DESIGN CHALLENGES IN NANOPARTICLE-BASED PLATFORMS:
IMPLICATIONS FOR TARGETED DRUG DELIVERY SYSTEMS

by

Douglas Gurnett Mullen

A dissertation submitted in partial fulfillment
of the requirements for the degree of
Doctor of Philosophy
(Macromolecular Science and Engineering)
in The University of Michigan
2010

Doctoral Committee:

       Professor Mark M. Banaszak Holl, Chair
       Professor James R. Baker Jr.
       Professor Jinsang Kim
       Associate Professor Xue-min Cheng

To my parents

Acknowledgements

My graduate career would not have been possible without the support, dedication and hard work of a number of individuals. It is not a trivial task to transition from the undergraduate training of a mechanical engineer to someone that works in synthetic polymer chemistry, designing platforms for targeted drug delivery. Taking on the learning curve associated with this transition is a success shared with many and I am truly grateful for all those that have helped me to navigate the space between the two fields. These individuals have each made remarkable contributions to my professional development.

Without question, my graduate school experience was positively impacted by my graduate advisor, Dr. Mark Banaszak Holl. I am continually impressed by the multi-path approach that Mark employs for tackling research questions and his willingness to modify and adjust research plans based on data. *Diversified research* could be another term for this strategy. My project probably would not have evolved in the way that it has, if Mark had not developed an initial research strategy that had several different objectives to be pursued in parallel. Mark's leadership and mentorship styles are ones that I hope to be able to emulate in the future as well as willingness to be available to those in this research group.

The other members of my thesis committee, Dr. James Baker Jr., Dr. Jinsang Kim, and Dr. Xue-min Cheng, were also huge influences on my graduate career. Dr. Baker never fails to amaze me in his ability to be an expert in so many different fields and his ability to juggle a plethora of responsibilities. He has been a great role model for someone interested in translating research to commercial use. Dr. Kim taught me very important lessons on the biological applications of polymeric materials. Finally, Dr. Xue-min Cheng was a critical resource for me in learning small molecule organic synthesis techniques. Dr. Cheng worked with me directly in the lab and was always willing to answer even the most basic organic chemistry questions.

I was very fortunate that Dr. Stassi DiMaggio temporarily left New Orleans to join our lab in Michigan for a year. Stassi spent many hours in the lab teaching me dendrimer synthesis, functionalization, and characterization techniques. It's hard to imagine how I would have learned all of the necessary skills for my projects without her help. She made every day in lab a delight with her humorous stories.

Dr. Istvan Majoros was a great source of information regarding dendrimer techniques and properties. He was always willing to share his insight into problems and I greatly enjoyed our discussions on the present challenges associated with the use of dendrimers as well as future possibilities.

Ankur Desai has been easily one of the most important team members on my graduate projects. From early-on Ankur has been my analytical "coach," instructing me on a number of different techniques and instrument operations. Ankur has gone above and beyond his responsibility as the MNIMBS analytical specialist on countless occasions, coming in to lab during the evening or weekend and logging into the HPLC computers remotely in the middle of the night to ensure that the HPLC systems were working properly. I am enormously grateful for all of the work and extra effort that Ankur made on my behalf.

Dr. Brad Orr has been a great source of support throughout graduate school. He was a huge resource for analyzing my dendrimer-ligand distribution data and developing initial models for the systems.

Dr. Elliott Hill was a great source of wisdom and guidance particularly in dealing with challenges that one typically encounters in graduate school. No graduate experience is complete without obstacles that grind forward progress to a standstill. For at least a year and a half, my own project did not work. I will always remember the great advice that Dr. Hill had at this point.

My academic 'twin,' Dan McNerny has been a great sounding board for ideas and the problem solving. Dan is always willing to drop what he is doing and help in any way that he can. I count myself very lucky to have Dan as a friend.

Similarly, Dr. Pascale Leroueil has been a great colleague and friend. She is always willing to listen to my unsolicited comments and advice, and has been a great advocate over the years.

I have been privileged to be able to work with a remarkably talented and hard working group of junior graduate and undergraduate students: Mark Barash, Emilee Byrne, Mallory van Dongen-Sohmer, Ming (Flora) Fang, Steven Holland, Becky Lahti, and Chris Sarra. These individuals have each made significant contributions towards advancing my own thesis work and I would not have been able to cover so many projects without their help. They were a great source of motivation for me.

The other members of the Banaszak Holl Group, Dr. Christopher Kelly, Dr. Seungpyo Hong, Dr. Kyung-hoon Lee, Dr. Lisa Prevette, Dr. Randon Walker, Dr. Joseph Wallace, Jiumei Chen, Blake Erickson, Ajdin Kavara, Damian Khan, Rahul Rattan, Ahleah Rohr, and Devon Triplett, have been truly great friends, mentors and collaborators. It has be a privilege to be a member of such a hard working group of individuals. Additionally, Dr. Jack Waddell and Dr. Len Sander have been very helpful in developing models for the ligand distribution data.

Being able to participate as a member of the interdisciplinary team in the Michigan Nanotechnology Institute for Medicine and Biological Sciences has been very enlightening and I feel very lucky to have had such a unique and enriched graduate career. Dr. Peter Cao, Dr. Seok Ki Choi, Dr. Jolanta Kukowska-Latallo, Dr. Baohua Huang, Dr. Paul Mackidon, Dr. Theodore Norris, Dr. Ramesh

Shukla, Dr. Thommey Thomas, Dr. Brent Ward, Dr. Hong Zong, Alina Kotlyar, and Mike Parise were all excellent mentors, always willing to take time out of their busy days to help and provide advice.

I am very thankful for the love and support that Annie has given me over the years. She has made grad school a great experience and has been a major source of balance in my life.

Finally, I'd like to thank my parents for all of their hard work, love and support. I simply would not be where I am today without them.

Table of Contents

List of Figures

List of Tables

Abstract

Characterization and control of heterogeneous distributions of nanoparticle-ligand components are major design challenges for nanoparticle-based platforms. This dissertation begins with an examination of poly(amidoamine) (PAMAM) dendrimer-based targeted delivery platform. A folic acid targeted modular platform was developed to target human epithelial cancer cells. Although active targeting was observed *in vitro*, active targeting was not found *in vivo* using a mouse tumor model. A major flaw of this platform design was that it did not provide for characterization or control of the component distribution.

Motivated by the problems experienced with the modular design, the actual composition of nanoparticle-ligand distributions were examined using a model dendrimer-ligand system. High Pressure Liquid Chromatography (HPLC) resolved the distribution of components in samples with mean ligand/dendrimer ratios ranging from 0.4 to 13. A peak fitting analysis enabled the quantification of the component distribution. Quantified distributions were found to be significantly more heterogeneous than commonly expected and standard analytical parameters, namely the mean ligand/nanoparticle ratio, failed to adequately represent the component heterogeneity. The distribution of components was also found to be sensitive to particle modifications that preceded the ligand conjugation.

With the knowledge gained from this detailed distribution analysis, a new platform design was developed to provide a system with dramatically improved control over the number of components and with improved batch reproducibility. Using semi-preparative HPLC, individual dendrimer-ligand components were isolated. The isolated dendrimer with precise numbers of ligands were characterized by NMR and analytical HPLC. In total, nine different dendrimer-ligand components were obtained with degrees

of purity $\geq 80\%$. This system has the potential to serve as a platform to which a precise number of functional molecules can be attached and has the potential to dramatically improve platform efficacy.

An additional investigation of reproducibility challenges for current dendrimer-based platform designs is also described. The mass transport quality during the partial acetylation reaction of the dendrimer was found to have a major impact on subsequent dendrimer-ligand distributions that cannot be detected by standard analytical techniques. Consequently, this reaction should be eliminated from the platform design. Finally, optimized protocols for purification and characterization of PAMAM dendrimer were detailed.

Chapter 1
Heterogeneous nanoparticle-ligand distributions: a major obstacle to scientific understanding and commercial translation

Introduction

The development of nanoparticle-based platforms conjugated with functional ligands has been an exciting area of activity in the past two decades. This class of material has been developed for a remarkably wide range of applications including nano-assemblies and structures,[1-2] sensing,[3-6] imaging and diagnostics,[7-9] probes of biological structure,[10] and targeted delivery.[11-15] Because small molecular ligands are often conjugated to the nanoparticle surface with an excess of attachment sites relative to the amount of ligand added, the resulting material is composed of a Poisson distribution of particles with different numbers of ligands. In our experience, however, the magnitude of this heterogeneity is frequently underestimated and explicit consideration of distributions is often not found in platform design. There remains a major need for better characterization and definition of the material composition as well as a better understanding of the relationship between the distribution of functional components and activity.

The most widely used parameter to characterize the distribution of nanoparticle-ligand components is the arithmetic mean number of ligands per particle. Although defining the nanoparticle-ligand composition by the arithmetic mean is an accepted standard of practice, this single value is insufficient to understand the material composition and ultimately predict the material activity. The problem is frequently compounded by the naive expectation that if a distribution of ligands exists, it will take the form of a Gaussian centered at the arithmetic mean. This expectation results in a substantial misunderstanding of the actual material compositions, especially for low numbers of conjugated ligands (1-10). Furthermore, it is not reliable to assume material

1

with the same mean necessarily has the same distribution. Finally, although values such as the median and the mode do provide additional information about the distribution, a comprehensive understanding requires characterization of the whole distribution.

This account provides our perspective on the problems that heterogeneous distributions present to the field at large. As part of an interdisciplinary team at the Michigan Nanotechnology Institute for Medicine and Biological Sciences (MNIMBS), our laboratory has been focused on the development of PAMAM dendrimer-based platforms for targeted drug delivery and diagnostic applications. In order to improve the platform design, we have developed a detailed understanding of the material composition in these systems as well as defining the level of characterization necessary to facilitate commercial translation. This account is generally applicable to nanoparticle-ligand systems where-in the ligand is conjugated with an excess of attachment sites on the nanoparticle and where the ligand is small relative to the nanoparticle such that site blocking is limited to the single attachment site.

Our efforts in characterizing and defining nanoparticle-ligand distributions have been greatly facilitated by two model nanoparticle-ligand systems for which the distribution of components can be resolved by HPLC. The platform, a generation five (G5) PAMAM dendrimer, has a very low level of polydispersity (PDI = 1.01) and is structurally well defined relative to other available platforms. The two model ligands in this system, 3-(4-(prop-2-ynyloxy)phenyl)propanoic acid (Alkyne Ligand) and 3-(4-(2-azidoethoxy)phenyl)propanoic acid (Azide Ligand) have characteristics similar to many functional ligands that are commonly used including size, functional groups and method of conjugation to the platform. The results of this work provide important information regarding questions of adequate characterization and also provide valuable insight into batch reproducibility challenges that several of these systems face.

Distributions in Nanoparticle-ligand Systems: Present but Often not Characterized

Distributions of nanoparticle-ligand components result because the synthetic methods used to conjugate ligand molecules to the particles are driven by random

2

collision and attachment events. The distributions detailed in this account are those that are generated when an excess of attachment sites on the nanoparticle is present relative to the molar amount of ligand molecules being conjugated. Although the theory behind these reactions has long been described,[16] very little experimental information exists that shows what these distributions look like in practice. Consequently, in practice, the heterogeneity and functional impact of the distribution is grossly underestimated.

The lack of understanding of the actual distributions in nanoparticle-ligand systems is in large part due to an inability of analytical techniques to identify the distribution. Several of the most common techniques are only capable of measuring the arithmetic mean number of ligands per particle. These methods include NMR spectroscopy, UV-visible spectroscopy, Fourier Transform Infrared Spectroscopy and elemental analysis. While techniques such as GPC, HPLC, MALDI-TOF, CE, and gel electrophoresis have the potential to resolve the distribution of nanoparticle-ligand components, the frequent outcome of these forms of characterization reveals no information about the distribution of components. This result is likely due to several factors including sub-optimized chromatographic conditions and/or the structural heterogeneity of the nanoparticle itself masking the distribution of nanoparticle-ligand components.

A common chromatographic result is the elution of the nanoparticle-ligand material in a single peak. In some cases, the chromatographic conditions have actually been tuned to produce idealized single peaks rather than multiple peaks corresponding to each of the different components in the distribution (**Figure 1.1**). In our experience, this single peak can lead to incorrect conclusions of homogeneous nanoparticle-ligand distributions. If the nanoparticle-ligand system is produced under the conditions described earlier, the single peak physically cannot be composed of a single nanoparticle-ligand component. The reality is that the single peak masks the actual distribution.

We have generated our share of chromatographic single peaks in our laboratory's research in dendrimer-based platforms for targeted drug delivery. In one such example,[10]

GPC chromatographs for PAMAM dendrimer conjugated with the dye AlexaFluor488 and with varying amounts of the targeting agent folic acid (means ranging from 0 to 15) contained only a single peak for each sample. In the HPLC elution traces for the same material, while two different peaks were observed, in no way does this come close to identifying the actual components in the material. In reality, each of these materials is composed of *hundreds* of components with different numbers of dye molecules and folic acid molecules.

Even for the dendrimer conjugated with the Alkyne or Azide ligands, with the exception of HPLC, all of the characterization techniques have failed to identify the different components in the material. **Figure 1.2a** shows GPC light scattering signals for four of these dendrimer-ligand samples.[17] The samples had mean ligand/dendrimer ratios between 0.4 and 1.5 (measured by NMR). Although all four samples elute as single peaks with similar peak shapes and elution times, the material was shown to have significantly different distributions. Sample A with a mean of 0.4 ligands per dendrimer was composed of 4 components, while Sample D had a mean of 1.5 ligands per dendrimer and was composed of 9 different dendrimer-ligand components. Similarly, characterization of the four dendrimer-ligand samples by a mass-based technique, MALDI-TOF (**Figure 1.2b**), provided no information about the distribution of components. In this case, the polydispersity in the dendrimer platform itself along with artifacts such as salt and matrix adducts, fragmentation and time-of-flight artifacts, prevents resolution of the different dendrimer-ligand components.

Although the distribution of components in most nanoparticle-ligand systems is inadequately defined, several groups have successfully worked to characterize the distributions. A number of these studies have provided qualitative evidence of resolved nanoparticle-ligand distributions. The Alivisatos group has used both gel electrophoresis and anion exchange chromatography to resolve the distribution of Au Nanoparticle-DNA components.[18] Gel electrophoresis was also used by Sperling et al. to resolve nanoparticles with different numbers of PEG ligands.[19] Because the resolution strategy was based on the incremental change in size from added PEG ligands, Sperling and co-

workers were able to resolve components in both Au-PEG and CdSe/ZnS-PEG systems. A third technique, UPLC, was used by Cason and colleagues to resolve different components in generation 4 (G4) PAMAM dendrimer conjugated with biotin molecules.[20] At least 7 different dendrimer-biotin components were resolved by this method. The same distribution was also resolved to a lesser extent using HPLC. Finally, in several detailed studies by the Murray group, mass spectrometry (MALDI and ESI-MS) was used to identify different gold nanoparticle components with different numbers of ligands.[21]

In addition to these qualitative studies, two studies have successfully quantified the distribution of nanoparticle components with different numbers of ligands. Working with quantum dots conjugated with fluorescently tagged proteins (ligand means of 8, 0.85, and 0.3 per particle), Casanova et al. used stepwise photobleaching to quantify the number of proteins bound to each nanoparticle and the ensemble distribution.[22] Finally, Pons and co-workers used single particle FRET measurements to quantify the distribution of quantum dot-protein components.[23] They reported experimental distributions consistent with Poisson distributions.

These studies represent major progress in understanding the material composition of nanoparticle-ligand systems. At a minimum, they provide direct experimental evidence from a wide variety of nanoparticle-ligand systems that the conditions used to synthesize nanoparticle-ligand conjugates produce highly heterogeneous mixtures of components. These studies stand in marked contrast to characterization that only provided the mean nanoparticle-ligand ratio and did not resolve the distribution.

Motivated, in part, by the above studies, we sought to develop a comprehensive understanding of the actual distribution of components in nanoparticle-ligand materials.

Quantification of Nanoparticle-ligand Distributions

As described in the introduction, our work in this area has been greatly facilitated by two small molecule ligands: the Alkyne and Azide Ligands. These molecules are

similar in size to a wide number of functional ligands that have been conjugated to nanoparticles including siRNA, fluorescent tags, oligonucleotides, folic acid, peptides, therapeutic agents, and other small molecules. Additionally, the coupling chemistry employed to conjugate the Alkyne and Azide ligands to the dendrimer, amide coupling via activated esters formed by EDC or PyBOP, is a standard method for nanoparticle-ligand conjugation. Most importantly, reverse-phase HPLC conditions have been developed to resolve the distribution of components in samples of dendrimer-ligand conjugates. We have leveraged this resolution to provide a quantitative analysis of dendrimer-ligand conjugates with ligand means ranging from 0.4 to 13.

A representative HPLC trace of one such dendrimer-ligand conjugate can be found in **Figure 1.3a**. The dendrimer sample in this figure had a mean of 2.7 ± 0.3 Azide Ligands per dendrimer as calculated by the combination of ^{1}H NMR, GPC and potentiometric titration. Five different peaks (labeled 0-4) can be clearly seen in the trace with an additional tailing region between 20 and 22 minutes. Peak 0, at approximately 18.8 minutes, had the same retention time as the parent unmodified dendrimer. The peaks with longer retention times as well as the "tailing" region, beginning at 20 minutes, were found to contain dendrimer particles with increasing numbers of conjugate ligands. A peak fitting method, using multiple copies of a fitting peak, shown in **Figure 1.3b** in green, made it possible to deconstruct the entire HPLC trace, including the tailing region, and quantify the relative amount of each dendrimer-ligand component. The shape of the fitting peak was developed based on the peak shape for the unmodified dendrimer. The distribution of dendrimer-ligand components, quantified by the peak fitting analysis, is plotted in **Figure 1.3c**. With this analysis, the arithmetic mean ligand/dendrimer ratio was determined to be 2.8 ± 0.1 which is identical (within experimental error) to the arithmetic mean determined by the combined NMR, GPC and potentiometric analysis (2.7 ± 0.3). With the entire distribution quantified, additional parameters such as the median (2), the mode (1) and the number of components in the distribution (12) were calculated.

In two initial studies,[17,24] distributions were quantified for samples produced using 100% amine terminated PAMAM dendrimer (G5-(NH$_2$)$_{112}$) and samples produced with partially acetylated dendrimer (G5-Ac$_{80}$-(NH$_2$)$_{34}$). The partial acetylation of the dendrimer prior to the conjugation of biologically active ligands has been a key design approach to prevent non-specific interactions between biological systems and the final device.

Quantified distributions for some of these dendrimer-ligand conjugates are shown in **Figure 1.4**, grouped in 3 different ranges of ligand means: 0.4 to 1.1, 2.7 to 6.8 and 10.2 to 12.9. The combined results from these two studies lead to several key observations. First, the distributions of components in these samples are very heterogeneous. The sample with a mean of 1.1 ligands (**Figure 1.4c**), for example, is composed of 6 different components with the mode (0) comprising over 45% of the entire material. Note that if this ligand were biologically active and being used in a drug delivery system, almost half of the material would be inactive. This is a significant amount of material, which will have no positive benefit, to inject into a patient. In the sample with a ligand man of 12.9 (**Figure 1.4a**), the distribution is made up of 27 different components. No individual component comprises more than 9% of the total material. Comparisons of each sample against the Poissonian distribution with the same ligand mean revealed the distribution to be skewed and slightly more heterogeneous than the theoretically expected result. Specifically, in all samples, the components at both extremes of the distribution were present in larger quantities than in the Poisson distribution and the components close to the mean were present in slightly smaller quantities. These experimentally quantified distributions are also significantly more heterogeneous than a narrow Gaussian distribution with a standard deviation of 1 or 2.

The second key observation is that pre-existing distributions increase the heterogeneity of subsequent ligand distributions. This observation was made by comparing distributions in dendrimer-ligand material made with the G5-(NH$_2$)$_{112}$ dendrimer with the distributions in the material made with the partially acetylated dendrimer. Increased skewing from the Poisson distribution was observed for the

partially acetylated material. Because the acetic anhydride is itself a very small ligand in the partial acetylation reaction and because an excess of modification sites on the dendrimer (primary amines) are present relative to the amount of acetic anhydride added, the reaction results in a distribution of dendrimer with different numbers of acetyl groups. In the subsequent Alkyne Ligand conjugation, the pre-existing distribution of acetyl groups per dendrimer increases the heterogeneity of the Alkyne Ligand distribution. This observation is very important because one of the advantages of using nanoparticles as platforms is that multiple copies of several different functional ligands can be conjugated to the same particle to obtain synergistic properties. In our own work, we frequently combine multiple copies of a targeting agent, a therapeutic agent, and a dye or imaging agent to the same dendrimer. With each conjugation step, however, the pre-existing distribution becomes increasingly heterogeneous. Additionally, simply changing the sequence in which different ligands are added to the nanoparticle could change the final material.

In a third study, the effect of the mass transport quality during the partial acetylation reaction on subsequent dendrimer-ligand distributions was investigated. This study was motivated by an observation in our laboratory that dendrimer-ligand distribution profiles had a dependence on the batch of partially acetylated dendrimer. These different batches were produced under supposedly the same experimental conditions and yet they introduced a high level of variability into the system. **Figure 1.5** displays the distribution analysis of two different dendrimer-ligand samples. Both samples had identical mean ligand/dendrimer ratios (6.6 ± 0.7 and 6.8 ± 0.7). The parent partially acetylated dendrimer for each sample was produced under different reaction conditions. For the dendrimer-ligand sample in panel **a** and **c**, the parent batch of partially acetylated dendrimer was produced with optimal mass transport conditions (dilution of acetic anhydride, rate of addition, and mixing efficiency). The parent dendrimer for the dendrimer-ligand sample in panel **b** and **d** was produced with sub-optimal mass transport conditions. Two dramatically different distribution profiles result as a direct consequence of the changes in mass transport. These differences were

extreme versions of the variability observed across batches of materials that were intended to have the same reaction conditions. Alarmingly, the characterization methods used to assess both the batches of partially acetylated dendrimer, HPLC and NMR, as well as the NMR characterization o f the dendrimer-ligand samples found not differences between the material.

The Arithmetic Mean is Insufficient

The combined knowledge gained from these three studies has provided critical insight into the heterogeneous distributions that are present in nanoparticle-ligand systems. Perhaps one of the most important lessons from these studies is that efforts to characterize these nanomaterials that only determine the mean nanoparticle/ligand ratio are wholly insufficient. The mean value alone provides no information about the number of different components in the material or the relative amount of each component in the distribution. For a first approximation, a Poisson distribution could be considered in the case where only the mean number of ligands is known. This form of distribution, however, is the "best case" distribution in terms of material homogeneity. All of our experimental data has found the actual distributions in these materials to be more heterogeneous than Poisson. The mean is also not capable of telling if the material is being produced consistently. The possibility that two samples can have the same mean number of ligands and yet have completely different distributions should no longer be considered unlikely. Finally, attempting to investigate composition-property relationships using the mean number of ligands as the representative material parameter is inadequate. In systems that combine multiple different ligand molecules to the nanoparticle, the component that has the same number of ligands as the mean number is likely to make up no more than 4% of the material.

Challenges for Reproducible Synthesis

In providing this account, it is not our intention to contend that distributions in nanoparticle-ligand materials are a fatal flaw. Certainly, there are many different systems in widespread use today that are heterogeneous mixtures. Polymeric materials are a

prime example. From a commercial translation perspective, however, nanoparticle-ligand distributions are major challenge to reproducibility. This is mainly because controls have not been incorporated to ensure that the distribution is reproduced in each manufactured batch. As described above, batches of material with consistent ligand means can have very different distributions. These can be caused by small changes in the starting material, mass transport conditions and reaction kinetics. These changes, however, will almost certainly not be detected by the standard levels of characterization being used by the field. There remains a great deal of progress to be made in order to identify the tolerable levels of variability in these materials as well as ways to implement control. These are likely to be very application and material specific.

New Platform Designs

In order to address the challenges inherent in systems with heterogeneous distributions of functional components, several groups have worked to design nanoparticle-ligand systems with improved distribution control. These systems include PAMAM dendrons,[25] dendrimer with single orthogonal modification sites,[26-27] and gold nanoparticles with precise numbers of ligands.[18-19,28-33]

Most recently our laboratory has focused on developing PAMAM dendrimer with precise numbers of 'click' modifiable ligands. Using semi-preparative HPLC, we were successful in isolating nine different dendrimer-ligand components with 0-8 Ligands from a dendrimer-ligand distribution. Analytical HPLC characterization of these "Precision Dendrimer" can be found in **Figure 1.6**. Using peak fitting, the degree of purity for each of these components was found to be 80% or greater, representing an order of magnitude increase in purity. Because the ligand in this system was the Azide Ligand, the isolated dendrimer components each had a precise number of orthogonal sites which could be modified with the alkyne-azide 'click' reaction. This approach has several attractive features. First, due to the highly reproducible separation of the dendrimer-ligand components on the HPLC column, dendrimer with precise numbers of Alkyne or Azide ligands can be obtained with great consistency. This is a major

advantage of this approach because column loading limitations can be overcome by isolating material over multiple runs. Second, the precision dendrimer have great potential to be a versatile platform that can be modified by a wide range of functional molecules via the click reaction to obtain dendrimer with precise numbers of functional molecules.

Conclusion

In conclusion, nanoparticle-ligand materials are composed of heterogeneous distributions that are widely unappreciated. The present reliance on the mean number of ligands per dendrimer should be replaced with a full characterization of the entire distribution that the mean is meant to represent. Furthermore, without the introduction of sufficient controls in platform designs distributions are a major obstacle to successful translation of nanoparticle-ligand systems.
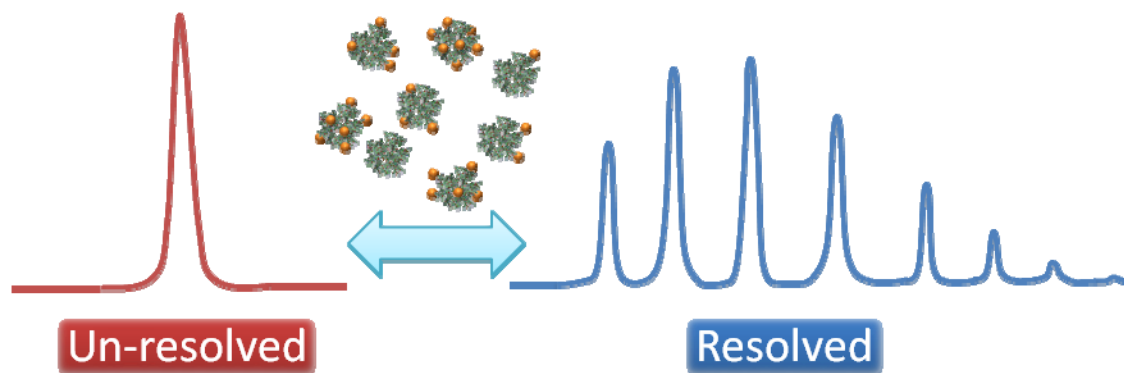
Figure 1.1: For many nanoparticle-ligand systems, chromatographic-based characterization produces a single peak that fails to resolve the actual distribution of components. This single peak frequently causes the actual distribution of components to be significantly underestimated. If, in the nanoparticle-ligand conjugation reaction, there is an excess of attachment sites relative to the amount of ligand added the most uniform distribution follow a Poisson distribution.
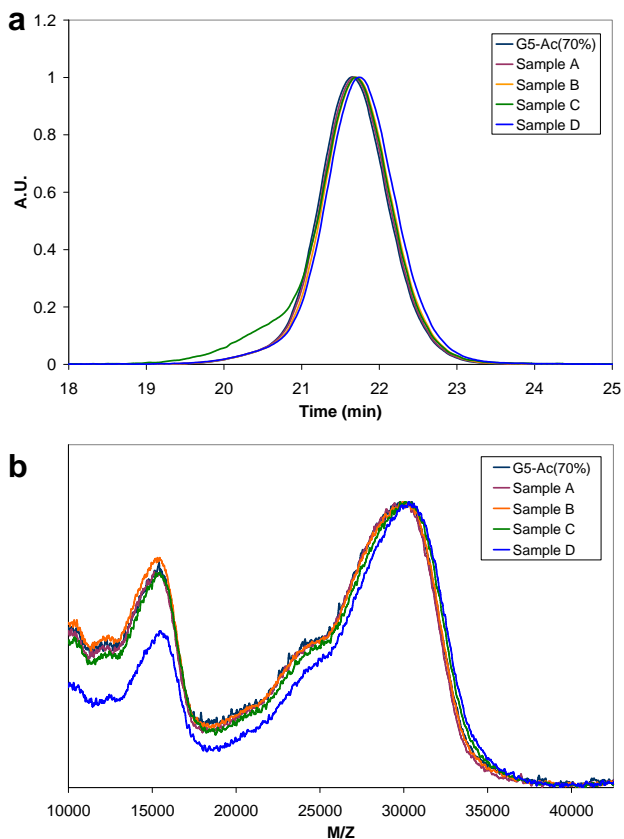
Figure 1.2: Examples of nanoparticle-ligand distributions that fail to be resolved using standard analytical techniques (GPC and MALDI-TOF). Samples A-D are composed of a series of dendrimer-ligand conjugates. The mean numbers of ligands for each sample is 0.2, 0.6, 1.04, and 1.47, respectively. HPLC analysis determined the number of dendrimer-ligand components in each sample to be a) The GPC light scattering data of the four samples produces only single peaks.   The different dendrimer-ligand distributions are indistinguishable by this technique.   b) Similarly, MALDI-TOF characterization is unsuccessful at resolving the different dendrimer-ligand components. One of the challenges of this mass based technique is that the structural heterogeneity of the dendrimer alone masks the different dendrimer-ligand components.

13
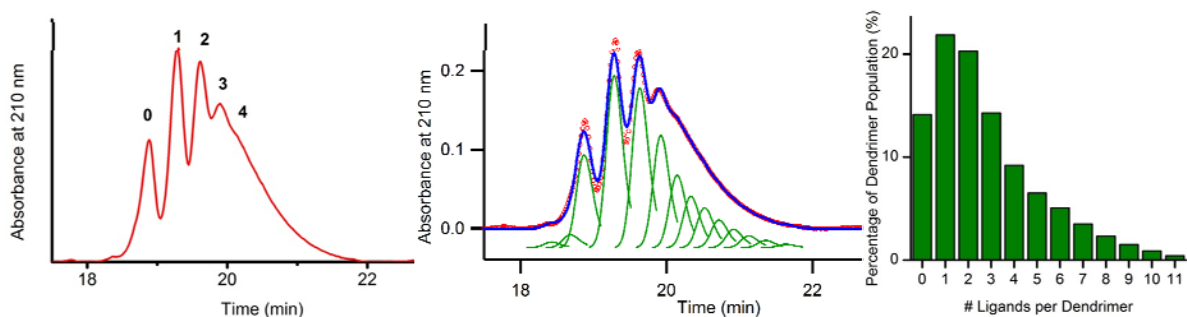
Figure 1.3: Peak fitting analysis deconstructs the HPLC trace of a dendrimer-ligand sample to provide the quantified distribution of dendrimer-ligand components. a) The HPLC trace at 210 nm for a dendrimer-ligand sample with a mean of 2.7 Alkyne Ligands per dendrimer is shown in red. Peak 0 had the same retention time as the un-modified parent dendrimer. b) Peak fitting analysis deconstructs the HPLC trace to provide the relative concentration of each dendrimer-ligand component. HPLC data is shown in red dots and the multiple copies of the fitting peak are shown in green. The shape of the fitting peak is based on the HPLC peak shape for the un-modified parent dendrimer. The summation of the fitting peaks is in blue. c) The relative amount of each dendrimer-ligand component in the distribution.
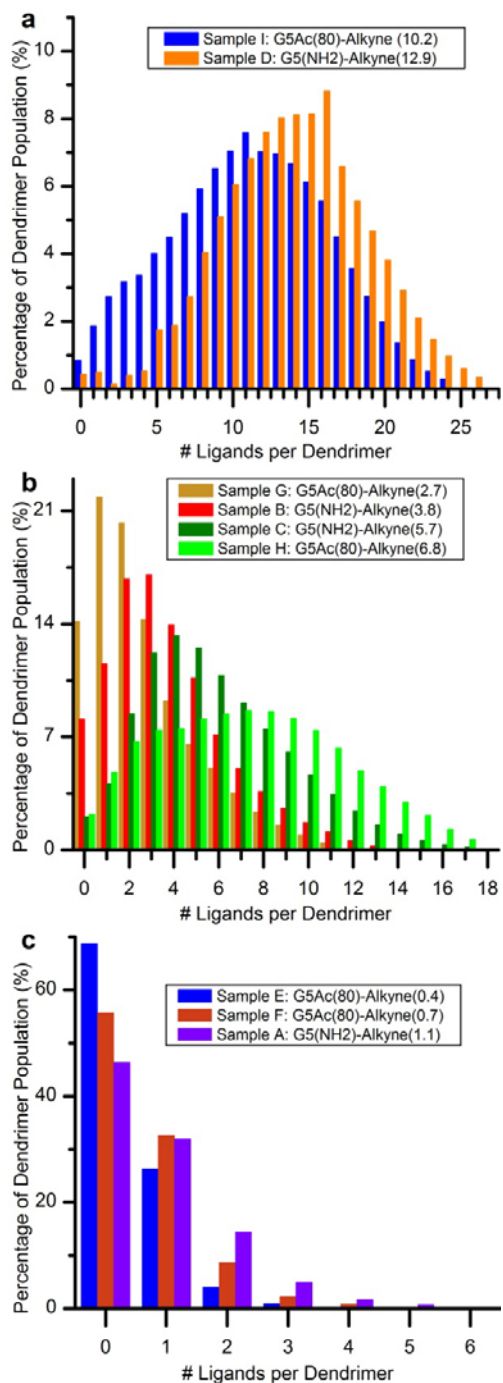
Figure 1.4: Quantified dendrimer-ligand distributions for samples with ligand means ranging from 0.4 to 12.9. Samples were prepared using either a partially acetylated dendrimer (G5-Ac$_{80}$-(NH$_2$)$_{34}$) or a 100% amine terminated dendrimer (G5-(NH$_2$)$_{112}$) **a)** Dendrimer-ligand distributions for samples with mean ligand/dendrimer ratios of 10.2 and 12.9. **b)** Distributions for samples with mean ligand/dendrimer ratios between 2.7 and 6.8. **c)** Distributions for dendrimer-ligand samples with mean ligand/dendrimer ratios ranging from 0.4 to 1.1.

15
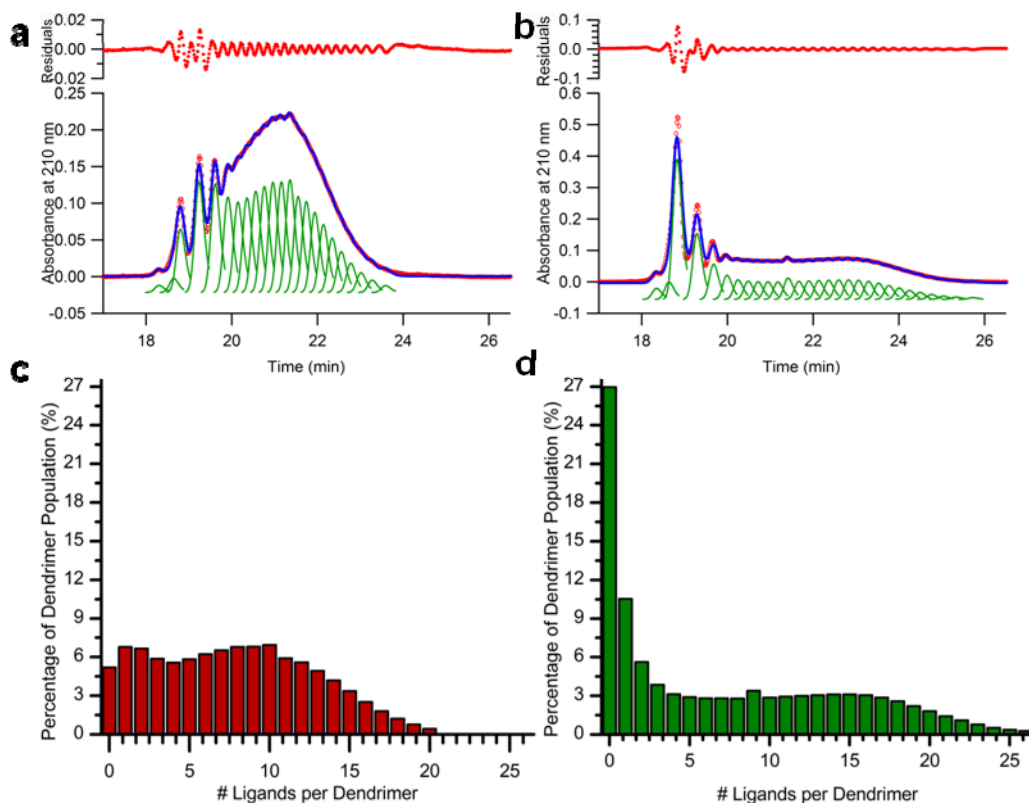
Figure 1.5: Quantified distributions of two dendrimer-ligand conjugates with mean ligand/dendrimer ratios of 6.6 ± 0.7 (**a** and **c**) and 6.8 ± 0.7 (**b** and **d**). Although the samples have the same arithmetic means, they have dramatically different distributions of dendrimer-ligand components. The dendrimer samples were produced using two different batches of partially acetylated dendrimer and the differences in dendrimer-ligand distributions were found to be caused by differences in dendrimer-acetyl group distributions in the parent partially acetylated dendrimer batches. For the sample in panel **a** and **c**, the parent partially acetylated dendrimer was produced under effective mass transport conditions. The parent dendrimer for the sample in b and d was produced with ineffective mass transport during the partial aceylation reaction.
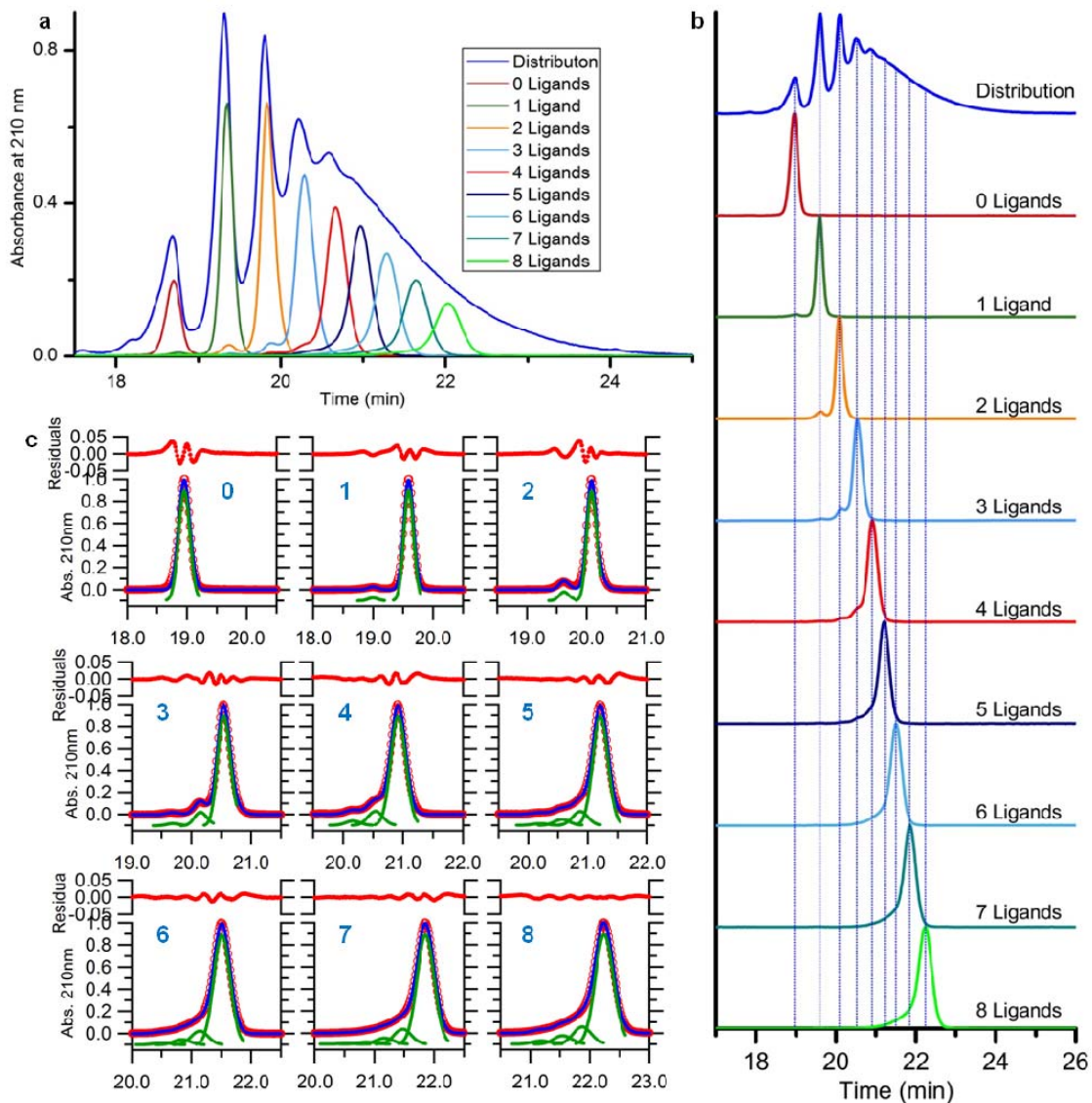
Figure 1.6: Dendrimer with precise numbers of ligands isolated from a distribution of dendrimer-ligand components. A total of nine different Precision Dendrimer were successfully isolated **a)** Analytical HPLC characterization of the Precision Dendrimer taken at the isolated concentration. **b**) Normalized analytical HPLC traces for the nine different Precision Dendrimer. Blue lines show the relationship between the isolated material and the distribution of dendrimer-ligand components. **c**) Peak fitting found the degree of purity for each isolated dendrimer component to be 80% or greater.

References

(1)   Maye, M. M.; Nykypanchuk, D.; Cuisinier, M.; van der Lelie, D.; Gang, O. *Nature Materials* **2009**, *8*, 388-391.

(2)   Maye, M. M.; Kumara, M. T.; Nykypanchuk, D.; Sherman, W. B.; Gang, O. *Nature Nanotechnology* **2010**, *5*, 116-120.

(3)   Medintz, I. L.; Clapp, A. R.; Mattoussi, H.; Goldman, E. R.; Fisher, B.; Mauro, J. M. *Nature Materials* **2003**, *2*, 630-638.

(4)   Jain, K. K. *Clinica Chimica Acta* **2005**, *358*, 37-54.

(5)   Park, S. J.; Taton, T. A.; Mirkin, C. A. *Science* **2002**, *295*, 1503-1506.

(6)   Pandana, H.; Aschenbach, K. H.; Gomez, R. D. *Ieee Sensors Journal* **2008**, *8*, 661-666.

(7)   Nie, S. M.; Xing, Y.; Kim, G. J.; Simons, J. W. *Annual Review of Biomedical Engineering* **2007**, *9*, 257-288.

(8)   Landmark, K. J.; DiMaggio, S.; Ward, J.; Kelly, C.; Vogt, S.; Hong, S.; Kotlyar, A.; Myc, A.; Thomas, T. P.; Penner-Hahn, J. E.; Baker, J. R.; Holl, M. M. B.; Orr, B. G. *ACS Nano* **2008**, *2*, 773-783.

(9)   Thaxton, C. S.; Elghanian, R.; Thomas, A. D.; Stoeva, S. I.; Lee, J. S.; Smith, N. D.; Schaeffer, A. J.; Klocker, H.; Horninger, W.; Bartsch, G.; Mirkin, C. A. *Proceedings of the National Academy of Sciences of the United States of America* **2009**, *106*, 18437-18442.

(10)   Hong, S.; Leroueil, P. R.; Majoros, I. J.; Orr, B. G.; Baker, J. R.; Holl, M. M. B. *Chemistry and Biology* **2007**, *14*, 107-115.

(11)   Tong, R.; Cheng, J. J. *Polymer Reviews* **2007**, *47*, 345-381.

(12)   Peer, D.; Karp, J. M.; Hong, S.; FaroKhzad, O. C.; Margalit, R.; Langer, R. *Nature Nanotechnology* **2007**, *2*, 751-760.

(13)   Choi, H. S.; Liu, W.; Liu, F.; Nasr, K.; Misra, P.; Bawendi, M. G.; Frangioni, J. V. *Nat Nanotechnol* **2010**, *5*, 42-47.

(14)   Rawat, M.; Singh, D.; Saraf, S.; Saraf, S. *Biological and Pharmaceutical Bulletin* **2006**, *29*, 1790-1798.

(15)   Patri, A. K.; Majoros, I. J.; Baker, J. R. *Current Opinion in Chemical Biology* **2002**, *6*, 466-471.

(16)   Beichelt, F. E.; Fatti, L. P. *Stochastic processes and their applications*; Taylor & Francis: London, 2002.

(17)   Mullen, D. G.; Desai, A. M.; Waddell, J. N.; Cheng, X.-M.; Kelly, C. V.; McNerny, D. Q.; Majoros, I. J.; Baker, J. R.; Sander, L. M.; Orr, B. G.; Banaszak Holl, M. M. *Bioconjug Chem* **2008**, *19*, 1748-1752.

(18)   Claridge, S. A.; Liang, H. Y. W.; Basu, S. R.; Frechet, J. M. J.; Alivisatos, A. P. *Nano Letters* **2008**, *8*, 1202-1206.

(19)   Sperling, R. A.; Pellegrino, T.; Li, J. K.; Chang, W. H.; Parak, W. J. *Advanced Functional Materials* **2006**, *16*, 943-948.

(20)   Cason, C. A.; Oehrle, S. A.; Fabre, T. A.; Girten, C. D.; Walters, K. A.; Tomalia, D. A.; Haik, K. L.; Bullen, H. A. *Journal of Nanomaterials* **2008**, doi:10.1155/2008/456082.

(21)   Tracy, J. B.; Kalyuzhny, G.; Crowe, M. C.; Balasubramanian, R.; Choi, J. P.; Murray, R. W. *Journal of the American Chemical Society* **2007**, *129*, 6706-6707.

(22)   Casanova, D.; Giaume, D.; Moreau, M.; Martin, J. L.; Gacoin, T.; Boilot, J. P.; Alexandrou, A. *Journal of the American Chemical Society* **2007**, *129*, 12592-12593.

(23)   Pons, T.; Medintz, I. L.; Wang, X.; English, D. S.; Mattoussi, H. *Journal of the American Chemical Society* **2006**, *128*, 15324-15331.

(24)   Mullen, D. G.; Fang, M.; Desai, A. M.; Baker, J. R.; Orr, B. G.; Banaszak Holl, M. M. *ACS Nano* **2010**, *4*, 657-670.

(25)   McNerny, D. Q.; Kukowska-Latallo, J. F.; Mullen, D. G.; Wallace, J. M.; Desai, A. M.; Shukla, R.; Huang, B. H.; Holl, M. M. B.; Baker, J. R. *Bioconjugate Chemistry* **2009**, *20*, 1853-1859.

(26)   Goyal, P.; Yoon, K.; Weck, M. *Chemistry-a European Journal* **2007**, *13*, 8801-8810.

(27)   Yoon, K.; Goyal, P.; Weck, M. *Organic Letters* **2007**, *9*, 2051-2054.

(28)   Hainfeld, J. F.; Powell, R. D. *Journal of Histochemistry & Cytochemistry* **2000**, *48*, 471-480.

(29)   Chak, C. P.; Xuan, S. H.; Mendes, P. M.; Yu, J. C.; Cheng, C. H. K.; Leung, K. C. F. *ACS Nano* **2009**, *3*, 2129-2138.

(30)   Wilson, R.; Chen, Y.; Aveyard, J. *Chemical Communications* **2004**, 1156-1157.

(31)   Zanchet, D.; Micheel, C. M.; Parak, W. J.; Gerion, D.; Alivisatos, A. P. *Nano Letters* **2001**, *1*, 32-35.

(32)   Zanchet, D.; Micheel, C. M.; Parak, W. J.; Gerion, D.; Williams, S. C.; Alivisatos, A. P. *Journal of Physical Chemistry B* **2002**, *106*, 11758-11763.

(33)   Zikich, D.; Borovok, N.; Molotsky, T.; Kotlyar, A. *Bioconjugate Chemistry* **2010**, *ASAP*.

Chapter 2
Design, synthesis, and biological functionality of a dendrimer-based modular drug delivery platform

Introduction

The high toxicity of conventional cytotoxic anti-cancer drugs often forces these agents to be given at sub-optimal dosages and this can result in treatment failure.[1] To resolve this problem, delivery platforms that can discriminate between healthy and malignant cells have been developed.[1-2] Actively targeted therapeutic delivery platforms consist of three different components: a targeting component comprised of targeting ligands with affinities for molecules expressed on cancer cells; a payload consisting of drug and/or imaging agents; and a nano-scale structure to which the targeting and payload moieties are attached. This platform targeting of anti-cancer drugs with cancer cell-specific ligands can dramatically improve a drug's therapeutic index. Conjugating multiple targeting ligands to a single platform molecule further increases the potential for specific targeting of cancer cells by allowing the possibility of multivalent interactions.[3-4]

The structural design of these types of delivery platforms is critical to the success of the delivery device. Numerous classes of targeted drug delivery platforms have been developed that potentially meet the requirements needed to combine targeting ligands, imaging agents, and drug molecules together to deliver the therapeutic payload to a desired location in the body. These include drug-target conjugates, linear polymers, lipid-based carriers (liposomes and micelles), carbon nanotubes, inorganic nanoparticles, and dendrimers. Several of these different delivery platforms are progressing towards or through clinical trials for cancer treatments with promising results.[2] Each approach, however, is not without limitations and the potential for widespread application of these platforms in their present design is unclear.

Dendrimer-based platforms have a unique branching structure which results in exceptionally high degrees of monodispersity and well defined terminal groups that provide the ability to form soluble conjugates containing multiple copies of hydrophobic drug and/or targeting molecules. The compact, branched structures appear to enhance the ability of the targeting molecules to interact in a fashion conducive to multivalent binding to cell membrane receptors.[3] The dendrimer's small size enables efficient diffusion across the vascular endothelium to find tumors and also allows the rapid clearance of these molecules from the blood stream. This clearance avoids potential long-term toxicities and reduces the necessity of a rapidly-degradable platform. The most widely used dendrimer in biomedical applications, poly(amidoamine) (PAMAM), is non-imunogenetic and non-toxic once the surface primary amines have been modified [5-10]. There have been numerous, recent examples describing the development of dendrimer-based targeted delivery systems using a wide variety of targeting ligands including monoclonal antibodies,[11-15] peptides,[16] T-antigens,[17-19] and folic acid.[20-29]

Despite the success of these dendrimer-based platforms, this approach has several challenges associated with its implementation. First, the synthesis of dendrimers with different functional groups for targeted delivery (including targeting, drug, and imaging agents) requires a laborious chemical process that is unique for each different molecular combination. Second, the carrying capacity of a single dendrimer, although significantly better than other types of delivery platforms, is finite due to limits in surface molecule density and solubility. This becomes a problem when one attempts to conjugate multiple copies of the target, drug, and/or dye molecules to the same dendrimer. Third, significant increases in heterogeneity occur with the conjugation of each additional molecule to a single dendrimer platform due to the stochastic nature of these chemical reactions.[30] This has limited the flexibility of these systems.

To address the drawbacks of the single dendrimer platforms, several groups have sought to apply modular design concepts to dendrimer systems.[31-41] The common premise of this new approach is to use dendrimers or dendrons as modular units, each with multiple copies of a single functional molecule. Multi-functional platforms can be

generated by combining different modules through a universal coupling mechanism. The main benefits of this design are two fold: First, segregating each functional group (drug/target/dye) to a different dendrimer module avoids the need to develop a new orthogonal coupling chemistry for each new combination of functional groups. This advantage should not be underestimated. Significant time is spent developing new orthogonal coupling strategies for desired functional combinations because many of the component drug molecules and targeting ligands (Taxol and RGD for example) are susceptible to a loss of activity due to undesired cross reactions as well as degradation by hydrolysis. The second benefit of the modular strategy is a greater carrying capacity of the delivery platform because the different functional molecules are localized on separate dendrimer units and the water solubilizing dendrimer backbone is effectively double the mass of the single dendrimer.

In the modular dendrimer systems synthesized to-date two coupling strategies have been used to combine different dendrimer-based modules together: oligonucleotide self-assembly and the 1,3-dipolar cycloaddition between an azide and an alkyne, commonly called 'click' chemistry. Oligonucleotide self-assembly has been used to link both dendron and dendrimer modular units. Choi and co-workers demonstrated this strategy by using two complementary oligonucleotides to link two PAMAM dendrimers together.[31-32] DeMattie, Huang, and Tomalia used the same method to connect two un-functionalized PAMAM dendrons together.[33] Characterization of these systems was accomplished by gel electrophoresis, AFM, MALDI, and UV/vis due to the small synthetic scales employed. For the dendrimer-based system, isolated dendrimer samples were not obtained, rather the samples were generated in solution. Choi et al. did demonstrate biological functionality of the modular system in a cell culture assay[32] and an *in vivo* model.[34]

The use of 'click' chemistry to create dendritic modular systems has mainly involved dendrons. 'Click' chemistry is a particularly attractive coupling method because it can be performed with a wide variety of solvent conditions including aqueous environments. The stable triazole ring bridge, resulting from coupling alkyne with azide

moieties, is frequently achieved at near quantitative yields and is considered to be biologically stable.[42-44] Furthermore, the 'click' coupling chemistry is orthogonal to the coupling chemistries typically used to attach functional groups to the dendrimer. Lee and co-workers have detailed the synthesis of multi-module platforms using both un-functionalized PAMAM dendrons[35-37] as well as un-functionalized Frechet-type dendrons[38] for each of the modules. In all of these systems, the focal point of the dendron possessed either an azide or alkyne moiety. Wu and co-workers developed a 2,2-bis(hydroxymethyl)propionic acid (bis-MPA) based asymmetric modular dendron with 16 mannose units and 2 coumarin chromaphores, and demonstrated binding in a hemagglutination assay.[39] Goyal, Yoon, and Weck have also developed a poly(amine) dendrimer that possessed a single aldehyde or azide moiety on the dendrimer periphery capable of orthogonal functionalization by small molecule functional groups.[40-41] These approaches appear promising but only the bis-MPA dendron system has been demonstrated to have function as a targeted drug delivery platform. In all cases, the dendrons used were G3 or smaller. This has significant limitations for widespread therapeutic use because of the limited carrying capacity of low generation dendrons. To date, click chemistry has not been applied to a modular dendrimer system.

In this paper we report on a new modular approach based upon 'clicking' together generation 5 (G5) PAMAM dendrimers containing either the targeting agent folic acid (FA) (**13**) or the dye fluorescein isothiocyanate (FITC) (**14**). The molecules were characterized by ^{1}H NMR spectroscopy and two-dimensional Nuclear Overhauser Effect spectroscopy (NOESY). To the best of our knowledge, this is the first example of the successful 'click' chemistry conjugation of dendrimers (as opposed to dendrons). Linking together two dendrimer-based modules was achieved by first conjugating one dendrimer module to an alkyne linker (**2b**) and conjugating a second dendrimer module to an azide linker (**3c**). The ability of this modular system to specifically target folic acid receptor (FAR) expressing cells has been verified by flow cytometic documentation of the uptake of the clicked FA-FITC modules into KB cells.

This dendrimer-based modular system has several potential benefits over is predisessor systems. In using 'click' chemistry rather than oligonucleotide linking, the modular system can be scaled up with far greater ease and at a substantially lower cost. Oligonucleotides are typically purchased in nano-gram quantities where-as the 'click' linkers in this study were produced at the gram scale. Additionally, because the clicked dendrimers are covalently linked rather than joined via the hydrogen-bond base-pairing oligonucleotide bridge, the platform is less likely to become unlinked. This characteristic proves beneficial when attempting to isolate and characterize multi-module platforms. In using generation 5 dendrimers with diameters of approximately 5 nm and over 630 hydrogen bonding sites, the carrying capacity is substantially greater than the previously used dendrons which were approximately 2 nm in diameter and possess approximately 150 hydrogen bonding sites. In fact, efforts in our group to generate G2 and G3 PAMAM dendrons functionalized with folic acid, failed due to a loss of platform solubility.

Experimental Procedures

Reagents and Materials

Biomedical grade, generation 5 PAMAM (poly(amidoamine)) dendrimer was purchased from Dendritech Inc. and purified by dialysis, as previously described,[30] to remove lower molecular weight impurities including trailing generation dendrimer defect structures.

MeOH (99.8%), acetic anhydride (99.5%), triethylamine (99.5%), dimethyl sulfoxide (99.9%), fluorescein isothiocyanate (98%), dimethylformamide (99.8%), 1-[3-(dimethylamino)-propyl-3-ethylcarbodiimide HCl (EDC) (98%), acetone (ACS reagent grade ≥ 99.5%), methyl 3-(4-hydroxyphenyl)propanoate (97%), sodium azide (99.99%), 1-bromo-2-chloroethane (98%), ethyl acetate (EtOAc) (99.5%), copper sulfate pentahydrate (99%), sodium ascorbate, 18-crown-6, K_2CO_3, tetrahydrofuran (99.9%), N,N-diisopropylethylamine, benzotriazol-1-yl-oxytripyrrolidinophosphonium hexafluorophosphate (98%), D_2O, NaCl, 1 N HCl, 2 M KOH, and volumetric solutions

(0.1 M HCl and 0.1 M NaOH) for potentiometric titration were purchased from Sigma Aldrich Co. and used as received. Hexanes (HPLC grade) and 10,000 molecular weight cut-off centrifugal filters (Amicon Ultra) were from Fisher Scientific. 1x phosphate buffer saline (PBS) (Ph = 7.4) without calcium or magnesium was purchased from Invitrogen. Sephadex G-25 and Sephadex LH-20 were purchased from GE Lifesciences.

Nuclear Magnetic Resonance Spectroscopy

All ^{1}H NMR experiments were conducted using a Varian Inova 500 MHz instrument. For all dendrimer samples the delay time was 10s. No delay time was used for small molecule samples. NOESY experiments on the dendrimer samples found in Figure 1 and utilized for Table 1 were also conducted using a Varian Inova 500 MHz instrument. For these experiments the mixing time was 250 ms, the relaxation time was 1s, and the number of increments was 128 with 32 scans per increment. Temperature was controlled at 25 °C. The NOESY experiments on the small molecule model system found in Figure 1 and utilized in Table 1 were conducted using a Varian MR400 (400 MHz) instrument. For the experiments on the small molecules, the mixing time was 800 ms, the relaxation time was 1.2s, and the number of increments was 200 with 4 scans per increment. Based on work published by Hoffman, the internal solvent reference peak for all experiments in $CDCl_3$ was set to 7.261 ppm. For experiments conducted in D_2O, the internal reference peak was set to 4.717 ppm.[45]

Gel Permeation Chromatography

GPC experiments were performed on an Alliance Waters 2690 separation module equipped with a 2487 dual wavelength UV absorbance detector (Waters Corporation), a Wyatt Dawn DSP laser photometer, and an Optilab DSP interferometric refractometer (Wyatt Technology Corporation). Columns employed were TosoHaas TSK-Gel Guard PHW 06762 (75 mm × 7.5 mm, 12 μm), G 2000 PW 05761 (300 mm × 7.5 mm, 10 μm), G 3000 PW 05762 (300 mm × 7.5 mm, 10 μm), and G 4000 PW (300 mm × 7.5 mm, 17 μm). Column temperature was maintained at 25 ± 0.1 °C with a Waters temperature control module. The isocratic mobile phase was 0.1 M citric acid and 0.025 wt % sodium azide, pH 2.74, at a flow rate of 1 mL/min. The sample concentration was 10 mg/5 mL

with an injection volume of 100 μL. The weight average molecular weight, M_w, has been determined by GPC, and the number average molecular weight, M_n, was calculated with Astra 4.7 software (Wyatt Technology Corporation) based on the molecular weight distribution.

Reverse Phase High Performance Liquid Chromatography

HPLC analysis was carried out on a Waters Delta 600 HPLC system equipped with a Waters 2996 photodiode array detector, a Waters 717 Plus auto sampler, and Waters Fraction collector III. The instrument was controlled by Empower 2 software. For analysis of the conjugates, a C5 silica-based RP-HPLC column (250 x 4.6 mm, 300 Å) connected to a C5 guard column (4 x 3 mm) was used. The mobile phase for elution of the conjugates was a linear gradient beginning with 90:10 (v/v) water/acetonitrile and ending with 10:90 (v/v) water/acetonitrile over 25 min at a flow rate of 1 mL/min. Trifluoroacetic acid (TFA) at 0.14 wt % concentration in water as well as in acetonitrile was used as a counter ion to make the dendrimer surfaces hydrophobic.

Cell Culture and Treatment

The uptake of the synthesized conjugates was performed using FA-receptor-expressing KB cells (ATCC #CCL-17) as we have described previously.[23] Cells were maintained in FA-free Roswell Park Memorial Institute-1640 (RPMI 1640) medium supplemented with 10% Fetal Bovine serum (FBS), 2 μM L-glutamine, 100 U/ml penicillin and 100 μg/ml streptomycin in 5% CO_2 at 37° C. Cells were planted into 24 wells plate at density 250,000 per well and allowed to reach ~90% confluent on the day of the experiment. They were rinsed and incubated in serum free medium with conjugates for 1 hour at 37° C in 5% CO_2. In some wells, a 20-fold excess of free folic acid or the folic acid conjugated dendrimer was added 30 minutes prior to the addition of the dendrimer platform for the blocking of folate receptors.

Flow Cytometric Analysis

The cellular fluorescence was quantified on a Beckman-Coulter EPICS-XL MCL flow cytometer, and the data were analyzed using Expo32 software (Beckman-Coulter,

Miami, FL). Cells were trypsinized, rinsed and suspended in PBS containing 0.1% bovine serum albumin (PBSB). The viable cells were gated, and the mean FL1-fluorescence of 10,000 cells was quantified. Error bars are calculated using the half-peak coefficient of variation (HPCV).[46]

Recipient Animal and Tumor Model

Immunodeficient, Five- to 6-week-old Fox Chase severe combined immunodeficient (SCID; CB-17/lcrCrl-scidBR) female mice were purchased from the Charles River Laboratories (Wilmington, MA) and housed in a specific pathogen-free animal facility at the University of Michigan Medical Center in accordance with the regulations of the University's Committee on the Use and Care of Animals as well as with federal guidelines, including the Principles of Laboratory Animal Care. Animals were fed ad libitum with Laboratory Autoclavable Rodent Diet 5010 (PMI Nutrition International, St. Louis, MO). Four weeks before tumor cell injection, the food was changed to a folate-deficient diet (TestDiet, Richmond, IN).

Tumor Cell Line

The KB human cell line, which overexpresses the folate receptor, was purchased from the American Type Tissue Collection (Manassas, VA) and maintained in vitro at 37ºC, 5% CO_2 in folate-deficient RPMI 1640 supplemented with penicillin (100 units/mL), streptomycin (100 μg/mL), and 10% heat-inactivated fetal bovine serum. Before injection in the mice, the cells were harvested with trypsin-EDTA solution, washed, and resuspended in PBS. The cell suspension (2×10^6 cells in 0.2 mL) was injected s.c. into both flanks of each mouse using a 30- gauge needle. In the biodistribution studies, the tumors were allowed to grow for 3 weeks until reaching 0.9 cm^3 in volume. The formula chosen to compute tumor volume was for a standard volume of an ellipsoid, where $V = 4/3\pi$ (1/2 length $\times$ 1/2 width $\times$ 1/2 depth). With an assumption that width equals depth and π equals 3, the formula used was $V = 1/2 \times$ length $\times$ width^2. Targeted drug delivery using conjugate injections was started 6 hours prior to harvest of the tumors.

Biodistribution of the Folic Acid Targeted Dendrimer System with 6TAMRA

Mice were injected via lateral tail vein with 0.2 mL saline solution containing 15 nmole of the dendrimer conjugates. At 6 hours postinjection, the animals were euthanized and samples of tumor were taken and immediately frozen for sectioning and imaging.

Flow cytometry analysis was done with single-cell suspension isolated from tumor. Tumor was crushed, cell suspension filtered through 70 μm nylon mesh (Becton Dickinson, Franklin Lakes, NJ), and washed with PBS. Samples were analyzed using an Vantage 2 flow cytometer (Becton Dickinson, Franklin Lakes, NJ). Data were reported as the mean channel fluorescence of the cell population.

For laser scanning confocal microscope imaging, tissue was dissected, embedded in OCT, and frozen in 2-methyl-butane in a dry ice bath. Sections (15 μm) were cut on a cryostat, thaw mounted onto slides, and stored at -80ºC until imaging. Prior to imaging, slides were allowed to air dry. Samples were imaged using an Olympus FluoView 500 laser scanning confocal microscope using a 60X, 1.5 numerical aperture oil immersion objective. Fluorescence and differential interference contrast (DIC) images were collected simultaneously using a Green Helium-Neon laser with 543 nm excitation. Images were recorded using FluoView software at 1024 x 1024 pixels with a scale of 0.21 x 0.21 μm per pixel and a height of 0.40 μm per imaging slice.

Synthesis

Dendrimers are identified by the core dendrimer (G5) and conjugated groups: Ac, Alkyne, Azide, FA, and FITC. In the cases where dendrimers are linked together via the triazole ring, Alkyne and Azide labels are replaced with "L." Ac refers to the acetamide termination, alkyne to linker **2b**, azide to linker **3c**, FA to folic acid, and FITC to fluorescein isothiocyanate.

1. Synthesis of Partially Acetylated Dendrimer

Partial acetylation of G5 PAMAM dendrimer was previously described.[5,30] The number average molecular weight (27,336 g/mol) and PDI (1.018) of the un-acetylated

dendrimer was determined by GPC. Potentiometric titration was conducted to determine the average number of primary amines per dendrimer (112 ± 5). Three batches of partially acetylated dendrimer were synthesized for further modification. **1' G5Ac$_{72\%}$:** ^{1}H NMR integration determined the degree of acetylation to be 72%. Number average molecular weight (30,722 g/mol) was computed based on the addition of mass to the dendrimer from the acetyl groups as determined by NMR. PDI (1.019) of the purified acetylated dendrimer were determined by GPC. **1" G5Ac$_{65\%}$:** ^{1}H NMR integration determined the degree of acetylation to be 65%. Number average molecular weight (30,394 g/mol) was computed based on the addition of mass to the dendrimer from the acetyl groups as determined by NMR. PDI (1.060) of the purified acetylated dendrimer were determined by GPC. **1''' G5Ac$_{67\%}$:** ^{1}H NMR integration determined the degree of acetylation to be 67%. Number average molecular weight (30,473 g/mol) was computed based on the addition of mass to the dendrimer from the acetyl groups as determined by NMR. **1'''' G5Ac$_{58\%}$:** ^{1}H NMR integration determined the degree of acetylation to be 58%. Number average molecular weight (30,064 g/mol) was computed based on the addition of mass to the dendrimer from the acetyl groups as determined by NMR. **1''''' G5Ac$_{68.8\%}$:** ^{1}H NMR integration determined the degree of acetylation to be 68.8%. Number average molecular weight (30,572 g/mol) was computed based on the addition of mass to the dendrimer from the acetyl groups as determined by NMR. **1'''''' G5Ac$_{64\%}$:** ^{1}H NMR integration determined the degree of acetylation to be 64%. Number average molecular weight (30,347 g/mol) was computed based on the addition of mass to the dendrimer from the acetyl groups as determined by NMR.

2. Synthesis of Alkyne Linker (3-(4-(prop-2-ynyloxy)phenyl)propanoic acid)

2a. Synthesis of methyl 3-(4-(prop-2-ynyloxy)phenyl)propanoate has been previously reported.[30]

2b. Synthesis of (3-(4-(prop-2-ynyloxy)phenyl)propanoic acid) has also been previously reported.[30]

3. Synthesis of Azide Linker (3-(4-(2-azidoethoxy)phenyl)propanoic acid)

3a. To a solution of methyl 3-(4-hydroxyphenyl)propanoate (1.699 g, 9.43 mmole) in dry acetone (47.5 mL) was added anhydrous K_2CO_3 (3.909 g, 0.0283 mole) followed by 1-bromo-2-chloroethane (1.563 mL, 0.01886 mole). The resulting suspension was refluxed for 43 h with vigorous stirring. The reaction mixture was cooled to room temperature and the salt was removed by filtration followed by washing with portions of EtOAc (3 x 70 mL). The crude material was purified by silica chromatography (25:75 EtOAc:Hexane) and the solvent was removed under vacuum to give the desired product, methyl 3-(4-(2-chloroethoxy)phenyl)propanoate **3a**, as an oil (0.75 g, 33%). ^{1}H NMR (500 MHz, CDCl$_3$) δ 7.121 (d, J = 8.7, 2H), 6.843 (d, J = 8.7, 2H), 4.206 (t, J = 5.9, 2H), 3.798 (t, J = 5.9, 2H), 3.664 (s, 3H), 2.895 (t, J = 7.8, 2H), 2.598 (t, J = 7.8, 2H).

3b. To a solution of methyl 3-(4-(2-chloroethoxy)phenyl)propanoate **3a** (0.75 g 3.1 mmole) in anhydrous DMF (6.1 mL) was added 18-crown-6 (3.4 mg, 0.013 mmole) and sodium azide (0.44 g, 6.8 mmole). The resulting solution was heated at 78 °C for 11 h. The reaction mixture was cooled to room temperature, diluted with ethyl acetate (50 mL), washed with a saturated $NaHCO_3$ solution (4 x 70 mL), and then dried over $MgSO_4$. The solvent was removed under vacuum to give methyl 3-(4-(2-azidoethoxy)phenyl)propanoate **3b** as a yellow oil (0.58 g, 75%) ^{1}H NMR (500 MHz, CDCl$_3$) δ 7.125 (d, J = 8.6, 2H), 6.849 (d, J = 8.6, 2H), 4.129 (t, J = 5.0 2H), 3.666 (s, 3H), 3.581 (t, J = 5.0, 2H), 2.899 (t, J = 7.8, 2H), 2.600 (t, J = 7.8, 2H).

3c. To a solution of methyl 3-(4-(2-azidoethoxy)phenyl)propanoate **3b** (3.88 g, 0.0156 mole) in methanol (102 mL) was added potassium hydroxide (2 M, 28.3 mL, 0.0566 mole). The resulting solution was refluxed at 70 °C for 3 h. The solution was cooled to room temperature and condensed under reduced pressure. The residue was dissolved in water (30 mL) and was acidified by addition of 1N HCl to pH 1. The white cloudy solution was diluted with EtOAc. Layers were separated and the aqueous layer was extracted with EtOAc (2 x 70 mL). The combined organic extracts were washed with a saturated NaCl solution and dried over $MgSO_4$. Solvent was evaporated under vacuum

to give the (3-(4-(2-azidoethoxy)phenyl)propanoic acid) **3c** as a white solid (3.44 g, 93.9%). ^{1}H NMR (500 MHz, CDCl$_3$) δ 7.139 (d, J = 8.5, 2H), 6.859 (d, J = 8.5, 2H), 4.132 (t, J = 5.0 2H), 3.584 (t, J = 5.0, 2H), 2.909 (t, J = 7.7, 2H), 2.653 (t, J = 7.7, 2H).

4. Synthesis of Small Molecule Model System

The methyl-ester forms of the Alkyne Linker **2a** (448.0 mg, 1.80 mmole) and Azide Linker **3b** (371.5 mg, 1.70 mmole) were dissolved in a mixture of THF (1.6 mL) and water (0.4 mL). To this mixture was added copper sulfate pentahydrate (43.1 mg, 86.0μmole) and sodium ascorbate (170.9 mg, 431 μmole). The resulting reaction mixture was stirred at room temperature for 24 hrs. The solution was then diluted in EtOAc (60 mL) and water (60mL). Layers were separated and the aqueous layer was extracted twice with EtOAc solution (2 x 70 mL). The combined organic extracts were washed with a saturated NaHCO$_3$ solution (3 x 70 mL) and then with saturated NaCl solution (2 x 70 mL). The organic extracts were finally dried over MgSO$_4$. Solvent was evaporated under reduced pressure to give the desired product **4** as a white solid (0.54 g, 95%). ^{1}H NMR (500 MHz, CDCl$_3$) δ 7.799 (s, 1H), 7.108 (overlapping d, J = 8.4, 4H), 6.911 (d, J = 8.6, 2H), 6.778 (d, J = 8.6, 2H), 5.185 (s, 2H), 4.749 (t, J = 5.0, 2H), 4.329 (t, J = 5.0, 2H), 3.663 (s, 3H), 3.657 (s, 3H), 2.889 (t, J = 7.8, 2H), 2.885 (t, J = 7.7, 2H), 2.592 (t, J = 7.8, 2H), 2.586 (t, J = 7.7, 2H).

5. Synthesis of G5-Ac$_{72\%}$-Alkyne$_{1.4}$

A solution of partially acetylated dendrimer **1'** (54.6 mg, 1.78 μmole) was prepared with anhydrous DMSO (12.133 mL). The Alkyne Linker **2b** (0.9 mg, 4.4 μmole) was dissolved in DMSO (453 μL) and add to the dendrimer-DMSO solution. To this mixture was added N,N-Diisopropylethylamine (4.6 μL, 26 μmole) and the resulting solution was stirred for 45 minutes. Benzotriazol-1-yl-oxytripyrrolidinophosphonium hexafluorophosphate (2.3 mg, 4.4 μmole) was dissolved in DMSO (462 μL) and added in a dropwise manner to the dendrimer/Alkyne Linker solution. The resulting solution was stirred for 24 hrs. All reaction steps were carried out in glass flasks at room temperature under nitrogen.

The reaction mixture was purified using 10,000 MWCO centrifugal filtration devices. Purification consisted of two cycles using 1x PBS and eight cycles using DI water. All cycles were 10 minutes at 5,000 rpm. The resulting product **5** was lyophilized for three days to yield a white solid (41.5 mg, 75.4%). ^{1}H NMR integration determined an average of 1.4 Alkyne Linkers coupled to the dendrimer. The quantification of the number of linkers by NMR integration is described previously.[30] See Appendix A for ^{1}H NMR spetrum of **5**.

6. Synthesis of G5-Ac$_{72\%}$-Azide$_{1.3}$

A solution of partially acetylated dendrimer **1'** (60.5 mg, 1.97 μmole) was prepared with anhydrous DMSO (13.444 mL). The Azide Linker **3c** (1.2 mg, 4.9 μmole) was dissolved in DMSO (578 μL) and add to the dendrimer-DMSO solution. To this mixture was added N,N-Diisopropylethylamine (5.1 μL, 30 μmole) and the resulting solution was stirred for 45 minutes. Benzotriazol-1-yl-oxytripyrrolidinophosphonium hexafluorophosphate (2.6 mg, 4.9 μmole) was dissolved in DMSO (511 μL) and added in a dropwise manner to the dendrimer/Azide Linker solution. The resulting solution was stirred for 24 hrs. All reaction steps were carried out in glass flasks at room temperature under nitrogen.

The reaction mixture was purified using 10,000 MWCO centrifugal filtration devices. Purification consisted of two cycles using 1x PBS and eight cycles using DI water. All cycles were 10 minutes at 5,000 rpm. The resulting product **6** was lyophilized for three days to yield a white solid (50.3 mg, 91.3%). ^{1}H NMR integration determined an average of 1.3 Alkyne Linkers coupled to the dendrimer. See Appendix A for ^{1}H NMR spetrum of **6**.

7. Synthesis of Model Dendrimer System G5-Ac$_{72\%}$-L-G5Ac$_{72\%}$

Partially acetylated dendrimer with an average of 1.4 Alkyne Linkers **5** (15.30 mg, 0.493 μmole) and partially acetylated dendrimer with an average of 1.3 Azide Linkers **6** (15.4 mg, 0.496 μmole) was dissolved in deuterium oxide (0.820 mL) and placed in a glass microwave reactor vessel. Sodium ascorbate (6.9 mg, 35 μmole) and

copper sulfate pentahydrate (5.9 mg, 24 μmole) was added to the dendrimer solution. The resulting solution was placed in a microwave reactor for 40 seconds at 100 watts with a cut-off temperature of 100 °C. The microwave conditions were repeated for an additional 40 seconds. The cut-off temperature was then increased to 110 °C and the microwave was run at 100 watts for 2 minutes. The resulting crude product was a turbid yellow. The crude product was transferred to an NMR tube and analyzed by NOESY and ^{1}H NMR. After two days, the crude product in solution turned to a red-brown solution with a precipitate at the bottom of the NMR tube. NOESY and ^{1}H NMR experiments were repeated at this time point. The supernatant was separated from the precipitate and lyophilized to yield 4.9 mg of a brown solid. See Appendix A for ^{1}H NMR spetrum of **7.**

8. Synthesis of G5-Ac$_{65\%}$-Alkyne$_{1.6}$

The Alkyne Linker was conjugated to the partially acetylated dendrimer in two consecutive reactions. First, a stock solution of the Alkyne Linker **2b** (9.5 mg, 0.047 mmole) was generated with a mixture of DMF (6.198 mL) and DMSO (3.099 mL). To this mixture was added EDC (124.9 mg, 0.651 mmole). The resulting solution was stirred for 2 h at room temperature to create the active ester form of the Alkyne Linker.

A solution of partially acetylated dendrimer **1"** (58.8 mg, 1.930 μmole) was prepared with DI water (13.099 mL). The active ester form of the Alkyne Linker (5.784 mL, 0.0289 mmole) in DMF/DMSO was added in a dropwise manner (0.13 mL/min) to the dendrimer-water solution. The resulting reaction mixture was stirred for 2 days. All reaction steps were carried out in glass flasks at room temperature under nitrogen. The reaction mixture was purified using 10,000 MWCO centrifugal filtration devices. Purification consisted of five cycles using 1x PBS and five cycles using DI water. All cycles were 30 minutes at 5,000 rpm. The resulting product **8** was lyophilized for three days to yield a white solid (55.0 mg, 92.5%). ^{1}H NMR integration determined an average of 1.6 Alkyne Linkers coupled to the dendrimer. See Appendix A for ^{1}H NMR spetrum of **8.**

9. Synthesis of G5-Ac$_{65\%}$-Azide$_{2.5}$

The Azide Linker was conjugated to the partially acetylated dendrimer in two consecutive reactions. First, a stock solution of the Azide Linker **3c** (7.6 mg, 0.032 mmole) was generated with a mixture of DMF (4.958 mL) and DMSO (2.479 mL). To this mixture was added EDC (86.7 mg, 0.452 mmole). The resulting solution was stirred for 1.75 h at room temperature to create the active ester form of the Azide Linker.

A solution of partially acetylated dendrimer **1''** (58.8 mg, 1.930 μmole) was prepared with DI water (13.099 mL). The active ester form of the Azide Linker (6.663 mL, 0.0289 mmole) in DMF/DMSO was added in a dropwise manner (0.13 mL/min) to the first dendrimer-water aliquot. The resulting mixture was stirred for 2 days. All reaction steps were carried out in glass flasks at room temperature under nitrogen. The reaction mixture was purified using 10,000 MWCO centrifugal filtration devices. Purification consisted of five cycles using 1x PBS and five cycles using DI water. All cycles were 10 minutes at 5,000 rpm. The resulting product **9** was lyophilized for three days to yield a white solid (55.0 mg, 88.8%). ^{1}H NMR integration determined an average of 2.5 Azide linkers coupled to the dendrimer. See Appendix A for ^{1}H NMR spetrum of **9.**

10. Synthesis of G5-Ac$_{65\%}$-Alkyne$_{1.6}$-FA$_{1.7}$

Folic acid was conjugated to the Alkyne Linker-conjugated dendrimer **8** in two consecutive reactions. First, a solution of folic acid (1.9 mg, 4.26 μmole) was generated with a mixture of DMF (1.234 mL) and DMSO (0.617 mL). To this mixture was added EDC (11.4 mg, 59.7 μmole). The resulting solution was stirred for 1 h at room temperature to create the active ester form of folic acid.

A solution of partially acetylated dendrimer with an average number of 1.6 Alkyne Linkers **8** (20.8 mg, 0.752 μmole) was prepared with DI water (4.638 mL). The active ester form of folic acid (1.850 mL, 4.26 μmole) in DMF/DMSO was added in a dropwise manner to the dendrimer-water solution. The resulting reaction mixture was stirred for 3 days. All reaction steps were carried out in glass flasks at room temperature

under nitrogen. The reaction mixture was purified using 10,000 MWCO centrifugal filtration devices. Purification consisted of five cycles using 1x PBS and four cycles using DI water. All cycles were 10 minutes at 5,000 rpm. The resulting product **10** was lyophilized for three days to yield a white solid (15.6 mg, 73.2%). ^{1}H NMR integration determined an average of 1.7 folic acid molecules coupled to the dendrimer. See Appendix A for ^{1}H NMR spetrum of **10.**

11. Synthesis of G5-Ac$_{65\%}$-Azide$_{2.5}$-FITC$_{3.2}$

Partially acetylated dendrimer with an average number of 2.5 Azide Linkers **9** (21.5 mg, 0.694 µmole) was dissolved in DMSO (1.5 mL). Fluorescene isothiocyanate (1.4 mg, 3.5 µmole) was dissolved in DMSO (0.54 mL) and added in a dropwise fashion to the dendrimer solution. The resulting mixture was stirred for 24 hours at room temperature. The reaction mixture was purified using 10,000 MWCO centrifugal filtration devices. Purification consisted of six cycles using 1x PBS and six cycles using DI water. All 1x PBS cycles were 15 minutes at 5,000 rpm and all DI water cycles were 15 minutes at 5,000 rpm. HPLC analysis of the lyophilized product detected un-conjugated FITC remaining in the sample. To remove the remaining un-reacted FITC, the conjugate was purified by size exclusion chromatography using Sephadex G-25 beads in 1x PBS. The dendrimer fraction was collected and the elution buffer was exchanged with DI water using 10,000 MWCO centrifugal filtration devices (four cycles of 10 minutes at 5,000 rpm). The purified product **11** was lyophilized to yield a yellow-orange solid (10.1 mg, 45.6%). ^{1}H NMR integration determined an average of 3.2 FITC coupled to the dendrimer. See Appendix A for ^{1}H NMR spetrum of **11.**

12. Synthesis of G5-Ac$_{65\%}$-Alkyne$_{1.6}$-FA$_{3.5}$

Additional folic acid was conjugated to the partially acetylated dendrimer with an average of 1.6 Alkyne Linkers and 1.7 folic acid molecules **10** in two consecutive reactions. First, a solution of folic acid (1.1 mg, 2.4 µmole) was generated with a mixture of DMF (0.687 mL) and DMSO (0.344 mL). To this mixture was added EDC (6.3 mg, 33 µmole). The resulting solution was stirred for 1 h at room temperature to create the active ester form of the folic acid.

35

A solution of partially acetylated dendrimer with an average number of 1.6 Alkyne Linkers and 1.7 folic acid molecules **10** (8.5 mg, 0.298 μmole) was prepared with DI water (1.895 mL). The active ester form of folic acid (1.031 mL, 2.4 μmole) in DMF/DMSO was added in a dropwise manner to the dendrimer-water solution. The resulting reaction mixture was stirred for 3 days. All reaction steps were carried out in glass flasks at room temperature under nitrogen. The reaction mixture was purified by size exclusion chromatography using Sephadex G-25 in 1x PBS. The dendrimer fraction was collected and the elution buffer was exchanged with DI water using 10,000 MWCO centrifugal filtration devices (four cycles of 10 minutes at 5,000 rpm). The purified product **12** was lyophilized for three days to yield a yellow solid (7.0 mg, 80.5%). ^{1}H NMR integration determined an average of 3.5 folic acid molecules coupled to the dendrimer. See Appendix A for ^{1}H NMR spetrum of **12.**

13. Synthesis of G5-Ac$_{107}$-Alkyne$_{1.6}$-FA$_{3.5}$

Partially acetylated dendrimer with an average number of 1.6 Alkyne Linkers and 3.5 folic acid **12** (7.0 mg, 0.22 μmole) was dissolved in anhydrous methanol (1.124 mL). Triethylamine (1.7 μL, 0.012 mmole) was added to this mixture and stirred for 30 minutes. Acetic anhydride (0.9 μL, 9.6 μmole) was added in a dropwise manner to the dendrimer solution. The reaction was carried out in a glass flask, under nitrogen, at room temperature for 24 hours. Methanol was evaporated from the resulting solution and the product was purified by size exclusion chromatography using Sephadex LH-20 in methanol. The purified dendrimer **13** was lyophilized for three days to yield a white solid (6.6 mg, 90.3%). ^{1}H NMR integration determined the degree of acetylation to be 100%. See Appendix A for ^{1}H NMR spetrum of **13.**

14. Synthesis of G5-Ac$_{106}$-Azide$_{2.5}$-FITC$_{3.2}$

Partially acetylated dendrimer with an average number of 2.5 Azide Linkers and 3.2 FITC **11** (7.5 mg, 0.23 μmole) was dissolved in anhydrous methanol (1.206 mL). Triethylamine (1.8 μL, 0.013 mmole) was added to this mixture and stirred for 30 minutes. Acetic anhydride (1.0 μL, 10.0 μmole) was added in a dropwise manner to the dendrimer solution. The reaction was carried out in a glass flask, under nitrogen, at room

temperature for 24 hours. Methanol was evaporated from the resulting solution and the product was purified by size exclusion chromatography using Sephadex LH-20 in methanol. The purified dendrimer **14** was lyophilized for three days to yield a white solid (7.1 mg, 90.6%). ^{1}H NMR integration determined the degree of acetylation to be 100%. See Appendix A for ^{1}H NMR spetrum of **14.**

15. Synthesis of Folic Acid Targeted Dendrimer System $FA_{3.5}$-$G5$-Ac_{107}-L-$G5$-Ac_{106}-$FITC_{3.2}$

Dendrimer with an average of 1.6 Alkyne Linkers and 3.5 folic acid molecules **13** (3.1 mg, 91 nmole) and dendrimer with an average of 2.5 Azide Linkers and 3.2 FITC molecules **14** (3.0 mg, 88 nmole) were dissolved in deuterium oxide (0.650 mL) and placed in a glass microwave reactor vessel. Sodium ascorbate (1.1 mg, 4.5 μmole) and copper sulfate pentahydrate (1.1 mg, 5.4 μmole) was added to the dendrimer solution. The resulting solution was placed in a microwave reactor for 6.5 minutes at 100 watts with a cut-off temperature of 100 °C. The reaction mixture was transferred to an NMR tube and analyzed by NOESY and ^{1}H NMR spectroscopy using. Lyophilization yielded 6.7 mg of a red solid. See Appendix A for ^{1}H NMR spetrum of **15.**

16. Synthesis of $G5$-$Ac_{67\%}$-$Alkyne_{1.3}$

A solution of partially acetylated dendrimer **1'''** (176.7 mg, 5.8 μmole) was prepared with anhydrous DMSO (39.27 mL). The Alkyne Linker **2b** (2.6 mg, 13 μmole) was dissolved in DMSO (1.306 mL) and add to the dendrimer-DMSO solution. To this mixture was added N,N-Diisopropylethylamine (13.4 μL, 76.7 μmole) and the resulting solution was stirred for 45 minutes. Benzotriazol-1-yl-oxytripyrrolidinophosphonium hexafluorophosphate (6.7 mg, 13 μmole) was dissolved in DMSO (1.331 mL) and added in a dropwise manner to the dendrimer/Alkyne Linker solution. The resulting solution was stirred for 24 hrs. All reaction steps were carried out in glass flasks at room temperature under nitrogen.

The reaction mixture was purified using 10,000 MWCO centrifugal filtration devices. Purification consisted of two cycles using 1x PBS and eight cycles using DI

water. All cycles were 10 minutes at 5,000 rpm. The resulting product **5** was lyophilized for three days to yield a white solid (116.2 mg, 65.2%). ^{1}H NMR integration determined an average of 1.3 Alkyne Linkers coupled to the dendrimer. See Appendix A for ^{1}H NMR spetrum of **16.**

17. Synthesis of G5-Ac$_{110.7}$-Alkyne$_{1.3}$

Partially acetylated dendrimer with an average number of 1.3 Alkyne Linkers **16** (22.6 mg, 0.737 μmole) was dissolved in anhydrous methanol (3.0 mL). Triethylamine (5.8 μL, 0.042 mmole) was added to this mixture and stirred for 30 minutes. Acetic anhydride (3.2 μL, 34 μmole) was added in a dropwise manner to the dendrimer solution. The reaction was carried out in a glass flask, under nitrogen, at room temperature for 24 hours. Methanol was evaporated from the resulting solution and the product was purified by size exclusion chromatography using Sephadex LH-20 in methanol. The purified dendrimer **17** was lyophilized for three days to yield a white solid (19.1 mg, 80.5%). ^{1}H NMR integration determined the degree of acetylation to be 100%. See Appendix A for ^{1}H NMR spetrum of **17.**

18. Synthesis of Un-targeted Dendrimer System G5-Ac$_{110.7}$-L-G5-Ac$_{106}$-FITC$_{3.2}$

Dendrimer with an average of 1.3 Alkyne Linkers **17** (1.0 mg, 31 nmole) and dendrimer with an average of 2.5 Azide Linkers and 3.2 FITC molecules **14** (1.0 mg, 29 nmole) were dissolved in deuterium oxide (0.741 mL) and placed in a glass microwave reactor vessel. Sodium ascorbate (0.36 mg, 1.8 μmole) and copper sulfate pentahydrate (0.38 mg, 1.5 μmole) was added to the dendrimer solution. The resulting solution was placed in a microwave reactor for 6.5 minutes at 100 watts with a cut-off temperature of 100 °C. The reaction mixture was transferred to an NMR tube and analyzed by NOESY and ^{1}H NMR spectroscopy using. Lyophilization yielded 2.4 mg of a red solid. See Appendix A for ^{1}H NMR spetrum of **18.**

19. Synthesis of G5-Ac$_{58\%}$-Alkyne$_{1.2}$

The Alkyne Ligand **2b** (2.3 mg, 11 μmole) in anhydrous DMSO (1.141 mL), was added to a solution of partially acetylated dendrimer **1''''** (152.0 mg, 5.06 μmole) in

anhydrous DMSO (33.7 mL). N,N-diisopropylethylamine (8.6 mg, 11.7 μL, 67 μmole) was added to the reaction mixture and the resulting solution was stirred for 30 minutes. A solution of PyBOP (5.8 mg, 11 μmole) in anhydrous DMSO (1.163 mL) was added in a dropwise manner (0.1 mL/min) to the dendrimer solution. The resulting reaction mixture was stirred for 24 hrs under nitrogen and then purified as described earlier. The purified product, **19**, was lyophilized for three days to yield a white solid (86mg, 56%). ^{1}H NMR integration determined the mean number of Alkyne Ligands per dendrimer to be 1.2.

20. Synthesis of G5-Ac$_{68\%}$-Azide$_{1.1}$

The Azide Ligand **3c** (1.6 mg, 6.6 μmole) in anhydrous DMSO (0.780 mL), was added to a solution of partially acetylated dendrimer **1''''** (91.8 mg, 3.0 μmole) in anhydrous DMSO (20.4 mL). N,N-diisopropylethylamine (5.1 mg, 6.9 μL, 6.6 μmole) was added to the reaction mixture and the resulting solution was stirred for 30 minutes. A solution of PyBOP (3.5 mg, 6.6 μmole) in anhydrous DMSO (0.690 mL) was added in a dropwise manner (0.1 mL/min) to the dendrimer solution. The resulting reaction mixture was stirred for 24 hrs under nitrogen and then purified as described earlier. The purified product, **20**, was lyophilized for three days to yield a white solid (71 mg, 77%). ^{1}H NMR integration determined the mean number of Azide Ligands per dendrimer to be 1.1.

21. Synthesis of G5-Ac$_{58\%}$-Alkyne$_{1.2}$-FA$_{3.7}$

Folic acid was conjugated to the Alkyne Linker-conjugated dendrimer **19** in two consecutive reactions. First, a solution of folic acid (10.8 mg, 24.4 μmole) was generated with a mixture of DMF (7.9 mL) and DMSO (2.6 mL). To this mixture was added EDC (64.6 mg, 0.337 μmole). The resulting solution was stirred for 1 h at room temperature to create the active ester form of folic acid.

A solution of partially acetylated dendrimer with an average number of 1.2 Alkyne Linkers 19 (74.1 mg, 2.44 μmole) was prepared with DI water (16.5 mL). The active ester form of folic acid in DMF/DMSO was added in a dropwise manner to the

dendrimer-water solution. The resulting reaction mixture was stirred for 3 days. All reaction steps were carried out in glass flasks at room temperature under nitrogen. The reaction mixture was purified using 10,000 MWCO centrifugal filtration devices. Purification consisted of one cycle using 1x PBS and four cycles using DI water (Amicon Ultra). All cycles were 10 minutes at 5,000 rpm. The resulting product **21** was lyophilized for three days to yield a white solid (59.9 mg, 76%). ^{1}H NMR integration determined an average of 3.7 folic acid molecules coupled to the dendrimer.

22. Synthesis of G5-Ac$_{65\%}$-Azide$_{1.1}$-6TAMRA$_{6.8}$

Partially acetylated dendrimer with an average number of 1.1 Azide Linkers **20** (54.9 mg, 1.78 μmole) was dissolved in DMSO (4.5 mL). 6TAMRA (7.5 mg, 14 μmole) was dissolved in DMSO (0.915 mL) and added in a dropwise fashion to the dendrimer solution. The resulting mixture was stirred for 24 hours at room temperature. The reaction mixture was purified by size-exclusion chromatography using Sephadex G-25 beads equilibrated with 1x PBS. After separation by size-exclusion, the dendrimer fraction was collected and the elution buffer was exchanged with DI water using 10,000 MWCO centrifugal filtration devices (four cycles of 10 minutes at 5,000 rpm). The purified product **22** was lyophilized to yield a purple-pink solid (42.4 mg, 68%). ^{1}H NMR integration determined an average of 6.8 6TAMRA coupled to the dendrimer.

23. Synthesis of G5-Ac$_{107}$-Alkyne$_{1.2}$-FA$_{3.7}$

Partially acetylated dendrimer with an average number of 1.2 Alkyne Linkers and 3.7 folic acid **21** (57.0 mg, 1.8 μmole) was dissolved in anhydrous methanol (7.2 mL). Triethylamine (17 μL, 0.12 mmole) was added to this mixture and stirred for 30 minutes. Acetic anhydride (9.3 μL, 98 μmole) was added in a dropwise manner to the dendrimer solution. The reaction was carried out in a glass flask, under nitrogen, at room temperature for 24 hours. Methanol was evaporated from the resulting solution and the reaction mixture was purified using 10,000 MWCO centrifugal filtration devices. Purification consisted of one cycle using 1x PBS and four cycles using DI water (Amicon Ultra). All cycles were 10 minutes at 5,000 rpm. Due to the presence of particulate, the product was filtered with at 0.45 μm filter. The purified dendrimer **23** was lyophilized

for three days to yield a white solid (39.2 mg, 62%). ^{1}H NMR integration determined the degree of acetylation to be 100%.

24. Synthesis of G5-Ac$_{104}$-Azide$_{1.1}$-6TAMRA$_{6.8}$

Partially acetylated dendrimer with an average number of 1.1 Azide Linkers and 6.8 6TAMRA **22** (36.2 mg, 1.1 μmole) was dissolved in anhydrous methanol (4.5 mL). Triethylamine (7.3 μL, 0.053 mmole) was added to this mixture and stirred for 30 minutes. Acetic anhydride (4.0 μL, 42 μmole) was added in a dropwise manner to the dendrimer solution. The reaction was carried out in a glass flask, under nitrogen, at room temperature for 24 hours. Methanol was evaporated from the resulting solution and the reaction mixture was purified using 10,000 MWCO centrifugal filtration devices. Purification consisted of one cycle using 1x PBS and five cycles using DI water (Amicon Ultra). All cycles were 10 minutes at 5,000 rpm. The purified dendrimer **24** was lyophilized for three days to yield a white solid (26.3 mg, 90%). ^{1}H NMR integration determined the degree of acetylation to be 100%.

25. Synthesis of Folic Acid Targeted Dendrimer System with 6TAMRA FA$_{3.7}$-G5-Ac$_{107}$-L-G5-Ac$_{104}$-6TAMRA$_{6.8}$

Dendrimer with an average of 1.2 Alkyne Linkers and 3.7 folic acid molecules **23** (10.0 mg, 0.29 mmole) and dendrimer with an average of 1.1Azide Linkers and 6.8 6TAMRA molecules **24** (10.1 mg, 0.29 mmole) were dissolved in deuterium oxide (0.842 mL) and placed in a glass microwave reactor vessel. Sodium ascorbate (3.5 mg, 18 μmole) and copper sulfate pentahydrate (3.7 mg, 15 μmole) was added to the dendrimer solution. The resulting solution was placed in a microwave reactor for five 30s intervals at 100 watts with a cut-off temperature of 100 °C. The reaction mixture was transferred to an NMR tube and analyzed by NOESY and ^{1}H NMR spectroscopy using. Lyophilization yielded 24.6 mg of a red solid.

26. Synthesis of Un-targeted Dendrimer System G5-Ac$_{110.7}$-L-G5-Ac$_{104}$-6TAMRA$_{6.8}$

Dendrimer with an average of 1.3 Alkyne Linkers **17** (6.6 mg, 0.20 μmole) and dendrimer with an average of 1.1 Azide Linkers and 6.8 6TAMRA molecules **24** (7.2 mg,

0.20 μmole) were dissolved in deuterium oxide (0.744 mL) and placed in a glass microwave reactor vessel. Sodium ascorbate (2.4 mg, 12 μmole) and copper sulfate pentahydrate (2.5 mg, 10 μmole) was added to the dendrimer solution. The resulting solution was placed in a microwave reactor for five 30s intervals minutes at 100 watts with a cut-off temperature of 100 °C. The reaction mixture was transferred to an NMR tube and analyzed by NOESY and ^{1}H NMR spectroscopy using. Lyophilization yielded 12.2 mg of a red solid.

27. Synthesis of G5-Ac$_{64\%}$-6TAMRA$_{7.1}$

Partially acetylated dendrimer **1'''''''** (75.3 mg, 2.48 μmole) was dissolved in DMSO (6.3 mL). 6TAMRA (10.2 mg, 19.3 μmole) was dissolved in DMSO (1.3 mL) and added in a dropwise fashion to the dendrimer solution. The resulting mixture was stirred for 24 hours at room temperature. The reaction mixture was purified by size-exclusion chromatography using Sephadex G-25 beads equilibrated with DI water. The purified product **27** was lyophilized to yield a purple-pink solid (71.9 mg, 85%). ^{1}H NMR integration determined an average of 7.1 6TAMRA coupled to the dendrimer.

28. Synthesis of G5-Ac$_{64\%}$-6TAMRA$_{7.1}$-FA$_{4.0}$

Folic acid was conjugated to the 6TAMRA-conjugated dendrimer **27** in two consecutive reactions. First, a solution of folic acid (8.7 mg, 19 μmole) was generated with a mixture of DMF (6.4 mL) and DMSO (2.1 mL). To this mixture was added EDC (53.7 mg, 0.280 μmole). The resulting solution was stirred for 1 h at room temperature to create the active ester form of folic acid.

A solution of partially acetylated dendrimer with an average number of 7.1 6TAMRA **27** (65.7 mg, 1.97 μmole) was prepared with DI water (14.6 mL). The active ester form of folic acid in DMF/DMSO was added in a dropwise manner to the dendrimer-water solution using a syringe pump. The resulting reaction mixture was stirred for 3 days. All reaction steps were carried out in glass flasks at room temperature under nitrogen. The reaction mixture was purified by size-exclusion chromatography using Sephadex G-25 beads equilibrated with 1x PBS. Buffer was then exchanges for the

isolated product with DI water using 10,000 MWCO centrifugal filtration devices (Amicon Ultra). Purification consisted of four cycles using DI water. All cycles were 10 minutes at 5,000 rpm. The resulting product **28** was lyophilized for three days to yield a white solid (59.0 mg, 85%). ^{1}H NMR integration determined an average of 4.0 folic acid molecules coupled to the dendrimer.

29. Synthesis of G5-Ac$_{101}$-6TAMRA$_{7.1}$-FA$_{4.0}$

Partially acetylated dendrimer with an average number of 7.1 6TAMRA and 4.0 FA **28** (46.3 mg, 1.29 μmole) was dissolved in anhydrous methanol (5.3 mL). Triethylamine (7.9 μL, 57 μmole) was added to this mixture and stirred for 30 minutes. Acetic anhydride (4.3 μL, 45 μmole) was added in a dropwise manner to the dendrimer solution.   The reaction was carried out in a glass flask, under nitrogen, at room temperature for 24 hours. Methanol was evaporated from the resulting solution and the reaction mixture was purified by size-exclusion chromatography using Sephadex G-25 beads equilibrated with 1x PBS. Buffer was then exchanges for the isolated product with DI water using 10,000 MWCO centrifugal filtration devices (Amicon Ultra). Purification consisted of two cycles using DI water. All cycles were 10 minutes at 5,000 rpm.The purified dendrimer **29** was lyophilized for three days to yield a white solid (35.6 mg, 74%). ^{1}H NMR integration determined the degree of acetylation to be 100%.

Results and Discussion

Synthesis and Characterization of the Small-molecule Model System

A small molecule model system (**4**) was first synthesized to facilitate the spectroscopic assignment of triazole-related atoms resulting from successful 'click' reactions between dendrimer modules with an azide linker (**3c**) and dendrimer modules possessing an alkyne linker (**2b**). This model system utilized the methyl ester forms of the two linkers (**2a** and **3b**). Proton assignments were based upon ^{1}H NMR and NOESY experiments in CDCl$_3$. **Figure 2.1**, panel a, displays the cross-peaks for the triazole related protons in the clicked product (**4**) and **Table 2.1** contains the chemical shifts for these in both the pre- and post-'click' reaction states. Protons c, e, and f experience the

greatest change in chemical shift as a result of the 'click' reaction. Also of interest is the region between 6.4 and 8.5 ppm (**Figure 2.2**, panel a and b), which shows the up-field shift for peak g from 6.85 ppm to 6.78 ppm.

Synthesis and Characterization of the Model Dendrimer System

Dendrimers without target or dye functionalities, possessing only the 'click' reaction functional groups (**5** and **6**), were employed to develop 'click' reaction conditions (**Figure 2.3**). Because many of the proton peaks associated with the dendrimer-conjugated alkyne and azide linkers (particularly those closest to the 'click' reaction sites) overlap in the ^{1}H NMR spectra with other protons belonging to the PAMAM dendrimer, NOESY experiments were used to document proton chemical shifts via the resolution of cross peaks in the 2-D spectra (**Figure 2.1**, panel b). The chemical shifts for the triazole related protons in the dendrimer system both pre- and post-'click' reaction can be found in **Table 2.1**. The region between 6.4 and 8.5 ppm in the proton spectra for the pre- and post-'click'ed dendrimer samples can be found in **Figure 2.2**, panel c and d. In the spectra for the pre-'click' reaction mixture (panel c), both sets of aromatic protons overlap at 6.90 ppm (b and g) and 7.13 ppm (a and h). In the sample post-'click' reaction (panel d), the aromatic protons no longer overlap. Protons a and h partially overlap at 7.09 ppm and 7.06 ppm, and protons b and g are found at 6.90 ppm and 6.74 ppm, respectively.

A comparison of the chemical shifts in **Table 2.1** for the small molecule system and the dendrimer system reveals good correlations for both the pre- and post-reaction states. This indicates that a successful 'click' reaction has occurred between the azide and alkyne conjugated dendrimers. It is important to note that whereas chemical shifts for the small molecule model system are determined in $CDCl_3$, the chemical shifts for the dendrimer sample were detected in D_2O. Although the different solvents could influence the proton chemical shifts, this does not appear to be an issue for these particular molecules.

A peak for the single proton in the triazole ring is absent from both the NOESY and 1D experiments. In the small molecule system this peak is found at 7.80 ppm (**Figure 2.2**, panel b). Working with a similar system using PAMAM dendrons that contained the alkyne and azide moieties at the dendron focal point, Lee et. al. found that the triazole proton peak gradually shifted down-field from 7.77 ppm to 7.93 ppm as the generation of the clicked dendrons increased from 1 to 3.[47] If this downfield change in chemical shift also holds for the generation 5 dendrimer case, the triazole proton would be overlapped by several peaks between 7.80 ppm and 8.20 ppm associated with the dendrimer (**Figure 2.2**, panel d). The NOESY spectra did not expose any cross peaks in this region with other protons in the linkers that are in close proximity to the triazole ring. The cross-peaks associated with the triazole proton appear to be below the intensity required for NMR detection.

Synthesis and Characterization of the Folic Acid Targeted Dendrimer System

Synthesis of the folic acid targeted modular dendrimer platform is outlined in **Figure 2.4**. Dendrimers with an average of 1.6 alkyne linkers (**8**) were functionalized with the targeting molecule folic acid. The formation of an amide linkage between one of the remaining primary amines on the dendrimer and one of the carboxylic acid groups in folic acid was achieved by EDC coupling chemistry as previously reported [22]. This reaction conjugated an average of 1.7 folic acid molecules per dendrimer as determined by NMR (**10**). Because this average was below the optimal range for multi-valent binding,[3] the reaction was repeated using the dendrimer with an average of 1.6 alkyne linkers and 1.7 folic acid (**10**). The second reaction resulted in the addition of 1.8 folic acid molecules per dendrimer bringing the final average to 3.5 folic acid molecules per dendrimer (**12**). The remaining dendrimer primary amines were then fully acetylated to avoid positive charge-based cellular interactions (**13**).[6,9-10] Dendrimers with 2.5 azide linkers (**9**) were functionalized with the dye molecule FITC. Using conditions similar to previously published work,[25] an average of 3.2 FITC molecules were coupled to the dendrimer via the formation of a thiourea bond between the primary amine on the dendrimer and the isothiocyanate group in FITC (**11**). This dendrimer conjugate also was

fully acetylated (**14**). Reverse phase HPLC confirmed that any un-reacted FITC or folic acid molecules had been removed by purification of dendrimer **13** and **14**.

The two dendrimer modules (**13** and **14**) were coupled together using the Cu-catalysed 1,3-dipolar cycloaddition reaction under conditions similar to those used with the model dendrimer system. NOESY experiments provided direct spectroscopic proof that the functionalized dendrimers had been clicked together. Specifically, the AA'BB' pattern was observed to shift in a fashion identical to that observed for the two model systems previously described (**Table 2.1** and **Figure 2.2**).

In vitro **Testing of the Folic Acid Targeted Dendrimer System with KB cells**

Cellular uptake of the folic acid targeted dendrimer system (**15**) at four different concentrations (30 nM, 100 nM, 300 nM, and 1000 nM of **15**) was measured in KB cells that express a high cellular membrane concentration of folic acid receptor (FAR). Fluorescence uptake was quantified by Flow Cytometry. As seen in **Figure 2.5a** and **Figure 2.5f-blue**, a dose dependent uptake was observed with saturation occurring at 100 nM. This binding affinity is consistent with previous studies on single dendrimer platforms possessing multiple FITC and multiple FA molecules.[23]

A series of control experiments were performed in order to ensure that uptake of the folic acid targeted dendrimer system (**15**) was occurring via receptor-mediated endocytosis and not non-specific membrane interactions. The first set of controls measured uptake of single dendrimers possessing the azide linker and multiple FITC (**14**) at 30 nM, 100 nM, 300 nM, and 1000 nM (**Figure 2.5b** and **Figure 2.5f-purple**). No uptake was observed for this sample above the background level. The second control sample contained a non-conjugated (un-clicked) mixture of the two dendrimers functionalized with either FITC or folic acid (**13** and **14**). Uptake of this mixture was quantified at 30 nM, 100 nM, and 300 nM (**Figure 2.5c** and **Figure 2.5f-teal**). At all three concentrations, no florescence uptake was observed. This control eliminates the possibility that the dendrimer modules could form a non-covalently linked complex that would be internalized. A third control sample (**18**) was composed of an un-targeted

dendrimer module (**17**) coupled to the FITC conjugated imaging module (**14**). The un-targeted dual module platform (**18**) was assembled under the same conditions used to form the folic acid targeted platform (**15**). Mean fluorescence uptake of the un-targeted platform can be found in the Appendix A. At concentrations up to 300 nM, no uptake was observed beyond the background level. This un-targeted dendrimer platform is an essential control because it matches the molecular weight and size of the folic acid targeted dendrimer system (**15**). This control will become even more important as evaluation of this system moves to an *in vivo* model.

The final set of controls investigated active blocking of the folic acid receptor by either free folic acid (**Figure 2.5d** and **Figure 2.5f-green**) or a folic acid-dendrimer conjugate without a fluorescent dye (**13**) (**Figure 2.5e** and **Figure 2.5f-orange**) to prevent the specific up-take of the folic acid targeted dendrimer system. A 20 fold excess of blocking agent was employed relative to the targeted platform. For the blocking experiment using the single dendrimer-folic acid conjugate (**13**), molar equivalence was based on the folic acid content of the sample rather than the dendrimer content. Both blocking agents were evaluated at 30 nM, 100 nM, 300 nM, and 1000 nM. Complete blocking is achieved using free folic acid concentrations up to 100 nM. While the dendrimer-folic acid conjugate is not as effective at blocking as the free folic acid, approximately 75% blocking is achieved. These binding data indicate that the cellular association of the folic acid targeted dendrimer system occurs through the folic acid receptor rather than via non-specific interactions. On a more fundamental level, the biological results prove again that the folic acid conjugate dendrimer module is covalently linked by 'click' chemistry to dendrimer module functionalized with FITC.

In vivo Testing

A second dual dendrimer platform was tested in vivo using immunodeficient mice bearing human epithelial tumors that have high concentrations of the folic acid receptor. The dendrimer platform for this study (**25**) was composed of a targeting module with folic acid and an imaging module with the dye 6TAMRA. 3 control platforms, one positive control and two negative controls, and a PBS control were utilized to assess the

active tumor targeting capabilities of the dual dendrimer platform. The positive control was a single dendrimer platform (**29**) conjugated with folic acid and 6TAMRA. The negative controls were an untargeted dual dendrimer platform with a 6TAMRA module (**26**), and an uncoupled mixture of the folic acid module (**23**) and the 6TAMRA module (**24**). For each group, three animals with tumors on both flanks were used. Analysis of the tumors was performed with confocal microscopy, flow cytometry, and 2-photon microscopy. All three of these techniques found that the targeted dual dendrimer platform (**25**) did not demonstrate active tumor targeting. While the presence of both the targeted platform and the positive control were detected in the tumors, the negative control dendrimer platforms were detected at similar levels in the tumor. Consequently, the dual dendrimer platform was not found to actively target the tumor.

Design Analysis

One of the limitations of the modular platform design in its current iteration is that each module is composed of a heterogeneous distribution of dendrimer-ligand components.[30,48] To a first approximation, these distributions are consistent with Poissonian statistics. Not only are the modules composed of a distribution of dendrimer particles with different numbers of the biologically active ligand (folic acid, FITC, 6TAMRA), the modules are also composed of a distribution of dendrimer with different numbers of the coupling ligands (Azide and Alkyne). The implication of these distributions is that the final 'dual' module platform is most likely composed of a large number of different platforms with different numbers of modules linked together and different numbers of ligands per module. Future designs should incorporate characterization and control of these distributions in order to make a more controlled, reproducible material.

<div align="center">

Conclusion

</div>

A delivery platform covalently linking two different PAMAM dendrimer modules through 'click' chemistry was successfully designed and synthesized. Two model systems were also generated to assist in the NMR spectroscopy characterization of the

modular platform. The folic acid targeted system was evaluated for functional activity *in vitro* with KB cells and found to selectively target the cancer cell line through the high-affinity folate receptor. The same selective targeting was not observed *in vivo* in an animal model for human epithelial cancer.

Acknowledgements
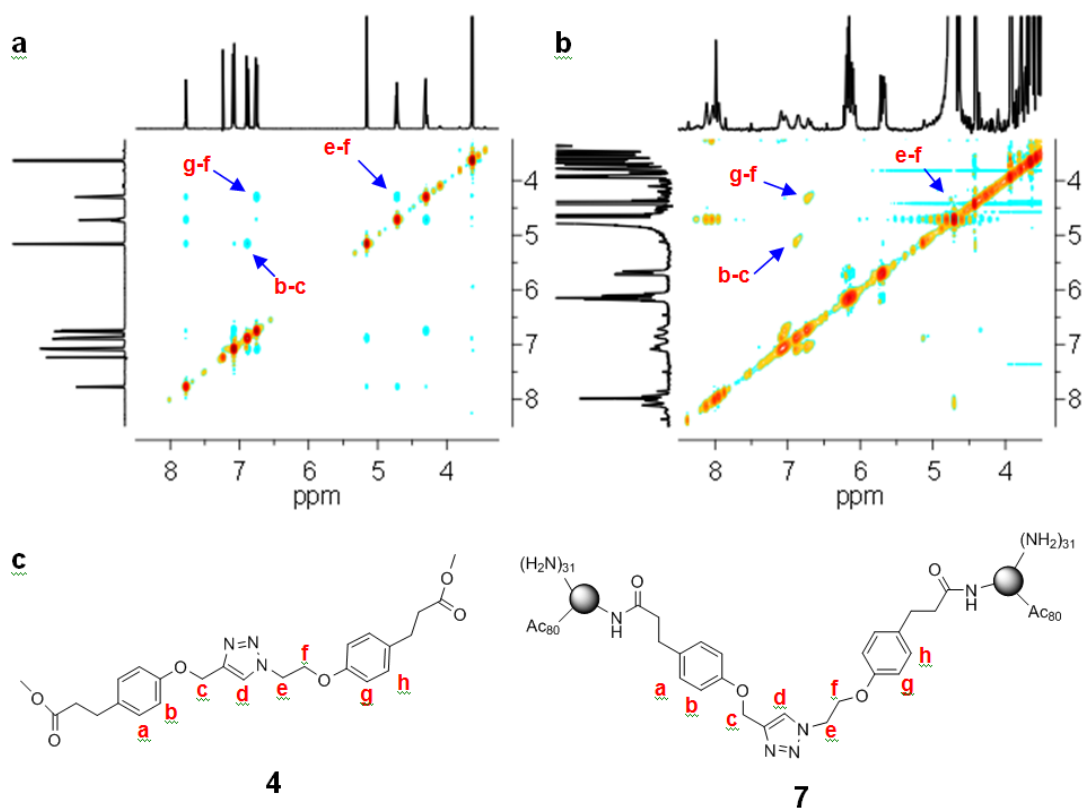
Figure 2.1: a) NOESY of the small-molecule model system after the 'click' reaction (**4**). NOE cross-peaks between triazole related protons (b, c, e, f, and g) are labeled. **b)** NOESY of the model dendrimer system after the 'click' reaction (**7**). NOE cross-peaks for the triazole related protons are similarly labeled. The cross-peaks in the 2D spectra reveal proton chemical shifts for the several of the triazole related protons that are otherwise obscured by overlapping dendrimer peaks. **c)** Chemical structure and proton labels for the clicked small molecule model system (**4**) and the clicked dendrimer model system (**7**). The G5 PAMAM dendrimer is represented by a gray sphere.

Table 2.1: Good correlation is found between the small molecule model system (**2a**, **3b**, and **4**) and the dendrimer model system (**5**, **6**, and **7**) for the chemical shifts (ppm) of triazole related protons (a-h) both before and after the 'click' reaction. Chemical shifts for protons in the model dendrimer system were detected primarily via NOESY experiments.

	Compound			
	Before Reaction		After Reaction	
Proton	2a and 3b	5 and 6	4	7
a	7.14	7.13	7.11	7.09
b	6.91	6.90	6.91	6.90
c	4.67	4.69	5.19	5.15
d	n.a.	n.a.	7.80	--
e	3.58	3.61	4.75	4.76
f	4.13	4.13	4.33	4.35
g	6.85	6.90	6.78	6.74
h	7.13	7.13	7.11	7.06
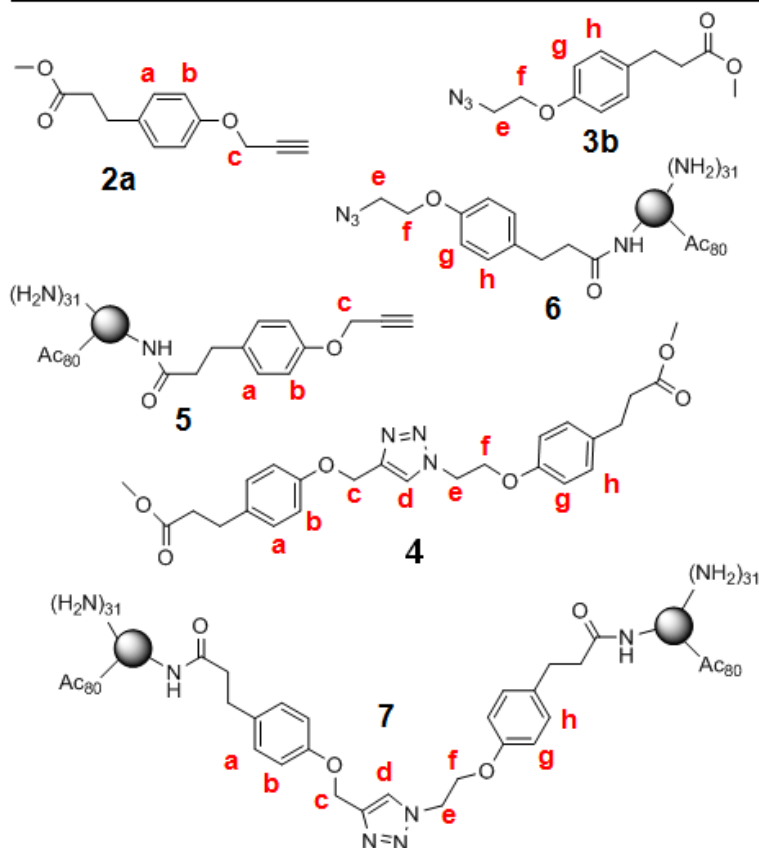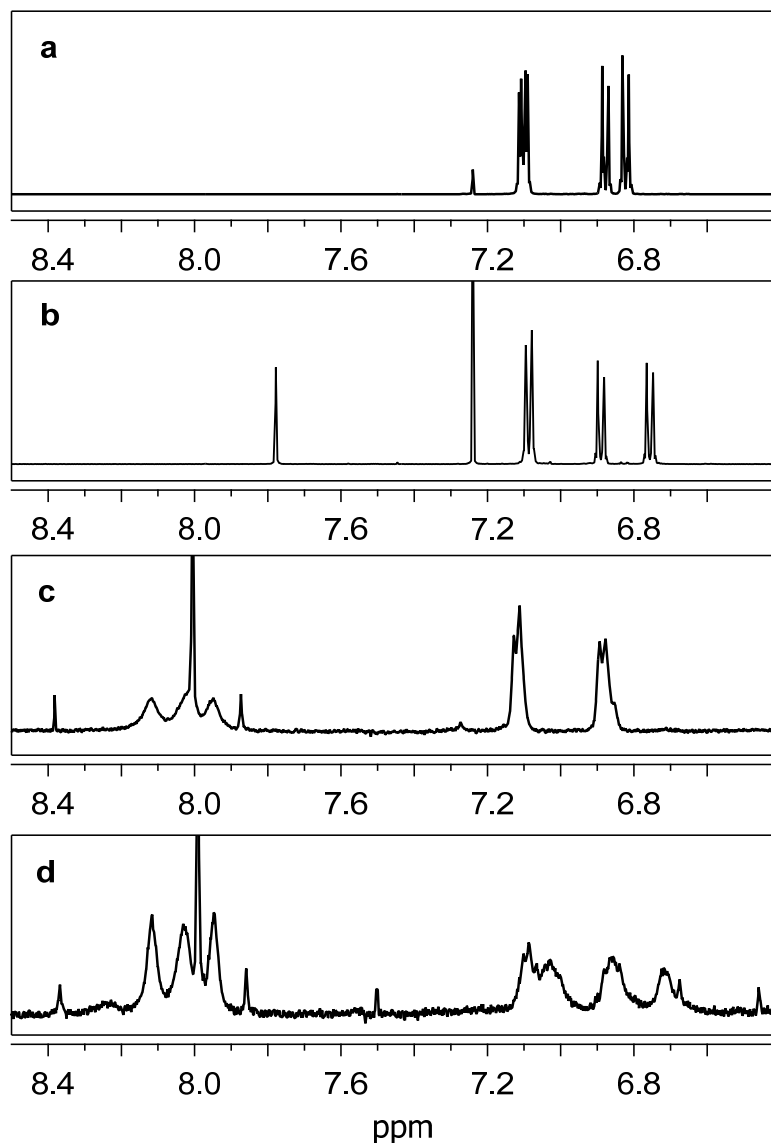
Figure 2.2: Proton NMR spectra of the small-molecule model system and model dendrimer system both pre- and post-'click' reaction. An up-field shift is observed for aromatic proton g as a result of the 'click' reaction. **a)** Spectrum of the small molecule model system before the 'click' reaction (2a and 3b), taken in CDCl$_3$. Proton g has a chemical shift of 6.85 ppm. **b)** Spectrum of the small molecule model system after the 'click' reaction (4), taken in CDCl$_3$. As a result of the 'click' reaction, g has experienced an up-field change to 6.78 ppm. **c)** Spectrum of the model dendrimer system before the 'click' reaction (5 and 6), taken in D$_2$O. Proton g overlaps proton b at 6.90 ppm. **d)** Spectrum of the model dendrimer system after the 'click' reaction (7), taken in D$_2$O. Similar to the small molecule model system, proton g experiences an up-field change as a result of the 'click' reaction. In the model dendrimer system, the new chemical shift is 6.74 ppm.
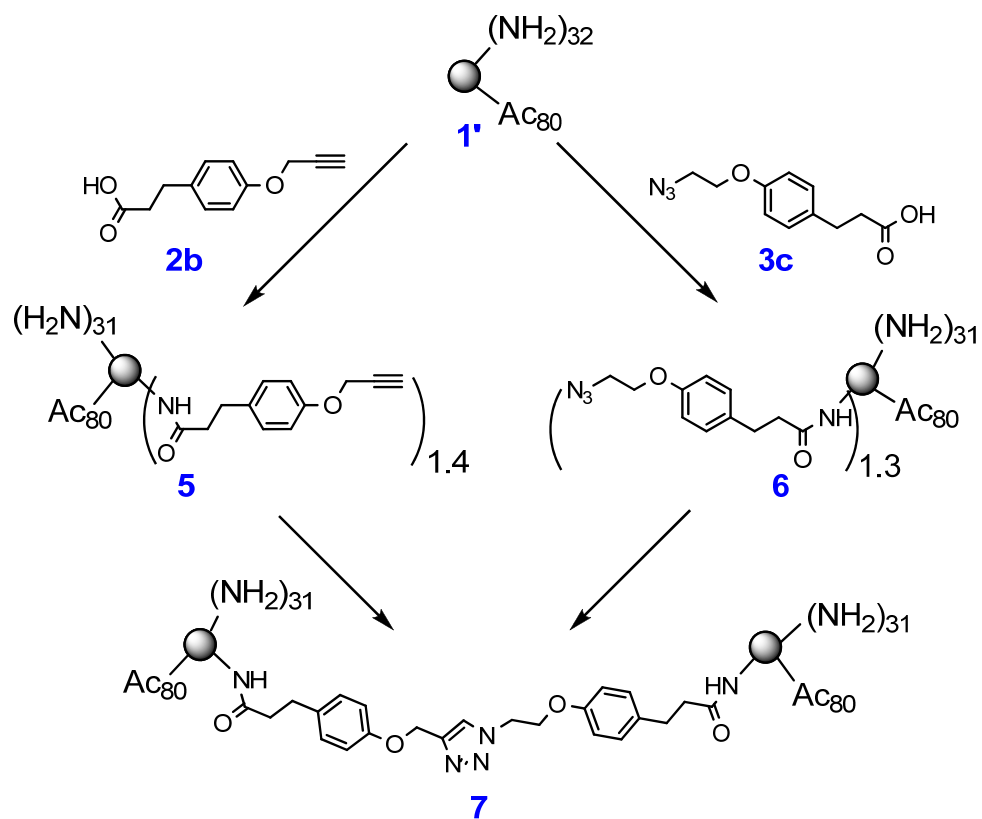
Figure 2.3: Synthetic scheme for the model dendrimer system (**7**). This simplified modular platform was developed to assist with the spectroscopic characterization of the folic acid targeted dendrimer system. The G5 dendrimer, used in this study, had an average of 112 end groups as determined by GPC and potentiometric titration.
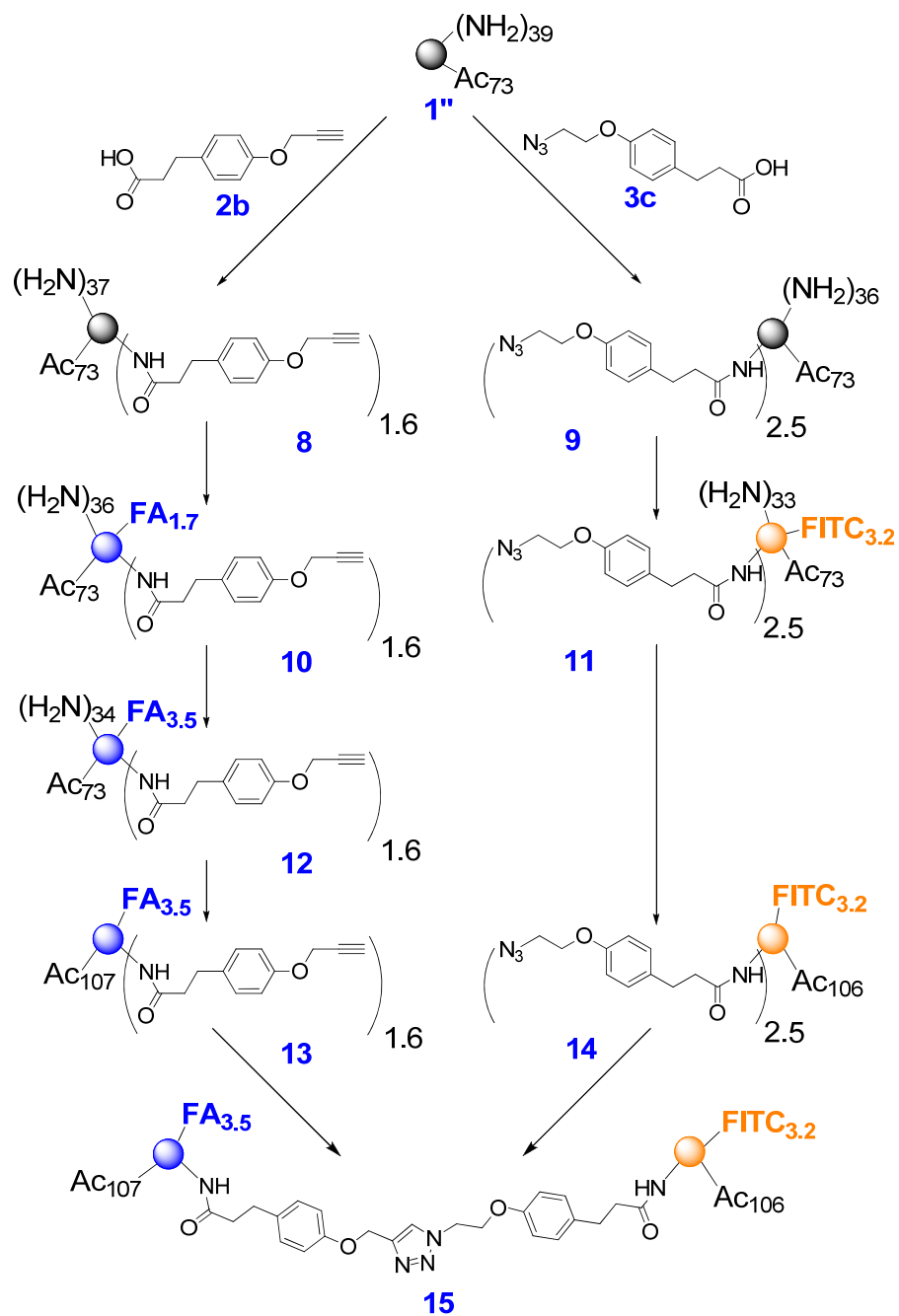
Figure 2.4: Synthetic scheme for the folic acid targeted modular dendrimer-based platform (**15**). A module possessing a terminal alkyne moiety and Folic Acid (**13**) is coupled to a second module possessing a terminal azide moiety and FITC (14) via the Cu-catalyzed 1,3-dipolar cycloaddition reaction. Both modules were fully acetylated to avoid non-specific cellular interactions.
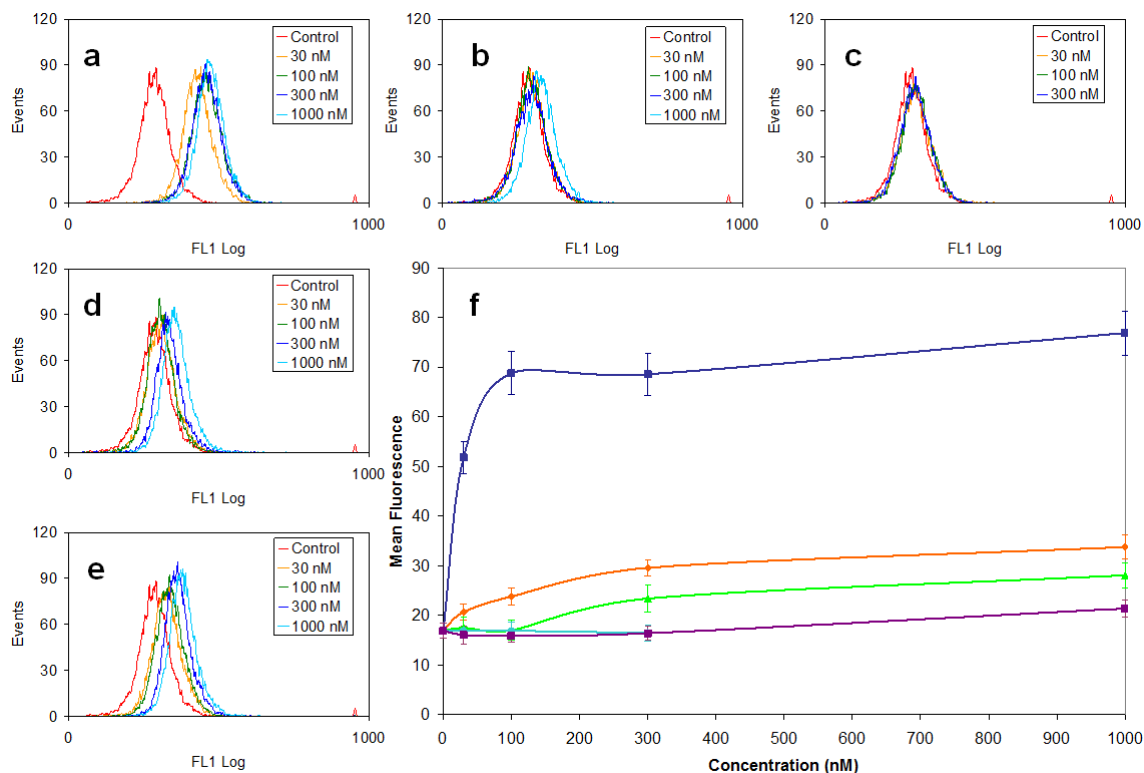
Figure 2.5: Binding and uptake of the fluorescent modular targeted dendrimer platform in KB cells as measured by Flow Cytometry. **a)** Uptake $FA_{3.5}$-G5-Ac_{107}-L-G5Ac_{106}-$FITC_{3.2}$ (**15**). **b)** Uptake of G5-Ac_{106}-$Azide_{2.5}$-$FITC_{3.2}$ (**14**) is not observed for 30 nM, 100 nM, and 300 nM. Very minimal uptake of this un-targeted module is observed at 1000 nM. **c)** Similarly, no uptake is observed for an uncoupled mixture of G5-Ac_{106}-$Azide_{2.5}$-$FITC_{3.2}$ (14) and G5-Ac_{107}-$Alkyne_{1.6}$-$FA_{3.5}$ (**13**). **d)** Uptake of $FA_{3.5}$-G5-Ac_{107}-L-G5Ac_{106}-$FITC_{3.2}$ (**15**) is successfully blocked using a 20 fold excess of free folic acid. e) Uptake of $FA_{3.5}$-G5-Ac_{107}-L-G5Ac_{106}-$FITC_{3.2}$ (**15**) is also successfully blocked using a 20 fold excess (with respect to the folic acid content) of G5-Ac_{107}-$Alkyne_{1.6}$-$FA_{3.5}$ (**13**). **f)** Summary of mean fluorescence values for **a-e**. Uptake of $FA_{3.5}$-G5-Ac_{107}-L-G5Ac_{106}-$FITC_{3.2}$ (**15**) is displayed in blue. Uptake of the targeted platform (**15**) blocked by a 20 fold excess of G5-Ac_{107}-$Alkyne_{1.6}$-$FA_{3.5}$ (**13**) is shown in orange. Uptake of the targeted platform (**15**) blocked by a 20 fold excess of free folic acid can be found in green. Uptake of a mixture of G5-Ac_{106}-$Azide_{2.5}$-$FITC_{3.2}$ (14) and G5-Ac_{106}-$Alkyne_{1.6}$-$FA_{3.5}$ (**13**) can be found in teal. Finally, uptake of G5-Ac_{106}-$Azide_{2.5}$-$FITC_{3.2}$ (**14**) can be found in purple. Error bars indicate standard deviation as computed from half-peak coefficient of variation (HPCV) values.

55

References

(1)   Allen, T. M. *Nature Reviews Cancer* **2002**, *2*, 750-763.

(2)   Peer, D.; Karp, J. M.; Hong, S.; FaroKhzad, O. C.; Margalit, R.; Langer, R. *Nature Nanotechnology* **2007**, *2*, 751-760.

(3)   Hong, S.; Leroueil, P. R.; Majoros, I. J.; Orr, B. G.; Baker, J. R.; Holl, M. M. B. *Chemistry and Biology* **2007**, *14*, 105-113.

(4)   Mammen, M.; Choi, S. K.; Whitesides, G. M. *Angewandte Chemie-International Edition* **1998**, *37*, 2755-2794.

(5)   Majoros, I. J.; Keszler, B.; Woehler, S.; Bull, T.; Baker, J. R. *Macromolecules* **2003**, *36*, 5526-5529.

(6)   Hong, S. P.; Bielinska, A. U.; Mecke, A.; Keszler, B.; Beals, J. L.; Shi, X. Y.; Balogh, L.; Orr, B. G.; Baker, J. R.; Holl, M. M. B. *Bioconjugate Chemistry* **2004**, *15*, 774-782.

(7)   Lee, C. C.; MacKay, J. A.; Frechet, J. M. J.; Szoka, F. C. *Nature Biotechnology* **2005**, *23*, 1517-1526.

(8)   Svenson, S.; Tomalia, D. A. *Advanced Drug Delivery Reviews* **2005**, *57*, 2106-2129.

(9)   Hong, S. P.; Leroueil, P. R.; Janus, E. K.; Peters, J. L.; Kober, M. M.; Islam, M. T.; Orr, B. G.; Baker, J. R.; Holl, M. M. B. *Bioconjugate Chemistry* **2006**, *17*, 728-734.

(10)   Leroueil, P. R.; Hong, S. Y.; Mecke, A.; Baker, J. R.; Orr, B. G.; Holl, M. M. B. *Accounts of Chemical Research* **2007**, *40*, 335-342.

(11)   Patri, A. K.; Myc, A.; Beals, J.; Thomas, T. P.; Bander, N. H.; Baker, J. R. *Bioconjugate Chemistry* **2004**, *15*, 1174-1181.

(12)   Shukla, R.; Thomas, T. P.; Peters, J. L.; Desai, A. M.; Kukowska-Latallo, J.; Patri, A. K.; Kotlyar, A.; Baker, J. R. *Bioconjugate Chemistry* **2006**, *17*, 1109-1115.

(13)   Wu, G.; Barth, R. F.; Yang, W. L.; Kawabata, S.; Zhang, L. W.; Green-Church, K. *Molecular Cancer Therapeutics* **2006**, *5*, 52-59.

(14)   Wu, G.; Barth, R. F.; Yang, W. L.; Chatterjee, M.; Tjarks, W.; Ciesielski, M. J.; Fenstermaker, R. A. *Bioconjugate Chemistry* **2004**, *15*, 185-194.

(15)   Backer, M. V.; Gaynutdinov, T. I.; Patel, V.; Bandyopadhyaya, A. K.; Thirumamagal, B. T. S.; Tjarks, W.; Barth, R. F.; Claffey, K.; Backer, J. M. *Molecular Cancer Therapeutics* **2005**, *4*, 1423-1429.

(16)   Shukla, R.; Thomas, T. P.; Peters, J.; Kotlyar, A.; Myc, A.; Baker, J. R. *Chemical Communications* **2005**, 5739-5741.

(17)   Sheng, K. C.; Kalkanidis, M.; Pouniotis, D. S.; Esparon, S.; Tang, C. K.; Apostolopoulos, V.; Pietersz, G. A. *European Journal of Immunology* **2008**, *38*, 424-436.

(18)   Baek, M. G.; Roy, R. *Bioorganic and Medicinal Chemistry* **2002**, *10*, 11-17.

(19)   Taite, L. J.; West, J. L. *Journal of Biomaterials Science-Polymer Edition* **2006**, *17*, 1159-1172.

(20)   Kono, K.; Liu, M. J.; Frechet, J. M. J. *Bioconjugate Chemistry* **1999**, *10*, 1115-1121.

(21)   Shukla, S.; Wu, G.; Chatterjee, M.; Yang, W. L.; Sekido, M.; Diop, L. A.; Muller, R.; Sudimack, J. J.; Lee, R. J.; Barth, R. F.; Tjarks, W. *Bioconjugate Chemistry* **2003**, *14*, 158-167.

(22)   Majoros, I. J.; Myc, A.; Thomas, T.; Mehta, C. B.; Baker, J. R. *Biomacromolecules* **2006**, *7*, 572-579.

(23)   Thomas, T. P.; Majoros, I. J.; Kotlyar, A.; Kukowska-Latallo, J. F.; Bielinska, A.; Myc, A.; Baker, J. R. *Journal of Medicinal Chemistry* **2005**, *48*, 3729-3735.

(24)   Myc, A.; Douce, T. B.; Ahuja, N.; Kotlyar, A.; Kukowska-Latallo, J.; Thomas, T. P.; Baker, J. R. *Anti-Cancer Drugs* **2008**, *19*, 143-149.

(25)   Majoros, I. J.; Thomas, T. P.; Mehta, C. B.; Baker, J. R. *Journal of Medicinal Chemistry* **2005**, *48*, 5892-5899.

(26)   Kukowska-Latallo, J. F.; Candido, K. A.; Cao, Z. Y.; Nigavekar, S. S.; Majoros, I. J.; Thomas, T. P.; Balogh, L. P.; Khan, M. K.; Baker, J. R. *Cancer Research* **2005**, *65*, 5317-5324.

(27)   Myc, A.; Patri, A. K.; Baker, J. R. *Biomacromolecules* **2007**, *8*, 2986-2989.

(28)   Myc, A.; Majoros, I. J.; Thomas, T. P.; Baker, J. R. *Biomacromolecules* **2007**, *8*, 13-18.

(29)   Landmark, K. J.; DiMaggio, S.; Ward, J.; Kelly, C.; Vogt, S.; Hong, S.; Kotlyar, A.; Myc, A.; Thomas, T. P.; Penner-Hahn, J. E.; Baker, J. R.; Holl, M. M. B.; Orr, B. G. *ACS Nano* **2008**, *2*, 773-783.

(30)   Mullen, D. G.; Desai, A. M.; Waddell, J. N.; Cheng, X.-M.; Kelly, C. V.; McNerny, D. Q.; Majoros, I. J.; Baker, J. R.; Sander, L. M.; Orr, B. G.; Banaszak Holl, M. M. *Bioconjugate Chemistry* **2008**, *19*, 1748-1752.

(31)   Choi, Y. S.; Mecke, A.; Orr, B. G.; Holl, M. M. B.; Baker, J. R. *Nano Letters* **2004**, *4*, 391-397.

(32)   Choi, Y.; Thomas, T.; Kotlyar, A.; Islam, M. T.; Baker, J. R. *Chemistry and Biology* **2005**, *12*, 35-43.

(33)   DeMattei, C. R.; Huang, B. H.; Tomalia, D. A. *Nano Letters* **2004**, *4*, 771-777.

(34)   Choi, Y. Dissertation, University of Michigan, 2005.

(35)   Lee, J. W.; Kim, J. H.; Kim, H. J.; Han, S. C.; Kim, J. H.; Shin, W. S.; Jin, S. H. *Bioconjugate Chemistry* **2007**, *18*, 579-584.

(36)   Lee, J. W.; Kim, H. J.; Han, S. C.; Kim, J. H.; Jin, S. H. *Journal of Polymer Science Part a-Polymer Chemistry* **2008**, *46*, 1083-1097.

(37)   Lee, J. W.; Kim, B. K.; Kim, H. J.; Han, S. C.; Shin, W. S.; Jin, S. H. *Macromolecules* **2006**, *39*, 2418-2422.

(38)   Lee, J. W.; Kim, J. H.; Kim, B. K.; Shin, W. S.; Jin, S. H. *Tetrahedron* **2006**, *62*, 894-900.

(39)   Wu, P.; Malkoch, M.; Hunt, J. N.; Vestberg, R.; Kaltgrad, E.; Finn, M. G.; Fokin, V. V.; Sharpless, K. B.; Hawker, C. J. *Chemical Communications* **2005**, 5775-5777.

(40)   Goyal, P.; Yoon, K.; Weck, M. *Chemistry-a European Journal* **2007**, *13*, 8801-8810.

(41)   Yoon, K.; Goyal, P.; Weck, M. *Organic Letters* **2007**, *9*, 2051-2054.

(42)   Rostovtsev, V. V.; Green, L. G.; Fokin, V. V.; Sharpless, K. B. *Angewandte Chemie-International Edition* **2002**, *41*, 2596-2599.

(43)   Wu, P.; Feldman, A. K.; Nugent, A. K.; Hawker, C. J.; Scheel, A.; Voit, B.; Pyun, J.; Frechet, J. M. J.; Sharpless, K. B.; Fokin, V. V. *Angewandte Chemie-International Edition* **2004**, *43*, 3928-3932.

(44)   Wu, P.; Fokin, V. V. *Aldrichimica Acta* **2007**, *40*, 7-17.

(45)   Hoffman, R. E. *Magnetic Resonance in Chemistry* **2006**, *44*, 606-616.

(46)   Marie, D.; Brown, S. C. *Biology of the Cell* **1993**, *78*, 41-51.

(47)   Lee, J. W.; Kim, J. H.; Kim, B. K.; Kim, J. H.; Shin, W. S.; Jin, S. H. *Tetrahedron* **2006**, *62*, 9193-9200.

(48)   Mullen, D. G.; Fang, M.; Desai, A. M.; Baker, J. R.; Orr, B. G.; Banaszak Holl, M. M. *ACS Nano* **2010**, *4*, 657-670.

Chapter 3
A Quantitative Assessment of Nanoparticle-Ligand Distributions: Implications for Targeted Drug and Imaging Delivery in Dendrimer Conjugates

Introduction

Conjugation strategies commonly employed to attach ligands to the surfaces of nanoparticles generate stochastic distributions of products. Commonly used techniques, including nuclear magnetic resonance (NMR), ultraviolet/visible (UV/Vis) spectroscopy, Fourier transformed infrared spectroscopy (FTIR), and elemental analysis are only capable of determining the mean ligand to nanoparticle ratio and do not provide information about the distribution of components present in the nanomaterial. Other techniques with potential to resolve the distribution of components such as gel permeation chromatography (GPC), high performance liquid chromatography (HPLC), and matrix assisted laser desorption ionization - time of flight (MALDI-TOF) are often unable to do so. The observation of unresolved distributions of macromolecules as "single peaks" using these techniques often leads to optimistic interpretations of sample homogeneity. As such, distributions of nanoparticle-ligand components are not adequately considered in either research studies or systems design. Important questions to ask about the nature of the "average" number of ligands and the distribution from which it arises include:

1. What are the mean, median, and mode of nanoparticle populations in terms of number of conjugated ligands per particle and how are they related to each other?
2. What is the specific number of components that constitute the observed distributions? What mathematical form best approximates the experimentally observed distribution? Does the mean appropriately represent the material composition?

3. How does a pre-existing distribution of attachment sites in a population of nanoparticles affect nanoparticle-ligand distributions? This is of particular interest since partial acetylation has been an important step for creating biological functional, targeted PAMAM dendrimers.[1-5] Broadly speaking, this question is relevant to nanoparticle systems that use sequential conjugations of different ligands to the same particle.

4. How does knowledge of the average (mean, median, and mode) and distribution of nanoparticle components affect design and application of nanoparticle-ligand conjugates?

Given the great potential that ligand conjugated nanomaterials possess with respect to therapeutic delivery,[6-11] cell targeting,[12-13] biomedical diagnostics,[14-17] and sensing,[18-19] a comprehensive understanding of the distributions that result from the conjugation of ligands to nanoparticles is paramount. In this chapter, we focus on the distribution of nanoparticle-ligand components that exists for samples produced using poly(amidoamine) (PAMAM) dendrimers and a small molecule ligand. **Figure 3.1** contains space filling models for 3 such components. The results from this chapter are generalizable to a broad range of nanoparticles. Relevant examples include particles composed of gold, iron oxide, polymers, silica, albumin, quantum dots, carbon nanotubes, and dendrimers.[4-5,20-29] This chapter is most relevant to nanoparticle-based systems produced using stochastic synthesis techniques with an excess of attachment sites on the nanoparticle relative to the number of conjugated ligands, and with the resulting mean number of conjugated ligands ranging from 0.4 to 13. Additionally, this chapter applies primarily to small and moderate sized ligands relative to the size of the nanoparticle such that site-blocking effects are not introduced by the conjugation of a ligand beyond the single site to which the ligand is covalently linked. This chapter is therefore less applicable to systems using large ligands such as proteins.[30] A non-exhaustive list of nanoparticle-ligand systems that fit directly in this category include Quantum Dots conjugated to siRNA,[22] iron oxide nanoparticles conjugated to fluorescein isothiocyanate (FITC)[23] and other small organic molecules,[23-24] and finally, dendrimers

conjugated to oligonucleotides,[25-26] folic acid,[4,20-21,27-28] peptides,[5,29] FITC,[29] and other small molecules.[4]

The diversity of ligands that have been conjugated to dendrimers makes the dendrimer a compelling system to study.[31-35] Several of these dendrimer-ligand combinations have been found to be highly effective in biological systems both *in vitro* and *in vivo* with potential to advance to human clinical trials.[2-3,36-41] To facilitate the development of these dendrimer-based nanomaterials into systems with consistent biological activities, it is vital to have knowledge of the distribution of dendrimer-ligand components that compose the material. A final factor making the dendrimer an attractive system to study is that dendrimers are structurally well-defined and well-characterized. This is especially true for PAMAM dendrimers. PAMAM dendrimers have a well defined branched structure which leads to exceptionally high degrees of monodispersity (PDI = 1.01) and a quantifiable mean number of surface functional groups. With just two exceptions,[42-43] however, only the mean number of ligands bound per dendrimer has been reported.

The situation is exemplified by the PAMAM dendrimer-ligand system developed for targeted drug delivery by Majoros *et al.*[27] This dendrimer was modified sequentially with a mean of 72 acetyl groups, 4 FITC dye molecules, 4 folic acid (FA) targeting ligands, 60 alcohols from glycidilation, and 5 methotrexate (MTX) drug molecules. Cellular-uptake of this targeted nanotheraputic in epidermal carcinoma (KB) cells was studied by Thomas *et al.*[37] Kukowska-Latallo and co-workers found that the dendrimer-based nanomaterial increased the antitumor activity of MTX and substantially decreased its toxicity relative to the free drug in mice bearing human epithelial cancer tumors.[36] These biological results are very promising, and yet at time of publication no knowledge existed about the distribution of dendrimer-ligand components that composed the material and gave rise to the observed biological results. For example, the specific number of different G5-FA components that are represented by the mean of 4 FA was not known, nor was it known if the largest population was even the dendrimer component with 4 FA molecules. Furthermore, no information existed about how the various ligand

distributions were affected by conducting each ligand conjugation reaction in a step-wise fashion with distributions forming in the presence of pre-existing ligand distributions.

In this chapter, we quantitatively analyze the HPLC traces of three different sets of nanoparticle-ligand samples. The nanoparticle-ligand sets were formed using three different nanoparticles: a partially acetylated PAMAM dendrimer with a mean of 78 Ac and 34 NH_2 groups, a G5 PAMAM dendrimer with a mean of 112 primary amines and a partially acetylated G5 PAMAM dendrimer with a mean of 80 Ac and 32 NH_2 groups; and a small molecule ligand: 3-(4-(prop-2-ynyloxy)phenyl)propanoic acid (Alkyne Ligand). Within each of the three sets (G5-Ac_{78}-Alkyne, G5-NH_2-Alkyne and G5-Ac_{80}-Alkyne), samples were synthesized to have ligand means in the range commonly used in dendrimer applications, as well as many other nanoparticle-ligand systems described earlier. The products were analyzed by ^{1}H NMR spectroscopy to determine the mean ligand-nanoparticle ratio. When combined with GPC and potentiometric titration data, the mean number of ligands per nanoparticle was computed. HPLC combined with a peak fitting method resolved the distribution of dendrimer-ligand components and provided the mean, median, and mode of the number of ligands per particle. Two statistical models were employed to confirm that the observed heterogeneity is consistent with theoretical expectations.

Experimental Methods

Reagents and Materials

Biomedical grade Generation 5 PAMAM (poly(amidoamine)) dendrimer was purchased from Dendritech Inc. and purified as described in the synthesis section. MeOH (99.8%), acetic anhydride (99.5%), triethylamine (99.5%), dimethyl sulfoxide (99.9%), dimethylformamide (99.8%), acetone (ACS reagent grade $\geq$ 99.5%), N,N-diisopropylethylamine, benzotriazol-1-yl-oxytripyrrolidinophosphonium hexafluorophosphate (98%), D_2O, and volumetric solutions (0.1 M HCl and 0.1 M NaOH) for potentiometric titration were purchased from Sigma Aldrich Co. and used as received. 10,000 molecular weight cut-off centrifugal filters (Amicon Ultra) were obtained from Fisher Scientific. 1x phosphate buffer saline (PBS) (Ph = 7.4) without calcium or magnesium was purchased from Invitrogen.

Nuclear Magnetic Resonance Spectroscopy

All ^{1}H NMR experiments were conducted using a Varian Inova 400 MHz instrument. 10s delay time and 64 scans were set for each dendrimer sample. Temperature was controlled at 25 °C. For experiments conducted in D_2O, the internal reference peak was set to 4.717 ppm. Based upon measuring T_2* values and empirical studies to ensure that the chosen delay was long enough to avoid any decreased peak intensity associated with spin saturation, the delay for all integration studies was set to 10 s.

Gel Permeation Chromatography

GPC experiments were performed on an Alliance Waters 2695 separation module equipped with a 2487 dual wavelength UV absorbance detector (Waters Corporation), a Wyatt HELEOS Multi Angle Laser Light Scattering (MALLS) detector, and an Optilab rEX differential refractometer (Wyatt Technology Corporation). Columns employed were TosoHaas TSK-Gel Guard PHW 06762 (75 mm × 7.5 mm, 12 μm), G 2000 PW 05761 (300 mm × 7.5 mm, 10 μm), G 3000 PW 05762 (300 mm × 7.5 mm, 10 μm), and G 4000 PW (300 mm × 7.5 mm, 17 μm). Column temperature was maintained at 25 ±

63

0.1 °C with a Waters temperature control module. The isocratic mobile phase was 0.1 M citric acid and 0.025 wt % sodium azide, pH 2.74, at a flow rate of 1 mL/min. The sample concentration was 10 mg/5 mL with an injection volume of 100 μL. The weight average molecular weight, M_w, has been determined by GPC, and the number average molecular weight, M_n, was calculated with Astra 5.3.14 software (Wyatt Technology Corporation) based on the molecular weight distribution.

Reverse Phase High Performance Liquid Chromatography

HPLC analysis was carried out on a Waters Delta 600 HPLC system equipped with a Waters 2996 photodiode array detector, a Waters 717 Plus auto sampler, and Waters Fraction collector III. The instrument was controlled by Empower 2 software. For analysis of the conjugates, a C5 silica-based RP-HPLC column (250 x 4.6 mm, 300 Å) connected to a C5 guard column (4 x 3 mm) was used. The mobile phase for elution of the conjugates was a linear gradient beginning with 100:0 (v/v) water/acetonitrile and ending with 20:80 (v/v) water/acetonitrile over 30 min at a flow rate of 1 mL/min. Trifluoroacetic acid (TFA) at 0.14 wt % concentration in water as well as in acetonitrile was used as a counter ion to make the dendrimer surfaces hydrophobic. Elution traces of the dendrimer-ligand conjugate were obtained at 210 nm. Run-to-run reproducibility of retention time was 0.016 min which is ~4% of the magnitude of the peak-to-peak separation noted in this analysis.

Beer's Law: Dilution Study

A dilution study of Sample D was performed to demonstrate that the dendrimer conjugates follow Beer's Law at 210 nm. Solutions of Sample D with different concentrations were injected on the HPLC. The elution profile at 210 nm of Sample D at varying concentrations can be found in **Figure 3.13**.

Using the fitting procedure described this chapter, peaks were fit to each of the elution profiles in **Figure 3.13**. Peak concentration was calculated as the product of the Peak Area Fraction and the Sample Concentration. The linear relationship found in

Figure 3.13 between Peak Area and Peak concentration clearly demonstrates that Beer's Law is followed at 210 nm for the dendrimer conjugates in this study.

Potentiometric Titration

Potentiometric titration was carried out using a Mettler Toledo MP220 pH meter and a Mettler Toledo InLab 430 pH electrode at room temperature, 23 °C. A 10 mL solution of 0.1 N NaCl was added to purified G5 PAMAM dendrimer **1** (127.5 mg) to shield amine group interactions. The pH of the dendrimer solution was lowered to pH = 2.01 using 0.1034 N HCl. A 25 mL Brand Digital Burette^{TM} III was used for the titration with 0.0987 N NaOH. The numbers of primary and tertiary amines were determined by from the titration curve with NaOH as previously described.[4]

Synthesis

The G5-$(NH_2)_{112}$ dendrimer was conjugated to Ac, and Alkyne groups. Ac refers to the acetyl termination, and Alkyne to the Alkyne Ligand.

Dendrimer 1: Purification of Generation 5 PAMAM Dendrimer G5-$(NH_2)_{112}$

The purchased G5 PAMAM dendrimer was purified by dialysis to remove lower molecular weight impurities including trailing generation dendrimer defect structures. dendrimer was dialysed with a 10,000 MWCO membrane against DI water for three days, exchanging washes every 4 hours. The number average molecular weight (27,100 g/mol± 1,000) and PDI (1.018 +/- 0.014) was determined by GPC. Potentiometric titration was conducted to determine the mean number of primary amines (112 ± 5).

Dendrimer 2: Synthesis of Partially Acetylated Dendrimer 1 G5-Ac_{78}-$(NH_2)_{34}$

Purified Generation 5 PAMAM dendrimer **1** (133.7 mg, 4.89 μmole) was dissolved in anhydrous methanol (21 mL). Triethylamine (68.5 μL, 0.491 mmole) was added to this mixture and stirred for 30 minutes. Acetic anhydride (37.1 μL, 0.393 mmole) was added to anhydrous methanol (4 mL) and the resulting mixture was added in a dropwise manner to the dendrimer solution. The reaction was carried out in a glass

flask, under nitrogen, at room temperature for 24 hours. Methanol was evaporated from the resulting solution and the product was purified using 10,000 MWCO centrifugal filtration devices (Centricon). Purification consisted of five cycles (30 minutes at 5,000 rpm) using 1x PBS and five cycles using DI water. The purified dendrimer was lyophilized for three days to yield a white solid (138.4 mg, 92%). Number average molecular weight (30,660 g/mol) and PDI (1.026 +/- 0.015) were determined by GPC. ^{1}H NMR integration determined the degree of acetylation to be 70%.

Dendrimer 3: Synthesis of Partially Acetylated Dendrimer G5-Ac$_{80}$-(NH$_2$)$_{32}$

Purified G5 PAMAM dendrimer **1** (180.1 mg, 6.588 μmole) was dissolved in anhydrous methanol (26.8 mL). Triethylamine (83.6 μL, 0.600 mmole) was added to this mixture and stirred for 30 minutes. Acetic anhydride (45.3 μL, 0.480 mmole) was added to anhydrous methanol (7.3 mL) and the resulting mixture was added in a dropwise manner to the dendrimer solution. The reaction was carried out in a glass flask, under nitrogen, at room temperature for 24 hours. Methanol was evaporated from the resulting solution and the product was purified using 10,000 MWCO centrifugal filtration devices (Amicon Ultra). Purification consisted of six cycles (10 minutes at 5,000 rpm) using 1x PBS (without magnesium and calcium) and six cycles using DI water. The purified dendrimer was lyophilized for three days to yield a white solid (124.5 mg, 62%). ^{1}H NMR integration determined the degree of acetylation to be 71.5%.

Ligand Synthesis (3-(4-(prop-2-ynyloxy)phenyl)propanoic acid)

To a solution of methyl 3-(4-hydroxyphenyl)propanoate (2.18 g, 0.0121 mol) in dry acetone (56 mL) was added anhydrous K$_2$CO$_3$ (4.60 g, 0.0333 mol) followed by propargyl bromide (80% solution in toluene, 1.88 mL, 0.0126 mol). The resulting suspension was refluxed for 24 h with vigorous stirring. The reaction mixture was cooled to room temperature and the salt was removed by filtration followed by washing with portions of EtOAc. The filtrate was evaporated under vacuum to give the desired product as an oil (2.43g, 92%).

The crude product from above was dissolved in MeOH (60 mL). KOH (8 M, 5.0 mL, 0.040 mol) was added and the resulting mixture was heated at 70 °C for 1.5 h. The solution was cooled to room temperature and condensed under reduced pressure. The residue was dissolved in water (30 mL) and was acidified by addition of 1N HCl to pH 1. The white cloudy solution was diluted with EtOAc. Layers were separated and the aqueous layer was extracted with EtOAc (2 x 70 mL). The combined organic extracts were washed with a saturated NaCl solution and dried over $MgSO_4$. Solvent was evaporated under reduced pressure to give the desired product as a yellowish solid. (2.21 g, 97%).

^{1}H NMR (500 MHz, $CDCl_3$) δ 7.12, (d, 2H, J = 8.74 Hz), 6.89 (d, 2H, J = 8.71 Hz), 6.89 (d, 2H, J = 8.71 Hz), 4.65 (d, 2H, J = 2.40 Hz), 2.89 (t, 2H, J = 7.74 Hz), 2.64 (t, 2H, J = 7.75 Hz), 2.49 (t, 1H, J = 2.40 Hz)

Synthesis of Dendrimer-Ligand Samples

All reaction steps were carried out in glass scintillation vials at room temperature under nitrogen. All samples were purified using 10,000 MWCO centrifugal filtration devices (Amicon Ultra). Purification consisted of one cycle (10 minutes at 5,000 rpm) using 1x PBS (without magnesium or calcium) and five cycles using DI water unless otherwise noted.

Samples A-D: G5-Ac$_{78}$-Alkyne$_{(0.2, 0.6, 1.04, 1.47)}$

The ligand was conjugated to the partially acetylated dendrimer **2** in two consecutive reactions. First, a stock solution of the ligand 3-(4-(prop-2-ynyloxy)phenyl)propanoic acid (9.4 mg, 0.046 mmole) was generated with a mixture of DMF (6.899 mL) and DMSO (2.300 mL). To this mixture was added 1-Ethyl-3-[3-dimethylaminopropyl]carbodiimide hydrochloride (EDC) (123.5 mg, 0.644 mmole). The resulting solution was stirred for 4 h at room temperature to create the active ester form of the ligand.

A stock solution of partially acetylated dendrimer **2** (77.1 mg, 2.51 μmole) was made with DI water (17.190 mL). This solution was partitioned into four aliquots, A-D (15.0 mg,

0.489 μmole each). Additional DI water (2.520 mL, 2.016 mL, 1.512 mL) was added to the first three aliquots (A-C). The active ester form of the ligand (0.504 mL, 2.521 μmole) in DMF/DMSO was added in a dropwise manner (0.1 mL/min) to the first aliquot (A) of dendrimer-water solution. Similarly, the activated ester form of the ligand was added to the second, third, and fourth aliquots (5.043 μmole, 7.565 μmole, and 10.087 μmole respectively). The resulting mixtures were stirred for 2.5 days. All reaction steps were carried out in glass flasks at room temperature under nitrogen. The four reaction mixtures were purified using 10,000 MWCO centrifugal filtration devices (Centricon). Purification consisted of five cycles using 1x PBS and six cycles using DI water. All cycles were 30 minutes at 5,000 rpm. The resulting products (A-D) were lyophilized for three days to yield a white solid (14.6 mg, 16.5 mg, 15.7 mg, and 15.5 mg respectively).

Samples E-H: G5-NH$_2$-Alkyne$_{(1.1,\ 3.8,\ 5.7,\ 12.9)}$

Three stock solutions were generated to synthesize Samples E-H. A solution of G5 PAMAM dendrimer **1** (37.6 mg, 1.38 μmole) was prepared with anhydrous DMSO (7.000 mL). The Alkyne Ligand (5.7 mg, 28 μmole) was dissolved in DMSO (2.85 mL). Benzotriazol-1-yl-oxytripyrrolidinophosphonium hexafluorophosphate (PyBOP) (5.5 mg, 10.6 μmole) was dissolved in DMSO (1.10 mL).

Sample E

The Alkyne Ligand (0.10 mg, 0.49 μmole) solution in anhydrous DMSO (43.9 μL), was added to a solution of G5-NH$_2$ **1** (8.0 mg, 0.29 μmole) in anhydrous DMSO (1.489 mL). N,N-diisopropylethylamine (0.30 mg, 0.40 μL, 2.3 μmole) was added to the reaction mixture together with 1.091 mL additional DMSO and the resulting solution was stirred for 30 minutes. A solution of PyBOP (0.20 mg, 0.38 μmole) in anhydrous DMSO (44.8 μL) was added in a dropwise manner (0.1 mL/min) to the dendrimer solution. The resulting reaction mixture was stirred for 24 hrs under nitrogen and then purified as described earlier. The purified product, Sample E, was lyophilized for three days to yield a white solid (5.7 mg, 71%). ^{1}H NMR integration determined the mean number of Alkyne Ligands per dendrimer to be 1.1.

Sample F

Sample F was synthesized in the same manner as Sample E, using G5-NH$_2$ **1** (8.0 mg, 0.29 μmole) in anhydrous DMSO (1.489 mL), the Alkyne Ligand (0.26 mg, 1.3 μmole) in DMSO (131.8 μL), N,N-diisopropylethylamine (1.0 mg, 1.3 μL, 7.5 μmole), 0.913 mL additional DMSO and PyBOP (0.70 mg, 1.3 μmole) in anhydrous DMSO (134.4 μL). Sample F was purified and lyophilized in the same manner as Sample E. The purified product, Sample F, was a white solid (8.0 mg, 97%). ^{1}H NMR integration determined the mean number of Alkyne Ligands per dendrimer to be 3.8.

Sample G

Sample G was synthesized in the same manner as Sample E, using G5-NH$_2$ **1** (8.0 mg, 0.29 μmole) in anhydrous DMSO (1.489 mL), the Alkyne Ligand (0.44 mg, 2.2 μmole) in DMSO (219.7 μL), N,N-diisopropylethylamine (1.7 mg, 2.2 μL, 13 μmole), 0.734 mL additional DMSO and PyBOP (1.1 mg, 2.2 μmole) in anhydrous DMSO (224.0 μL). Sample G was purified and lyophilized in the same manner as Sample E. The purified product, Sample G, was a white solid (6.9 mg, 83%). ^{1}H NMR integration determined the mean number of Alkyne Ligands per dendrimer to be 5.7.

Sample H

Sample H was synthesized in the same manner as Sample E, using G5-NH$_2$ **1** (8.0 mg, 0.29 μmole) in anhydrous DMSO (1.489 mL), the Alkyne Ligand (0.88 mg, 4.3 μmole) in DMSO (439.5 μL), N,N-diisopropylethylamine (3.3 mg, 4.5 μL, 26 μmole), 0.288 mL additional DMSO and PyBOP (2.2 mg, 4.30 μmole) in anhydrous DMSO (447.9 μL). Sample H was purified and lyophilized in the same manner as Sample E. The purified product, Sample H, was a white solid (8.1 mg, 92%). ^{1}H NMR integration determined the mean number of Alkyne Ligands per dendrimer to be 12.9.

Samples I-M: G5-Ac$_{80}$-Alkyne$_{(0.4, 0.7, 2.7, 6.8, 10.2)}$

Three stock solutions were generated to synthesize Samples I-M. A solution of the partially acetylated dendrimer **3** (22.4 mg, 0.728 μmole) was prepared with anhydrous DMSO (4.9778 mL). The Alkyne Ligand (9.9 mg, 49 μmole) was dissolved in DMSO

(4.9500 mL). Benzotriazol-1-yl-oxytripyrrolidinophosphonium hexafluorophosphate (PyBOP) (5.4 mg, 10 μmole) was dissolved in DMSO (1.000 mL).

Sample I

The Alkyne Ligand (29.0 μg, 0.146 μmole) in anhydrous DMSO (14.6 μL), was added to a solution of partially acetylated dendrimer **3** (4.4 mg, 0.14 μmole) in anhydrous DMSO (0.978 mL). N,N-diisopropylethylamine (1.1 mg, 1.5 μL, 8.6 μmole) was added to the reaction mixture and the resulting solution was stirred for 30 minutes. A solution of PyBOP (74.0 μg, 0.143 μmole) in anhydrous DMSO (13.8 μL) was added in a dropwise manner (0.1 mL/min) to the dendrimer solution. The resulting reaction mixture was stirred for 24 hrs under nitrogen and then purified as described earlier. The purified product, Sample I, was lyophilized for three days to yield a white solid (3.7 mg, 84%). ^{1}H NMR integration determined the mean number of Alkyne Ligands per dendrimer to be 0.4.

Sample J

Sample J was synthesized in the same manner as Sample I, using partially acetylated dendrimer **3** (4.4 mg, 0.14 μmole) in anhydrous DMSO (0.978 mL), the Alkyne Ligand (58.0 μg, 0.286 μmole) in DMSO (29.2 μL), N,N-diisopropylethylamine (0.2 mg, 0.3 μL, 2 μmole), and PyBOP (0.15 mg, 0.29 μmole) in anhydrous DMSO (28 μL). Sample J was purified and lyophilized in the same manner as Sample I. The purified product, Sample J, was a white solid (3.1 mg, 70%). ^{1}H NMR integration determined the mean number of Alkyne Ligands per dendrimer to be 0.7.

Sample K

Sample K was synthesized in the same manner as Sample I, using partially acetylated dendrimer **3** (4.4 mg, 0.14 μmole) in anhydrous DMSO (0.978 mL), the Alkyne Ligand (0.15 mg, 0.72 μmole) in DMSO (73.0 μL), N,N-diisopropylethylamine (0.6 mg, 0.7 μL, 4 μmole), and PyBOP (0.37 mg, 0.72 μmole) in anhydrous DMSO (69 μL). Sample K was purified and lyophilized in the same manner as Sample I. The

purified product, Sample K, was a white solid (3.6 mg, 80%). ^{1}H NMR integration determined the mean number of Alkyne Ligands per dendrimer to be 2.7.

Sample L

Sample L was synthesized in the same manner as Sample I, using partially acetylated dendrimer **3** (4.4 mg, 0.14 μmole) in anhydrous DMSO (0.978 mL), the Alkyne Ligand (0.29 mg, 1.4 μmole) in DMSO (146 μL), N,N-diisopropylethylamine (1.1 mg, 1.5 μL, 8.6 μmole), and PyBOP (0.74 mg, 1.4 μmole) in anhydrous DMSO (138 μL). Sample L was purified and lyophilized in the same manner as Sample I. The purified product, Sample L, was a white solid (3.5 mg, 76%). ^{1}H NMR integration determined the mean number of Alkyne Ligands per dendrimer to be 6.8.

Sample M

Sample M was synthesized in the same manner as Sample I, using partially acetylated dendrimer **3** (4.4 mg, 0.14 μmole) in anhydrous DMSO (0.978 mL), the Alkyne Ligand (0.44 mg, 0.14 μmole) in DMSO (978 μL), N,N-diisopropylethylamine (1.7 mg, 2.2 μL, 13 μmole), and PyBOP (1.1 mg, 2.1 μmole) in anhydrous DMSO (207 μL). Sample M was purified and lyophilized in the same manner as Sample I. The purified product, Sample M, was a white solid (2.7 mg, 57%). ^{1}H NMR integration determined the mean number of Alkyne Ligands per dendrimer to be 10.2.

<center>**Results**</center>

Characterization of the Mean Ligand-dendrimer Ratio by ^{1}H NMR Spectroscopy

^{1}H NMR spectroscopy can directly measure the number and type of protons present in a sample. In order to obtain peak areas to compare the integrated ratios of the ligand to dendrimer, it is important to set an appropriate relaxation delay time in the ^{1}H NMR pulse sequence, especially since methyne aromatic protons are being compared to methylene protons. A ten second delay is sufficient to give quantitative integrations of the ligand/dendrimer ratio. When combined with GPC and potentiometic titration, this ratio was converted to the mean number of ligands per dendrimer in the following manner. The combination of potentiometric titration and number average molecular weight

measurements from GPC were used to calculate the mean number of end groups (112 ± 5) per amine-terminated dendrimer (G5-NH$_2$) as described.[4] Experimental characterization of this value rather than using the theoretical value (128) is critical to this process as many defect structures exist in PAMAM dendrimer.[44-46] Next, the ratio of methylene protons on the amine-terminated dendrimer arms (**Figure 3.2**, **panel a**, peaks c and e) to the methyl protons in the acetyl terminated arms (**Figure 3.2, panel a**, peak j) were combined with the total number of end groups per dendrimer to compute the mean number of methyl protons in the partially acetylated dendrimer **3** (240.0). The same calculation was performed for dendrimer **2**. For ligand-dendrimer samples in the partially acetylated dendrimer sets (Sample A-D and E-I), the integrated methyl proton peak was used as the internal reference peak to quantify the mean number of ligands based on integration of the aromatic aa' bb' pattern proton peaks in the Alkyne Ligand (**Figure 3.2, panel b**).

The number of methyl protons per partially acetylated dendrimer **3** also provided the basis to quantify the mean number of protons in the dendrimer interior. Because the partially acetylated dendrimer was synthesized from the same lot of amine-terminated dendrimer **1** (G5-NH$_2$) as was used in this chapter for the G5-NH$_2$ based sample set, it was assumed that the number of interior protons was constant for both dendrimer forms (partially acetylated **2 & 3** and un-acetylated **1**). Thus, the interior proton peaks f, h, and i were used as internal reference peaks to quantify the mean number of conjugated ligands in the G5-NH$_2$ samples (E-H) (**Figure 2, panel c**).

Table 3.1 contains the mean number of ligands per dendrimer computed based on the ^{1}H NMR spectroscopic characterization for Sample A-D and **Table 3.2** contains the mean number of ligands for Samples E-M. A comparison of the aa' bb' proton peaks for Samples E-H can be found in **Figure 3.3**. As the mean number of ligands per dendrimer increases, the peak full-width at half max (FWHM) was observed to increase. A linear fit was obtained ($R^2 = 0.98$) indicating that the FWHM of the aa' bb' proton peaks could be used to provide an estimate of the mean number of conjugated ligands. A linear relationship was also found between the FWHM and the total number of dendrimer-

ligand components present in each sample. This trend was also found for the aa' bb'
proton peaks for Samples I-M.

**HPLC Characterization of Dendrimer-ligand Samples Resolves Distributions of
Dendrimer-ligand Components and Provides the Mean, Median, and Mode**

HPLC separates samples based upon their interaction with the stationary phase
and the eluting solvent. Recently, we have discovered that certain alkyne and azide
ligands used for click chemistry also provide excellent tags for separation of the
distribution of dendrimer-ligand components using reverse phase HPLC. Although the
dendrimer alone is composed of a number of different structural forms as a result of
defects in the polymer backbone, the separation that is achieved using the alkyne and
azide ligands is limited to the number of ligands on the different structural forms of the
dendrimer. As such, the term "dendrimer-ligand component" in this manuscript refers to
any number of structurally different dendrimer conjugated with a specific number of
ligands.

Elution traces of the dendrimer-ligand conjugates were obtained at 210 nm using
a C5 reverse phase column under a gradient elution conditions. The 210 nm wavelength
was selected because it is convenient for monitoring the PAMAM dendrimers and is not
significantly affected by varying amounts of conjugated ligands.[47] Since the absorbance
at 210 nm scales linearly with dendrimer concentration, we can use the area of each
absorbance peak to obtain the relative concentration of each different dendrimer/ligand
conjugate. Dilution studies of the conjugates demonstrate that Beer's law is followed and
that each of the fitted peaks has the same extinction coefficient (**Figure 3.13**). The data
taken at 276 nm is useful in helping to confirm the HPLC peak assignments, but cannot
be used quantitatively for concentration determinations because each dendrimer/ligand
conjugate generates a dramatically different local concentration of ligand thus causing a
deviation from Beer's law.

The HPLC elution profiles obtained at 210 nm for samples A-D are illustrated in
Figure 3.4a, solid traces. The first large peak (0) appears at an elution time consistent

with unmodified $G5(Ac)_{78}(NH_2)_{34}$. The small peaks preceding peak 0 are also present in the original $G5(Ac)_{78}(NH_2)_{34}$ sample and likely result from a small amount of lower generation dendrimer.[48] The second large peak (1) was preliminarily assigned as $G5(Ac)_{78}(NH_2)_{33}(L)_1$ (L = $NHCO(CH_2)_2C_6H_4OCH_2C_2H$) based upon elution order (Figure 3a, solid traces A-D). Additional data supporting this assignment was obtained from the elution profile monitored at 276 nm (sample D, dashed trace). At 276 nm, an absorbance maximum for the ligand with minimal contribution from the dendrimer, peak 0 ($G5(Ac)_{78}(NH_2)_{34}$) largely disappears as anticipated for dendrimer with no ligand conjugated. In this case, the first major feature observed (peak 1) was assigned as the dendrimer component containing one conjugated ligand ($G5(Ac)_{78}(NH_2)_{33}(L)_1$). Note that this is consistent with the assignment obtained based on monitoring dendrimer at 210 nm.

The HPLC traces for Samples I-M are grouped in **Figure 3.5** by conjugate type (G5-NH$_2$-Alkyne, and G5-Ac$_{80}$-Alkyne). Traces were normalized and plotted on the vertical axis based on each sample's mean number of conjugated ligands. The trace of un-modified dendrimer for each conjugate set (**1**: $G5\text{-}(NH_2)_{112}$ and **3**: $G5\text{-}Ac_{80}\text{-}(NH_2)_{32}$) is also included.

Two major features were observed in **Figure 3.5**. The first feature, found in both conjugate sets, is the trend of increasing trace width as the sample mean increases. This trend is rather dramatic when one considers the width of the unmodified dendrimer profile. The second feature is the partial resolution of distinct peaks within each trace that have the same peak shape as the un-modified dendrimer. As in **Figure 3.4a**, these resolved peaks begin at the same retention time as the unmodified dendrimer and also occur at later retention times.

A comparison between the elution profiles of the G5-NH$_2$ set (Samples E-H) and the G5-Ac$_{80}$ set (Samples I-M) in **Figure 3.5**, columns a and b respectively, reveals several additional observations. Both the trace width and the relative amount of the initially resolved peaks within the sample trace are greater in the G5-Ac$_{80}$ based samples

74

than in the G5-NH$_2$ based samples with comparable means. The G5-NH$_2$ based conjugates exhibit a slightly skewed Poissonian profile where-as the G5-Ac$_{80}$ conjugates show an enhanced skewing. Finally, resolution of the initial peaks in the HPLC traces for the G5-Ac$_{80}$ set is greater compared to the G5-NH$_2$ set.

Deconvolution of HPLC Traces Using Peak Fitting

Peak fitting analysis provided a means to both identify additional dendrimer-ligand components in the "tailing" region of the HPLC traces and to quantify the relative concentration of each dendrimer-ligand component in a given sample. A fitting peak for each of the samples was developed by fitting the elution profile of each sample type's unmodified dendrimer (**2**: G5-Ac$_{78}$-(NH$_2$)$_{34}$, **1**: G5-(NH$_2$)$_{112}$ and **3**: G5-Ac$_{80}$-(NH$_2$)$_{32}$) using Igor Pro 6.01. The functional form employed for the fitting peak was a Gaussian with an exponential decay tail to the right side of the elution peak. Each of the elution profiles for all of the samples in this chapter were fit with multiple copies of this fitting peak. The position and area of the multiple fitting peaks were not constrained. The fit for sample D, which has a 1.47 ligand/dendrimer ratio measured by ^{1}H NMR spectroscopy, is illustrated in Figure 4b. **Figure 3.6** illustrates this multi-peak fitting process with Sample F and K. **Panel a** and **b** contain each sample's respective HPLC trace. The mean number of ligands for these samples is 3.8 and 2.7 respectively. In **Figure 3.6, panel c** and **d** the fits for Sample F and K are shown with the HPLC trace in red, the multiple copies of the fitting peak in green, and the summation of the fitting peak copies in blue. The position and area of each fitting peak copy were not constrained. Two copies of the fitting peaks were added to the left of peak 0 and constrained in position. These two small peaks were present in the un-modified dendrimer profile and are likely a result of a small amount of lower generation dendrimer.[48] With the fits for each sample, the relative concentration of each dendrimer-ligand component in the sample was determined.

In both HPLC traces in **Figure 3.6, panel a** and **b**, the first large peak (0) has the same retention time as the un-modified dendrimer: G5-(NH$_2$)$_{112}$ for **panel a** and G5-Ac$_{80}$-(NH$_2$)$_{32}$ for **panel b**. The second peak in both panels was assigned as being composed of

the dendrimer component with exactly 1 ligand (G5-$(NH_2)_{111}$-Alkyne$_1$ and G5-Ac$_{80}$-$(NH_2)_{30}$-Alkyne$_1$). It should be noted that in the naming of these components, the number of Alkyne ligands is an exact number while the number of –Ac groups and -NH_2 groups is actually the mean number. The four remaining partially resolved peaks in **panel a** and three in **panel b** were assigned to be dendrimer components with sequentially increasing numbers of ligands based on elution order. The additional peaks in the tailing region of the HPLC traces to the left of these partially resolved peaks that were identified by peak fitting (**panel c** and **d**) were similarly assigned. Analogous peak assignments were made for all of the dendrimer-ligand samples in this chapter.

Mean, Median, and Mode of Ligand-dendrimer Populations Obtained Using HPLC

The relative concentrations of dendrimer components, resolved by HPLC and quantified through the peak fitting analysis, were used to calculate the weighted arithmetic mean of ligands per dendrimer for each sample. This value can be directly compared to the value obtained using ^{1}H NMR spectroscopy (**Table 1** and **Table 2**). For all samples the HPLC mean is identical, within error, to the mean determined independently by the combined NMR/GPC/titration analysis. The weighted median and the mode were also determined for each sample.

Distribution Features

Relative concentrations of dendrimer-ligand components for all samples are plotted in **Figure 7** for Samples A-D and **Figure 8** for Samples E-M. In **Figure 8**, these distributions are grouped by sample set (**panel a** for G5-NH_2-Alkyne, and **panel b** for G5-Ac$_{80}$-Alkyne). Three common trends exist across the panels. First, the number of dendrimer-ligand components present in a sample increases as the mean ligand number increases. Second, with the exception of Samples H, L and M, between 8% and 44% of each sample is composed of un-modified dendrimer. In many cases, the un-modified dendrimer is in fact the most abundant component present. The third trend, again with the exception of Samples H, L and M, is that the mean dendrimer-ligand component is not identical to the median or mode dendrimer-ligand component.

Additional observations can be made within each of the two sample sets in **Figure 3.5**. The G5-NH$_2$-Alkyne samples (**Figure 3.8**, **panel a**) have skewed-Poissonian distribution profiles. A close comparison between each of these distributions and a Poisson distribution with the matching mean reveals that the sample distributions have an over-abundance of dendrimer-ligand components at both low and high regions of the distribution and an under-abundance of the dendrimer-ligand components with similar numbers of ligands to the sample's mean. The quantified dendrimer-ligand distributions on partially acetylated dendrimer (**Figure 3.8, panel b**) exhibit a much more pronounced version of this feature.

Figure 3.9 provides an additional perspective by grouping the samples based on the sample ligand mean rather than sample set. **Panel a** contains the two samples with the highest ligand means (10.2 and 12.9). **Panel b** contains the four samples with medium level ligand means (2.7-6.8). Finally, **panel c** contains the three samples with the lowest ligand means (0.4-1.1). The initial acylation had a significant effect on the dendrimer-ligand distribution resulting in a significant departure from a pure Poissonian distribution, far greater than was observed for the G5-NH$_2$ based samples. Also evident in **Figure 3.9** is the greater number of dendrimer-ligand components for the samples that were produced with the partially acetylated dendrimer compared to the G5-NH$_2$-based sample set.

Statistical Models Confirm Experimental Results

Three statistical models were employed for comparison with the experimentally determined distributions in Samples A-D (**Figure 3.7, Table 3.1**). Poisson model I assumed that ligand conjugation with the nanoparticle proceeds in a stochastic fashion. The total number of available attachment points on the dendrimer surface (34) and the average ligand/dendrimer ratio determined by NMR were used as input. This fit gave a χ^2 per degree of freedom of 66. In Poisson model II, the ligand/dendrimer ratios were allowed to vary as fitting parameters in a simultaneous χ^2 minimization using all four data sets. This fit gave a χ^2 per degree of freedom of 47. Both Poisson models match

the 0.20 and 0.60 ligand/dendrimer distributions quite well but begin to deviate from the experimental data as the ligand/dendrimer ratio increases.

In order to better reproduce the experimental ligand distributions, a two path kinetic model was used. It allowed for deviations from the Poisson distribution by varying the activation energy of the reaction as a function of n ligands on the nanoparticle (eq 1). This two path model was also motivated by previous publications which indicate product amide autocatalysis should be expected for this reaction [49-51].

$$R_n = A_1 e^{-E_{a1}/RT} + nA_2 e^{-E_{a2}/RT} \tag{1}$$

The two paths correspond to attaching a ligand far from other ligands or near enough to previously attached ligands so that the barrier for attachment is reduced. These rates are fed into a master equation for the concentrations, c_n, of dendrimers with n ligands attached: $\dot{c}_n = R_{n-1}c_{n-1} - R_n c_n$. $A_{1,2}$ were adjusted to account for the number of available sites for the two paths. The solutions of the master equations were fit to all four data sets simultaneously using five independent parameters (E_{a1}-E_{a2}, and four independent values for the A's), resulting in a χ^2 per degree of freedom of 9. The best fit reproduced the experimental changes in concentration which is a strong confirmation that the approach had physical meaning for this system. The difference in activation barrier between the two paths could be extracted from the fit and was determined to be $E_{a1} - E_{a2}$ = 4.0 ± 1.5 kJ/mol or 0.041 ± 0.016 eV.

Dendrimer-ligand Distributions are Not Resolved by GPC or MALDI-TOF

The resolution of the various conjugated components by HPLC stands in stark contrast to the results obtained by NMR in which no resolution of the various numbers of ligands conjugated is obtained. Gel permeation chromatography (GPC) of Samples A-D exhibits a trend towards longer retention time but does not resolve the components (**Figure 3.10a**). Note that the longer retention time indicates the conjugates are effectively smaller, as measured by GPC, although the light scattering and refractive index detectors verify that the mass has increased upon conjugation. MALDI-TOF of

Samples A-D also exhibits a trend to higher mass, but once again the individual components are not resolved (**Figure 3.10b**).

Distribution Estimations for Folic Acid and Methotrexate Conjugated Dendrimer

Based on the quantified dendrimer - alkyne ligand distributions described above, the ligand distributions for the FA- and MTX-conjugated dendrimer, described in the introduction, can be explored. As noted earlier, this particular dendrimer conjugate was determined to have a mean of 4 FA and 5 MTX molecules per dendrimer. Where-as the experimentally determined distributions in this chapter follow skewed-Poissonian functional forms, the mathematical model used for this investigation is a true Poisson model with a prescribed mean and number of available attachment points. Ligand distributions resulting from this model with means of 4 and 5 representing the FA and MTX ligand distributions are displayed in **Figure 3.11, panel a**. Both distributions are combined in a two-dimensional matrix in order to describe all of the different G5-FA-MTX components. The bar plot in **Figure 3.11, panel b** contains the sample concentrations for all of the different dendrimer components based on the Poisson distributions for the individual ligands. Approximately 182 (13x14) different G5-FA-MTX components are found in this plot. Only 3.9% of the total sample consists of a dendrimer with exactly 4 folic acid and 5 methotrexate molecules. It should be noted that these concentrations assume that the distribution of methotrexate, for example, is not influenced by the pre-existing distributions of acetyl groups, folic acid molecules and dye molecules that were present during the methotrexate conjugation.

The number of different components in **Figure 3.11, panel b** also does not take into account the different regioisomers of folic acid and methotrexate conjugates that have significantly different biological activities. Both compounds have two carboxylic acid groups (α and γ). Several studies have found that folic acid and methotrexate maintain their biological activity when conjugated through the γ-carboxylic acid and either completely lose or experience a substantial reduction in biological activity when conjugated via the α-carboxylic acid.[52-55] The EDC coupling method that is used to conjugate both folic acid and methotrexate to the dendrimer is not regiospecific and

79

results in three different derivatives of both folic acid and methotrexate: amide bond at the γ-position, amide bond at the α-position, and amide bonds at both α− and γ− positions. Taking the 3 different versions of methotrexate and folic acid into account means that this particular dendrimer system is composed of ~1638 different dendrimer components. Taking into account folic acid and methotrexate regiochemistry into the consideration of the percentage of sample containing 4 fully active folic acid and 5 fully active methotrexate significantly reduces the estimate from the 3.9% given above. Experimentally determined ratios of γ− vs. α− modified forms of folic acid and methotrexate vary from roughly 80% to 30% of the active γ−form relative to the other forms.[52,56-57] The amount of fully active material, when also including the effects of proper regiochemistry, ranges from 0.3% to less than 0.01%.

Discussion

A number of groups have sought to characterize nanoparticle-ligand distributions. Several different methods have been employed including gel electrophoresis[58], anion-exchange HPLC,[59] ultra performance liquid chromatography,[43] fluorescence resonance energy transfer,[60] mass spectrometry,[61] and fluorescence quenching.[62] The nature of the distribution of dendrimer-ligand components quantified in this manuscript suggest that, when possible, investigations of nanoparticle-ligand distributions should be incorporated in all future research studies pertaining to nanoparticle-ligand conjugates, as well as in the design of new generation nanoparticle-based systems. To fully understand the functionality of a nanoparticle-ligand system, knowledge of only the mean ligand/nanoparticle ratio is inadequate. This chapter provides new information about the relationship between the typically measured average and the actual material composition. Here we seek to address the questions raised earlier in this manuscript.

Relationship Between Mean, Median, and Mode

To the best of our knowledge, the average values for all nanoparticle-ligand systems published to-date have been arithmetic means. Values for the median and mode have never before been reported. This is a consequence of a reliance on mean-producing

characterization techniques and a lack of emphasis on determining the number and relative amount of the different components that gives rise to the mean. Differences between these three forms of the average can be indicative of distribution features. As seen in **Table 3.2**, in samples with means of ~6 or below, the mean, median, and mode can differ substantially. For Samples E, I, and J, which all have arithmetic means of 1 or less, the mode of the samples is actually 0. For Sample G, which has an arithmetic mean of 6, the mode is actually 4. Also note that for all samples except H, the mean is always the same or greater than the median and the mode. The significance of considering the various forms of the average value is most apparent when considering Samples E and K. In Sample E, although the mean is ~1, the mode is zero. If this ligand was a targeting agent, drug, or dye, the most common component in the dendrimer distribution would have no activity. In Sample K, although the mean is ~3, the mode is 1. If one was designing materials for multivalent targeting, the most common component would exhibit no multivalent binding. For such systems, cartoons that present the mean numbers of ligands are particularly misleading with regards to the biological activity that can be expected.

Dendrimer-ligand Samples are Heterogeneous

The dendrimer-ligand distributions that have been quantified in this chapter contradict the concept that such samples are functionally homogeneous, composed of a relatively small number of constituent components. Although G5 PAMAM dendrimers are, with PDIs as low as 1.01, characterized by high degrees of structural uniformity, this polymeric mono-dispersity is derived from a synthetic process that exposes a vast molar excess of the monomer unit to the number of attachment points available on the dendrimer. The ligand conjugation reactions to the dendrimer are distinctly different from the dendrimer synthesis because there is instead an excess of attachment points on the dendrimer relative to the molar amount of ligand added. The consequence of this stochastic condition is seen in the number of different dendrimer components for each sample, listed in **Table 3.2**. Sample I, with a ligand mean of 0.4 is composed of 4 different dendrimer-ligand components ranging from un-modified dendrimer to

dendrimer with 3 ligands. Sample H with the highest mean in this chapter (12.9) has 27 different components present ranging from dendrimer with no ligands up to dendrimer with 26 ligands.

The mathematical form that the distributions follow in dendrimer-ligand samples is a skewed-Poisson distribution. A comparison of experimentally quantified distributions with Poisson and Gaussian distribution models can be found in **Figure 3.12** for three of the G5Ac-based samples. The Gaussian comparisons are provided only because many scientists are used to thinking about a distribution of this form and it therefore provides an interesting comparison to the Poisson distribution. In addition, previous work quantifying biotin-dendrimer distributions compared the experimental results to a Gaussian distribution.[29] **Panel a** displays the distribution for Sample L with a mean of 6.8. Three distribution models are included: a Poisson distribution with a mean of 6.8 and 32 available attachment sites, and two Gaussian distributions with means of 6.8 and standard deviations of 1 and 4. Note that the Gaussian with a standard deviation of 1 resembles what one might expect to see in a "homogeneous" sample. This Gaussian distribution does not, however, agree with the heterogeneity observed in the experimental data. In fact, the standard deviation has to be increased to 4 in order to obtain a distribution that resembles Sample L. The distribution for Sample L is skewed from both the Gaussian w/ SD=4 and the Poisson distribution in that there is a systematic over-abundance of components with low and high ligand numbers and an under representation of components with numbers close to the mean.

The heterogeneity observed in these dendrimer-ligand conjugates raises substantial doubt that the mean alone is an adequate measurement to understand nanoparticle-ligand composition and function. As a single value, the mean does not capture the true diversity of components present in the material. Certainly, it is incorrect to infer that the majority of the population is within ± 1 ligands of the mean. The only exceptions, in Samples E-M, are samples E, I, and J. Note that all of these samples have low mean values (1.1 and lower), below the means typically used for functional dendrimer conjugates. In fact, for samples with ligand means of 6.8 and higher, the

majority of dendrimer components present is not even within ± 2 ligands of the mean. In addition to this, in many cases, the mean is not the component with the largest relative concentration (the mode). The final problem with relying exclusively on the mean to describe the material composition is that it is completely unable to detect changes in heterogeneity that are caused by differences in the dendrimers' synthetic history (for example, pre-existing distributions).

Pre-existing Distributions Increase Sample Heterogeneity

Many dendrimer-ligand systems employ a partial acylation step before conjugating additional ligands such as FA or MTX. Furthermore, when attaching different ligands it is common to utilize a sequential reaction strategy. In both of these situations, ligands are conjugated in the presence of a pre-existing distribution making ligand distributions highly sensitive to the nanoparticles' synthetic history.

It is clear from the distribution data that the partially acetylated dendrimer causes an enhanced departure from the slightly skewed Poisson distribution observed in G5-NH$_2$ based samples. Given that the acetylation reaction takes place with an excess of amine groups on the dendrimer relative to the amount of acetic anhydride added, the acetylation reaction itself should result in a distribution composed of dendrimer molecules with different numbers of acetyl groups and consequently a distribution of primary amines for future reactions. The key implication is that the ligand conjugation with the partially acetylated dendrimer takes place in the presence of a pre-existing distribution of primary amines in the dendrimer material. This pre-existing distribution creates a situation where-in dendrimer molecules with high degrees of acetylation have a lower likelihood of reacting with a ligand than the dendrimer molecules in the same sample that have lower degrees of acetylation. The broader implication of this effect is that when conjugating multiple different functional groups to the dendrimer using conjugation reactions conducted in series, each additional conjugation will experience an increased skewing of the distribution and sample heterogeneity.

In light of the effect that pre-existing distributions have on subsequent ligand conjugations, it is important to point out that the HPLC traces for the three un-modified dendrimer (**1**: G5-(NH$_2$), **2**: G5-Ac$_{78}$-(NH$_2$)$_{34}$ and **3**: G5-Ac$_{80}$-(NH$_2$)$_{32}$) are nearly identical. Indeed, the difference in surface-amine group heterogeneity between these two samples is not identified by this chromatographic technique. This case should serve as a warning in terms of the problems associated with making conclusions about sample mono-dispersity based on single peaks.

Implications of Nanoparticle-ligand Distributions for Understanding Nanoparticle-ligand Function

This chapter provides valuable insight into the functional ligand distributions that exist in nanoparticle-based systems particularly those highlighted in the introduction. For many of these systems, the distribution of nanoparticle-ligand components has not been incorporated into the interpretation of the nanomaterial's biological activity. One particularly relevant example is the multivalent targeting that has been observed for FA-conjugated dendrimer. Previously, Hong and colleagues studied the relationship between multivalent targeting and the mean number of FA per dendrimer using surface plasmon resonance (SPR) and flow cytometry.[63] Five dendrimer samples were generated with means between 2.6 to 13.7. Based on the distributions reported earlier in this manuscript, the dendrimer-folic acid samples were likely composed of between 12 and 27 different components.

In the context of multivalent targeting, consider Sample K and L. In Sample K, which has a mean of 2.7, approximately 36% of the total dendrimer are not capable of multivalent targeting because they have either 0 or 1 ligand. Approximately 50% of the sample has between 2 and 5 conjugated ligands which one might reasonably expect to have a multivalent capacity. The 14% of the sample composed of dendrimer with 6 or more ligands may actually be less effective at multivalent targeting both because of a decreased water solubility from the high number of hydrophobic ligand molecules and/or due to ligand-ligand self-aggregation problems.[64] Sample L, with a mean of 6.8, has about 65% of its dendrimer material in this high ligand range. About, 29% of the

dendrimer population is in the predicted optimal range necessary to achieve multi-valencey and about 6% appear incapable of multivalent targeting. This type of analysis can also be applied to multi-ligand systems such as the G5-FA-MTX dendrimer, which would have very complex distributions of its three components (FA, MTX, and acetyl groups). With over 1600 different components, it appears evident that not all components have equal functionalities. In fact, it is very likely that only a small portion of the total material is actually capable of the desired activity. Given the diversity of components in these materials, interpreting biological results based solely on the mean number of functional groups ignores the varying contributions of individual dendrimer components and their concentration relative to the other components present. Incorporating this reality into future studies may lead to significant improvements in nanoparticle-ligand systems design particularly if specific dendrimer components are identified as having significantly enhanced biological activity.

Implications of Distributions for Platform Design

For dendrimer-ligand systems we propose three modifications to the current multi-functional dendrimer design and synthesis strategy to better control the distribution of dendrimer-ligand components. First, attempts should be made to eliminate the initial partial acetylation of the dendrimer. Although the partially acetylated dendrimer does have the benefit of enhanced solubility in several solvents that are commonly used for functional ligand conjugations, this chapter demonstrates that skipping this step will lead to a less disperse dendrimer-ligand sample. Second, synthetic strategies that reduce the number of sequential conjugations to the dendrimer should be explored. This could include both combining different functional ligands together before conjugation to the dendrimer, as well as limiting the number of different ligands being conjugated to the dendrimer. Finally, synthetic strategies and separation techniques should be developed that can reduce the distribution of dendrimer components within a sample.

Conclusion

The distributions of dendrimer-ligand components in samples with means between 0.4 and 13 ligands per dendrimer were resolved and quantified using HPLC. The use of partially acetylated dendrimer was found to have a significant effect upon the distribution of dendrimer-ligand components causing a greater skewing from a Poissonian distribution compared to samples prepared using the amine terminated dendrimer. This suggests that dendrimer-ligand distributions are highly sensitive to the particular dendrimer batch's synthetic history and that these results are applicable to a number of different functional ligands. For the range of dendrimer-ligand samples covered in this chapter, the average structure does a poor job reflecting the diversity of dendrimer-ligand components that exist in each sample. In many cases, the dendrimer-ligand component with the same number of ligands as the mean number is not even the most abundant component. Knowledge of these distributions for functional nanomaterials can lead to improved system design and predictions of structure, function and activity of the generated material.

Acknowledgements

Table 3.1: Comparison of the average number of ligands per dendrimer independently computed by NMR and HPLC techniques with the three statistical models.

	NMR Average	HPLC Average[a]	Poisson I ($\chi^2 = 66$)[b]	Poisson II ($\chi^2 = 47$)	Two Path ($\chi^2 = 9$)
Sample A	0.20 ± 0.02	0.20 ± 0.01	0.20	0.21	0.21
Sample B	0.60 ± 0.06	0.54 ± 0.02	0.60	0.53	0.54
Sample C	1.04 ± 0.10	0.98 ± 0.04	1.04	0.91	0.93
Sample D	1.47 ± 0.15	1.45 ± 0.06	1.47	1.17	1.32

[a]Determination of HPLC error is discussed in the Experimental Methods section of the Supporting Information.

[b]The Poisson I model uses the experimental NMR averages as input parameters.

Table 3.2: Comparison of the average number of ligands per dendrimer computed by two independent techniques (NMR spectroscopy and HPLC).

	G5-NH$_2$-Alkyne				
	NMR	**HPLC**			
	Arithmetic Mean	**Arithmetic Mean**	**Median**	**Mode**	**# Dendrimer Species**
Sample E	1.1 ± 0.1	0.9 ± 0.04	1	0	6
Sample F	3.8 ± 0.4	3.7 ± 0.2	3	3	14
Sample G	5.7 ± 0.6	5.8 ± 0.2	5	4	18
Sample H	12.9 ± 1.3	13.9 ± 0.6	14	16	27
	G5-Ac$_{80}$-Alkyne				
	NMR	**HPLC**			
	Arithmetic Mean	**Arithmetic Mean**	**Median**	**Mode**	**# Dendrimer Species**
Sample I	0.43 ± 0.04	0.4 ± 0.01	0	0	4
Sample J	0.7 ± 0.07	0.6 ± 0.02	0	0	5
Sample K	2.7 ± 0.3	2.8 ± 0.1	2	1	12
Sample L	6.8 ± 0.7	7.2 ± 0.3	7	7	18
Sample M	10.2 ± 1.0	11.2 ± 0.5	11	11	24
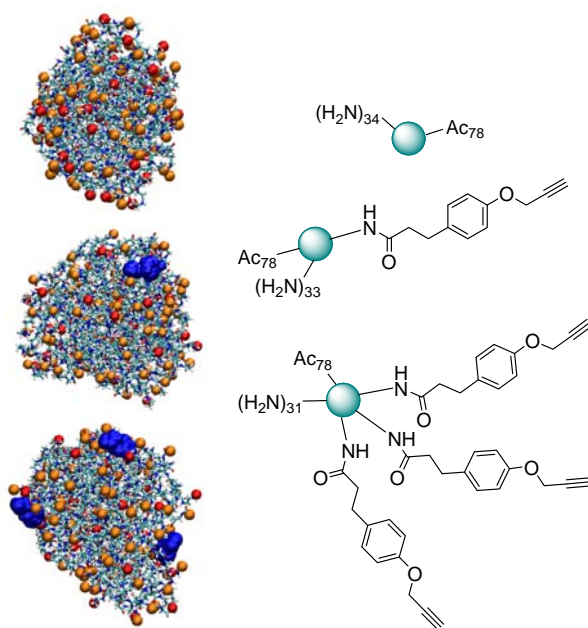
Figure 3.1: Equilibrated molecular dynamics models and schematics of G5 PAMAM dendrimers with different numbers of ligands. Terminal amines (red), acetyl groups (orange), and ligands (blue) are depicted in the models. Corresponding schematic representations show the dendrimer in teal with terminal groups. PAMAM dendrimers are monodisperse, highly ordered, water soluble, polymeric nanoparticles (~4.5 nm diameter). Terminal amines can be used as coupling points to attach different ligands.

Figure 3.2: ^{1}H NMR spectra of PAMAM dendrimer conjugates. a) Spectrum of the partially acetylated dendrimer G5-Ac$_{80}$-(NH$_2$)$_{32}$ **2**. Comparison of 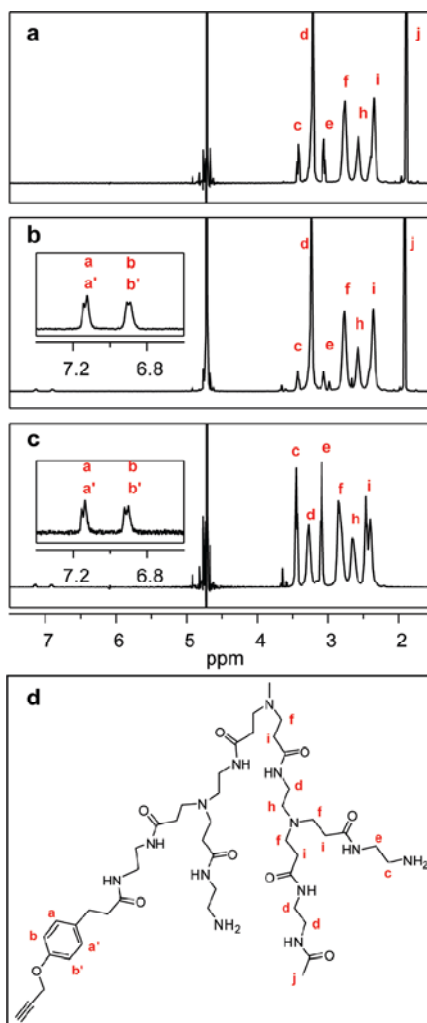peak integrals for the methylene protons (c and e) on primary amine terminated dendrimer arms with the methyl protons (j) that are unique to acetamide terminated arms was used to determine the mean ratio of dendrimer arms. Combining this ratio with the mean total number of arms per dendrimer, determined by potentiometric titration and the number average molecular weight measurement from GPC, provides the mean number of amine and acetamide terminated arms per dendrimer. These peaks were used as internal reference peaks to determine the mean number of dendrimer interior protons (f, h, and i). b) Spectrum of the partially acetylated dendrimer with a mean of 2.7 alkyne ligands G5-Ac$_{80}$-(NH$_2$)$_{29}$-Alkyne$_{2.7}$ (Sample K). The mean number of ligands was calculated using the aromatic aa' bb' proton peaks in the alkyne ligand and the methyl proton peak j. c) Spectrum of the amine-terminated dendrimer with a mean of 3.8 alkyne ligands G5-(NH$_2$)$_{108}$-Alkyne$_{3.8}$ (Sample F). The mean number of ligands was calculated using the aromatic aa' bb' proton peaks in the alkyne ligand and the internal dendrimer proton peaks f, h, and i. d) Chemical structure and proton labels of four terminal dendrimer arms with three different end group terminations: amine, actyl, amine, and the alkyne ligand (listed right to left).

90
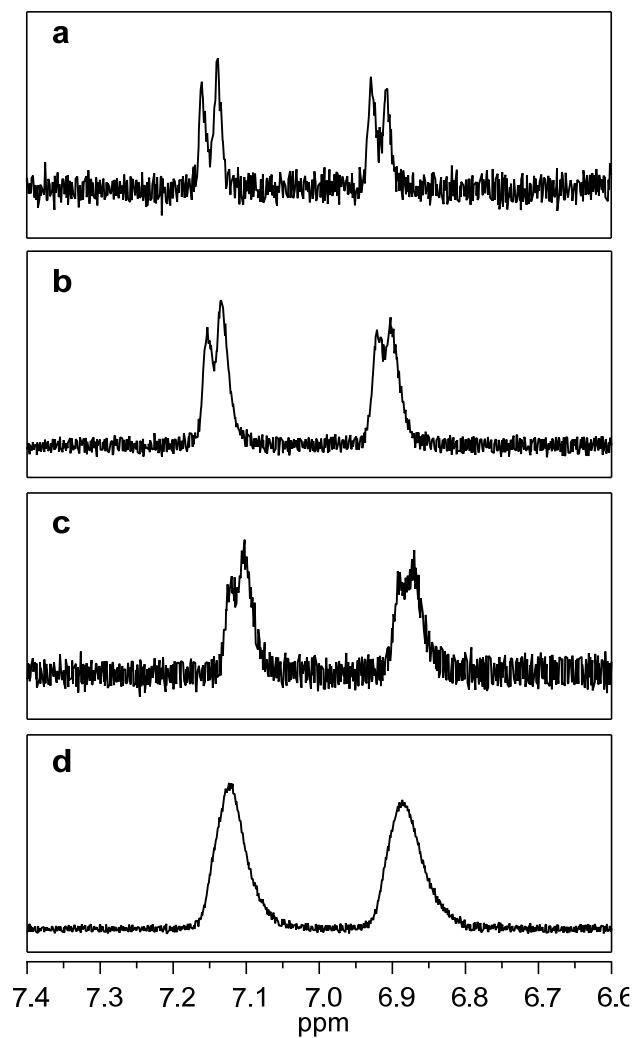
Figure 3.3: Expanded view of the aa' bb' proton peaks in the ^{1}H NMR spectra of Samples E-H (panel a-d respectively). As the mean number of ligands increases from 1.1 to 12.9, the full width at half max (FWHM) of both aromatic peaks increases: 13.1 Hz, 15.6 Hz, 17.3 Hz, and 21.3 Hz respectively.
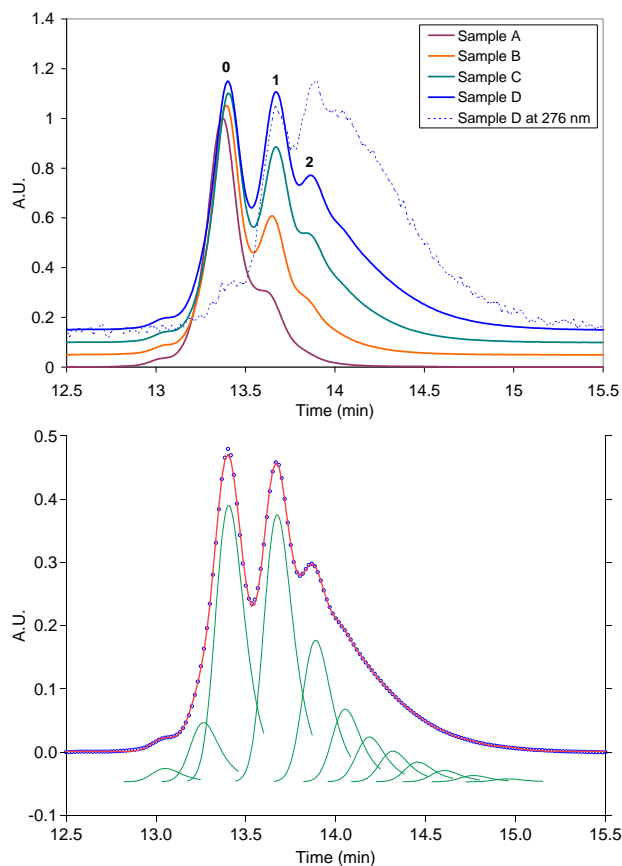
Figure 3.4: HPLC elution data for dendrimer-ligand conjugates: (a) Dendrimer concentration monitored at 210 nm for Samples A-D are shown with solid lines. The elution profile of Sample D at 276 nm, which is the maximum absorbance for the ligand, is displayed with a dashed line. Absorbance is normalized to the peak maximum. (b) The elution profile at 210 nm for Sample D is shown in blue. Individual fitted peaks are presented in green and the summation of the fitted peaks are in red.
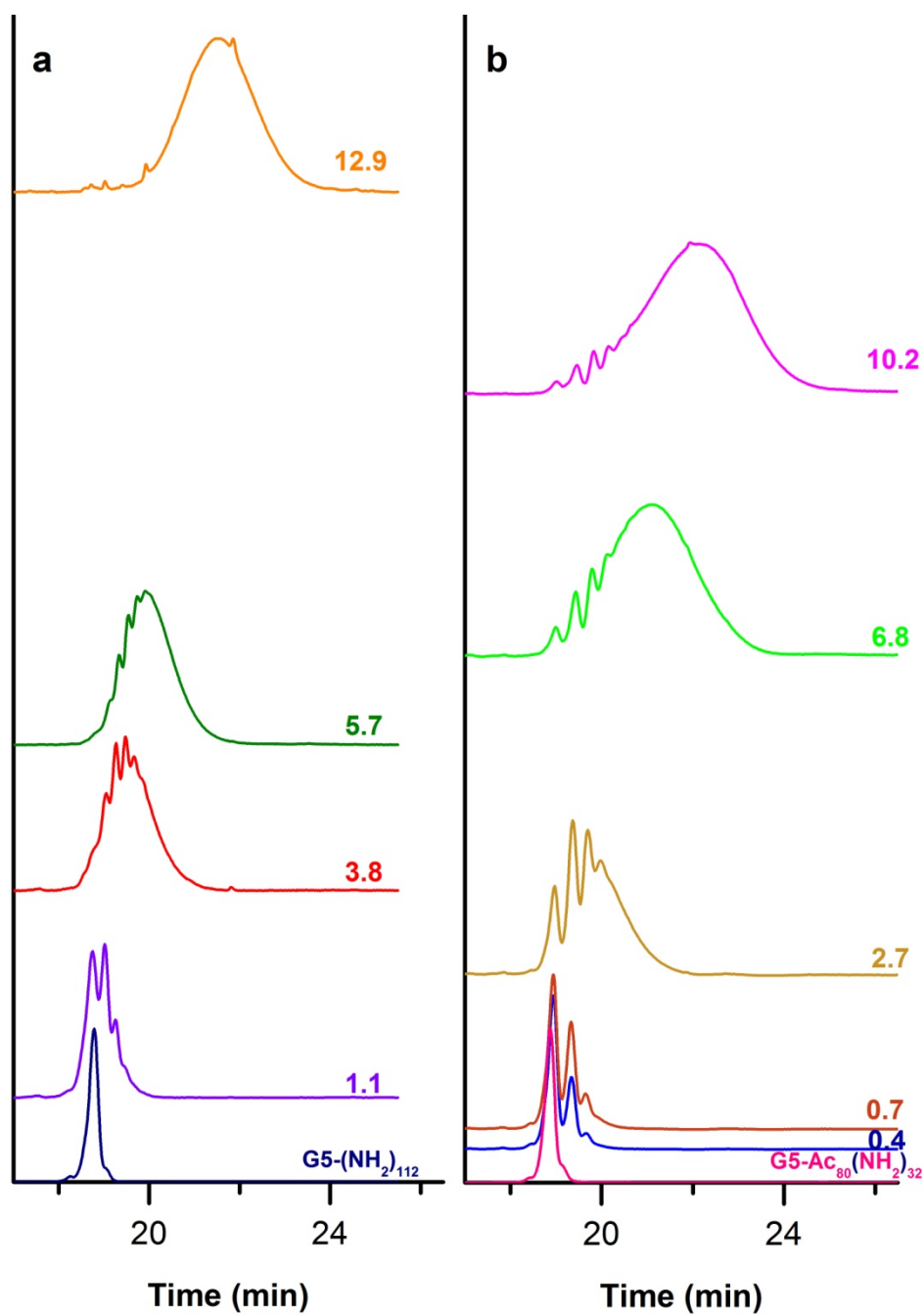
Figure 3.5: HPLC elution traces of dendrimer-ligand conjugates at 210 nm. Traces were normalized to the largest peak and off-set on the vertical axis based on the mean number of ligands per dendrimer. The HPLC trace of the un-modified parent dendrimer for each sample set is provided at the base of each panel (G5-$(NH_2)_{112}$ and G5-Ac_{80}-$(NH_2)_{32}$). a) HPLC traces for the G5-NH_2-Alkyne sample set (Samples E-H). b) HPLC traces for the G5-Ac_{80}-Alkyne sample set (Samples I-M).
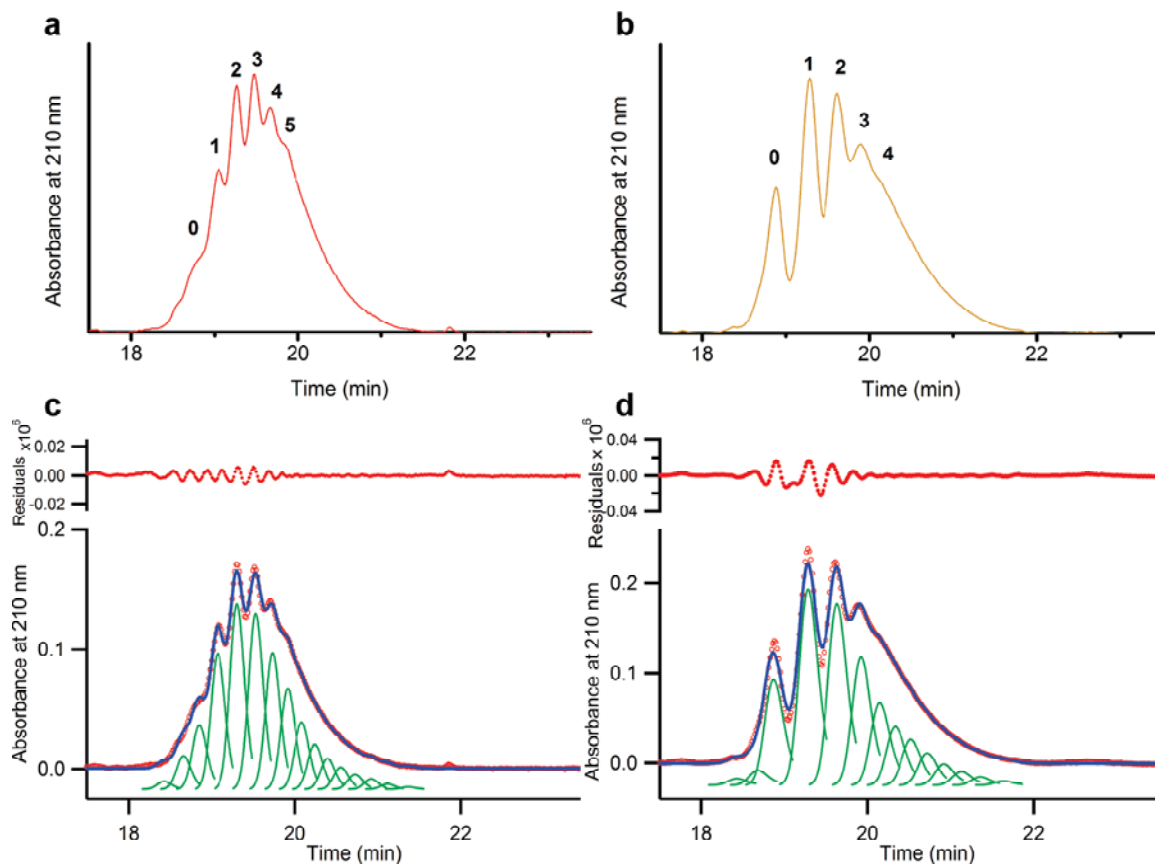
Figure 3.6: Peak fitting method quantifies the distribution of dendrimer-ligand components resolved in the HPLC elution traces. a) HPLC trace at 210 nm of Sample F (G5-$(NH_2)_{108}$-Alkyne$_{3.8}$). Six different peaks (0-5) were observed in the sample's trace. Peak 0 had the same retention time as the parent dendrimer (G5-$(NH_2)_{112}$). b) HPLC trace at 210 nm of Sample K (G5-Ac$_{80}$-$(NH_2)_{109}$-Alkyne$_{2.7}$). Six different peaks (0-5) were observed in the sample's trace. Peak 0 had the same retention time as the parent dendrimer (G5-Ac$_{80}$-$(NH_2)_{32}$). c) Fitted HPLC trace for Sample F. The experimental HPLC data is shown with red dots, individual fitting peaks are plotted in green, and the summation of the fitting peaks is plotted in blue. The fitting peak was developed to have the same shape as the parent dendrimer. d) Fitted HPLC trace for Sample K. The color code for panel d is the same as panel c. Residual values for panels c and d are10^{-6}.
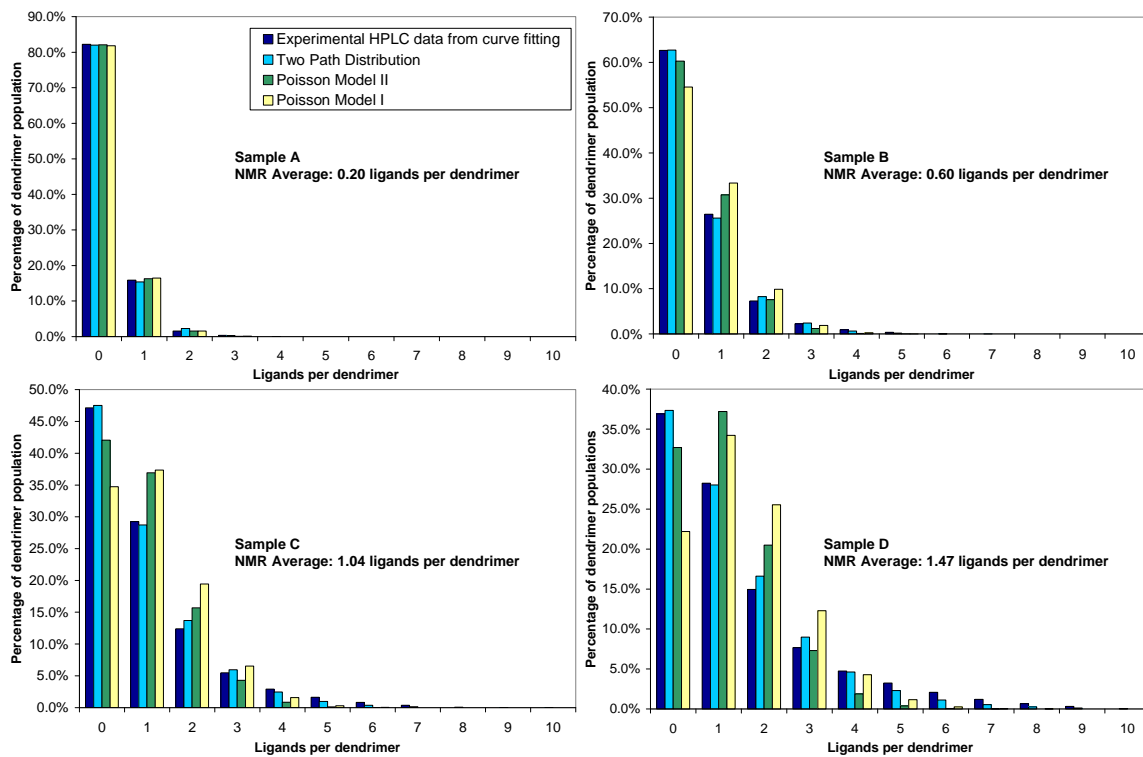
Figure 3.7: Experimental and statistical distributions of ligand-dendrimer conjugates A-D. Experimental distribution is calculated from fitted peaks to the HPLC elution profiles.
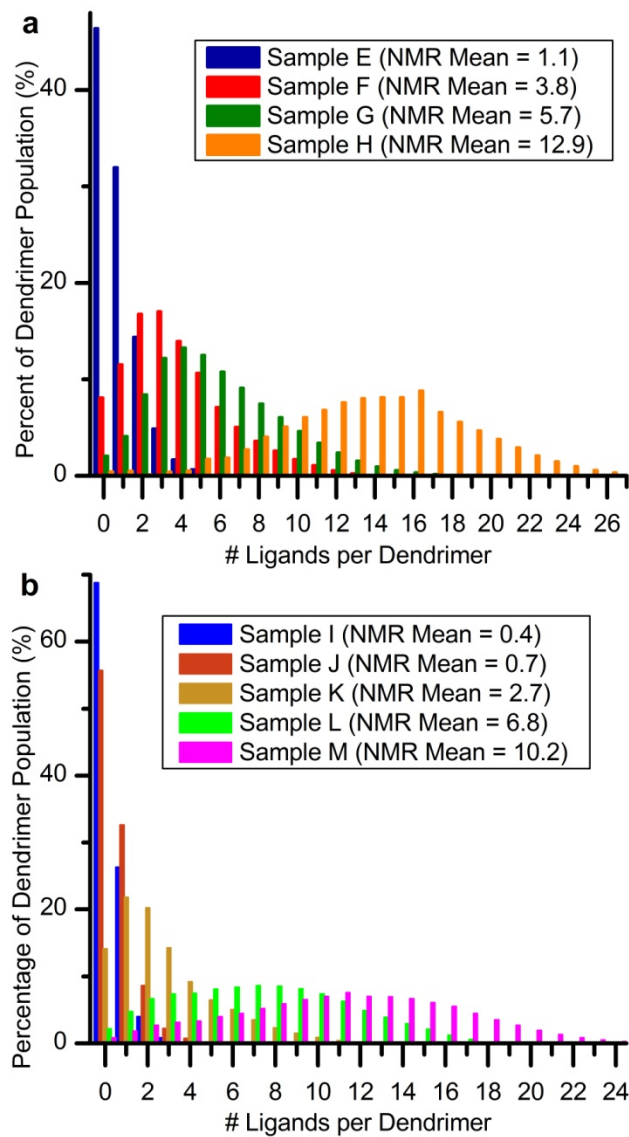
Figure 3.8: Quantified dendrimer-ligand distributions determined by the peak fitting enabled decovolution of the HPLC traces. a) Dendrimer-ligand distributions for G5-NH_2-based samples (Samples E-H). b) Dendrimer-ligand distributions for G5-Ac_{80}-$(NH_2)_{32}$-based samples (Samples I-M).
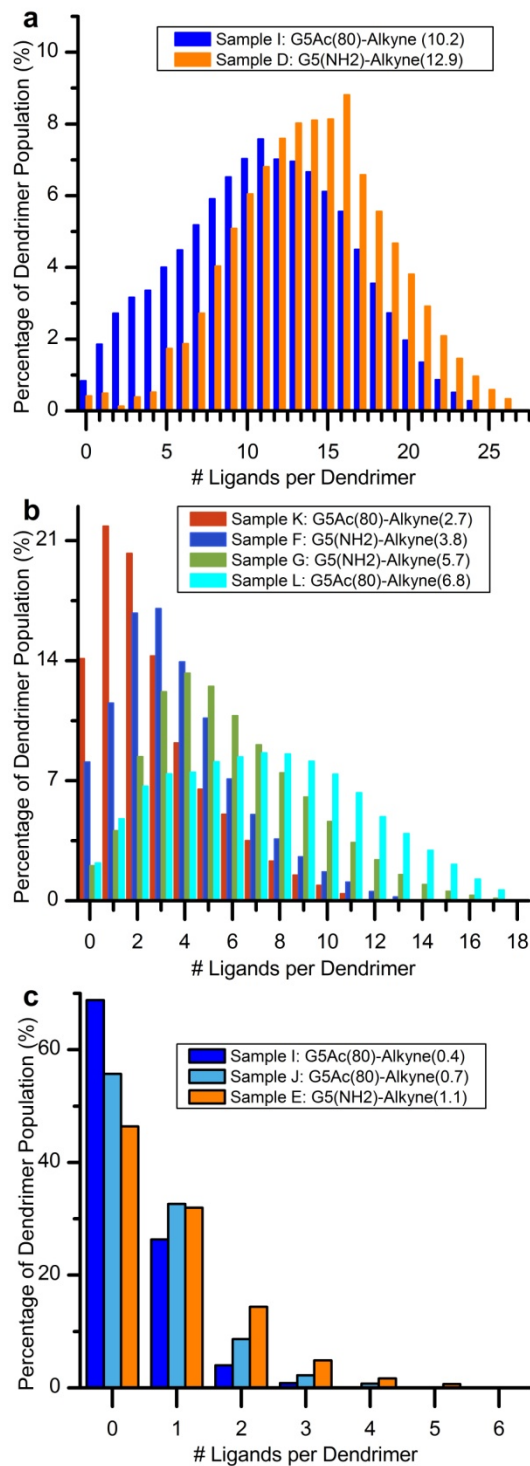
Figure 3.9: Comparison of dendrimer-ligand distributions for samples with similar ligand means. a) Distributions for Samples I and D with ligand means of 10.2 and 12.9, respectively. b) Distributions for samples with means between 2.7 and 6.8 (Samples G, B, C and H). c) Distributions for samples with means between 0.4 and 1.1 (Samples E, F and A).
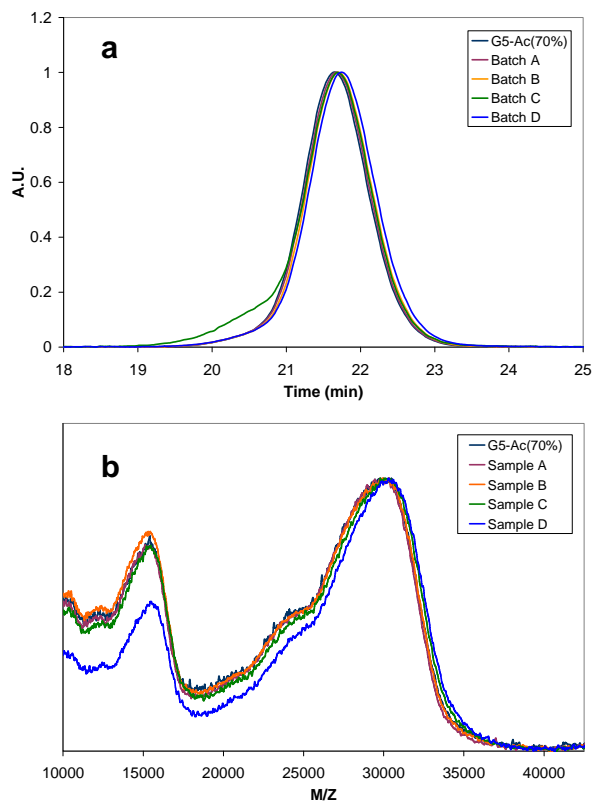
Figure 3.10: Standard analytical techniques that are commonly utilized to characterize nanoparticle conjugates fail to detect the different dendrimer-ligand populations: (a) The light scattering data of four dendrimer-ligand samples and partially acetylated dendrimer starting material, as separated by Gel Permeation Chromatography (GPC), clearly demonstrates the challenges in detecting the different populations based on differences in size. The single peak resolution achieved by GPC is in stark contrast to the multiple peak resolution achieved by HPLC (See Supporting Information for GPC conditions). (b) Similarly, molecular weight analysis of the same material by Matrix-Assisted, Laser-Desorption Time-of-Flight Mass Spectroscopy (MALDI-TOF) cannot detect significant differences between the five samples. (See Supporting Information for MALDI-TOF conditions)
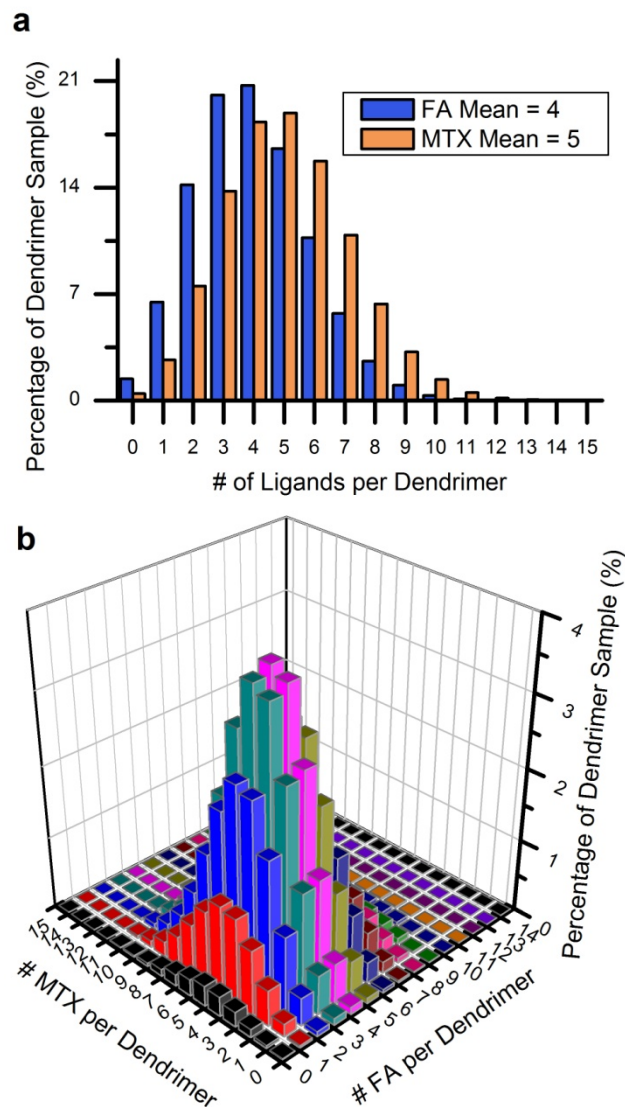
Figure 3.11: Theoretical distribution of dendrimer components that compose a dendrimer sample with a mean of 4 folic acid and 5 methotrexate molecules per dendrimer. This figure assumes that folic acid and methotrexate follow Poissonian distributions (statistically distributed). a) Poisson distributions with means of 4 and 5 molecules per dendrimer. b) The relative concentration of dendrimer components with different numbers of folic acid and methotrexate. Approximately 4% of the dendrimer sample is composed of a dendrimer with exactly 4 folic acid and 5 methotrexate molecules. Only 0.3 to < 0.01% is expected to consist 4 folic acid and 5 methotrexate molecules with the optimally active γ regiochemistry.
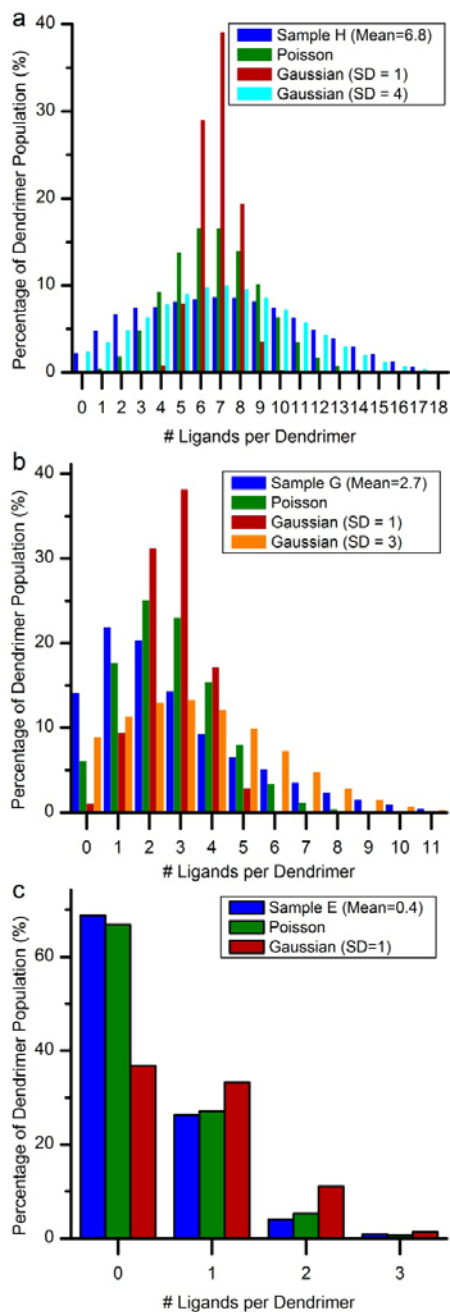
Figure 3.12: Comparison of dendrimer-ligand distributions with Poisson and Gaussian distributions. In all cases, the Poisson distribution has two inputs: the ligand mean and the total number of available attachment points on the dendrimer surface (32). The Gaussian distribution also has two inputs: the ligand mean and the standard deviation. a) The distribution for Sample H with a mean of 6.8 ligands per dendrimer. Two Gaussian distributions are show, each with means of 6.8 and with standard deviations of 1 (gold) and 4 (blue). b) The distribution for Sample G with a mean of 2.7 ligands per dendrimer. Two Gaussian distributions are show, each with means of 2.7 and with standard deviations of 1 (pink) and 3 (green). c) The distribution for Sample E with a mean of 0.4 ligands per dendrimer. The Gaussian distribution has a mean of 0.4 and a standard deviation of 1 (navy).

100
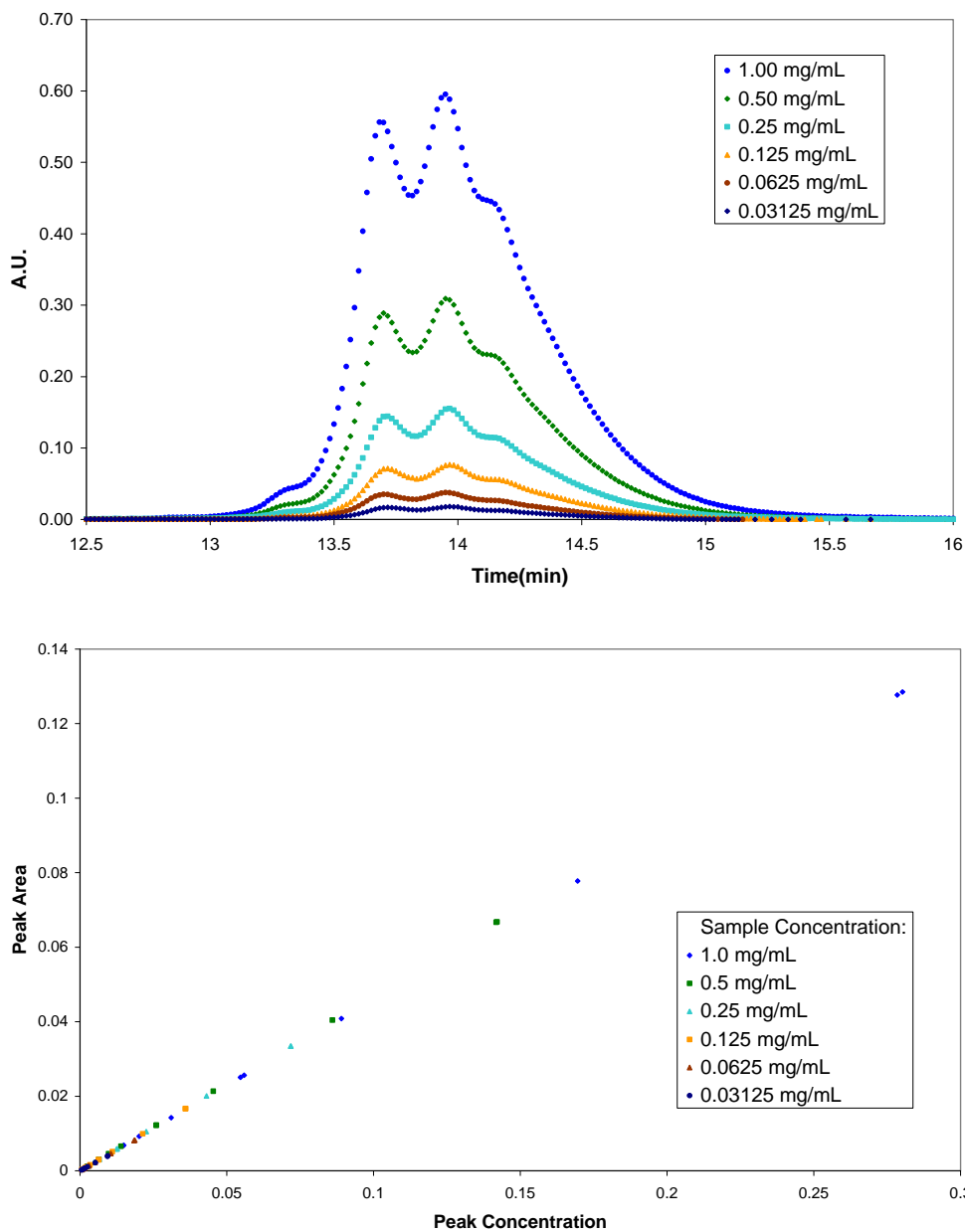
Figure 3.13: Beer's Law analysis for dendrimer-ligand conjugates at 210nm. A dilution study of Sample D was performed to demonstrate that the dendrimer conjugates follow Beer's Law at 210 nm. Solutions of Sample D with different concentrations were injected on the HPLC using the conditions detailed in the Methods section of this publication. **a)** The elution profile at 210 nm of Sample D at varying concentrations. **b)** Using the fitting procedure described earlier in this publication, peaks were fit to each of the elution profiles for the different sample concentrations. Peak concentration was calculated as the product of the Peak Area Fraction and the Sample Concentration. The linear relationship found between Peak Area and Peak concentration clearly demonstrates that Beer's Law is followed at 210 nm for the dendrimer conjugates in this study.

References

(1)   Majoros, I. J.; Keszler, B.; Woehler, S.; Bull, T.; Baker, J. R. *Macromolecules* **2003**, *36*, 5526-5529.

(2)   Quintana, A.; Raczka, E.; Piehler, L.; Lee, I.; Myc, A.; Majoros, I.; Patri, A. K.; Thomas, T.; Mule, J.; Baker, J. R. *Pharmaceutical Research* **2002**, *19*, 1310-1316.

(3)   Patri, A. K.; Myc, A.; Beals, J.; Thomas, T. P.; Bander, N. H.; Baker, J. R. *Bioconjugate Chemistry* **2004**, *15*, 1174-1181.

(4)   Majoros, I. J.; Thomas, T. P.; Mehta, C. B.; Baker, J. R. *Journal of Medicinal Chemistry* **2005**, *48*, 5892-5899.

(5)   Shukla, R.; Thomas, T. P.; Peters, J.; Kotlyar, A.; Myc, A.; Baker, J. R. *Chemical Communications* **2005**, 5739-5741.

(6)   Tong, R.; Cheng, J. J. *Polymer Reviews* **2007**, *47*, 345-381.

(7)   Rawat, M.; Singh, D.; Saraf, S.; Saraf, S. *Biological and Pharmaceutical Bulletin* **2006**, *29*, 1790-1798.

(8)   Patri, A. K.; Majoros, I. J.; Baker, J. R. *Current Opinion in Chemical Biology* **2002**, *6*, 466-471.

(9)   Peer, D.; Karp, J. M.; Hong, S.; FaroKhzad, O. C.; Margalit, R.; Langer, R. *Nature Nanotechnology* **2007**, *2*, 751-760.

(10)   Fortin, J. P.; Wilhelm, C.; Servais, J.; Menager, C.; Bacri, J. C.; Gazeau, F. *Journal of the American Chemical Society* **2007**, *129*, 2628-2635.

(11)   Johns, R. E.; El-Sayed, M. E. H.; Bulmus, V.; Cuschieri, J.; Maier, R.; Hoffman, A. S.; Stayton, P. S. *Journal of Biomaterials Science-Polymer Edition* **2008**, *19*, 1333-1346.

(12)   Josephson, L.; Tung, C. H.; Moore, A.; Weissleder, R. *Bioconjugate Chemistry* **1999**, *10*, 186-191.

(13)   Babic, M.; Horak, D.; Trchova, M.; Jendelova, P.; Glogarova, K.; Lesny, P.; Herynek, V.; Hajek, M.; Sykova, E. *Bioconjugate Chemistry* **2008**, *19*, 740-750.

(14)   Nie, S. M.; Xing, Y.; Kim, G. J.; Simons, J. W. *Annual Review of Biomedical Engineering* **2007**, *9*, 257-288.

(15)   Landmark, K. J.; DiMaggio, S.; Ward, J.; Kelly, C.; Vogt, S.; Hong, S.; Kotlyar, A.; Myc, A.; Thomas, T. P.; Penner-Hahn, J. E.; Baker, J. R.; Holl, M. M. B.; Orr, B. G. *ACS Nano* **2008**, *2*, 773-783.

(16)   Kircher, M. F.; Mahmood, U.; King, R. S.; Weissleder, R.; Josephson, L. *Cancer Research* **2003**, *63*, 8122-8125.

(17)   Jain, K. K. *Clinica Chimica Acta* **2005**, *358*, 37-54.

(18)   Pandana, H.; Aschenbach, K. H.; Gomez, R. D. *Ieee Sensors Journal* **2008**, *8*, 661-666.

(19)   Park, S. J.; Taton, T. A.; Mirkin, C. A. *Science* **2002**, *295*, 1503-1506.

(20)   Myc, A.; Patri, A. K.; Baker, J. R. *Biomacromolecules* **2007**, *8*, 2986-2989.

(21)   Chandrasekar, D.; Sistla, R.; Ahmad, F. J.; Khar, R. K.; Diwan, P. V. *Biomaterials* **2007**, *28*, 504-512.

(22)   Derfus, A. M.; Chen, A. A.; Min, D. H.; Ruoslahti, E.; Bhatia, S. N. *Bioconjugate Chemistry* **2007**, *18*, 1391-1396.

(23)   Schellenberger, E. A.; Reynolds, F.; Weissleder, R.; Josephson, L. *ChemBioChem* **2004**, *5*, 275-279.

(24)   Polito, L.; Colombo, M.; Monti, D.; Melato, S.; Caneva, E.; Prosperi, D. *Journal of the American Chemical Society* **2008**, *130*, 12712-12724.

(25)   Choi, Y.; Thomas, T.; Kotlyar, A.; Islam, M. T.; Baker, J. R. *Chemistry and Biology* **2005**, *12*, 35-43.

(26)   Choi, Y. S.; Mecke, A.; Orr, B. G.; Holl, M. M. B.; Baker, J. R. *Nano Letters* **2004**, *4*, 391-397.

(27)   Majoros, I. J.; Myc, A.; Thomas, T.; Mehta, C. B.; Baker, J. R. *Biomacromolecules* **2006**, *7*, 572-579.

(28)   Chandrasekar, D.; Sistla, R.; Ahmad, F. J.; Khar, R. K.; Diwan, P. V. *Journal of Biomedical Materials Research Part A* **2007**, *82A*, 92-103.

(29)   Hill, E.; Shukla, R.; Park, S. S.; Baker, J. R. *Bioconjugate Chemistry* **2007**, *18*, 1756-1762.

(30)   Aubin-Tam, M. E.; Hamad-Schifferli, K. *Biomedical Materials* **2008**, *3*.

(31)   Cloninger, M. J. *Current Opinion in Chemical Biology* **2002**, *6*, 742-748.

(32)   Lee, C. C.; MacKay, J. A.; Frechet, J. M. J.; Szoka, F. C. *Nature Biotechnology* **2005**, *23*, 1517-1526.

(33)   Svenson, S.; Tomalia, D. A. *Advanced Drug Delivery Reviews* **2005**, *57*, 2106-2129.

(34)   Gillies, E. R.; Frechet, J. M. J. *Drug Discovery Today* **2005**, *10*, 35-43.

(35)   Wolinsky, J. B.; Grinstaff, M. W. *Advanced Drug Delivery Reviews* **2008**, *60*, 1037-1055.

(36)   Kukowska-Latallo, J. F.; Candido, K. A.; Cao, Z. Y.; Nigavekar, S. S.; Majoros, I. J.; Thomas, T. P.; Balogh, L. P.; Khan, M. K.; Baker, J. R. *Cancer Research* **2005**, *65*, 5317-5324.

(37)   Thomas, T. P.; Majoros, I. J.; Kotlyar, A.; Kukowska-Latallo, J. F.; Bielinska, A.; Myc, A.; Baker, J. R. *Journal of Medicinal Chemistry* **2005**, *48*, 3729-3735.

(38)   Myc, A.; Douce, T. B.; Ahuja, N.; Kotlyar, A.; Kukowska-Latallo, J.; Thomas, T. P.; Baker, J. R. *Anti-Cancer Drugs* **2008**, *19*, 143-149.

(39)   Baek, M. G.; Roy, R. *Bioorganic and Medicinal Chemistry* **2002**, *10*, 11-17.

(40)   Wu, G.; Barth, R. F.; Yang, W. L.; Chatterjee, M.; Tjarks, W.; Ciesielski, M. J.; Fenstermaker, R. A. *Bioconjugate Chemistry* **2004**, *15*, 185-194.

(41)   Wu, P.; Malkoch, M.; Hunt, J. N.; Vestberg, R.; Kaltgrad, E.; Finn, M. G.; Fokin, V. V.; Sharpless, K. B.; Hawker, C. J. *Chemical Communications* **2005**, 5775-5777.

(42)   Mullen, D. G.; Desai, A. M.; Waddell, J. N.; Cheng, X. M.; Kelly, C. V.; McNerny, D. Q.; Majoros, I. J.; Baker, J. R.; Sander, L. M.; Orr, B. G.; Holl, M. M. B. *Bioconjugate Chemistry* **2008**, *19*, 1748-1752.

(43)   Cason, C. A.; Oehrle, S. A.; Fabre, T. A.; Girten, C. D.; Walters, K. A.; Tomalia, D. A.; Haik, K. L.; Bullen, H. A. *Journal of Nanomaterials* **2008**, doi:10.1155/2008/456082.

(44)   Peterson, J.; Allikmaa, V.; Subbi, J.; Pehk, T.; Lopp, M. *European Polymer Journal* **2003**, *39*, 33-42.

(45)   Giordanengo, R.; Mazarin, M.; Wu, J. Y.; Peng, L.; Charles, L. *International Journal of Mass Spectrometry* **2007**, *266*, 62-75.

(46)   Tolic, L. P.; Anderson, G. A.; Smith, R. D.; Brothers, H. M.; Spindler, R.; Tomalia, D. A. *International Journal of Mass Spectrometry* **1997**, *165*, 405-418.

(47)   Islam, M. T.; Majoros, I. J.; Baker, J. R. *Journal of Chromatography B-Analytical Technologies in the Biomedical and Life Sciences* **2005**, *822*, 21-26.

(48)   Shi, X. Y.; Bi, X. D.; Ganser, T. R.; Hong, S. P.; Myc, L. A.; Desai, A.; Holl, M. M. B.; Baker, J. R. *Analyst* **2006**, *131*, 842-848.

(49)   Menger, F. M.; Eliseev, A. V.; Khanjin, N. A. *Journal of the American Chemical Society* **1994**, *116*, 3613-3614.

(50)   Menger, F. M.; Eliseev, A. V.; Khanjin, N. A.; Sherrod, M. J. *Journal of Organic Chemistry* **1995**, *60*, 2870-2878.

(51)   Titskii, G. D.; Litvinen, L. M. *Zhurnal Obshchei Khimii* **1970**, *40*, 2680-2688.

(52)   Wang, S.; Lee, R. J.; Mathias, C. J.; Green, M. A.; Low, P. S. *Bioconjugate Chemistry* **1996**, *7*, 56-62.

(53)   Ke, C. Y.; Mathias, C. J.; Green, M. A. *Advanced Drug Delivery Reviews* **2004**, *56*, 1143-1160.

(54)   Kralovec, J.; Spencer, G.; Blair, A. H.; Mammen, M.; Singh, M.; Ghose, T. *Journal of Medicinal Chemistry* **1989**, *32*, 2426-2431.

(55)   Rosowsky, A.; Forsch, R. A.; Galivan, J.; Susten, S. S.; Freisheim, J. H. *Molecular Pharmacology* **1985**, *27*, 141-147.

(56)   Wei, W. H.; Fountain, M.; Magda, D.; Wang, Z.; Lecane, P.; Mesfin, M.; Miles, D.; Sessler, J. L. *Organic & Biomolecular Chemistry* **2005**, *3*, 3290-3296.

(57)   Mezo, G.; Lang, O.; Jakab, A.; Bai, K. B.; Szabo, I.; Schlosser, G.; Lang, J.; Kohidai, L.; Hudecz, F. *Journal of Peptide Science* **2006**, *12*, 328-336.

(58)   Sperling, R. A.; Pellegrino, T.; Li, J. K.; Chang, W. H.; Parak, W. J. *Advanced Functional Materials* **2006**, *16*, 943-948.

(59)   Claridge, S. A.; Liang, H. Y. W.; Basu, S. R.; Frechet, J. M. J.; Alivisatos, A. P. *Nano Letters* **2008**, *8*, 1202-1206.

(60)   Pons, T.; Medintz, I. L.; Wang, X.; English, D. S.; Mattoussi, H. *Journal of the American Chemical Society* **2006**, *128*, 15324-15331.

(61)   Tracy, J. B.; Kalyuzhny, G.; Crowe, M. C.; Balasubramanian, R.; Choi, J. P.; Murray, R. W. *Journal of the American Chemical Society* **2007**, *129*, 6706-6707.

(62)   Casanova, D.; Giaume, D.; Moreau, M.; Martin, J. L.; Gacoin, T.; Boilot, J. P.; Alexandrou, A. *Journal of the American Chemical Society* **2007**, *129*, 12592-12593.

(63)   Hong, S.; Leroueil, P. R.; Majoros, I. J.; Orr, B. G.; Baker, J. R.; Holl, M. M. B. *Chemistry and Biology* **2007**, *14*, 107-115.

(64)   Reddy, J. A.; Abburi, C.; Hofland, H.; Howard, S. J.; Vlahov, I.; Wils, P.; Leamon, C. *Gene Therapy* **2002**, *9*, 1542-1550.

Chapter 4
Isolation and characterization of dendrimer with precise numbers of functional groups

Introduction

Conjugation Substantial attention has been devoted to nanoparticles conjugated with functional ligands. Application of these materials has included building blocks for nano-scale structures,[1-2] materials for sensing and detection,[3-4] platforms for targeted delivery,[5-7] imaging and diagnostic systems,[8-10] and probes of biological structure.[11] One of the challenging features of these systems is the heterogeneous distribution of ligands per particle. For the vast majority of systems reported, these distributions are not characterized nor are they incorporated in design parameters. The implications of this heterogeneity are two-fold: First, mixtures containing many ligand/particle ratios make studies that investigate composition-activity relationships complex. Second, production of material with a consistent distibution of ligand/particle ratios is problematic because of inconsistencies in the nanoparticle preparations and reaction kinetics. New methods that exhibit precise control over the number of ligands per particle have the potential for dramatically improved functional efficacy, batch reproducibility, and an enhanced ability to probe the relationship between activity and the number of ligands conjugated to a particle.

Significant progress has been made towards precisely controlled material using gold nanoparticles. A number of strategies exist in the literature to synthesize and/or isolate milligram quantities of gold nanoparticles with a single functional group[12-14] and up to 95% purity has been achieved. Gold nanoparticles with 0-5 conjugated ligands have also been isolated in sub milligram quantities using either gel electrophoresis or ion exchange chromatography.[15-19]

This level of control has not been attained for other nanoparticle-based systems. In fact, with few exceptions, the analytical techniques commonly used to characterize these systems (NMR, HPLC, GPC, MALDI-TOF, UV-Vis) have been unable to identify the distribution of nanoparticle-ligand components.

Recently, we have developed the ability to resolve the distribution of components using HPLC for poly(amidoamine) (PAMAM) dendrimer samples conjugated with 3-(4-(prop-2-ynyloxy)phenyl)propanoic acid (Alkyne Ligand).[20-21] The results of these studies revealed that dendrimer-ligand distributions are heterogeneous (a sample with a ligand mean of 5.7 was composed of 18 dendrimer-ligand components), are poorly represented by the arithmetic mean, and are sensitive to pre-existing distributions of conjugation sites on the parent dendrimer.

We have now employed semi-preparative HPLC to successfully isolate 9 different dendrimer components with precise numbers of ligands. Generation 5 (G5) PAMAM dendrimer was conjugated with (3-(4-(2-azidoethoxy)phenyl)propanoic acid) (Azide Ligand) to produce dendrimer with a mean of 4.3 ligands (**Scheme 1**). Dendrimer samples with 0, 1, 2, 3, 4, 5, 6, 7 and 8 Azide Ligands were isolated from the dendrimer conjugate 3 and characterized by ^{1}H NMR and analytical HPLC. Levels of purity for these samples were found to be greater than 80%.

<div align="center">Experimental Methods</div>

Reagents and Materials

Biomedical grade Generation 5 PAMAM (poly(amidoamine)) dendrimer was purchased from Dendritech Inc. and purified as described in the synthesis section. MeOH (99.8%), acetic anhydride (99.5%), triethylamine (99.5%), dimethylformamide (99.8%), acetone (ACS reagent grade $\geq$ 99.5%), methyl 3-(4-hydroxyphenyl)propanoate (97%), sodium azide (99.99%), 1-bromo-2-chloroethane (98%), ethyl acetate (EtOAc) 99.5%), 18-crown-6, K_2CO_3, NaCl, 1N HCl, 2 M KOH, *N*-(3-dimethylaminopropyl)N'-ethylcarbodiimide ($\geq$ 97.0%) (EDC), *N*-hydroxysuccinimide (98%) (NHS), D_2O, and volumetric solutions (0.1 M HCl and 0.1 M NaOH) for potentiometric titration were

purchased from Sigma Aldrich Co. and used as received. 10,000 molecular weight cut-off centrifugal filters (Amicon Ultra) and Hexanes (HPLC grade) were obtained from Fisher Scientific. 1x and 10x phosphate buffer saline (PBS) (Ph = 7.4) without calcium or magnesium was purchased from Invitrogen.

Nuclear Magnetic Resonance Spectroscopy

All ^{1}H NMR experiments were conducted using a Varian Inova 400 MHz instrument. 10s delay time and 64 scans were set for each dendrimer sample. Temperature was controlled at 25 ^{o}C. For experiments conducted in D_2O, the internal reference peak was set to 4.717 ppm. Based upon measuring T_2* values and empirical studies to ensure that the chosen delay was long enough to avoid any decreased peak intensity associated with spin saturation, the delay for all integration studies was set to 10s.

Gel Permeation Chromatography

GPC experiments were performed on an Alliance Waters 2695 separation module equipped with a 2487 dual wavelength UV absorbance detector (Waters Corporation), a Wyatt HELEOS Multi Angle Laser Light Scattering (MALLS) detector, and an Optilab rEX differential refractometer (Wyatt Technology Corporation). Columns employed were TosoHaas TSK-Gel Guard PHW 06762 (75 mm × 7.5 mm, 12 μm), G 2000 PW 05761 (300 mm × 7.5 mm, 10 μm), G 3000 PW 05762 (300 mm × 7.5 mm, 10 μm), and G 4000 PW (300 mm × 7.5 mm, 17 μm). Column temperature was maintained at 25 ± 0.1 °C with a Waters temperature control module. The isocratic mobile phase was 0.1 M citric acid and 0.025 wt % sodium azide, pH 2.74, at a flow rate of 1 mL/min. The sample concentration was 10 mg/5 mL with an injection volume of 100 μL. The weight average molecular weight, M_w, has been determined by GPC, and the number average molecular weight, M_n, was calculated with Astra 5.3.14 software (Wyatt Technology Corporation) based on the molecular weight distribution.

Potentiometric Titration

Potentiometric titration was carried out using a Mettler Toledo MP220 pH meter and a Mettler Toledo InLab 430 pH electrode at room temperature, 23 °C. A 10 mL solution of 0.1 N NaCl was added to purified G5 PAMAM dendrimer **1** (127.5 mg) to shield amine group interactions. The pH of the dendrimer solution was lowered to pH = 2.01 using 0.1034 N HCl. A 25 mL Brand Digital Burette[TM] III was used for the titration with 0.0987 N NaOH. The numbers of primary and tertiary amines were determined by from the titration curve with NaOH as previously described.[22]

Analytical Reverse Phase High Performance Liquid Chromatography

HPLC analysis was carried out on a Waters Delta 600 HPLC system equipped with a Waters 2996 photodiode array detector, a Waters 717 Plus auto sampler, and Waters Fraction collector III. The instrument was controlled by Empower 2 software. For analysis of the conjugates, a C5 silica-based RP-HPLC column (250 x 4.6 mm, 300 Å) connected to a C5 guard column (4 x 3 mm) was used. The mobile phase for elution of the conjugates was a linear gradient beginning with 100:0 (v/v) water/acetonitrile and ending with 20:80 (v/v) water/acetonitrile over 30 min at a flow rate of 1 mL/min. Trifluoroacetic acid (TFA) at 0.14 wt % concentration in water as well as in acetonitrile was used as a counter ion to make the dendrimer surfaces hydrophobic. Elution traces of the dendrimer-ligand conjugate were obtained at 210 nm. We have previously shown that 210 nm is a convenient wavelength to monitor PAMAM dendrimers because absorbance is not significantly affected by varying amounts of conjugated ligand and Beer's Law is followed.[20] Run-to-run reproducibility of retention time was 0.016 min which is ~4% of the magnitude of the peak-to-peak separation noted in this analysis.

Semi-preparative Reverse Phase High Performance Liquid Chromatography

HPLC isolation was carried out on a Waters Delta 600 HPLC system equipped with a Waters 2996 photodiode array detector, a Waters 2707 auto sampler, and Waters Fraction collector III. The instrument was controlled by Empower 2 software. For analysis of the conjugates, a C5 silica-based RP-HPLC column (250 x 21.20 mm, 10μ 300 Å) connected to a C5 guard column (50 x 21.20 mm) was used. The mobile phase for

elution of the conjugates was a linear gradient beginning with 100:0 (v/v) water/isopropanol and ending with 60:40 (v/v) water/isopropanol over 25 min at a flow rate of 10 mL/min. Trifluoroacetic acid (TFA) at 0.14 wt % concentration in water as well as in isopropanol was used as a counter ion to make the dendrimer surfaces hydrophobic. Elution traces of the dendrimer-ligand conjugate were obtained at 210 nm.

Synthesis

The G5-(NH$_2$)$_{112}$ dendrimer was conjugated to Azide and Ac groups. Ac refers to the acetyl termination, and Azide to the Azide Ligand.

Compound 1: Azide Ligand (3-(4-(2-azidoethoxy)phenyl)propanoic acid)

1a. To a solution of methyl 3-(4-hydroxyphenyl)propanoate (1.699 g, 9.43 mmole) in dry acetone (47.5 mL) was added anhydrous K$_2$CO$_3$ (3.909 g, 0.0283 mole) followed by 1-bromo-2-chloroethane (1.563 mL, 0.01886 mole). The resulting suspension was refluxed for 43 h with vigorous stirring. The reaction mixture was cooled to room temperature and the salt was removed by filtration followed by washing with portions of EtOAc (3 x 70 mL). The crude material was purified by silica chromatography (25:75 EtOAc:Hexane) and the solvent was removed under vacuum to give the desired product, methyl 3-(4-(2-chloroethoxy)phenyl)propanoate **1a**, as an oil (0.75 g, 33%). ^{1}H NMR (500 MHz, CDCl$_3$) δ 7.121 (d, J = 8.7, 2H), 6.843 (d, J = 8.7, 2H), 4.206 (t, J = 5.9, 2H), 3.798 (t, J = 5.9, 2H), 3.664 (s, 3H), 2.895 (t, J = 7.8, 2H), 2.598 (t, J = 7.8, 2H).

1b. To a solution of methyl 3-(4-(2-chloroethoxy)phenyl)propanoate **1a** (0.75 g 3.1 mmole) in anhydrous DMF (6.1 mL) was added 18-crown-6 (3.4 mg, 0.013 mmole) and sodium azide (0.44 g, 6.8 mmole). The resulting solution was heated at 78 °C for 11 h. The reaction mixture was cooled to room temperature, diluted with ethyl acetate (50 mL), washed with a saturated NaHCO$_3$ solution (4 x 70 mL), and then dried over MgSO$_4$. The solvent was removed under vacuum to give methyl 3-(4-(2-azidoethoxy)phenyl)propanoate **1b** as a yellow oil (0.58 g, 75%) ^{1}H NMR (500 MHz,

109

CDCl$_3$) δ 7.125 (d, J = 8.6, 2H), 6.849 (d, J = 8.6, 2H), 4.129 (t, J = 5.0 2H), 3.666 (s, 3H), 3.581 (t, J = 5.0, 2H), 2.899 (t, J = 7.8, 2H), 2.600 (t, J = 7.8, 2H).

1c. To a solution of methyl 3-(4-(2-azidoethoxy)phenyl)propanoate **1b** (3.88 g, 0.0156 mole) in methanol (102 mL) was added potassium hydroxide (2 M, 28.3 mL, 0.0566 mole). The resulting solution was refluxed at 70 °C for 3 h. The solution was cooled to room temperature and condensed under reduced pressure. The residue was dissolved in water (30 mL) and was acidified by addition of 1N HCl to pH 1. The white cloudy solution was diluted with EtOAc. Layers were separated and the aqueous layer was extracted with EtOAc (2 x 70 mL). The combined organic extracts were washed with a saturated NaCl solution and dried over MgSO$_4$. Solvent was evaporated under vacuum to give the (3-(4-(2-azidoethoxy)phenyl)propanoic acid) **1c** as a white solid (3.44 g, 93.9%). ^{1}H NMR (500 MHz, CDCl$_3$) δ 7.139 (d, J = 8.5, 2H), 6.859 (d, J = 8.5, 2H), 4.132 (t, J = 5.0 2H), 3.584 (t, J = 5.0, 2H), 2.909 (t, J = 7.7, 2H), 2.653 (t, J = 7.7, 2H).

Dendrimer 1: Purification of Generation 5 PAMAM Dendrimer G5-(NH$_2$)$_{112}$

The purchased G5 PAMAM dendrimer was purified by dialysis, as previously described,[20] to remove lower molecular weight impurities including trailing generation dendrimer defect structures. The number average molecular weight (27,100 g/mol± 1,000) and PDI (1.018 +/- 0.014) was determined by GPC. Potentiometric titration was conducted to determine the mean number of primary amines (112 ± 5).

Dendrimer 2: G5-(NH$_2$)$_{108}$-Azide$_{4.3}$

The Azide Ligand (19.4 mg, 82.7 μmole), EDC (31.7 mg, 0.165 mmole), and NHS (21.9 mg, 0.190 mmole) were dissolved in anhydrous acetonitrile (4.861 mL). The resulting solution was stirred under nitrogen for 1 hr. The resulting solution was added by syringe pump to a solution of G5 PAMAM dendrimer **1** (451.9 mg, 16.53 μmole) in DI water (100 mL). The resulting reaction mixture was stirred for 12 hrs under nitrogen at room temperature. The product was purified using 10,000 MWCO centrifugal filtration devices. Purification consisted of 2 cycles to concentrate the solution, 1 cycle using 1x PBS (without magnesium and calcium) and four cycles using DI water. Each

cycle was 10 minutes at 5,000 rpm. The purified dendrimer was lyophilized for three days to yield a white solid (368.9 mg, 79%). ^{1}H NMR integration determined the mean number of Azide Ligands per dendrimer to be 4.3.

Dendrimer 3: G5-Ac$_{108}$-Azide$_{4.3}$

Purified G5 PAMAM dendrimer **1** (365.2 mg, 12.89 μmole) was dissolved in anhydrous methanol (30.0 mL). Triethylamine (297 μL, 2.12 mmole) was added to this mixture and stirred for 30 minutes. Acetic anhydride (174 μL, 1.8 mmole) was added in a dropwise manner to the dendrimer solution. The reaction was carried out in a glass flask, under nitrogen, at room temperature for 24 hours. Methanol was evaporated from the resulting solution and the product was purified using 10,000 MWCO centrifugal filtration devices. Purification consisted of 1 cycles to concentrate the solution, 2 cycle using 1x PBS (without magnesium and calcium) and four cycles using DI water. The purified dendrimer was lyophilized for three days to yield a white solid (258.4 mg, 61%). ^{1}H NMR integration determined that the dendrimer was fully acetylated.

Isolation Procedure

Dendrimer 3 was injected into the HPLC system for 12 consecutive runs. Each injection used 18.2 mg of material in 910 μL of water w/0.14% TFA. A 30 minute run time and a 10 minute delay between runs were used. Beginning at 20 min 0 s in each run, 120 fractions were collected using the Waters Fraction Collector at 4 s intervals. Fractions for all 12 runs were collected in the same set of test tubes.

Fractions were combined based on the peak fitting analysis to obtain the 9 isolated dendrimer-ligand samples (Samples 0-8). 50 μL from each sample was removed and used for analytical HPLC characterization. Purification of each sample was necessary due to the low pH (~1.9) of the HPLC solvent system. This process is described in detail for Sample 0 and was repeated for Samples 1-8.

Sample 0: Fractions 11-18 (20m40s-21m12s) were combined, diluted with an equal volume of 1x PBS (w/o Mg or Ca) and aspirated with nitrogen to evaporate isopropanol. The concentrated sample was lyophilized for 1 day to yield a white powder.

The dried sample was then re-dissolved in 2.5 mL of 10x PBS (w/o Mg or Ca) and purified using PD-10 desalting columns. DI water was used as the mobile phase for the column purification step. The sample was then lyophilized for 2 days to yield a white solid (10.4 mg).

Sample 1: Fractions 34-38 (22m12s-22m32s) 10.1 mg. The purification process was repeated twice for Sample 1.

Sample 2: Fractions 52-55 (23m24s-23m40s) 8.5 mg.

Sample 3: Fractions 66-69 (24m20s-24m36s) 9.5 mg.

Sample 4: Fractions 78-81 (25m8s-25m24s) 8.7 mg.

Sample 5: Fractions 87-89 (25m44s-25m56s) 5.4 mg.

Sample 6: Fractions 96-98 (26m20s-26m32s) 6.7 mg.

Sample 7: Fractions 105-107 (26m56s-27m8s) 1.5 mg.

Sample 8: Fractions 115-117 (27m36s-27m48s) 1.8 mg.

Results and Discussion

Isolation of practical quantities of material was achieved by carrying out the HPLC process for 12 runs. **Figure 4.1a** shows the semi-prep HPLC traces along with grey lines demarking the fractions that were collected every 4s. A peak fitting analysis determined the retention time of each component (**Figure 4.1b**), thereby identifying the fractions in **Figure 4.1a** to combine for dendrimer samples with 0-8 ligands. These fractions are highlighted in **Figure 4.1a** by solid colored bars. The mass isolated by this process is listed in **Table 4.1**.

Analytical HPLC was used to characterize the samples both before and after purification. **Figure 4.2a** displays the sample traces before purification. A normalized trace of 3 is included for reference. The peak area for each of the samples directly relates to the amount of material that was isolated because samples were characterized at the

112

isolated concentration. Following purification, the samples were characterized again by analytical HPLC (**Figure 4.2b**) and ^{1}H NMR.

Three main features stand out in **Figure 4.2**. First, each isolated component has the same retention time as its original position in the distribution. Second, smaller peaks can be seen adjacent to the major peak in each sample. These smaller peaks have retention times consistent with other dendrimer-ligand components. The purity levels of the isolated samples (**Table 4.1**) were quantified by peak fitting (**Figure 4.2c**). Finally, no differences were observed in the HPLC traces before and after purification indicating that the samples did not degrade during the purification process.

NMR is the second technique used to characterize the isolated samples. **Figure 4.3** shows the ^{1}H spectrum for the sample with 1 ligand. Two different methods were used to calculate the ligand/dendrimer ratio for each sample (**Table 4.1**).

The first method has two assumptions: 1) All dendrimer end groups are either acetyl groups or ligands. 2) The mean number of end groups per dendrimer after HPLC isolation is 112. Method 1 uses the integrals for the aromatic ligand protons (aa' and bb'), normalized by the number of these protons per ligand (4), divided by the numerator plus the integral for the methyl protons at 1.9 ppm normalized by the number of protons per acetyl group. The product (the ratio of ligands to the total number of end groups per dendrimer) is multiplied by 112 to yield the number of ligands per dendrimer.

Overall, there is good agreement between the ratios determined by HPLC and by NMR method 1. For samples 5-8, the difference between these values is 3% or less. Samples with 1-4 ligands, however, have differences between 13% and 26%. These larger differences suggest that the assumptions in Method 1 may not be appropriate. In addition to 3 being composed of a distribution of dendrimer/ligand ratios, the dendrimer alone is a polymer with different backbone structures. Considering that a small section of each component peak was isolated from the distribution in **Figure 4.1a**, the isolated dendrimer particles in each sample may not have a mean of 112 end groups.

Using a different set of assumptions, a second method was used to calculate the NMR ratios. This method uses the protons from the interior of the dendrimer as a reference. The reference integral was determined using 4 which was also made from 1. In the ^{1}H NMR spectrum for this material, the integral of the methyl protons c was normalized to 336. This provided the number of interior protons, f, g, and e per dendrimer. These protons were then used as an internal reference to quantify the ligand/dendrimer ratio in the isolated samples.

Method 2 assumes that all of the amines in 4 were acetylated and that the number of interior protons is not sensitive to the isolation process. The ligand/dendrimer ratios, calculated by Method 2, are reported in **Table 4.1**. Similar to Method 1, there is generally good agreement between the number of ligands by HPLC and the NMR calculation. For samples 1-4, the difference is between 3% and 17%. Samples 5-8 have differences between 7% and 13%.

Our ability to generate dendrimer with precise numbers of ligands is significant for two reasons: First, this method produces material with precise numbers of functional ligands. In this study, over 80% of the material in each sample is a single dendrimer-ligand component. This is an order of magnitude improvement in the purity of the desired component (**Table 4.1**). Since the ligand in this study has a terminal azide group, the samples can be modified with biologically active molecules using alkyne-azide 'click' chemistry. The end result is a system in which $\geq$80% of the dendrimer particles have the same number of biologically active molecules. Second, our method directly addresses the batch-to-batch reproducibility challenge facing nanoparticle conjugate production. This is a problem that dendrimer-based systems have not escaped. Dendrimer-based drug delivery platforms with great in vivo activity, failed to advance to the clinic because of inconsistencies in the material being produced. Our new method achieves batch consistency because the resolution of dendrimer-ligand components by HPLC is highly reproducible. As a result of such consistent product, the process remains insensitive to variations in the dendrimer conjugate that usually results from bath to batch inconsistencies in the dendrimer synthesis and subsequent reaction kinetics.

Conclusion

In conclusion, we have successfully employed a semi-preparative HPLC to isolate dendrimer with 0-8 Azide Ligands. Peak fitting analysis on analytical HPLC traces determined the sample purity to be 80% or higher. The number of ligands per dendrimer, quantified by ^{1}H NMR, were in good agreement with the number quantified by HPLC and peak fitting. Significantly, for dendrimer compounds with 0-4 Ligands, over 8 mg of material was produced in this study. This approach shows great promise to overcome batch reproducibility challenges in dendrimer-based systems.

Acknowledgements
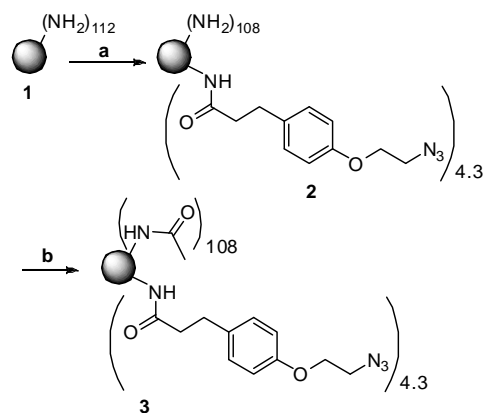
Scheme 1. a) Alkyne Ligand, NHS, EDC, acetonitrile, water, rt, 12 h, 79% yield; b) acetic anhydride, triethylamine, MeOH, rt, 12 h, 61% yield. Detailed experimental methods can be found in the Supporting Information.
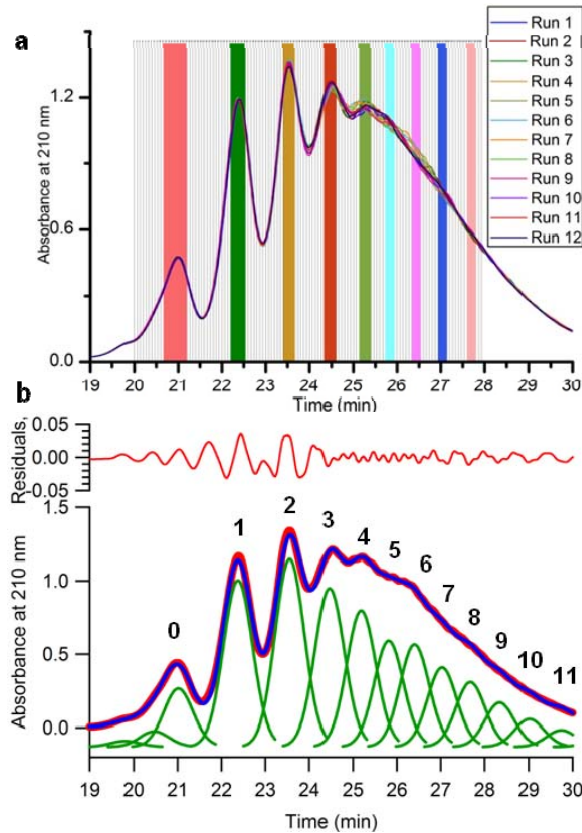
Figure 4.1: Isolation of dendrimer-ligand components by semi-preparative HPLC. a) Semi-preparative HPLC traces for the 12 identical runs. The 120 fractions starting at 20 minutes are shown in grey. The selected fractions for each of the different dendrimer-ligand components (0-8) are highlighted in solid colored lines. b) Peak fitting analysis of the trace for Run 6. The HPLC data is presented in red circles and the multiple copies of the fitting peak are shown in green. The summation of these fitting peaks is shown in blue. The residual values in panel b are multiplied by 10^6.

Figure 4.2: Analytical HPLC analysis for the isolated dendrimer-ligand components. a) Baseline-corrected traces for dendrimer-ligand components with 0-8 ligands run immediately after the isol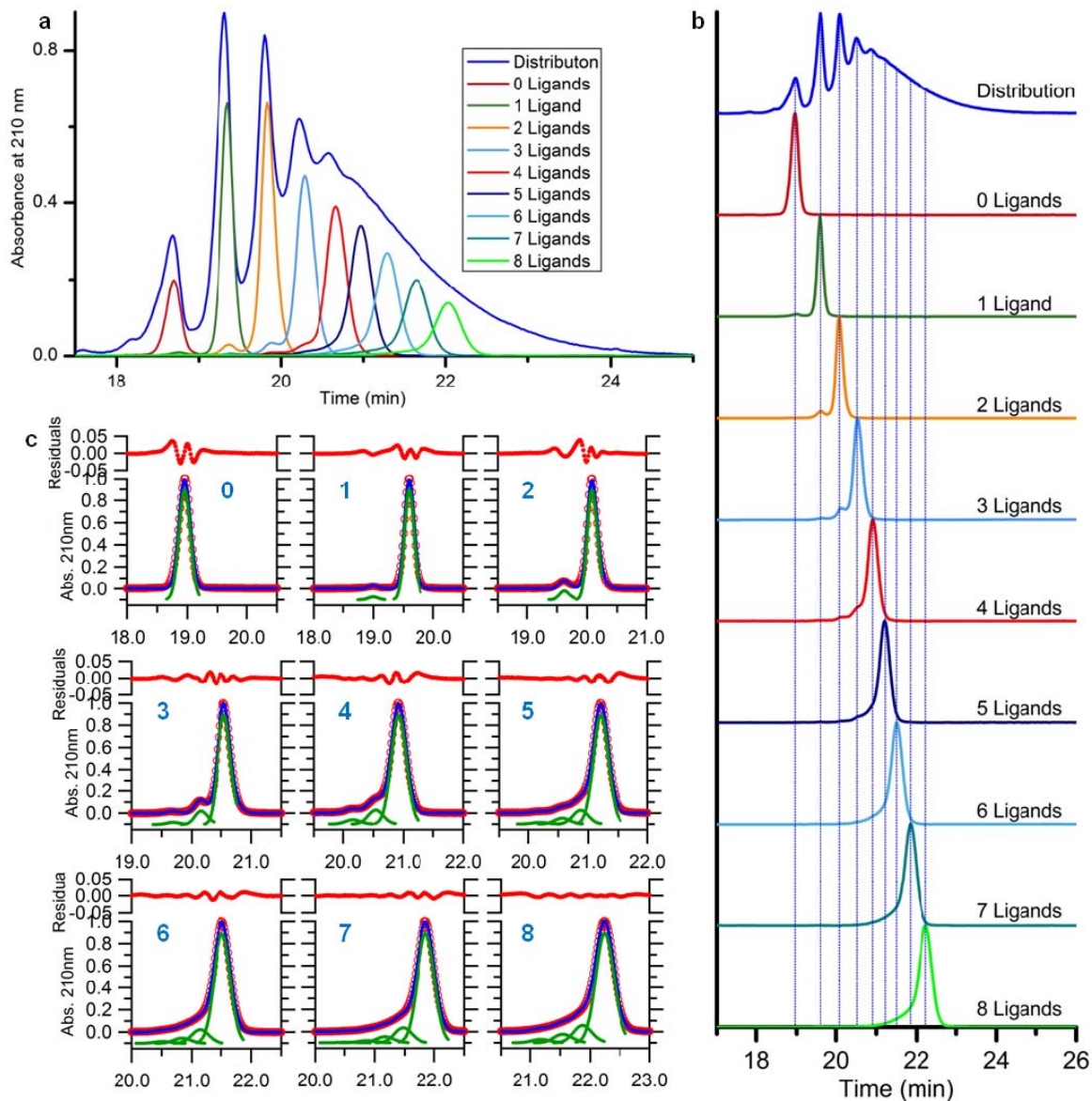ation process. The area of each peak is directly proportional to the amount of isolated material. The HPLC trace for the dendrimer distribution with a mean of 4.3 ligands is also included. This trace has been normalized. b) Traces for the isolated dendrimer-ligand components after purification. Each trace has been baseline corrected and normalized. Blue lines show relationship between the isolated component and the material with the distribution of components. In addition to the major peak in each component, small amount of other components have been detected. c) The peak fitting method was used to quantify the purity of each isolated component. Fitting peaks are shown in green, with the summation of these peaks in blue. The HPLC data is shown in red circles. The residual values in panel c are mulitiplied by 10^6.
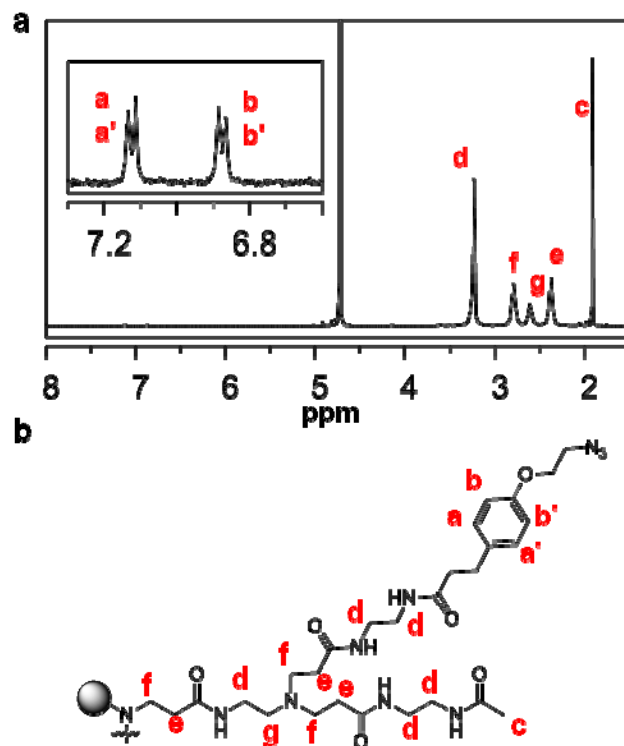
Figure 4.3: ^{1}H NMR characterization. a) Spectrum for the isolated dendrimer with 1 ligand. b) Chemical structure and proton labels for the Azide Ligand and acetyl terminated dendrimer arms.

Table 4.1: Characterization of isolated dendrimer with precise numbers of ligands

| | | HPLC Analysis | | | NMR Analysis | | | |
| | | | | | Method 1 | | Method 2 | |
Nominal # of Ligands per Dendrimer	Mass Recovered (mg)	# Ligands per Dendrimer	Purity[a]	Increase in Purity[b]	# Ligands per Dendrimer	Difference[c]	# Ligands per Dendrimer	Difference[c]
0	10.4	0.0	100%	14x	0	0	0	0
1	10.1	1.0	97%	6x	1.2	20%	1.1	10%
2	8.5	1.9	93%	6x	2.4	26%	2.2	14%
3	9.5	2.7	88%	7x	3.4	26%	3.2	17%
4	8.7	3.8	86%	9x	4.3	13%	3.9	3%
5	5.4	4.8	84%	10x	4.9	2%	4.5	7%
6	6.7	5.8	84%	12x	5.7	2%	5.2	10%
7	1.5	6.7	82%	14x	6.8	3%	5.8	13%
8	1.8	7.7	79%	16x	7.8	1%	6.9	10%

[a] Defined by the number of ligands per dendrimer.

[b] Fold increase in purity is relative to the amount of the component in the distribution (Dendrimer 3).

[c] Difference is calculated by the NMR ratio minus the HPLC ratio, divided by the HPLC ratio.

References

(1)   Maye, M. M.; Nykypanchuk, D.; Cuisinier, M.; van der Lelie, D.; Gang, O. *Nature Materials* **2009**, *8*, 388-391.

(2)   Maye, M. M.; Kumara, M. T.; Nykypanchuk, D.; Sherman, W. B.; Gang, O. *Nature Nanotechnology* **2010**, *5*, 116-120.

(3)   Medintz, I. L.; Clapp, A. R.; Mattoussi, H.; Goldman, E. R.; Fisher, B.; Mauro, J. M. *Nature Materials* **2003**, *2*, 630-638.

(4)   Jain, K. K. *Clinica Chimica Acta* **2005**, *358*, 37-54.

(5)   Tong, R.; Cheng, J. J. *Polymer Reviews* **2007**, *47*, 345-381.

(6)   Peer, D.; Karp, J. M.; Hong, S.; FaroKhzad, O. C.; Margalit, R.; Langer, R. *Nature Nanotechnology* **2007**, *2*, 751-760.

(7)   Choi, H. S.; Liu, W.; Liu, F.; Nasr, K.; Misra, P.; Bawendi, M. G.; Frangioni, J. V. *Nat Nanotechnol* **2010**, *5*, 42-47.

(8)   Nie, S. M.; Xing, Y.; Kim, G. J.; Simons, J. W. *Annual Review of Biomedical Engineering* **2007**, *9*, 257-288.

(9)   Landmark, K. J.; DiMaggio, S.; Ward, J.; Kelly, C.; Vogt, S.; Hong, S.; Kotlyar, A.; Myc, A.; Thomas, T. P.; Penner-Hahn, J. E.; Baker, J. R.; Holl, M. M. B.; Orr, B. G. *ACS Nano* **2008**, *2*, 773-783.

(10)   Thaxton, C. S.; Elghanian, R.; Thomas, A. D.; Stoeva, S. I.; Lee, J. S.; Smith, N. D.; Schaeffer, A. J.; Klocker, H.; Horninger, W.; Bartsch, G.; Mirkin, C. A. *Proceedings of the National Academy of Sciences of the United States of America* **2009**, *106*, 18437-18442.

(11)   Hong, S.; Leroueil, P. R.; Majoros, I. J.; Orr, B. G.; Baker, J. R.; Holl, M. M. B. *Chemistry & Biology* **2007**, *14*, 107-115.

(12)   Hainfeld, J. F.; Robinson, J. M. *Journal of Histochemistry & Cytochemistry* **2000**, *48*, 459-460.

(13)   Chak, C. P.; Xuan, S. H.; Mendes, P. M.; Yu, J. C.; Cheng, C. H. K.; Leung, K. C. F. *ACS Nano* **2009**, *3*, 2129-2138.

(14)   Wilson, R.; Chen, Y.; Aveyard, J. *Chemical Communications* **2004**, 1156-1157.

(15)   Zanchet, D.; Micheel, C. M.; Parak, W. J.; Gerion, D.; Alivisatos, A. P. *Nano Letters* **2001**, *1*, 32-35.

(16)   Zanchet, D.; Micheel, C. M.; Parak, W. J.; Gerion, D.; Williams, S. C.; Alivisatos, A. P. *Journal of Physical Chemistry B* **2002**, *106*, 11758-11763.

(17)   Claridge, S. A.; Liang, H. Y. W.; Basu, S. R.; Frechet, J. M. J.; Alivisatos, A. P. *Nano Letters* **2008**, *8*, 1202-1206.

(18)   Sperling, R. A.; Pellegrino, T.; Li, J. K.; Chang, W. H.; Parak, W. J. *Advanced Functional Materials* **2006**, *16*, 943-948.

(19)   Zikich, D.; Borovok, N.; Molotsky, T.; Kotlyar, A. *Bioconjugate Chemistry* **2010**, *ASAP*.

(20)   Mullen, D. G.; Desai, A. M.; Waddell, J. N.; Cheng, X. M.; Kelly, C. V.; McNerny, D. Q.; Majoros, I. J.; Baker, J. R.; Sander, L. M.; Orr, B. G.; Holl, M. M. B. *Bioconjugate Chemistry* **2008**, *19*, 1748-1752.

(21)   Mullen, D. G.; Fang, M.; Desai, A. M.; Baker, J. R.; Orr, B. G.; Holl, M. M. B. *ACS Nano* **2010**, *4*, 657-670.

(22)   Majoros, I. J.; Thomas, T. P.; Mehta, C. B.; Baker, J. R. *Journal of Medicinal Chemistry* **2005**, *48*, 5892-5899.

Chapter 5
The effect of mass transport in the synthesis of partially acetylated dendrimer:
Implications for functional ligand-nanoparticle distributions

Introduction

Nanoparticle-based platforms have emerged in the past decade as a truly disruptive technology with applications that include nanoassemblies,[1-2] sensing and detection,[3-6] targeted delivery,[7-11] imaging and diagnostics,[12-14] and probes of biological structure.[15] For many systems, an important design criterion is that the particles be charge neutral.[16-21] This requirement is often fulfilled with a surface modification step. In poly(amidoamine) (PAMAM) dendrimer-based systems, passivation of the surface primary amines has been frequently accomplished in a partial acetylation reaction.[22] Because the partial acetylation results in a distribution of dendrimer particles with different numbers of modification sites, this passivation step is likely to have a major impact on the subsequent distribution of dendrimer-ligand components. At present, however, no studies have investigated the effect of the partial acetylation reaction on subsequent dendrimer-ligand distributions especially in the context of batch reproducibility. Specifically, no information is known about how the dendrimer-ligand distributions are affected by changes in the effectiveness of mass transport during the partial acetylation of the parent dendrimer.

The limitations of commonly used analytical techniques are arguably the main reason that the relationships between the passivation step and dendrimer-ligand distributions have not been characterized. Techniques such as nuclear magnetic resonance (NMR), ultraviolet/visable (UV-vis) spectroscopy, and elemental analysis only provide the mean number of ligands per particle. While gel permeation chromatography (GPC), high-performance liquid chromatography (HPLC), and matrix-assisted laser desorption ionization time of flight (MALDI-TOF) have the potential to resolve the

different nanoparticle-ligand components in a distribution, these techniques often fail to do so. PAMAM dendrimer have been conjugated with a wide variety of ligands including peptides,[23-24] T-antigens,[25-26] monoclonal antibodies,[27] folic acid,[28-31] and therapeutic agents,[28,32-33] and yet only three studies exist where the distribution of dendrimer-ligand components was resolved.[34-36] Additionally, no examples exist where the distribution of dendrimer with different ratios of acetyl groups was resolved.

Our research group has become keenly interested in this subject because we found production of dendrimer-based platforms with consistent properties between batches to be challenging. In fact, one dendrimer platform that was approved for human trials is currently on hold due to insufficient control over batch consistency.[31,37-38]

Recently, we have noticed a dependence of the dendrimer-ligand distribution features on the batch of partially acetylated dendrimer. Our observations were made using two model ligands that enable us to resolve the distribution of dendrimer-ligand components with HPLC. This study presents three such sets of dendrimer-ligand conjugates ($G5Ac_{76}Alkyne$, $G5Ac_{76}Azide$, and $G5Ac_{80}Alkyne$) produced with two batches of partially acetylated dendrimer and two small molecule ligands. For each sample, the distribution of ligand/dendrimer ratios was quantified by HPLC and a peak fitting analysis. The distribution features were consistent for samples made with the same dendrimer, irrespective of the ligand. Major dendrimer-ligand distribution differences were found correlating with the batch of partially acetylated dendrimer. Our hypothesis was that the two dendrimer batches had different distributions of modification sites caused by differing acetyl group distributions. Furthermore, we hypothesized that the acetyl distribution differences resulted from the effectiveness of mass transport during the partial acetylation. This resulting distribution of modification sites then had a major impact on the subsequent dendrimer-ligand distributions.

To test our hypothesis, we conducted two partial acetylation reactions with effective and ineffective mass transport controlled by adjusting both dilution and stir rate parameters. No differences were detected between the two batches using NMR or HPLC

characterization. The ligand was then conjugated to both batches producing material with the same mean number of ligands. The two batches had distinctly different distribution profiles consistent with our earlier observations. Our results indicate that mass transport has a major impact on the acetyl group distribution which in turn effects the distributions of all subsequent conjugated ligands. This mass transport-induced difference in acetyl group distribution then limits, and for ligands that are not sterically constrained, controls the attainable distribution of the functional ligands that are subsequently attached. The sensitivity of the acetylation reaction to mass transport effects makes reproducible distributions very difficult to achieve which is a substantial problem for batch-to-batch reproducibility. Broadly, this is a cautionary tale for many nanoparticle-ligand conjugates because the final two dendrimer-ligand conjugates, appeared to be identical by common characterization techniques and yet had dramatically different distribution profiles.

Experimental

Reagents and Materials:

Biomedical grade Generation 5 PAMAM (poly(amidoamine)) dendrimer was purchased from Dendritech Inc. and purified as described in the synthesis section. MeOH (99.8%), acetic anhydride (99.5%), triethylamine (99.5%), dimethyl sulfoxide (99.9%), dimethylformamide (99.8%), acetone (ACS reagent grade $\geq$ 99.5%), N,N-diisopropylethylamine, benzotriazol-1-yl-oxytripyrrolidinophosphonium hexafluorophosphate (98%), D_2O, and volumetric solutions (0.1 M HCl and 0.1 M NaOH) for potentiometric titration were purchased from Sigma Aldrich Co. and used as received. 10,000 molecular weight cut-off centrifugal filters (Amicon Ultra) were obtained from Fisher Scientific. 1x phosphate buffer saline (PBS) (Ph = 7.4) without calcium or magnesium was purchased from Invitrogen. The Alkyne Ligand (3-(4-(prop-2-ynyloxy)phenyl)propanoic acid) was synthesized as described previously.[39] Synthesis of the Azide Ligand (3-(4-(2-azidoethoxy)phenyl)propanoic acid) was also previously described.[40]

Nuclear Magnetic Resonance Spectroscopy

All ^{1}H NMR experiments were conducted using a Varian Inova 400 MHz instrument. 10 s delay time and 64 scans were set for each dendrimer sample. Temperature was controlled at 25 ^{o}C. For experiments conducted in D_2O, the internal reference peak was set to 4.717 ppm.

Gel Permeation Chromatography

GPC experiments were performed on an Alliance Waters 2695 separation module equipped with a 2487 dual wavelength UV absorbance detector (Waters Corporation), a Wyatt HELEOS Multi Angle Laser Light Scattering (MALLS) detector, and an Optilab rEX differential refractometer (Wyatt Technology Corporation). Columns employed were TosoHaas TSK-Gel Guard PHW 06762 (75 mm × 7.5 mm, 12 μm), G 2000 PW 05761 (300 mm × 7.5 mm, 10 μm), G 3000 PW 05762 (300 mm × 7.5 mm, 10 μm), and G 4000 PW (300 mm × 7.5 mm, 17 μm). Column temperature was maintained at 25 ± 0.1 °C with a Waters temperature control module. The isocratic mobile phase was 0.1 M citric acid and 0.025 wt % sodium azide, pH 2.74, at a flow rate of 1 mL/min. The sample concentration was 10 mg/5 mL with an injection volume of 100 μL. The weight average molecular weight, M_w, has been determined by GPC, and the number average molecular weight, M_n, was calculated with Astra 5.3.14 software (Wyatt Technology Corporation) based on the molecular weight distribution.

Reverse Phase High Performance Liquid Chromatography

HPLC analysis was carried out on a Waters Delta 600 HPLC system equipped with a Waters 2996 photodiode array detector, a Waters 717 Plus auto sampler, and Waters Fraction collector III. The instrument was controlled by Empower 2 software. For analysis of the conjugates, a C5 silica-based RP-HPLC column (250 x 4.6 mm, 300 Å) connected to a C5 guard column (4 x 3 mm) was used. The mobile phase for elution of the conjugates was a linear gradient beginning with 100:0 (v/v) water/acetonitrile and ending with 20:80 (v/v) water/acetonitrile over 30 min at a flow rate of 1 mL/min. Trifluoroacetic acid (TFA) at 0.14 wt % concentration in water as well as in acetonitrile was used as a counter ion to make the dendrimer surfaces hydrophobic.

126

Synthesis

The G5-$(NH_2)_{112}$ dendrimer was conjugated to Ac, Alkyne and Azide groups. Ac refers to the acetyl termination, Alkyne to the Alkyne Ligand and Azide to the Azide Ligand.

Dendrimer 1: Purification of Generation 5 PAMAM Dendrimer G5-$(NH_2)_{112}$

The purchased G5 PAMAM dendrimer was purified by dialysis, as previously described,[39] to remove lower molecular weight impurities including trailing generation dendrimer defect structures. The number average molecular weight (27,100 g/mol± 1,000) and PDI (1.018 +/- 0.014) was determined by GPC. Potentiometric titration was conducted to determine the mean number of primary amines (112 ± 5).

Dendrimer 2: Synthesis of Partially Acetylated Dendrimer G5-Ac_{76}-$(NH_2)_{36}$

Purified G5 PAMAM dendrimer **1** (149.0 mg, 5.451 μmole) was dissolved in anhydrous methanol (22.0 mL). Triethylamine (69.1 μL, 0.496 mmole) was added to this mixture and stirred for 30 minutes. Acetic anhydride (40.5 μL, 0.397 mmole) was added to anhydrous methanol (5.0 mL) and the resulting mixture was added in a dropwise manner to the dendrimer solution using a addition funnel. The reaction was carried out in a glass flask, under nitrogen, at room temperature for 24 hours. Methanol was evaporated from the resulting solution and the product was purified using 10,000 MWCO centrifugal filtration devices. Purification consisted of one cycle (10 minutes at 5,000 rpm) using 1x PBS (without magnesium and calcium) and five cycles using DI water. The purified dendrimer was lyophilized for three days to yield a white solid (85.1 mg, 51%). ^{1}H NMR integration determined the degree of acetylation to be 68%.

Dendrimer 3: Synthesis of Partially Acetylated Dendrimer G5-Ac_{80}-$(NH_2)_{32}$

Purified G5 PAMAM dendrimer **1** (180.1 mg, 6.588 μmole) was dissolved in anhydrous methanol (26.8 mL). Triethylamine (83.6 μL, 0.600 mmole) was added to this mixture and stirred for 30 minutes. Acetic anhydride (45.3 μL, 0.480 mmole) was added to anhydrous methanol (7.3 mL) and the resulting mixture was added in a dropwise manner to the dendrimer solution using a addition funnel. The reaction was carried out in

a glass flask, under nitrogen, at room temperature for 24 hours. Methanol was evaporated from the resulting solution and the product was purified using 10,000 MWCO centrifugal filtration devices. Purification consisted of one cycle (10 minutes at 5,000 rpm) using 1x PBS (without magnesium and calcium) and five cycles using DI water. The purified dendrimer was lyophilized for three days to yield a white solid (124.5 mg, 62%). ^{1}H NMR integration determined the degree of acetylation to be 71.5%.

Synthesis of Dendrimer-Ligand Samples

All reaction steps were carried out in glass scintillation vials at room temperature under nitrogen. All samples were purified using 10,000 MWCO centrifugal filtration devices. Purification consisted of one cycle (10 minutes at 5,000 rpm) using 1x PBS (without magnesium or calcium) and five cycles using DI water.

Samples A-E: G5-Ac$_{76}$-Alkyne$_{(0.5, 2.1, 3.1, 3.8, 10.4)}$

Three stock solutions were prepared to synthesize Samples A-E. A solution of partially acetylated dendrimer **2** (52.3 mg, 1.71 μmole) was prepared with anhydrous DMSO (8.00 mL). The Alkyne Ligand (6.2 mg, 30.4 μmole) was dissolved in DMSO (3.1 mL). Last, PyBOP (10.2 mg, 19.6 μmole) was dissolved in DMSO (2.04 mL).

Sample A

The Alkyne Ligand (0.1 mg, 0.31 μmole) in anhydrous DMSO (31.5 μL), was added to a solution of partially acetylated dendrimer **2** (6.4 mg, 0.21 μmole) in anhydrous DMSO (0.979 mL). N,N-diisopropylethylamine (0.2 mg, 0.3 μL, 1.85 μmole) was added to the reaction mixture together with 1.018 mL additional DMSO and the resulting solution was stirred for 30 minutes. A solution of PyBOP (0.20 mg, 0.38 μmole) in anhydrous DMSO (32.1 μL) was added in a dropwise manner (0.1 mL/min) to the dendrimer solution. The resulting reaction mixture was stirred for 24 hrs under nitrogen and then purified using 10,000 MWCO centrifugal filtration devices. Purification consisted of one cycle (10 minutes at 5,000 rpm) using 1x PBS (without magnesium or calcium) and five cycles using DI water. The purified product **A** was lyophilized for three days to yield a white solid (2.9 mg, 45%). ^{1}H NMR integration determined the average number of Alkyne Ligands per dendrimer to be 0.5.

Sample B

Sample B was synthesized in the same manner as Sample A, using partially acetylated dendrimer **2** (6.4 mg, 0.21 μmole) in anhydrous DMSO (0.979 mL), the Alkyne Ligand (0.3 mg, 1.29 μmole) in DMSO (131.8 μL), N,N-diisopropylethylamine (0.7 mg, 1.0 μL, 5.4 μmole), 0.890 mL additional DMSO and PyBOP (0.5 mg, 0.93 μmole) in anhydrous DMSO (96.2 μL). Sample B was purified and lyophilized in the same manner as Sample A. The purified product **Sample B** was a white solid (4.7 mg, 72%). ^{1}H NMR integration determined the average number of Alkyne Ligands per dendrimer to be 2.1.

Sample C

Sample C was synthesized in the same manner as Sample A, using partially acetylated dendrimer **2** (6.4 mg, 0.21 μmole) in anhydrous DMSO (0.979 mL), the Alkyne Ligand (0.3 mg, 1.54 μmole) in DMSO (157.4 μL), N,N-diisopropylethylamine (1.2 mg, 1.6 μL, 9.25 μmole), 0.763 mL additional DMSO and PyBOP (0.8 mg, 1.54 μmole) in anhydrous DMSO (160.4 μL). Sample C was purified and lyophilized in the same manner as Sample A. The purified product **Sample C** was a white solid (7.1 mg, 108%). The extra mass indicated the presence of residual solvent. This did not affect the characterization of the material. ^{1}H NMR integration determined the average number of Alkyne Ligands per dendrimer to be 3.1.

Sample D

Sample D was synthesized in the same manner as Sample A, using partially acetylated dendrimer **2** (6.4 mg, 0.21 μmole) in anhydrous DMSO (0.979 mL), the Alkyne Ligand (0.6 mg, 3.08 μmole) in DMSO (314.7 μL), N,N-diisopropylethylamine (2.4 mg, 3.2 μL, 18.6 μmole), 0.443 mL additional DMSO and PyBOP (1.6 mg, 3.08 μmole) in anhydrous DMSO (320.8 μL). Sample D was purified and lyophilized in the same manner as Sample A. The purified product **Sample D** was a white solid (3.3 mg, 50%). ^{1}H NMR integration determined the average number of Alkyne Ligands per dendrimer to be 3.8.

Sample E

Sample E was synthesized in the same manner as Sample A, using stock solutions prepared in a different day. To partially acetylated dendrimer **2** (6.4 mg, 0.21 μmole) in anhydrous DMSO (1.730 mL), the Alkyne Ligand (0.6 mg, 3.08 μmole) in DMSO (314.7 μL), N,N-diisopropylethylamine (2.4 mg, 3.2 μL, 18.6 μmole), and PyBOP (1.6 mg, 3.08 μmole) in anhydrous DMSO (320.8 μL) were added. Sample E was purified and lyophilized in the same manner as Sample A. The purified product **Sample E** was a white solid (2.2 mg, 32%). ^{1}H NMR integration determined the average number of Alkyne Ligands per dendrimer to be 10.4.

Samples F-H: G5-Ac$_{76}$-Azide$_{(1.9, 4.4, 7.7)}$

Three stock solutions were prepared to synthesize Samples F-H. A solution of partially acetylated dendrimer **2** (52.3 mg, 1.71 μmole) was prepared with anhydrous DMSO (8.00 mL). The Azide Ligand (9.2 mg, 39.1 μmole) was dissolved in DMSO (4.6 mL). Last, PyBOP (10.2 mg, 19.6 μmole) was dissolved in DMSO (2.04 mL).

Sample F

The Azide Ligand (0.10 mg, 0.49 μmole) solution in anhydrous DMSO (43.9 μL), was added to a solution of partially acetylated dendrimer **2** (6.4 mg, 0.21 μmole) in anhydrous DMSO (0.979 mL). N,N-diisopropylethylamine (0.70 mg, 1.0 μL, 5.6 μmole) was added to the reaction mixture together with 0.924 mL additional DMSO and the resulting solution was stirred for 30 minutes. The solution of PyBOP (0.50 mg, 0.93 μmole) in anhydrous DMSO (96.2 μL) was added in a dropwise manner (0.1 mL/min) to the dendrimer solution. The resulting reaction mixture was stirred for 24 hrs under nitrogen and then purified as described earlier. The purified product, Sample F, was lyophilized for three days to yield a white solid (4.1 mg, 63%). ^{1}H NMR integration determined the mean number of Azide Ligands per dendrimer to be 1.9.

Sample G

Sample G was synthesized in the same manner as Sample F, using partially acetylated dendrimer **2** (6.4 mg, 0.21 μmole) in anhydrous DMSO (0.979 mL), the Azide Ligand (0.40 mg, 1.5 μmole) in DMSO (181.3 μL), N,N-diisopropylethylamine (1.2 mg,

1.6 μL, 9.3 μmole), 0.787 mL additional DMSO and PyBOP (0.80 mg, 1.5 μmole) in anhydrous DMSO (160.4 μL). Sample G was purified and lyophilized in the same manner as Sample F. The purified product, Sample G, was a white solid (4.2 mg, 63%). ^{1}H NMR integration determined the mean number of Azide Ligands per dendrimer to be 4.4.

Sample H

Sample H was synthesized in the same manner as Sample F, using partially acetylated dendrimer **2** (6.4 mg, 0.21 μmole) in anhydrous DMSO (0.979 mL), the Azide Ligand (0.70 mg, 3.1 μmole) in DMSO (362.5 μL), N,N-diisopropylethylamine (2.4 mg, 3.2 μL, 19 μmole), 0.443 mL additional DMSO and PyBOP (1.6 mg, 3.1 μmole) in anhydrous DMSO (320.8 μL). Sample H was purified and lyophilized in the same manner as Sample F. The purified product, Sample H, was a white solid (3.5 mg, 52%). ^{1}H NMR integration determined the mean number of Azide Ligands per dendrimer to be 7.7.

Samples I-M: G5-Ac$_{80}$-Alkyne$_{(0.4, 0.7, 2.7, 6.8, 10.2)}$

Three stock solutions were generated to synthesize Samples I-M. A solution of the partially acetylated dendrimer **3** (22.4 mg, 0.728 μmole) was prepared with anhydrous DMSO (4.9778 mL). The Alkyne Ligand (9.9 mg, 49 μmole) was dissolved in DMSO (4.9500 mL). Benzotriazol-1-yl-oxytripyrrolidinophosphonium hexafluorophosphate (PyBOP) (5.4 mg, 10 μmole) was dissolved in DMSO (1.000 mL).

Sample I

The Alkyne Ligand (29.0 μg, 0.146 μmole) in anhydrous DMSO (14.6 μL), was added to a solution of partially acetylated dendrimer **3** (4.4 mg, 0.14 μmole) in anhydrous DMSO (0.978 mL). N,N-diisopropylethylamine (1.1 mg, 1.5 μL, 8.6 μmole) was added to the reaction mixture and the resulting solution was stirred for 30 minutes. A solution of PyBOP (74.0 μg, 0.143 μmole) in anhydrous DMSO (13.8 μL) was added in a dropwise manner (0.1 mL/min) to the dendrimer solution. The resulting reaction mixture was stirred for 24 hrs under nitrogen and then purified as described earlier. The purified product, Sample I, was lyophilized for three days to yield a white solid (3.7 mg, 84%). [1]H

131

NMR integration determined the mean number of Alkyne Ligands per dendrimer to be 0.4.

Sample J

Sample J was synthesized in the same manner as Sample I, using partially acetylated dendrimer **3** (4.4 mg, 0.14 μmole) in anhydrous DMSO (0.978 mL), the Alkyne Ligand (58.0 μg, 0.286 μmole) in DMSO (29.2 μL), N,N-diisopropylethylamine (0.2 mg, 0.3 μL, 2 μmole), and PyBOP (0.15 mg, 0.29 μmole) in anhydrous DMSO (28 μL). Sample J was purified and lyophilized in the same manner as Sample I. The purified product, Sample J, was a white solid (3.1 mg, 70%). ^{1}H NMR integration determined the mean number of Alkyne Ligands per dendrimer to be 0.7.

Sample K

Sample K was synthesized in the same manner as Sample I, using partially acetylated dendrimer **3** (4.4 mg, 0.14 μmole) in anhydrous DMSO (0.978 mL), the Alkyne Ligand (0.15 mg, 0.72 μmole) in DMSO (73.0 μL), N,N-diisopropylethylamine (0.6 mg, 0.7 μL, 4 μmole), and PyBOP (0.37 mg, 0.72 μmole) in anhydrous DMSO (69 μL). Sample K was purified and lyophilized in the same manner as Sample I. The purified product, Sample K, was a white solid (3.6 mg, 80%). ^{1}H NMR integration determined the mean number of Alkyne Ligands per dendrimer to be 2.7.

Sample L

Sample L was synthesized in the same manner as Sample I, using partially acetylated dendrimer **3** (4.4 mg, 0.14 μmole) in anhydrous DMSO (0.978 mL), the Alkyne Ligand (0.29 mg, 1.4 μmole) in DMSO (146 μL), N,N-diisopropylethylamine (1.1 mg, 1.5 μL, 8.6 μmole), and PyBOP (0.74 mg, 1.4 μmole) in anhydrous DMSO (138 μL). Sample L was purified and lyophilized in the same manner as Sample I. The purified product, Sample L, was a white solid (3.5 mg, 76%). ^{1}H NMR integration determined the mean number of Alkyne Ligands per dendrimer to be 6.8.

Sample M

Sample M was synthesized in the same manner as Sample I, using partially acetylated dendrimer **3** (4.4 mg, 0.14 μmole) in anhydrous DMSO (0.978 mL), the

Alkyne Ligand (0.44 mg, 0.14 µmole) in DMSO (978 µL), N,N-diisopropylethylamine (1.7 mg, 2.2 µL, 13 µmole), and PyBOP (1.1 mg, 2.1 µmole) in anhydrous DMSO (207 µL). Sample M was purified and lyophilized in the same manner as Sample I. The purified product, Sample M, was a white solid (2.7 mg, 57%). ^{1}H NMR integration determined the mean number of Alkyne Ligands per dendrimer to be 10.2.

Dendrimer 4: Synthesis of Partially Acetylated Dendrimer G5-Ac$_{71}$-(NH$_2$)$_{41}$

Purified G5 PAMAM dendrimer **1** (53.1 mg, 1.94 µmole) was dissolved in anhydrous methanol (7.9 mL). Triethylamine (24.6 µL, 0.177 mmole) was added to this mixture and stirred for 30 minutes. Acetic anhydride (14.4 µL, 0.141 mmole) was added to anhydrous methanol (2.2 mL) and the resulting mixture was added with a syringe pump to the dendrimer solution. The dropwise addition rate was 11.9 mL/hr and the stir-rate in the dendrimer solution was ~900 rpm. The reaction was carried out in a glass flask, under nitrogen, at room temperature for 12 hours. Methanol was evaporated from the resulting solution and the product was purified using 10,000 MWCO centrifugal filtration devices. Purification consisted of one cycle (10 minutes at 5,000 rpm) using 1x PBS (without magnesium and calcium) and five cycles using DI water. The purified dendrimer was lyophilized for three days to yield a white solid (45.6 mg, 77%). ^{1}H NMR integration determined the degree of acetylation to be 63%.

Dendrimer 5: Synthesis of Partially Acetylated Dendrimer G5-Ac$_{82}$-(NH$_2$)$_{30}$

Purified G5 PAMAM dendrimer **1** (50.1 mg, 1.83 µmole) was dissolved in anhydrous methanol (9.5 mL). Triethylamine (23.2 µL, 0.167 mmole) was added to this mixture and stirred for 30 minutes. Acetic anhydride (12.6 µL, 0.133 mmole) was added in a dropwise manner to the dendrimer solution. The stir-rate in the dendrimer solution was low (600 rpm). The reaction was carried out in a glass flask, under nitrogen, at room temperature for 24 hours. Methanol was evaporated from the resulting solution and the product was purified using 10,000 MWCO centrifugal filtration devices. Purification consisted of one cycles (10 minutes at 5,000 rpm) using 1x PBS (without magnesium and calcium) and five cycles using DI water. The purified dendrimer was lyophilized for three

days to yield a white solid (46.6 mg, 62%). ^{1}H NMR integration determined the degree of acetylation to be 83%.

Samples N and O:

Two stock solutions were generated to synthesize Samples N and O. A solution of the Alkyne Ligand (7.2 mg, 35 μmole) was dissolved in DMSO (3.600 mL). Benzotriazol-1-yl-oxytripyrrolidinophosphonium hexafluorophosphate (PyBOP) (8.8 mg, 17 μmole) was dissolved in DMSO (1.760 mL).

Sample N

The Alkyne Ligand stock solution in anhydrous DMSO (1.1 mg, 5.1 μmole, 525.7 μL), was added to a solution of **dendrimer 4** (12.8 mg, 0.422 μmole) in anhydrous DMSO (2.889 mL). N,N-diisopropylethylamine (1.8 mg, 2.5 μL, 14 μmole) was added to the reaction mixture and the resulting solution was stirred for 30 minutes. The stock solution of PyBOP in anhydrous DMSO (2.7 mg, 5.2 μmole) 535.9 μL) was added in a dropwise manner (0.27 mL/min) to the dendrimer solution. The resulting reaction mixture was stirred for 24 hrs under nitrogen and then purified as described earlier. The purified product, Sample N, was lyophilized for three days to yield a white solid (12.4 mg, 93%). ^{1}H NMR integration determined the mean number of Alkyne Ligands per dendrimer to be 6.6.

Sample O

The Alkyne Ligand (13.0 μg, 0.146 μmole) in anhydrous DMSO (14.6 μL), was added to a solution of **dendrimer 5** (12.8 mg, 0.422 μmole) in anhydrous DMSO (2.889 mL). N,N-diisopropylethylamine (1.8 mg, 2.5 μL, 14 μmole) was added to the reaction mixture and the resulting solution was stirred for 30 minutes. The stock solution of PyBOP in anhydrous DMSO (2.7 mg, 5.2 μmole) 535.9 μL) was added in a dropwise manner (0.27 mL/min) to the dendrimer solution. The resulting reaction mixture was stirred for 24 hrs under nitrogen and then purified as described earlier. The purified product, Sample N, was lyophilized for three days to yield a white solid (13.0 mg, 96%). ^{1}H NMR integration determined the mean number of Alkyne Ligands per dendrimer to be 6.8.

134

<center>**Results**</center>

Characterization of the dendrimer-ligand Samples A-M

The three conjugate sets were characterized by ^{1}H NMR spectroscopy and HPLC. We have previously shown that NMR integration combined with GPC and potentiometric titration provides the mean number of ligands per dendrimer.[34-35] Briefly, the mean number of end groups per G5-(NH$_2$) dendrimer **1** (112) was found by potentiometric tritration and the number average molecular weight from GPC. The mean number of methyl protons per partially acetylated dendrimer was then calculated using the integral for the methyl protons, the integrals for the methylene protons on the amine-terminated arms and the mean number of end groups per dendrimer. Finally, the mean number of methyl protons per dendrimer was used as a reference integral to quantify the mean number of ligands per dendrimer in the NMR spectra for Samples A-M. The arithmetic mean number of ligands per dendrimer is reported in **Table 5.1** for each sample. Similar to many nanoparticle-based systems, including a plethora of dendrimer-ligand conjugates,[30,33,37,41] the mean ligand-dendrimer ratio for Samples A-M ranged from 0.4 to 10.4. In this table, and in all figures, data resulting from acetylated dendrimers that has been assigned are resulting from ineffective mass transport is identified with a   to assist the reader in keep track of the sample sets.

HPLC characterization of Samples A-M was also performed using a previously reported methods.[35] Elution traces recorded at 210 nm are plotted in **Figure 5.1** by sample set. The trace of the parent dendrimer (Dendrimer **2**: G5-Ac$_{76}$-(NH$_2$)$_{36}$ and Dendrimer **3**: G5-Ac$_{80}$-(NH$_2$)$_{32}$) is included at the base of each column. Discrete peaks, with the same peak shape as the parent dendrimer, can be seen within each HPLC trace. We have previously shown that each of these discrete peaks are composed of a dendrimer component with a different number of Alkyne or Azide Ligands per particle.[34-35,40] The first discrete peak in each trace was found to be composed of dendrimer with 0 ligands. Dendrimer components with 1, 2, 3… etc. ligands were found to have incrementally

<center>135</center>

longer retention times. A previously developed peak fitting method deconstructed the HPLC trace with multiple copies of a fitting peak that had the same shape as the HPLC trace for the unmodified dendrimer (dendrimer **2** and **3**). This fitting method quantified the relative concentration of each dendrimer-ligand component in the distribution. With the relative concentration of each dendrimer-ligand component, the mean, median, and mode for each sample were calculated and are reported in **Table 5.1**. Quantified distributions for each sample are plotted by sample set in **Figure 5.2** and in groups of similar ligand means in **Figure 5.3**.

Two major observations can be made from the quantified dendrimer-ligand distributions in **Figure 5.2** and **Figure 5.3**. First, the sample sets made using dendrimer **2** (G5-Ac$_{76}$-Alkyne and G5-Ac$_{76}$-Azide sample sets (Samples A-H)) have the same distribution features. Comparing the distributions for Sample B and F in **Figure 5.3c** found the number of components in each sample to be very similar (10 vs. 13) and the difference between the concentration of each dendrimer-ligand component to be 3% or less. Remarkably, for the samples in these two sets (Samples A-H) with means ranging from 0.5-10.4, the mode was 0. This highlights a very interesting distribution feature that is most apparent in Sample E and H (**Figure 5.2**). Instead of a skewed-Poisson profile, the distributions are bimodal. High concentrations of dendrimer with low numbers of ligands (0, 1 and 2) are present with a second mode at a much higher dendrimer-ligand component (13 for Sample H and 15 for Sample E).

The second major observation from **Figures 5- 1-3** is that the G5-Ac$_{80}$-Alkyne set (Samples I-M) which was produced using dendrimer **3**, does not have the same distribution features as the G5-Ac$_{76}$-Alkyne and G5-Ac$_{76}$-Azide sample sets (Samples A-H). This difference can be best seen between Sample E and M (**Figure 5.3a**). Whereas Sample E is bimodal with a median of 12 and a mode of 0, Sample M follows a skewed-Poisson distribution and has a median and mode of 11. The two samples have identical means by NMR (10.4 and 10.2), and yet Sample M has 6 fewer dendrimer-ligand components (24 vs. 30).

Characterization of partially acetylated dendrimer batches as a function of mass transport effectiveness

Characterization of the two partially acetylated batches of dendrimer by NMR spectroscopy followed previously established protocols.[35]   Peak integration provided a means to calculate the degree of acetylation.   Dendrimer 4, which was partially acetylated under effective stirring and dilution conditions, was found to be 63% acetylated.   Because GPC and potentiometric titration had determined the starting dendrimer **1** to have a mean of 112 terminal arms per particle, the dendrimer in this batch had a mean of 71 Ac groups and 41 NH_2 groups.   Dendrimer 5, acetylated with ineffective stirring and undiluted acetic anhydride, was 73% acetylated with a mean of 82 Ac and 30 NH_2 groups.

No direct information about the distribution of -Ac (and conversely -NH_2) groups can be obtained from the NMR spectra (**Figure 5.4**).   To the level of detail at which the spectra have been analyzed in the past, the samples appear to be the same.   A closer examination does find some interesting differences.   First, there is a downfield chemical shift (a change of approximately 0.05 ppm) in **Figure 5.4b** for protons in the interior of the dendrimer structure.   Second, the broad peak at 3.2 ppm in **Figure 5.4a** appears to be resolved into two different peaks in **Figure 5.4b**.   These changes, however, cannot be interpreted to provide information about different distributions in the dendrimer structure.

While close scrutiny of the NMR spectra in **Figure 5.4** does find small differences, HPLC characterization of the two dendrimer batches (4 and 5) in Figure 5.5 reveal no differences between the two batches.   The small peaks adjacent to the major peak have been previously determined to be different dendrimer defect structures (trailing generation and dimer defects).[42] The two major peaks do have slightly different retention times but this difference is within the run-to-run variability of the HPLC system (4%).

Characterization of dendrimer-ligand samples N and O

NMR spectra for Samples N and O are contained in **Figure 5.6**. The mean number of ligands per dendrimer was found to be 6.7 and 6.6 respectively. In addition to having the same ligand mean, the NMR spectra reveals very few clues about any differences in the dendrimer-ligand distributions. Chemical shifts between the two spectra are very similar and the resolved semi-overlapping peaks at 3.2 ppm in dendrimer 5 (**Figure 5.4b**) are no longer resolved in the ligand conjugated material. There is a difference in the FWMH for the ligand aa' bb' proton peaks at 7.1 and 6.9. FWHM is 7 hz wider for Sample O.

HPLC traces for Sample N and O are dramatically different (**Figure 5.7**). Sample N has a skewed-Poisson profile similar to the $G5-Ac_{80}$-Alkyne sample set (Samples I-M). Sample O has the same, if not more pronounced bimodal distribution features as sample sets $G5-Ac_{76}$-Alkyne and $G5-Ac_{76}$-Azide (Samples A-H). Differences between the two samples are even more apparent in the quantified distributions (**Figure 5.8** and **Table 5.2**). The mode for sample O is zero with this component making up 27% of the sample. Conversely, the mode for Sample N is 10 and this component makes up only about 7% of the sample. Furthermore, although the samples have the same means, Sample O is significantly more heterogeneous than Sample N (26 vs. 20 dendrimer-ligand components).

Discussion

The distinct HPLC profile differences within Samples A-M provided the motivation for this investigation. There is clear a dependence of the dendrimer-ligand distribution profile with the batch of partially acetylated dendrimer. In fact, the use of two different ligand molecules (Alkyne vs. Azide) does not result in any differences in distribution features. Although the additional data is not included in this manuscript, we have observed variations in all of the material produced using this system correlating with the batch of partially acetylated dendrimer. The distribution profiles exhibited by Samples O and N are the most and least heterogeneous profiles that we have observed.

Based on our observations of samples A-M, our hypothesis was that Dendrimer 2 and 3 had different distribution profiles of dendrimer-modification site ratios caused by a change in the quality of mass transport during the partial acetylation. Because the goal of the partial acetylation is to passivate an average of 60-80% of the dendrimer modification sites (primary amines), the reaction step occurs with an excess of modification sites per dendrimer relative to the molar amount of acetic anhydride. These conditions result in a distribution of dendrimer with different numbers of acetyl groups and consequently a distribution of dendrimer-modification site ratios. Assuming the partial acetylation reaction has perfect mass transport and is a purely stochastic process, the distribution profile would be expected to be similar to the Poisson distribution in **Figure 5.9a**. Such a distribution means that during the ligand conjugation reaction some dendrimer have a higher probability to react with ligand molecules. This causes an increase in the distribution heterogeneity.

We have observed such an increase in heterogeneity in our previous study that compared distributions between conjugates made with a $G5-(NH_2)_{112}$ dendrimer and with a partially acetylated dendrimer.[35] The dendrimer-ligand conjugates made with the $G5-(NH_2)_{112}$ had slightly skewed-Poisson distributions and the conjugate made with the partially acetylated dendrimer were more skewed. Given that ligand distributions do appear to be sensitive to a pre-existing acetyl group distribution, it is reasonable to hypothesize that the two dendrimer-ligand distribution profile types indicate that Dendrimer **2** and **3** have significantly different acetyl group distributions. Under our hypothesis, in dendrimer **3**, used to make Samples I-M, the acetyl distribution would be similar to the distribution in **Figure 5.9a**. For dendrimer **2**, the parent to Samples A-H, the distribution of acetyl group-dendrimer ratios would be more heterogeneous and would include a large percentage of dendrimer components with zero or very few modification sites. This sub-population would have a very low probability of subsequent ligand conjugation and would give rise to the high concentration of dendrimer with 0, 1, and 2 ligands in samples A-H.

The final part of our hypothesis is that this subpopulation of dendrimer-acetyl components is a consequence of ineffective mass transport. Due to the fast reaction kinetics of the acetylation reaction, locally high concentrations of acetic anhydride could easily generate the sub-population of dendrimer with very few modification sites. The remaining dendrimer components would have a significantly increased probability of reacting with ligand molecules leading to an increase in heterogeneity.

Dendrimer **4** and **5** were synthesized to test our hypothesis. Dendrimer **4** was produced under effective mass transport conditions, defined by a high stir rate, dilution of acetic anhydride in methanol prior to addition and use of a syringe pump to achieve a slow, uniform addition of acetic anhydride. The conditions used for Dendrimer **5** were characteristic of an ineffective mass transport regime. The stir rate was very low, acetic anhydride was not diluted with methanol before addition and a syringe pump was not used. As quantified in **Figure 5.8**, these two mass transport qualities ultimately result in dramatically different dendrimer-ligand distributions (Samples N and O).

The dendrimer-ligand distributions in Sample N and O are consistent with our hypothesis that the effectiveness of mass transport during the partial acetylation reaction has a major influence on subsequent dendrimer-ligand distributions. The ineffective mass transport dendrimer conjugate (Sample O) has a bimodal dendrimer-ligand distribution with 27% of the dendrimer particles left unmodified by the ligand conjugation reaction. This profile is an extreme form of the bimodal profile originally observed in the dendrimer-ligand samples made with dendrimer **2** (Samples A-H). Similar to the samples made with dendrimer **3** (Samples I-M), the effective mass transport dendrimer (4) produces a dendrimer-ligand distribution that is a skewed-Poisson (Sample N).

Even in this study, direct resolution of the distributions of dendrimer-actyl ratios is not achieved. It is clear, however, that the subsequent dendrimer-ligand distributions that are resolved provide indirect information about the distribution of dendrimer particles with different number of actyl groups. In the future, the Alkyne and Azide

ligands may find a use as quality control tests to monitor the reproducibility of the partial acetylation as well as other ligand conjugations for which resolution of the distribution is not achieved.

Implications

The findings of this study should serve as a cautionary tale for nanoparticle-ligand systems. First, control of the passivation step is very important for achieving reproducible products. In particular, for dendrimer-based systems the introduction of a partial acetylation step may be the main obstacle to batch reproducibility. The sensitivity of this reaction to slight changes in mass transport as well as to changes in the starting $G5-NH_2$ dendrimer (variable amounts of dendrimer defect structures) makes this reaction hard to control. New platform designs should seek to eliminate the partial acetylation step and perform ligand conjugations to the $G5-NH_2$ dendrimer because of the variability on functional ligand distribution that is enforced by the variability in the acetylation distribution.

By performing the reactions in this sequence, a reproducible Poisson distribution of ligands is achievable which is the narrowest distribution that can be physically obtained for such solution phase reactions of small ligands conjugated to an excess of surface sites.[34-35] Distributions of this kind can show excellent targeted drug delivery *in vitro* and *in vivo*.[31,37-38] The remaining primary amines can then be passivated in a final acetylation step. In other nanoparticle systems, platform designs need to consider the fact that the passivation step typically results in a distribution of modification sites. This distribution then increases the heterogeneity of subsequent nanoparticle-ligand distributions.

Second, systems that achieve a reproducible mean number of ligands per particle may still not have a consistent distribution. It is very alarming that Samples E and M had the same mean number of ligands per dendrimer and yet had completely different distributions. Only the HPLC analysis of the samples identified the differences. The batches of parent dendrimer for these samples (dendrimer **2** and **3**) were produced under

what was thought to be the same synthetic conditions. Characterization of dendrimer **2** and **3** found that they were nominally the same material. Clearly this was not the case. The quality of mass transport during the partial acetylation reaction for dendrimer **2** was impaired relative to dendrimer **3**. The result of this impairment was a major difference in the dendrimer-ligand distribution that was only detected by HPLC. Similarly, characterization of dendrimer **4** and **5** with intentionally different mass transport conditions, failed to detect any differences in the material. Again, only the HPLC characterization of Sample N and O revealed the even more extreme differences between the material. This is problematic because the capability to resolve the distribution of components does not exist for many nanoparticle-ligand systems in production today. Frequently, only the mean ligand-nanoparticle ratio is known for these systems. The results of this study indicate that it will be very important to go a step further and identify the distribution that gives rise to the mean. Failure to do so may make batch reproducibility a major challenge as these systems are moved to commercial scales. To this end, future studies need to focus on the relationships between the nanoparticle-ligand distributions and the material properties of the system. These studies will be very useful for defining the tolerable levels of variability in the distribution that will produce the same bulk properties.

Conclusion

In conclusion, the effectiveness of mass transport in the partial acetylation step has a major impact on subsequent dendrimer-ligand distributions. Our results indicate that mass transport effectiveness has a dramatic impact upon the dendrimer-acetyl distribution which in turn controls the distribution of ligands which can be acheived. Furthermore, this study demonstrates that using the mean ligand-nanoparticle ratio alone is insufficient to ensure that the batch reproducibility of the distribution is maintained.

Acknowledgements

Table 5.1: Comparison of the average number of ligands per dendrimer computed by two independent techniques (NMR spectroscopy and HPLC) for Samples A-M. Samples A-H were produced using Dendrimer 2 as the parent partially acetylated dendrimer. Samples I-M were produced with Dendrimer 3. Dendrimer samples containing a distribution of ligands that are assigned as resulting from ineffective mass transport in the acetylation step are identified with a .
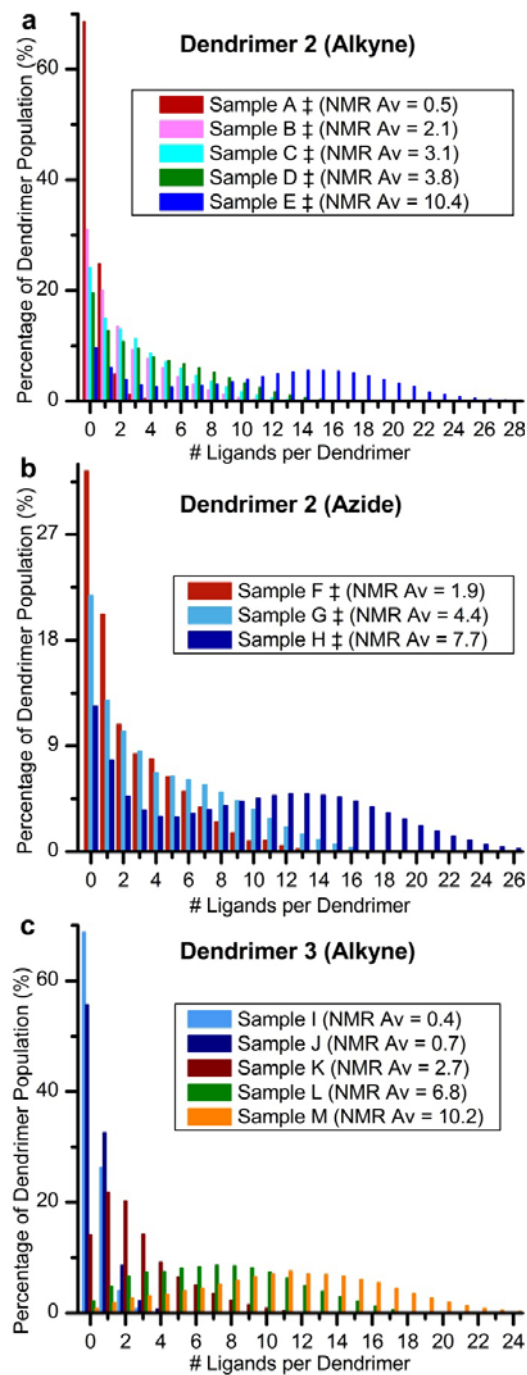
| | | G5-Ac$_{76}$-Alkyne | | | | |
| | | NMR | HPLC | | | |
		Arithmetic Mean	Arithmetic Mean	Median	Mode	# Dendrimer Species
Dendrimer 2	**Sample A**	0.5 ± 0.1	0.4 ± 0.02	0	0	5
	Sample B	2.1 ± 0.2	2.3 ± 0.09	1	0	10
	Sample C	3.1 ± 0.3	3.4 ± 0.1	2	0	13
	Sample D	3.8 ± 0.4	4.1 ± 0.2	3	0	13
	Sample E	10.4 ± 1.0	11.0 ± 0.4	12	0	30
		G5-Ac$_{76}$-Azide				
		NMR	HPLC			
		Arithmetic Mean	Arithmetic Mean	Median	Mode	# Dendrimer Species
	Sample F	1.9 ± 0.2	1.9 ± 0.08	1	0	13
	Sample G	4.4 ± 0.4	4.2 ± 0.2	3	0	16
	Sample H	7.7 ± 0.8	9.4 ± 0.4	10	0	26
		G5-Ac$_{80}$-Alkyne				
		NMR	HPLC			
		Arithmetic Mean	Arithmetic Mean	Median	Mode	# Dendrimer Species
Dendrimer 3	**Sample I**	0.4 ± 0.04	0.4 ± 0.01	0	0	3
	Sample J	0.7 ± 0.07	0.6 ± 0.02	0	0	4
	Sample K	2.7 ± 0.8	2.8 ± 0.1	2	1	11
	Sample L	6.8 ± 0.7	7.2 ± 0.3	7	7	17
	Sample M	10.2 ± 1.0	11.2 ± 0.5	11	11	24

Table 5.2: Comparison of the average number of ligands per dendrimer computed by NMR spectroscopy and HPLC for Sample N, produced with dendrimer 4, and Sample O, produced with dendrimer 5.

	NMR	HPLC

	Arithmetic Mean	Arithmetic Mean	Median	Mode	# Dendrimer Species
Sample N (Dendrimer 4)	6.7 ± 0.7	7.8 ± 0.3	8	10	20
Sample O (Dendrimer 5)	6.6 ± 0.7	7.0 ± 0.3	4	0	26
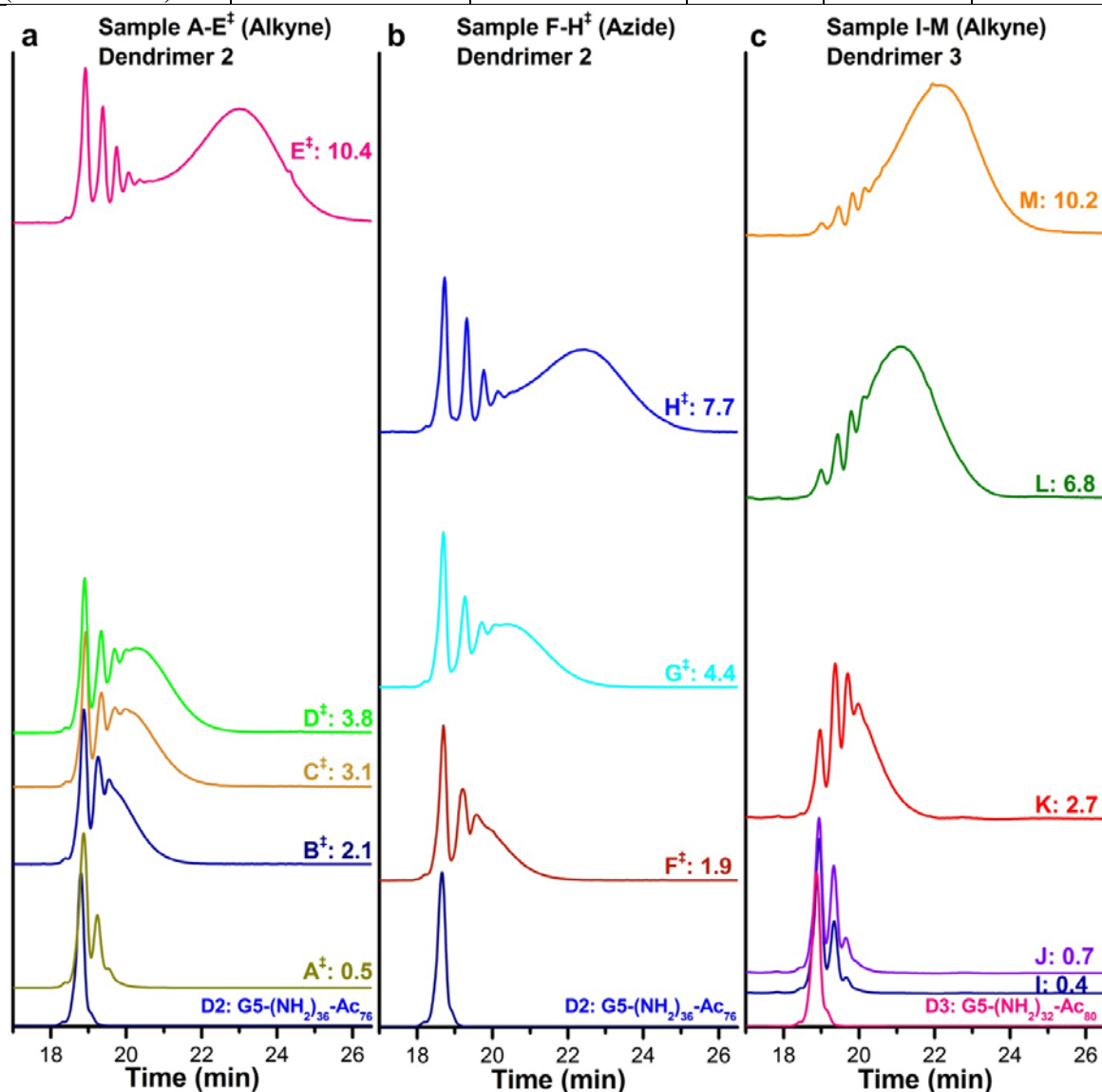
Figure 5.1: HPLC elution traces of dendrimer-ligand conjugates (Sample A-M) at 210 nm. Traces were normalized to the largest peak and off-set on the vertical axis based on the mean number of ligands per dendrimer. The mean number of ligands per dendrimer is listed by each trace. The HPLC trace of the un-modified parent dendrimer for each sample set is provided at the base of each panel (Dendrimer **2** G5-Ac$_{76}$-(NH$_2$)$_{36}$ for panel a and b, and Dendrimer **3** G5-Ac$_{80}$-(NH$_2$)$_{32}$ for panel c). a) HPLC traces for the G5-Ac$_{76}$-Alkyne sample set (Samples A-E). b) HPLC traces for the G5-Ac$_{76}$-Azide sample set (Samples F-H). c) HPLC traces for the G5-Ac$_{80}$-Alkyne sample set (Samples I-M). Dendrimer samples containing a

distribution of ligands that are assigned as resulting from ineffective mass transport in the acetylation step are identified with a   .

Figure 5.2: Quantified dendrimer-ligand distributions determined by the peak fitting enabled deconstruction of the HPLC traces. a) Dendrimer-ligand distributions for the G5-Ac$_{76}$-Alkyne sample set (Samples A-E). b) Dendrimer-ligand distributions for the G5-Ac$_{76}$-Azide sample set (Samples F-H). c) Dendrimer-ligand distributions for the G5-Ac$_{80}$-Alkyne sample set (Samples I-M). Dendrimer samples containing a distribution of ligands that are assigned as resulting from ineffective mass transport in the acetylation step are identified with a .
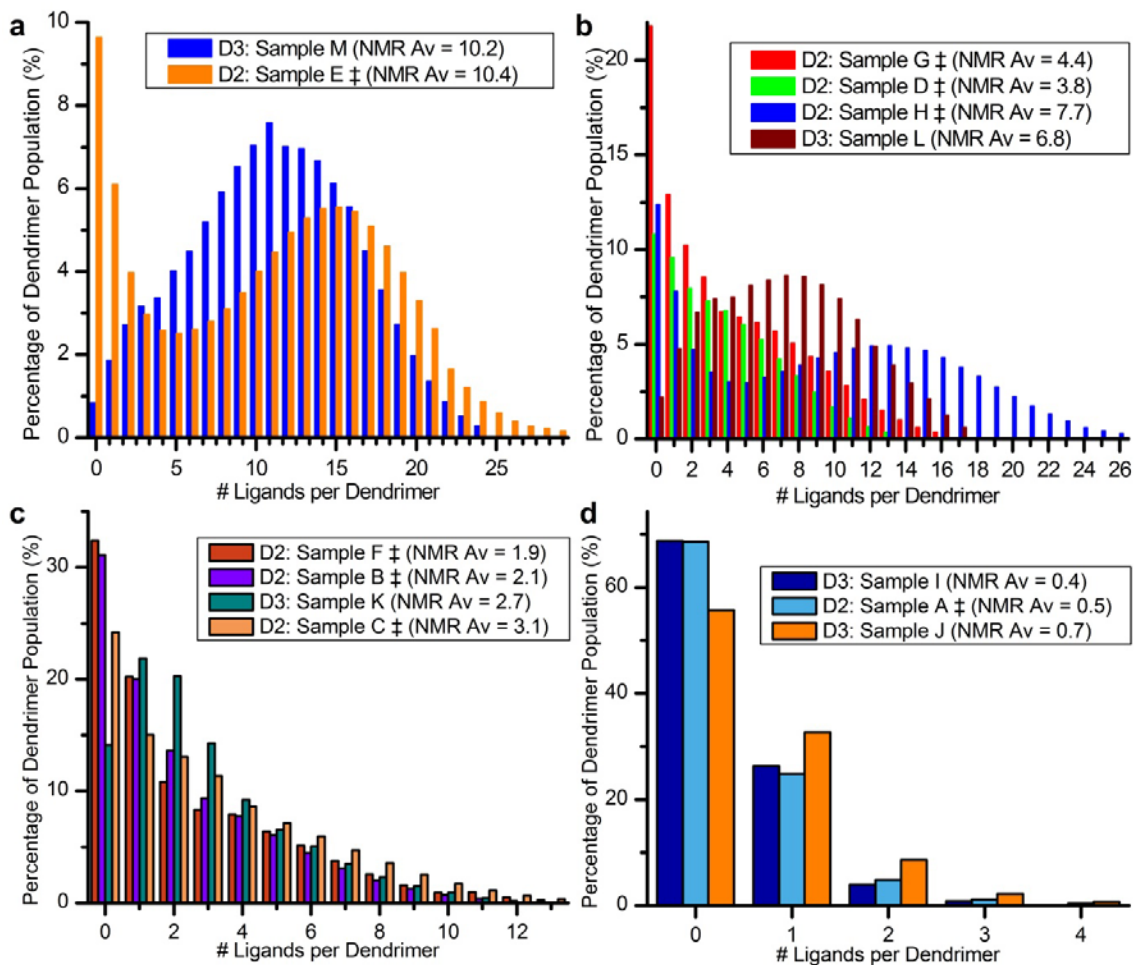
Figure 5.3: Comparison of the distribution of dendrimer-ligand species for samples with similar ligand means. The parent dendrimer is noted for each sample: D2 for dendrimer **2** and D3 for dendrimer **3**. a) Distributions for Samples M and E with ligand means of 10.2 and 10.4, respectively. b) Distributions for samples with means between 4.4 and 6.8 (Samples G, D, H and L). c) Distributions for samples with means between 1.9 and 3.1 (Samples F, B, K and C). d) Distributions for samples with means between 0.4 and 0.7 (Samples I, A and J). Dendrimer samples containing a distribution of ligands that are assigned as resulting from ineffective mass transport in the acetylation step are identified with a   .
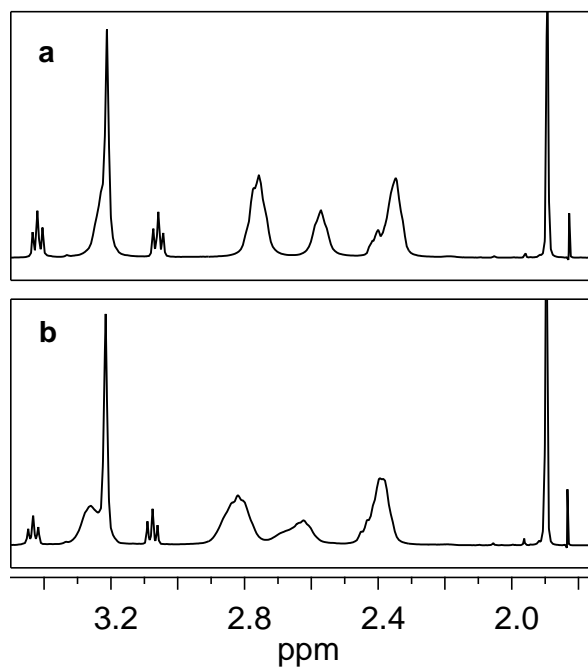
Figure 5.4: ^{1}H NMR spectra of partially acetylated dendrimer samples. **a**) Spectrum of the partially acetylated dendrimer **4** produced under effective mass transport conditions (G5-Ac$_{71}$-(NH$_2$)$_{41}$). NMR peak integration determined the average degree of acetylation to be 63%. **b**) Spectrum of the partially acetylated dendrimer **5** produced under ineffective mass transport conditions (G5-Ac$_{82}$-(NH$_2$)$_{30}$). NMR peak integration determined the average degree of acetylation to be 73%.
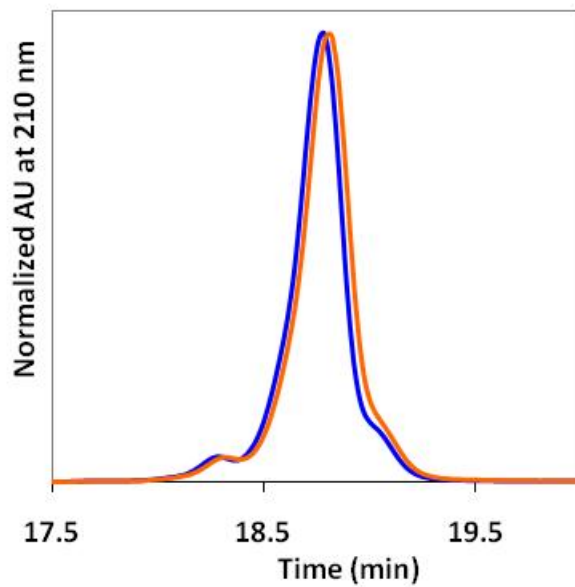
Figure 5.5: Normalized HPLC traces at 210 nm of partially acetylated dendrimer **4** (blue) and **5** (orange). Dendrimer **4** was synthesized under effective mass transport conditions while dendrimer **5** was produced with ineffective mass transport.
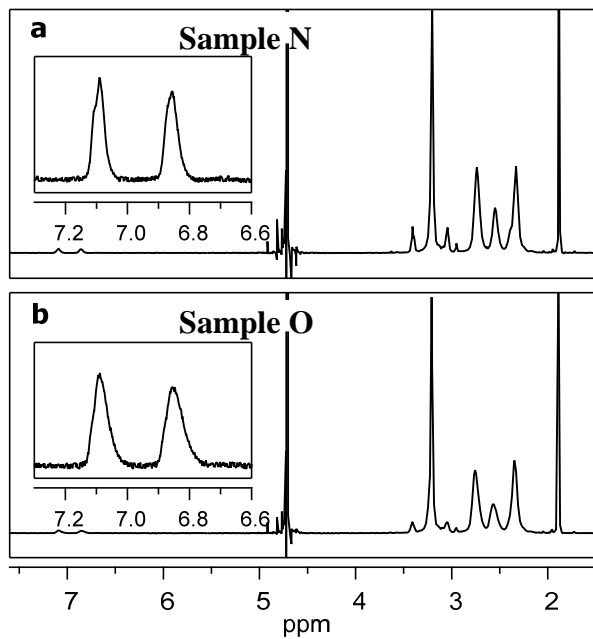
Figure 5.6: NMR spectra of Sample N (a), produced using dendrimer **4** and Sample O (b), produced using dendrimer **5**. An expanded view insert of the ligand aa' bb' protons at approximately 7.1 ppm and 6.85
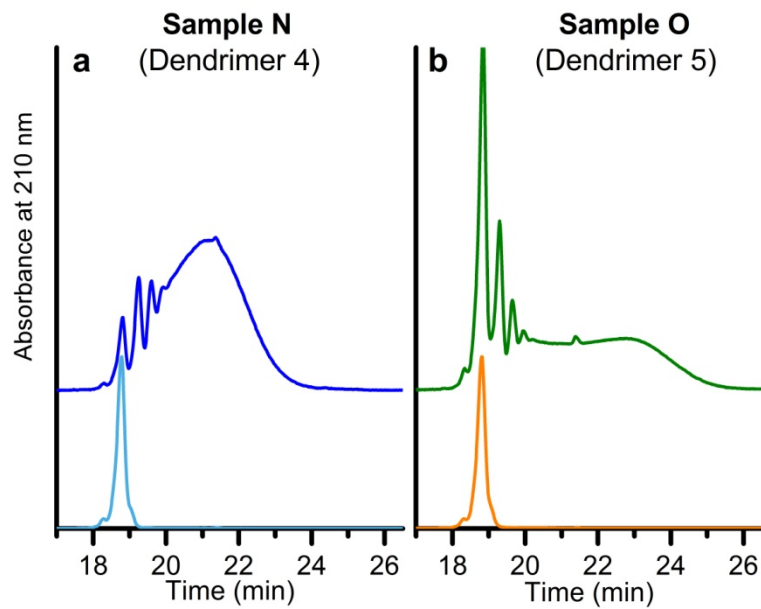
Figure 5.7: HPLC elution traces of Sample N (a) and O (b) at 210 nm. The elution profile of the parent partially acetylated dendrimer (**4** and **5**, respectively) is included at the base of each column.
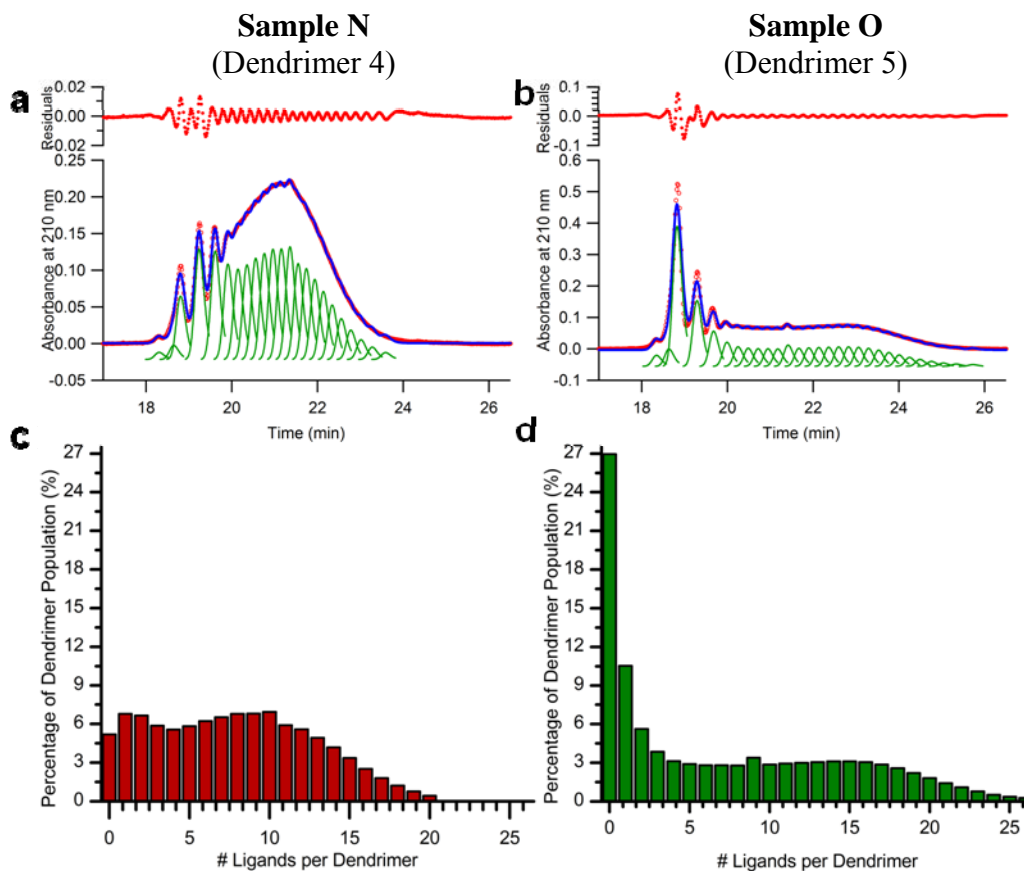
Figure 5.8: The distribution of dendrimer-ligand components for Sample N and O quantified by the peak fitting method. a) 210 nm HPLC elution data for Sample N are shown in red dots, the multiple copies of the fitting peak is shown in green, and the summation of the fitting peaks are plotted in blue. Residual values in red have been multiplied by 10^6. b) Fitted HPLC trace for Sample O. The color scheme for panel b is the same as panel a. Residual values in red have been multiplied by 10^6. c) Relative concentration of each dendrimer-ligand component in Sample N. d) Relative concentration of each dendrimer-ligand component in Sample O.
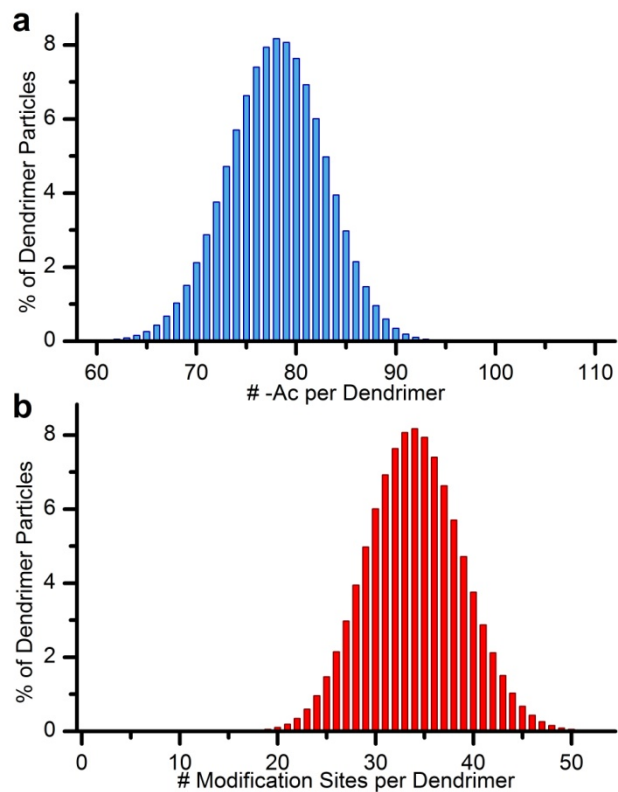
Figure 5.9: Theoretical distributions of dendrimer with different numbers of acetyl groups per particle (**a**) and the distribution of dendrimer with different numbers of modification sites that result from the partial acetylation (**b**).

References

(1)   Maye, M. M.; Nykypanchuk, D.; Cuisinier, M.; van der Lelie, D.; Gang, O. *Nature Materials* **2009**, *8*, 388-391.

(2)   Maye, M. M.; Kumara, M. T.; Nykypanchuk, D.; Sherman, W. B.; Gang, O. *Nature Nanotechnology* **2010**, *5*, 116-120.

(3)   Medintz, I. L.; Clapp, A. R.; Mattoussi, H.; Goldman, E. R.; Fisher, B.; Mauro, J. M. *Nature Materials* **2003**, *2*, 630-638.

(4)   Jain, K. K. *Clinica Chimica Acta* **2005**, *358*, 37-54.

(5)   Park, S. J.; Taton, T. A.; Mirkin, C. A. *Science* **2002**, *295*, 1503-1506.

(6)   Pandana, H.; Aschenbach, K. H.; Gomez, R. D. *IEEE Sensors Journal* **2008**, *8*, 661-666.

(7)   Tong, R.; Cheng, J. J. *Polymer Reviews* **2007**, *47*, 345-381.

(8)   Peer, D.; Karp, J. M.; Hong, S.; FaroKhzad, O. C.; Margalit, R.; Langer, R. *Nature Nanotechnology* **2007**, *2*, 751-760.

(9)   Choi, H. S.; Liu, W.; Liu, F.; Nasr, K.; Misra, P.; Bawendi, M. G.; Frangioni, J. V. *Nat Nanotechnol* **2010**, *5*, 42-47.

(10)   Rawat, M.; Singh, D.; Saraf, S.; Saraf, S. *Biological and Pharmaceutical Bulletin* **2006**, *29*, 1790-1798.

(11)   Patri, A. K.; Majoros, I. J.; Baker, J. R. *Current Opinion in Chemical Biology* **2002**, *6*, 466-471.

(12)   Nie, S. M.; Xing, Y.; Kim, G. J.; Simons, J. W. *Annual Review of Biomedical Engineering* **2007**, *9*, 257-288.

(13)   Landmark, K. J.; DiMaggio, S.; Ward, J.; Kelly, C.; Vogt, S.; Hong, S.; Kotlyar, A.; Myc, A.; Thomas, T. P.; Penner-Hahn, J. E.; Baker, J. R.; Holl, M. M. B.; Orr, B. G. *ACS Nano* **2008**, *2*, 773-783.

(14)   Thaxton, C. S.; Elghanian, R.; Thomas, A. D.; Stoeva, S. I.; Lee, J. S.; Smith, N. D.; Schaeffer, A. J.; Klocker, H.; Horninger, W.; Bartsch, G.; Mirkin, C. A. *Proceedings of the National Academy of Sciences of the United States of America* **2009**, *106*, 18437-18442.

(15)   Hong, S.; Leroueil, P. R.; Majoros, I. J.; Orr, B. G.; Baker, J. R.; Holl, M. M. B. *Chemistry and Biology* **2007**, *14*, 107-115.

(16)   Hong, S. P.; Leroueil, P. R.; Janus, E. K.; Peters, J. L.; Kober, M. M.; Islam, M. T.; Orr, B. G.; Baker, J. R.; Holl, M. M. B. *Bioconjugate Chemistry* **2006**, *17*, 728-734.

(17)   Leroueil, P. R.; Hong, S. Y.; Mecke, A.; Baker, J. R.; Orr, B. G.; Holl, M. M. B. *Accounts of Chemical Research* **2007**, *40*, 335-342.

(18)   Hong, S. P.; Bielinska, A. U.; Mecke, A.; Keszler, B.; Beals, J. L.; Shi, X. Y.; Balogh, L.; Orr, B. G.; Baker, J. R.; Holl, M. M. B. *Bioconjugate Chemistry* **2004**, *15*, 774-782.

(19)   Duncan, R.; Izzo, L. *Advanced Drug Delivery Reviews* **2005**, *57*, 2215-2237.

(20)   Bagwe, R. P.; Hilliard, L. R.; Tan, W. H. *Langmuir* **2006**, *22*, 4357-4362.

(21)   Zhang, Y.; Kohler, N.; Zhang, M. Q. *Biomaterials* **2002**, *23*, 1553-1561.

(22)   Majoros, I. J.; Keszler, B.; Woehler, S.; Bull, T.; Baker, J. R. *Macromolecules* **2003**, *36*, 5526-5529.

(23)   Shukla, R.; Thomas, T. P.; Peters, J.; Kotlyar, A.; Myc, A.; Baker, J. R. *Chemical Communications* **2005**, 5739-5741.

(24)   Hill, E.; Shukla, R.; Park, S. S.; Baker, J. R. *Bioconjugate Chemistry* **2007**, *18*, 1756-1762.

(25)   Sheng, K. C.; Kalkanidis, M.; Pouniotis, D. S.; Esparon, S.; Tang, C. K.; Apostolopoulos, V.; Pietersz, G. A. *European Journal of Immunology* **2008**, *38*, 424-436.

(26)   Baek, M. G.; Roy, R. *Bioorganic and Medicinal Chemistry* **2002**, *10*, 11-17.

(27)   Backer, M. V.; Gaynutdinov, T. I.; Patel, V.; Bandyopadhyaya, A. K.; Thirumamagal, B. T. S.; Tjarks, W.; Barth, R. F.; Claffey, K.; Backer, J. M. *Molecular Cancer Therapeutics* **2005**, *4*, 1423-1429.

(28)   Kono, K.; Liu, M. J.; Frechet, J. M. J. *Bioconjugate Chemistry* **1999**, *10*, 1115-1121.

(29)   Shukla, S.; Wu, G.; Chatterjee, M.; Yang, W. L.; Sekido, M.; Diop, L. A.; Muller, R.; Sudimack, J. J.; Lee, R. J.; Barth, R. F.; Tjarks, W. *Bioconjugate Chemistry* **2003**, *14*, 158-167.

(30)   Majoros, I. J.; Myc, A.; Thomas, T.; Mehta, C. B.; Baker, J. R. *Biomacromolecules* **2006**, *7*, 572-579.

(31)   Thomas, T. P.; Majoros, I. J.; Kotlyar, A.; Kukowska-Latallo, J. F.; Bielinska, A.; Myc, A.; Baker, J. R. *Journal of Medicinal Chemistry* **2005**, *48*, 3729-3735.

(32)   Myc, A.; Douce, T. B.; Ahuja, N.; Kotlyar, A.; Kukowska-Latallo, J.; Thomas, T. P.; Baker, J. R. *Anti-Cancer Drugs* **2008**, *19*, 143-149.

(33)   Kurtoglu, Y. E.; Mishra, M. K.; Kannan, S.; Kannan, R. M. *International Journal of Pharmaceutics* **2010**, *384*, 189-194.

(34)   Mullen, D. G.; Desai, A. M.; Waddell, J. N.; Cheng, X.-M.; Kelly, C. V.; McNerny, D. Q.; Majoros, I. J.; Baker, J. R.; Sander, L. M.; Orr, B. G.; Banaszak Holl, M. M. *Bioconjug Chem* **2008**, *19*, 1748-1752.

(35)   Mullen, D. G.; Fang, M.; Desai, A. M.; Baker, J. R.; Orr, B. G.; Banaszak Holl, M. M. *ACS Nano* **2010**, *4*, 657-670.

(36)   Cason, C. A.; Oehrle, S. A.; Fabre, T. A.; Girten, C. D.; Walters, K. A.; Tomalia, D. A.; Haik, K. L.; Bullen, H. A. *Journal of Nanomaterials* **2008**, doi:10.1155/2008/456082.

(37)   Majoros, I. J.; Thomas, T. P.; Mehta, C. B.; Baker, J. R. *Journal of Medicinal Chemistry* **2005**, *48*, 5892-5899.

(38)   Kukowska-Latallo, J. F.; Candido, K. A.; Cao, Z. Y.; Nigavekar, S. S.; Majoros, I. J.; Thomas, T. P.; Balogh, L. P.; Khan, M. K.; Baker, J. R. *Cancer Research* **2005**, *65*, 5317-5324.

(39)   Mullen, D. G.; Desai, A. M.; Waddell, J. N.; Cheng, X. M.; Kelly, C. V.; McNerny, D. Q.; Majoros, I. J.; Baker, J. R.; Sander, L. M.; Orr, B. G.; Holl, M. M. B. *Bioconjugate Chemistry* **2008**, *19*, 1748-1752.

(40)   Mullen, D. G.; Byrne, E. L.; Desai, A.; van Dongen, M. A.; Barash, M.; Cheng, X. M.; Baker, J. R.; Holl, M. M. B. *Submitted* **2010**.

(41)   Thomas, T. P.; Ye, J. Y.; Chang, Y. C.; Kotlyar, A.; Cao, Z.; Majoros, I. J.; Norris, T. B.; Baker, J. R. *Journal of Biomedical Optics* **2008**, *13*.

(42)   Islam, M. T.; Shi, X. Y.; Balogh, L.; Baker, J. R. *Analytical Chemistry* **2005**, *77*, 2063-2070.

Chapter 6
Best practices for purification and characterization of PAMAM dendrimer

Introduction

First developed in the 1970's, dendrimers are a unique class of branched polymers with unusually low polydispersities. This quality has made these macromolecules attractive for a number of different applications. In particular, poly(amido amine) dendrimers have received intense attention as candidates for a variety of biomedical applications including targeted drug delivery,[1-4] diagnostic imaging,[5] and gene delivery.[6] In addition to being relatively monodisperse (PDI = 1.01 for a generation 5 dendriemr), PAMAM dendrimers are an ideal size to interact with biological processes (1-10nm),[7] are structurally well-defined, possess a hydrophilic back-bone, and have numerous modification sites to which different functional ligands can be attached for synergistic effects. Although PAMAM dendrimers are a relatively uniform material,[8] the material is not molecularly perfect and substantial variation can exist across individual batches. Consequently, in order to effectively prepare PAMAM dendrimer for use in many of the mentioned applications it is necessary to carefully purify and characterize each individual batch of material.

The structural heterogeneity in PAMAM dendrimers results from undesired side-reactions that occur during the dendrimer synthesis. These structural defects have been described by several groups and include missing arms, dimers, and trailing generations.[9-12] Both the mean number of terminal arms as well as the number average molecular weight and PDI of the polymer are directly affected by these defect structures. Consequently, accurate characterization of these parameters for each batch of dendrimer is essential for the reproducibility of subsequent ligand conjugations as well as to understand the biological activity of the material. Additionally, by removing trailing

generation defect structures through purification, the variations between batches of dendrimer for these parameters can be reduced.

This note describes our current 'best practices' for purifying and characterizing PAMAM dendrimer. Generation 5 PAMAM dendrimer was purchased from Dendritech Inc. and then purified by dialysis to remove a portion of the trailing generation defect structures. The purified material was then characterized by GPC, potentiometric titration, HPLC, and ^{1}H NMR. This analysis provided the number average molecular weight, PDI, the mean number of primary amines per dendrimer and the relative amount of dimer molecules, G5 molecules and remaining trailing generation molecules.

Experimental Methods

Materials

Biomedical grade Generation 5 PAMAM dendrimer was purchased from Dendritech Inc. 10,000 molecular weight cut-off dialysis tubing (Spectra/Por 7 Dialysis membrane, nominal flat width: 45 mm, diameter: 29 mm) was purchased from Spectrum Laboratories Inc. and was washed with DI water before use. D_2O, and volumetric solutions (0.1 M HCl and 0.1 M NaOH) for potentiometric titration were purchased from Sigma Aldrich Co. and used as received.

Dendrimer Purification

Methanol was removed from a solution of G5 dendrimer under reduced pressure to produce a viscous oil. The dendrimer was redissolved in water and then lyophilized to obtain a dry weight (5.1310 g). The dry dendrimer was dissolved with 80 mL of DI water and divided into 4 aliquots. Four 10,000 MWCO dialysis membranes were prepared with a length of approximately 14 inches. Weighted clips were attached to one end of each dialysis tube and 20 mL of the dendrimer/water solution were added to each dialysis membrane tube. Residual air was removed from each tube and the tubes were sealed with floating clips, attached so that the length of each dialysis tube was approximately 7 inches. A foam float was affixed to each of the floating clips and the dialysis tubes and placed into glass jars filled with one gallon of DI water each. Slow

stirring was utilized. DI water was exchanged 9 times over 3 days. The minimum time between exchanges was 3 hrs. After purification, the dendrimer was removed from the dialysis tubes, placed in glass scintillation vials. The purified dendrimer was lyophilized for 3 days to yield 5.0238 g (98%) of a glassy material. The dried product was stored under nitrogen at -25 ºC.

GPC

GPC experiments were performed on an Alliance Waters 2695 separation module equipped with a 2487 dual wavelength UV absorbance detector (Waters Corporation), a Wyatt HELEOS Multi Angle Laser Light Scattering (MALLS) detector, and an Optilab rEX differential refractometer (Wyatt Technology Corporation). Columns employed were TosoHaas TSK-Gel Guard PHW 06762 (75 mm × 7.5 mm, 12 μm), G 2000 PW 05761 (300 mm × 7.5 mm, 10 μm), G 3000 PW 05762 (300 mm × 7.5 mm, 10 μm), and G 4000 PW (300 mm × 7.5 mm, 17 μm). Column temperature was maintained at 25 ± 0.1 °C with a Waters temperature control module. The isocratic mobile phase was 0.1 M citric acid and 0.025 wt % sodium azide, pH 2.74, at a flow rate of 1 mL/min. The sample concentration was 10 mg/5 mL with an injection volume of 100 μL. The weight average molecular weight, M_w, has been determined by GPC, and the number average molecular weight, M_n, was calculated with Astra 5.3.14 software (Wyatt Technology Corporation) based on the molecular weight distribution.

Potentiometric Titration

Potentiometric titration was carried out using a Mettler Toledo MP220 pH meter and a Mettler Toledo InLab 430 pH electrode at room temperature, 23 °C. A 20 mL solution of 0.1 N NaCl was added to purified G5 PAMAM dendrimer **1** (80.7 mg) to shield amine group interactions. The pH of the dendrimer solution was lowered to pH = 2.01 using 0.1034 N HCl. A 25 mL Brand Digital Buret III was used for the titration with 0.1024 N NaOH. NaOH was titrated into the dendrimer solution in 0.06 mL increments (2 drops). A high rate of stirring was maintained throughout the titration. The numbers of primary and tertiary amines were determined by from the titration curve with NaOH as previously described.[2] This process was also conducted for the unpurified dendrimer.

Reverse Phase High Performance Liquid Chromatography

HPLC analysis was carried out on a Waters Delta 600 HPLC system equipped with a Waters 2996 photodiode array detector, a Waters 717 Plus auto sampler, and Waters Fraction collector III. The instrument was controlled by Empower 2 software. For analysis of the conjugates, a C5 silica-based RP-HPLC column (250 x 4.6 mm, 300 Å) connected to a C5 guard column (4 x 3 mm) was used. The mobile phase for elution of the conjugates was a linear gradient beginning with 100:0 (v/v) water/acetonitrile and ending with 20:80 (v/v) water/acetonitrile over 30 min at a flow rate of 1 mL/min. Trifluoroacetic acid (TFA) at 0.14 wt % concentration in water as well as in acetonitrile was used as a counter ion to make the dendrimer surfaces hydrophobic.

NMR

All ^{1}H NMR experiments were conducted using a Varian Inova 400 MHz instrument. 10 s delay time and 64 scans were set for each dendrimer sample. Temperature was controlled at 25 ^{o}C. For experiments conducted in D_2O, the internal reference peak was set to 4.717 ppm.

Results and Discussion

The purification of G5 PAMAM dendrimer has been an important step in our laboratory to prepare material for gene therapy mechanistic studies, polycation-cellular membrane interaction studies and for modification with functional ligands such as a targeting moieties, therapeutic molecules and or imaging agents. By removing many of the trailing generation defect structures, the purification process improves the uniformity of the material. This is important because each batch of dendrimer has a varying amount of trailing generation defect structures which can effect the observed material properties.

GPC Molecular Weight Analysis

GPC was used to characterize the dendrimer both before and after purification. **Figure 6.1** shows the GPC data from the Light Scattering and Differential Refractive Index detectors for the received biomedical grade dendrimer sample as well as one of the four purified samples. A comparison of **panels a** and **b** reveals that the dialysis process

reduced the amount of smaller sized dendrimer particles that elute at 22.5 minutes. This reduction is consistent with the increase in the weight and number average molecular weight for the purified dendrimer samples. **Table 1** contains the number average molecular weight, the weight average molecular weight and the PDI for the different dendrimer samples. The dialysis process increased M_n of the material by approximately 3,000 g/mol and reduced the PDI from 1.043 to an average of 1.018. Previous studies have found that the error of the M_n measurement to be $\pm$ 1,000 g/mol. Consequently, by this measurement, the purification process had the same efficiency for all four dendrimer aliquots.

Mean Number of End Groups per Dendrimer

Accurate determination of the mean number of end groups (primary amines) per dendrimer is critical in order to calculate reaction stoichiometries as well as determine the mean number of functional ligands that become conjugated to the dendrimer. Theoretically, a G5 dendrimer has 128 primary amines. Due to the numerous defect structures, in practice this value is significantly lower. The use of potentiometric titration to calculate the mean number of primary amines per dendrimer has been described earlier.[2] Although we continue to use the same calculation, the titration procedure has been modified. Instead of using a glass burette, we have increased the precision of the titration by using a Digital Burette to add the 0.1024 N NaOH in 0.06 mL increments. The mean number of end groups for the purified dendrimer was found to be 109 $\pm$ 5 (**Figure 6.2**), which is an increase in the mean number of end groups per dendrimer from the received biomedical grade dendrimer (96 $\pm$ 5).

HPLC Resolves Major Dendrimer Defect Structures

Reverse phase HPLC has been previously developed for analysis of PAMAM dendrimer. HPLC traces at 210 nm for the four purified dendrimer aliquots as well as the unpurified dendrimer can be seen in Error! Reference source not found.**a**. In addition to he major peak in each trace, several smaller peaks can be seen. These peaks have been previously shown to be composed of trailing generation defect structures and the dimer defect structure.[13] In the trace for the unpurified dendrimer, two additional peaks can be

found with retention times at 16.9 min and 17.8 min. It is these dendrimer defect structures that are successfully removed by dialysis. Presumably these defects are the trailing generation with same size and molecular weight of a generation 2 and 3 dendrimer, respectively. Based on the fitted peak areas 70% of the material is composed of G5 dendrimer.

A peak fitting analysis can be used to quantify the relative concentration of the G5 dendrimer relative the other major defect structures. We have previously shown that Beer's law is valid at 210nm for PAMAM dendrimer.[14] The fitted HPLC trace for the unpurified dendrimer can be found in Error! Reference source not found.**b** with the HPLC signal in red dots, the fitting peaks in green and the summation of the fitting peaks in blue. The shape of the fitting peaks were set based on the shape of the G5 peak at 18.9 min. A shoulder was found to be present on the leading side of the main G5 peak. This shoulder was fit with an additional fitting peak. Our hypothesis is that this shoulder may contain dimer of a trailing generation.

Conclusion

Purification and characterization of each batch of PAMAM dendrimer is important for use. This note has described our current 'best practices' for purification of G5 PAMAM dendrimer by dialysis followed by characterization by GPC, potentiometric titration, and HPLC.

Table 6.1: Molecular weight analysis

Dendrimer	Mn	Mw	PDI
Unpurified	23,080	24,070	1.043
Purified Aliquot 1	27,030	27,490	1.017
Purified Aliquot 2	25,460	25,910	1.017
Purified Aliquot 3	26,730	27,200	1.018
Purified Aliquot 4	25,640	26,110	1.019
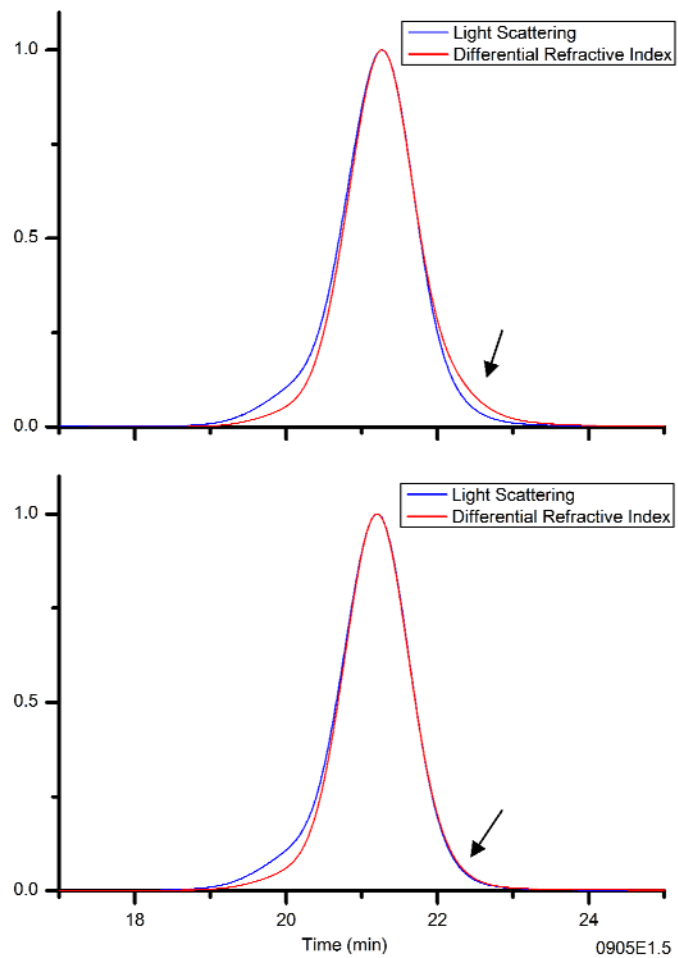
Figure 6.1: Characterization of PAMAM dendrimer using a GPC based Light Scattering Detector and a Differential Refractive Index Detector. **a)** Unpurified dendrimer. **b)** Purified dendrimer (aliquot 1).
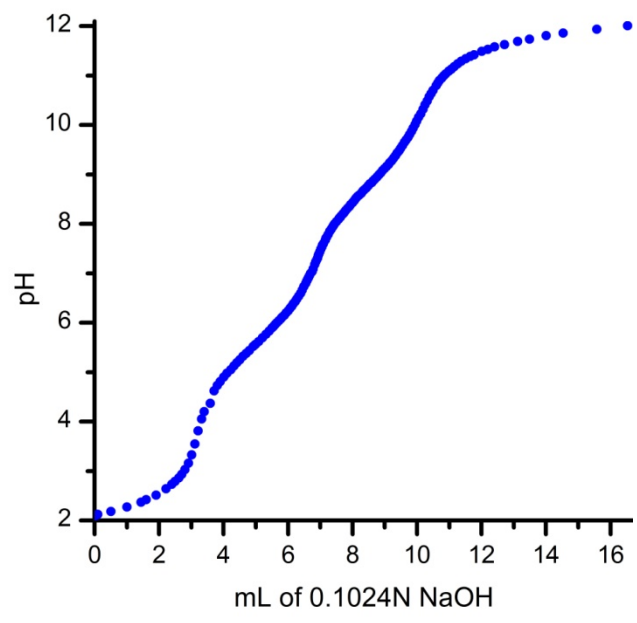
Figure 6.2: Potentiometric titration of the purified dendrimer.
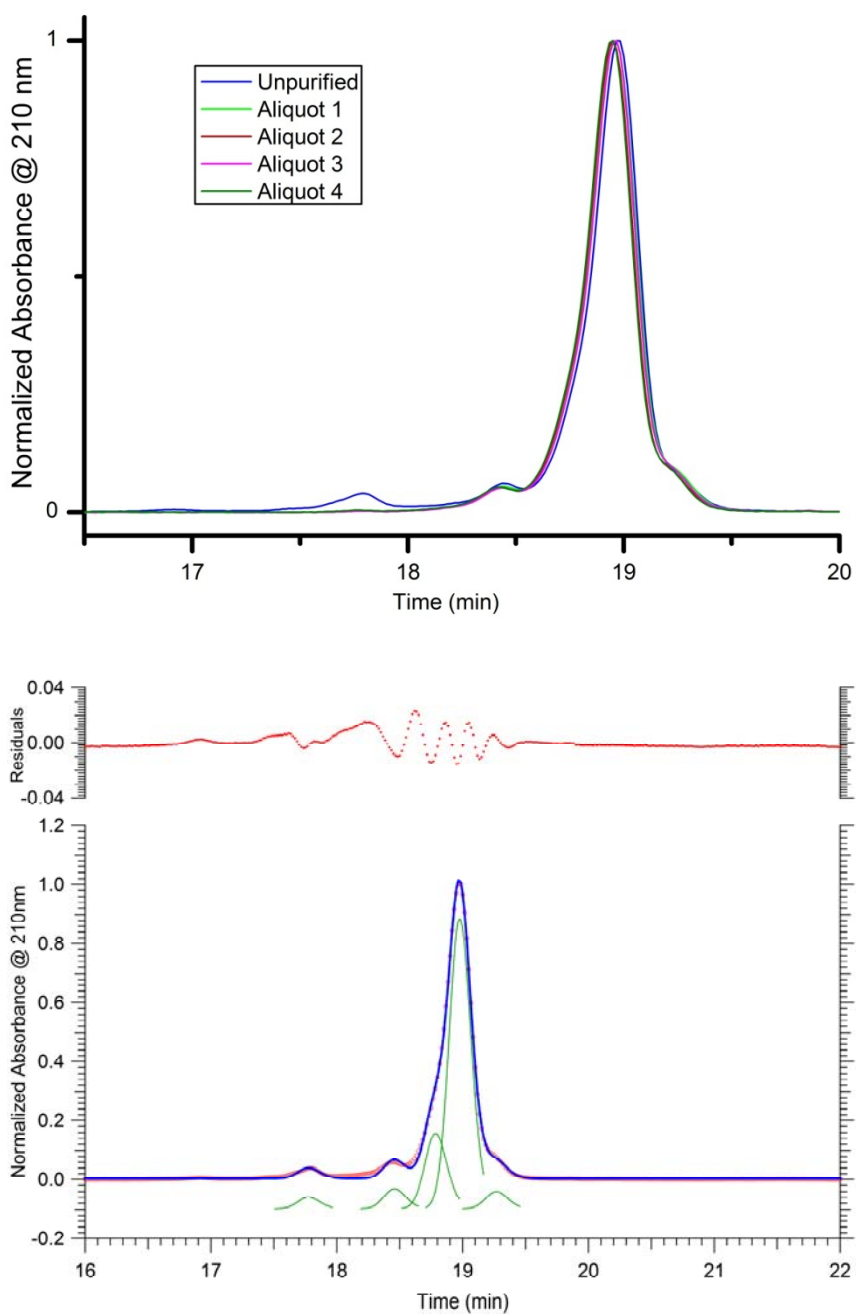
Figure 6.3: HPLC characterization of unpurified and purified dendrimer. **a**) HPLC traces at 210 nm. **b**) Peak fitting analysis of the unpurified dendrimer quantifies the relative concentration of dendrimer defect structures. Residuals are $\times 10^6$.

References:

(1)   Hong, S.; Leroueil, P. R.; Majoros, I. J.; Orr, B. G.; Baker, J. R.; Holl, M. M. B. *Chemistry and Biology* **2007**, *14*, 107-115.

(2)   Majoros, I. J.; Thomas, T. P.; Mehta, C. B.; Baker, J. R. *Journal of Medicinal Chemistry* **2005**, *48*, 5892-5899.

(3)   Kukowska-Latallo, J. F.; Candido, K. A.; Cao, Z. Y.; Nigavekar, S. S.; Majoros, I. J.; Thomas, T. P.; Balogh, L. P.; Khan, M. K.; Baker, J. R. *Cancer Research* **2005**, *65*, 5317-5324.

(4)   Thomas, T. P.; Majoros, I. J.; Kotlyar, A.; Kukowska-Latallo, J. F.; Bielinska, A.; Myc, A.; Baker, J. R. *Journal of Medicinal Chemistry* **2005**, *48*, 3729-3735.

(5)   Landmark, K. J.; DiMaggio, S.; Ward, J.; Kelly, C.; Vogt, S.; Hong, S.; Kotlyar, A.; Myc, A.; Thomas, T. P.; Penner-Hahn, J. E.; Baker, J. R.; Holl, M. M. B.; Orr, B. G. *ACS Nano* **2008**, *2*, 773-783.

(6)   Shakhbazau, A.; Isayenka, I.; Kartel, N.; Goncharova, N.; Seviaryn, I.; Kosmacheva, S.; Potapnev, M.; Shcharbin, D.; Bryszewska, M. *International Journal of Pharmaceutics* **2010**, *383*, 228-235.

(7)   Choi, H. S.; Liu, W. H.; Liu, F. B.; Nasr, K.; Misra, P.; Bawendi, M. G.; Frangioni, J. V. *Nature Nanotechnology* **2010**, *5*, 42-47.

(8)   Grayson, S. M.; Godbey, W. T. *Journal of Drug Targeting* **2008**, *16*, 329-356.

(9)   Peterson, J.; Allikmaa, V.; Subbi, J.; Pehk, T.; Lopp, M. *European Polymer Journal* **2003**, *39*, 33-42.

(10)   Tomalia, D. A.; Naylor, A. M.; Goddard, W. A. *Angewandte Chemie-International Edition in English* **1990**, *29*, 138-175.

(11)   Kallos, G. J.; Tomalia, D. A.; Hedstrand, D. M.; Lewis, S.; Zhou, J. *Rapid Communications in Mass Spectrometry* **1991**, *5*, 383-386.

(12)   Tolic, L. P.; Anderson, G. A.; Smith, R. D.; Brothers, H. M.; Spindler, R.; Tomalia, D. A. *International Journal of Mass Spectrometry* **1997**, *165*, 405-418.

(13)   Islam, M. T.; Majoros, I. J.; Baker, J. R. *Journal of Chromatography B-Analytical Technologies in the Biomedical and Life Sciences* **2005**, *822*, 21-26.

(14)   Mullen, D. G.; Desai, A. M.; Waddell, J. N.; Cheng, X. M.; Kelly, C. V.; McNerny, D. Q.; Majoros, I. J.; Baker, J. R.; Sander, L. M.; Orr, B. G.; Holl, M. M. B. *Bioconjugate Chemistry* **2008**, *19*, 1748-1752.

Chapter 7
Conclusions

This dissertation has investigated two of the main challenges in nanoparticle-based platform design: quantifying and controlling populations of heterogeneous nanoparticle-ligand components. Additionally, this dissertation has leveraged the knowledge gained about nanoparticle-ligand distributions to develop new platform designs with the goal of providing a reproducible system capable of translation to the clinic.

Chapter 2 provided an example of a targeted drug delivery platform design that failed to account for the complexity of component distributions in multi-functional dendrimer systems. This platform design used a modular approach to construct multi-functional platforms. The anticipated advantage of the modular design was to facilitate the production of platforms with different functionalities by segregating different functional ligand (folic acid, FITC, 6TAMRA ect.) to separate dendrimer-based modules. With one universal orthogonal coupling reaction, desired dendrimer modules with specific functionalities could be combined. The flaw of this design was that it grossly underestimated the true diversity of components that made up each functionalized dendrimer module, both in the distribution of components with different numbers of the biologically active ligands and also the distribution of components with different numbers of the modular assembly ligand. Although this platform demonstrated active targeting of epidermal carcinoma cells *in vitro*, the platform failed to show active tumor targeting above levels associated with non-specific targeting.

Chapter 3 examined the actual material composition in dendrimer-ligand systems. HPLC was used to resolve and quantify dendrimer components with different numbers of a model ligand. The distributions quantified in this study were found to be significantly more heterogeneous than commonly expected and yet consistent, to a first approximation,

169

with the theoretically expected Poisson distribution. Pre-existing distributions were found to increase the heterogeneity of the dendrimer-ligand distribution and it was concluded that the average structure, which is the standard parameter of the field to characterize nanoparticle-ligand systems, does a poor job reflecting the true diversity of components. This study represents the first time the distribution of components has been resolved and quantified for a dendrimer-ligand system and adds to a small number of publications that have addressed the problems of insufficient characterization for nanoparticle-ligand materials. Platform designs that do not account for the distributions of components described in this chapter may find it extremely difficult to produce material with reproducible results.

Leveraging the findings and design lessons from Chapter 3, a new platform design was described in Chapter 4. Using semi-preparative HPLC, a method was developed to isolate individual components from a distribution of dendrimer-ligand components. Nine different dendrimer components with precise numbers of ligands (0-8) were obtained by this method leading to an order of magnitude improvement in the purity of each component. This process is highly reproducible owing to the consistent HPLC retention times of the different dendrimer-ligand components. In this Chapter, for example, the process was repeated 12 consecutive times. While it is very difficult to synthetically produce a consistent *distribution* of dendrimer-ligand components across batches, this process is insensitive to changes in the distribution.

The product of the strategy described in Chapter 4, *Precision Dendrimer*, have great potential for use as a platform because the ligand molecule in this chapter possessed a terminal azide group that can be modified by both copper-catalyzed alkyne-azide 'click' reactions as well as copper free 'click' reactions. Because the Precision Dendrimer had a precise number of azide groups, the platform can be modified by any number of functional molecules possessing an alkyne moiety. The key advantages of this platform design are a highly controlled number of functional molecules per dendrimer, the ability to ensure batch reproducibility, and the capability to optimize platform loading for improved efficacy.

Chapter 5 continued to investigate the distributions of nanoparticle-ligand components in dendrimer-based systems. In this Chapter, the effect of the partial acetylation reaction on subsequent dendrimer-ligand distributions was examined. The partial acetylation has been one of the key modifications performed to the PAMAM dendrimer before the addition of functional ligands. This reaction was found to create a distribution of modification sites per dendrimer which then controls the distribution of any subsequent ligand. Furthermore, the distribution that results from the partial acetylation reaction was found to be highly sensitive to mass transport conditions making this reaction a major obstacle to achieving reproducible platform construction.

Finally, our current 'best practices' for purifying and characterizing poly(amidoamine) dendrimer was described in Chapter 6. When intended for a wide variety of applications including as platforms, it is essential to have a detailed understanding of the material properties for the specific batch of dendrimer. This is necessary due to the variability in properties between batches of commercially produced dendrimer. Our methods have been optimized to remove trailing generation defect structures from generation 5 poly(amidoamine) dendrimer as well as characterize the prepared material by GPC, potentiometric tritration.

Future Directions

The reality that most nanoparticle-ligand systems are composed of nanoparticle-ligand component distributions, is alone, not an insurmountable obstacle to commercial application. Indeed, there are many examples of materials that have been composed of heterogeneous mixtures of components and yet have made important societal and industrial impacts. The entire field of polymers, for example, has confronted this challenge for more than a century. Distributions of components are a major obstacle, however, when they vary uncontrollably between batches and result in different material activities. Distribution characterization and reproducibility as well as an understanding of the material composition-activity relationships are presently major challenges for nanoparticle-ligand systems.

171

To address these challenges, major improvements will need to be made in the ability to generate and characterize nanoparticle-ligand distributions that are consistent across multiple batches. For dendrimer-based systems, the Azide and Alkyne Ligand, described in this thesis, can be used during process development and scale-up to ensure distribution reproducibility. The Azide and Alkyne ligands can be temporarily substituted for functional ligands when the actual nanoparticle-ligand distribution cannot be directly resolved. These two model ligand systems can be used to test the effectiveness of the reaction conditions (mixing, temperature, reagent addition rate ect.) as well as to monitor the distribution dependence on variations in the starting dendrimer material (number of end groups, amount of trailing generations and dimer).

If future synthetic strategies to produce functional dendrimer-based platforms continue to employ stochastic conditions, the results of this dissertation indicate that distributions can be more reproducible and homogeneous if the partial acetylation step is eliminated and functional ligands are instead conjugated directly to the 100% amine terminated dendrimer. Not only does this approach bypass the poor control present in the partial acetylation reaction, it also may make functional ligand distributions less sensitive to varying amounts of dendrimer defect structures in different commercial lots. The dendrimer with precise numbers of Azide Ligands, described in Chapter 4, offers a truly exciting number of new opportunities. This material can be used as a tool kit to investigate the activity of different functional ligand-dendrimer components. To accomplish this, the functional ligand molecules will need to be modified with a terminal alkyne group and then coupled, using 'click' chemistry, to the dendrimer with precise numbers of Azide Ligands. In this coupling reaction, an excess of alkyne-modified functional ligands can be added relative to the number of Azide Ligands in order to produce non-stochastic conditions and ensure that all Azide Ligands are modified. From an engineering design perspective, this information will be valuable for identifying the most active dendrimer-ligand components as well as establishing the tolerable variations in distributions between batches of material that still maintain the same properties. With the most active components identified, this material should also be considered for use as

an actual product (a therapeutic in the case of a drug delivery application). The major feature of this material is reproducibility of properties and activity (and quite possibly, dramatically increased efficacy). This feature meets at least one major existing need in the field of targeted drug delivery. Although the current isolation method that produces the material is inefficient, this drawback may be outweighed by its benefits and furthermore, a number of strategies currently exist in the literature that could be leveraged to improve the conservation of material.

Conclusion

In closing, this dissertation has provided detailed findings regarding the actual material composition in nanoparticle-ligand systems and has provided new platform designs to account for the challenges that distributions create. Broadly speaking, there remains a definite need for improved characterization and control of nanoparticle-ligand distributions.

^{1}H NMR Spectra for Dendrimer Conjugates

1'. G5Ac$_{72\%}$
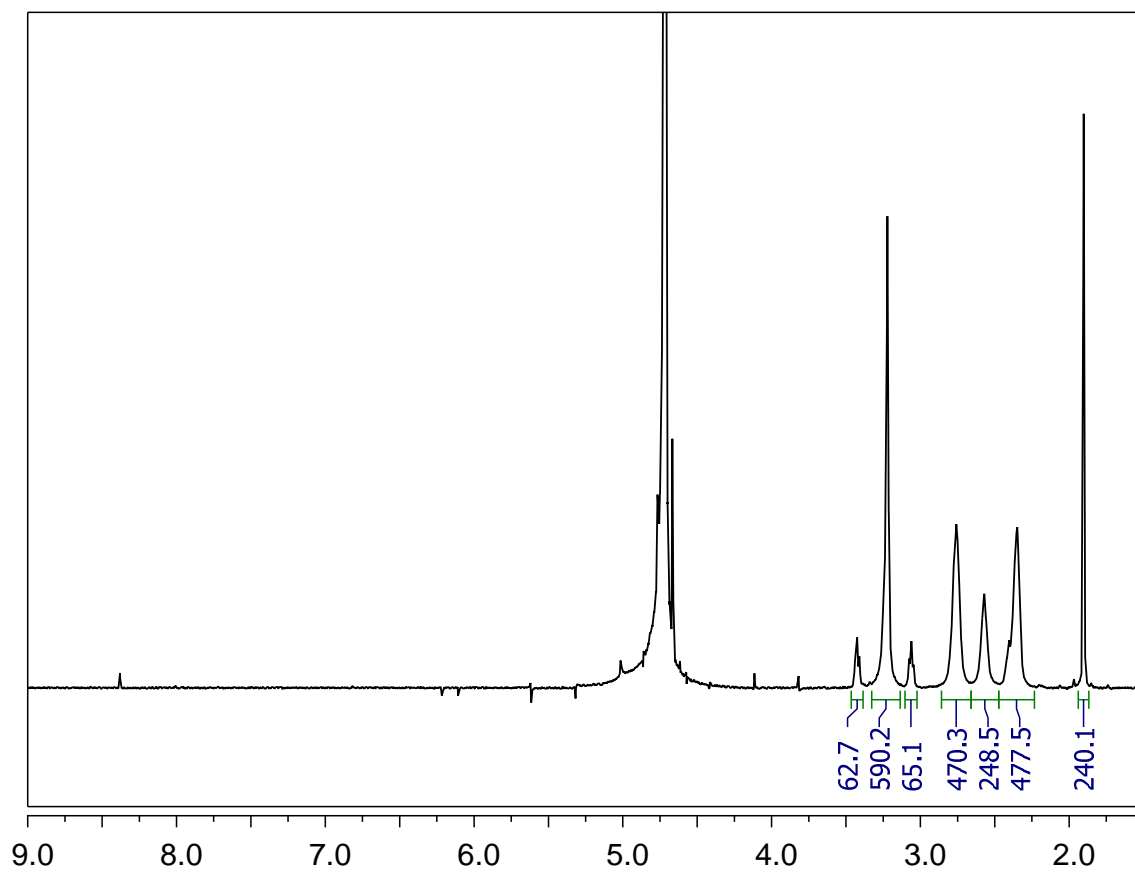
1''. G5Ac_{62%}
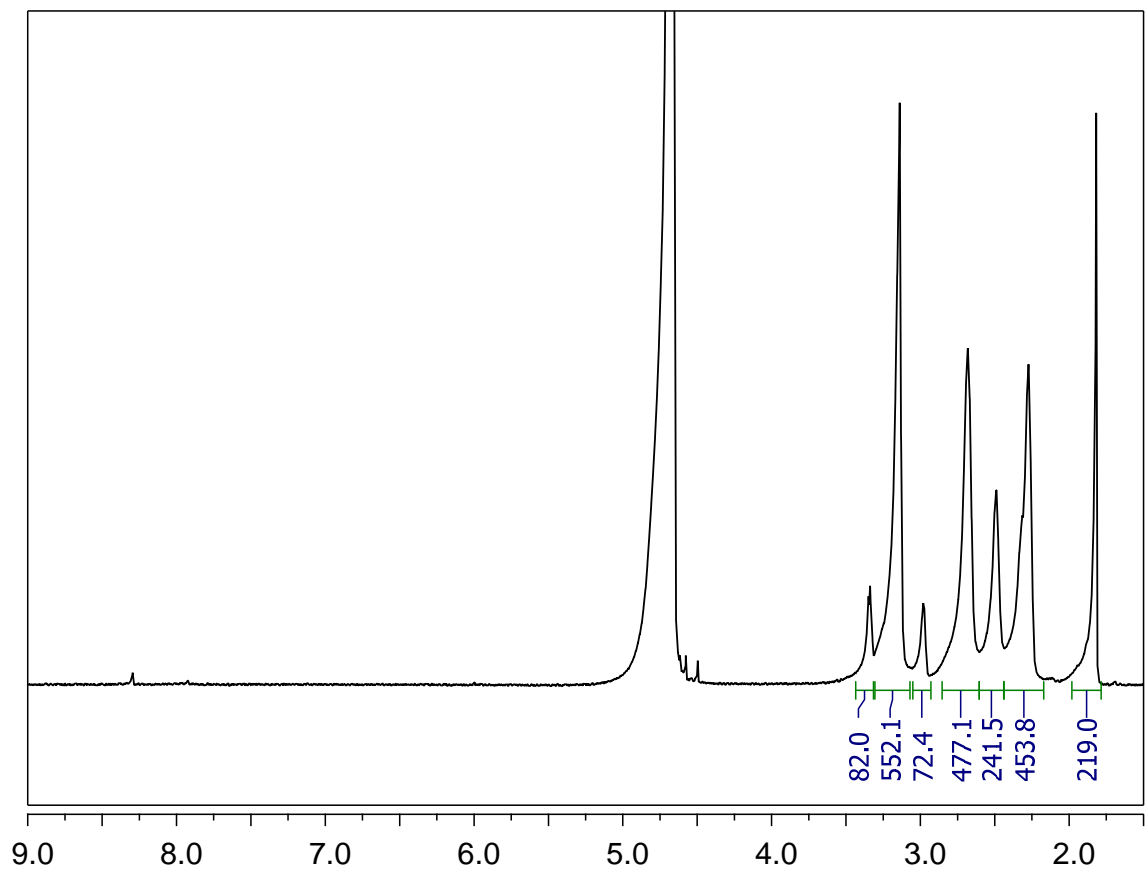
1'''. G5Ac₆₇%
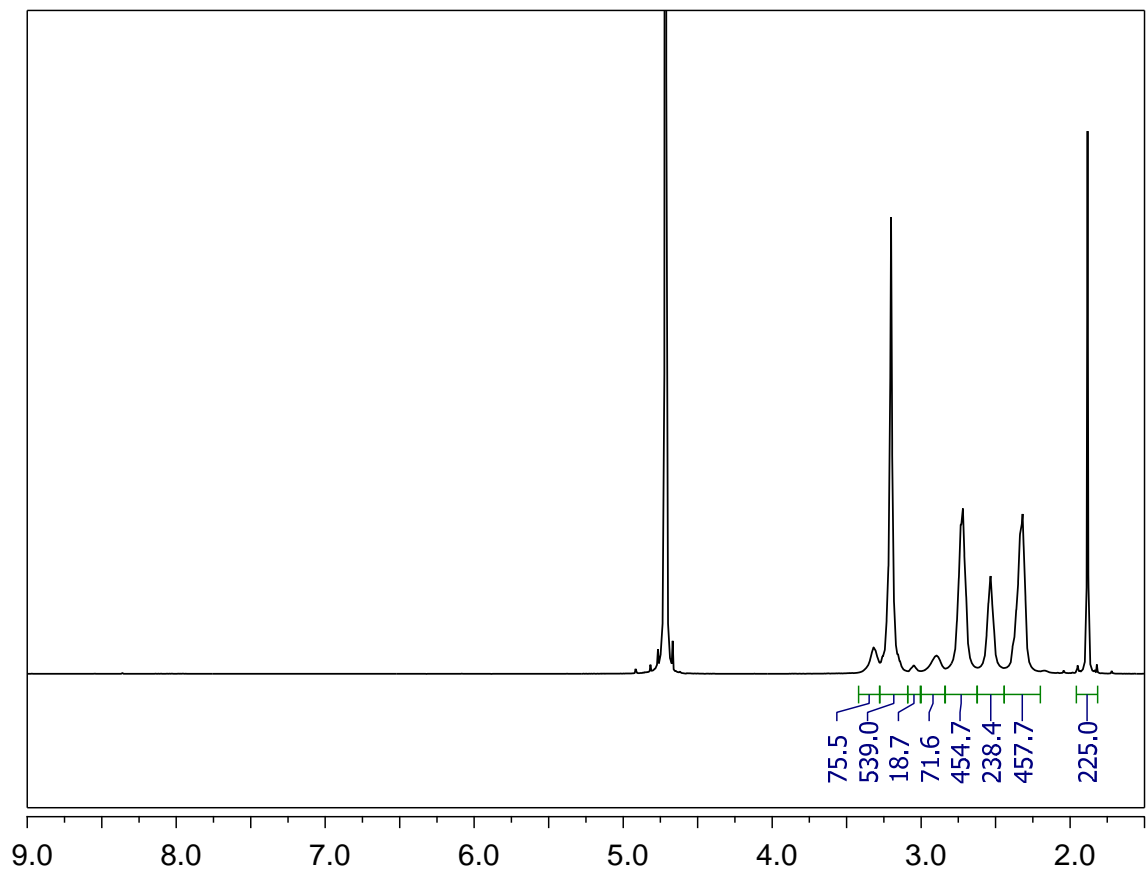
5. G5-Ac$_{72\%}$-Alkyne$_{1.4}$
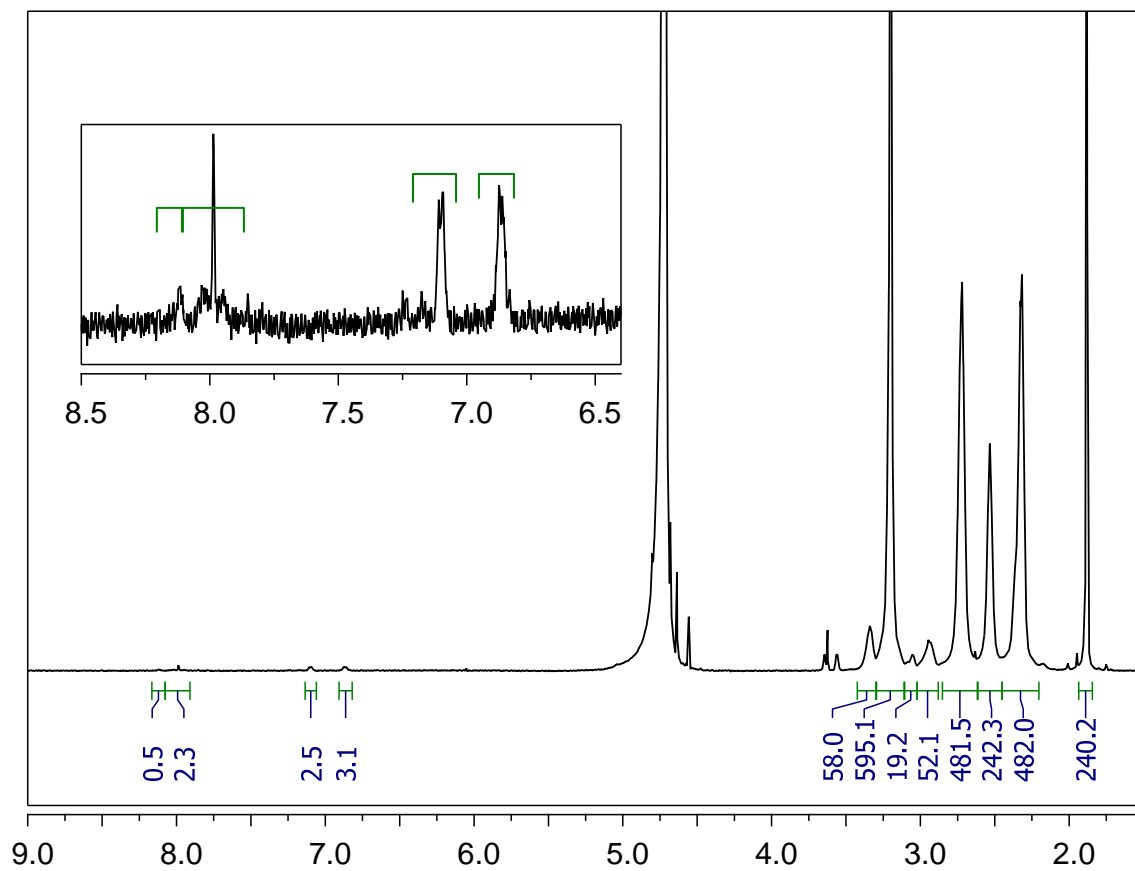
6. G5-Ac$_{72\%}$-Azide$_{1.3}$
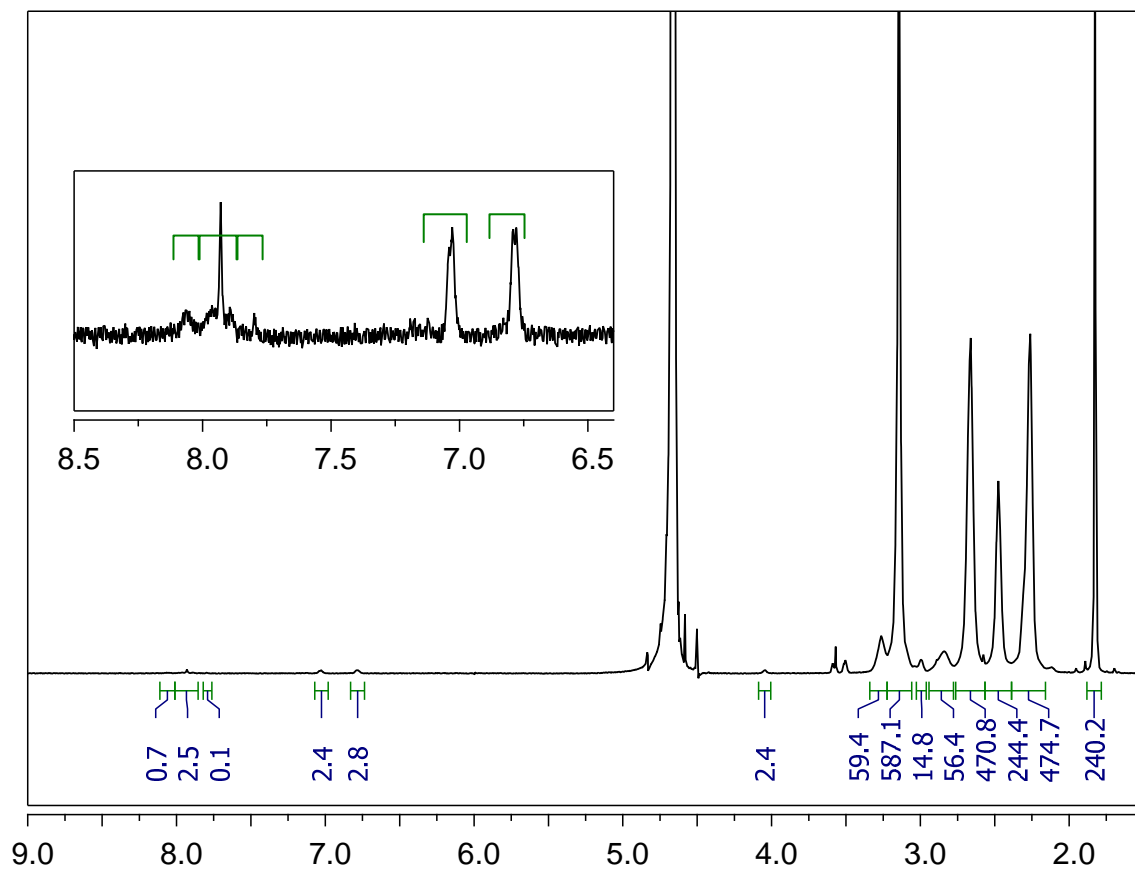
7. Model Dendrimer System G5-Ac$_{72\%}$-L-G5Ac$_{72\%}$
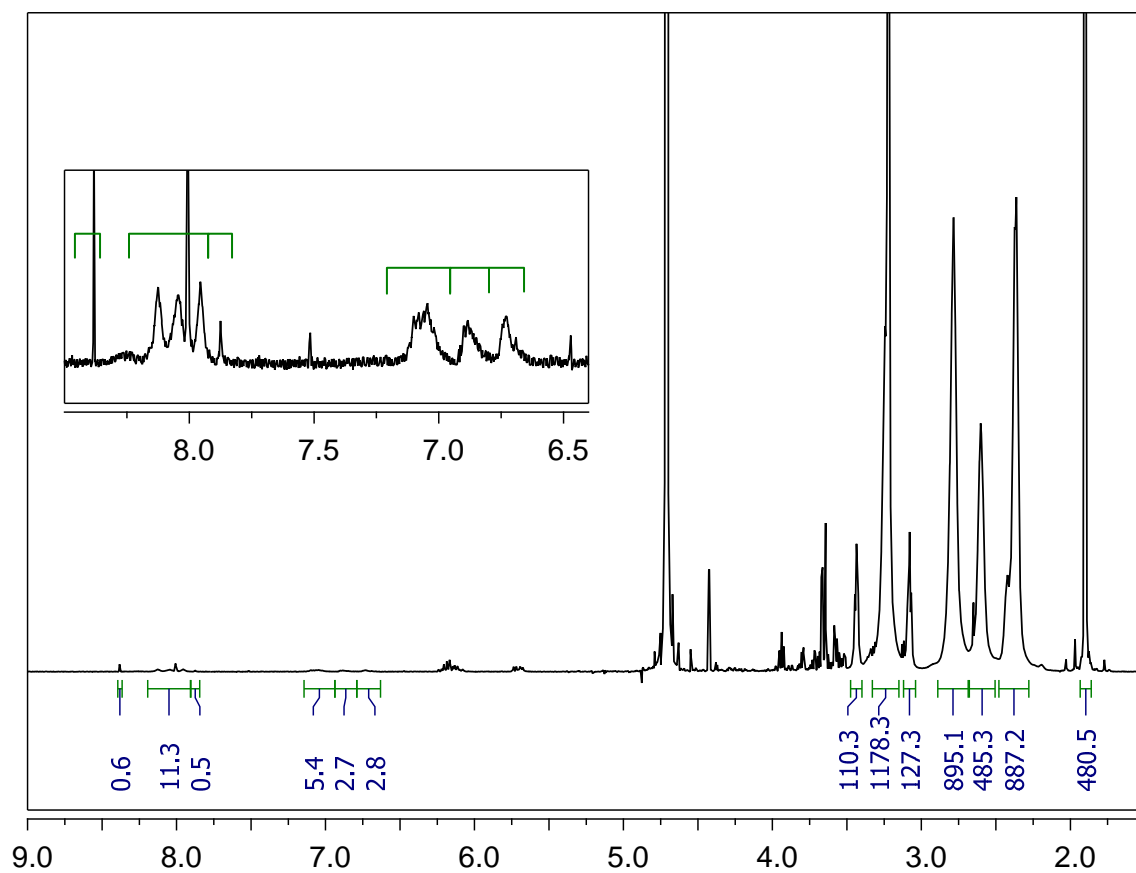
8. G5-Ac$_{65\%}$-Alkyne$_{1.6}$
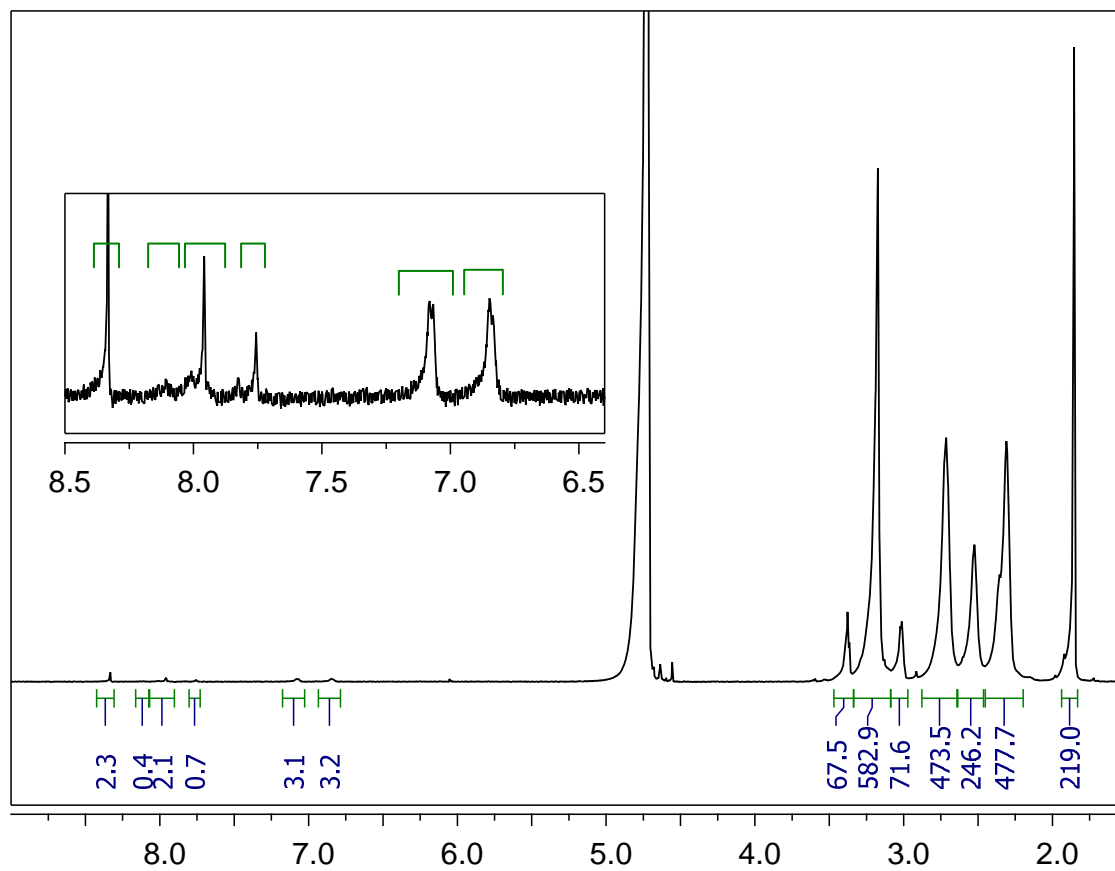
9. G5-Ac$_{65\%}$-Azide$_{2.5}$
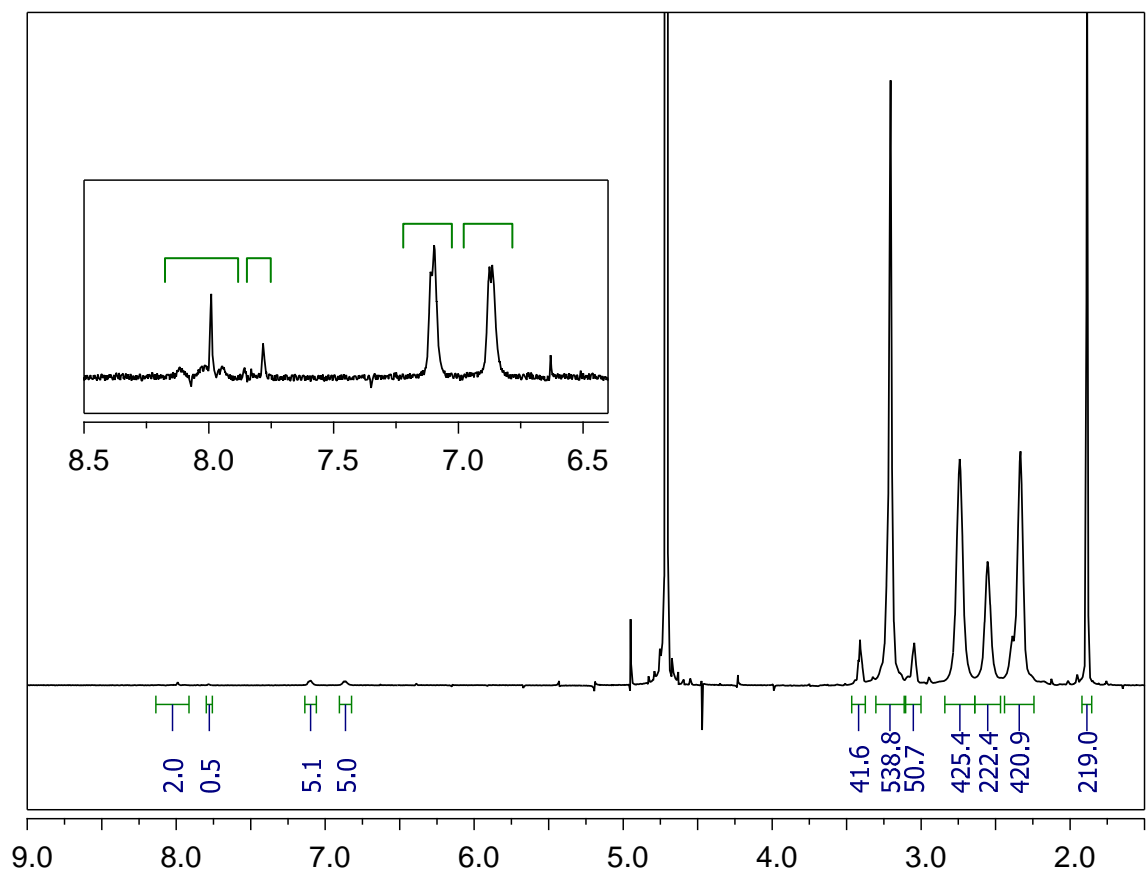
10. G5-Ac$_{65\%}$-Alkyne$_{1.6}$-FA$_{1.7}$
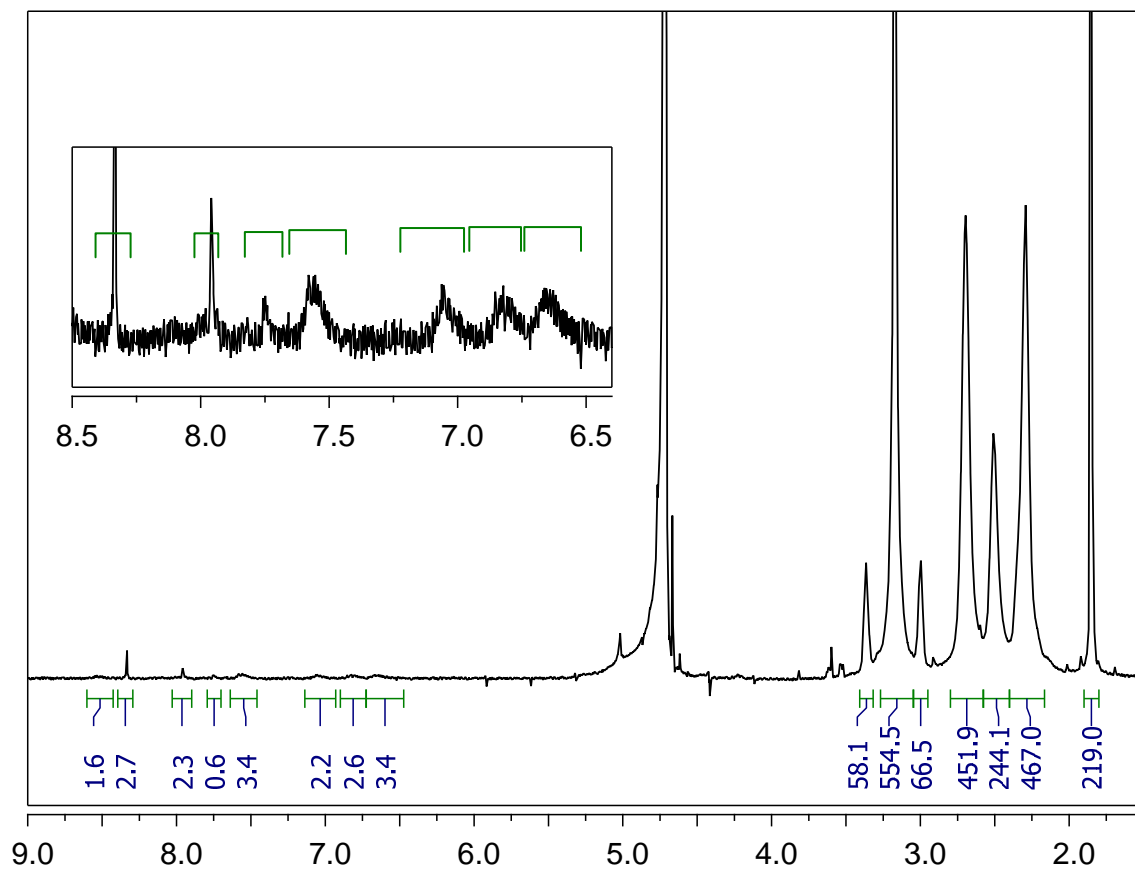
11. G5-Ac_{65%}-Azide_{2.5}-FITC_{3.2}
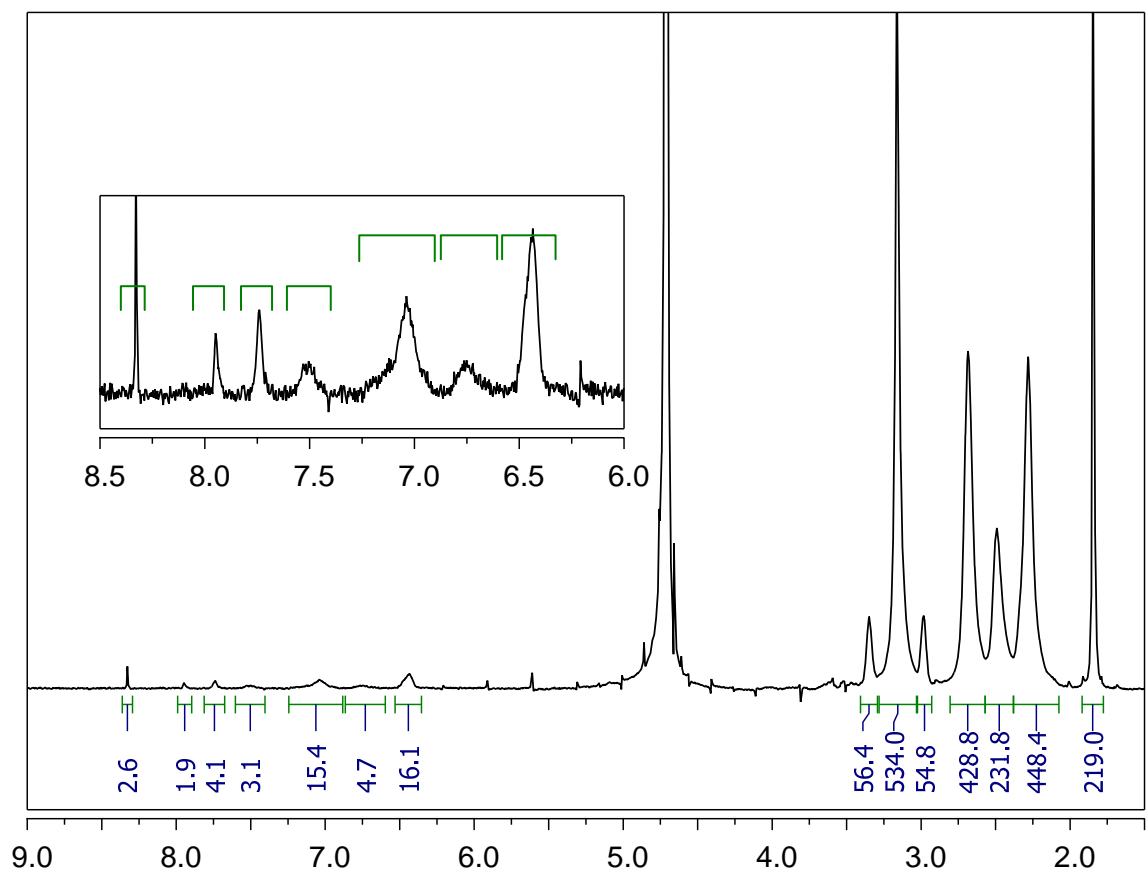
12. G5-Ac$_{65\%}$-Alkyne$_{1.6}$-FA$_{3.5}$
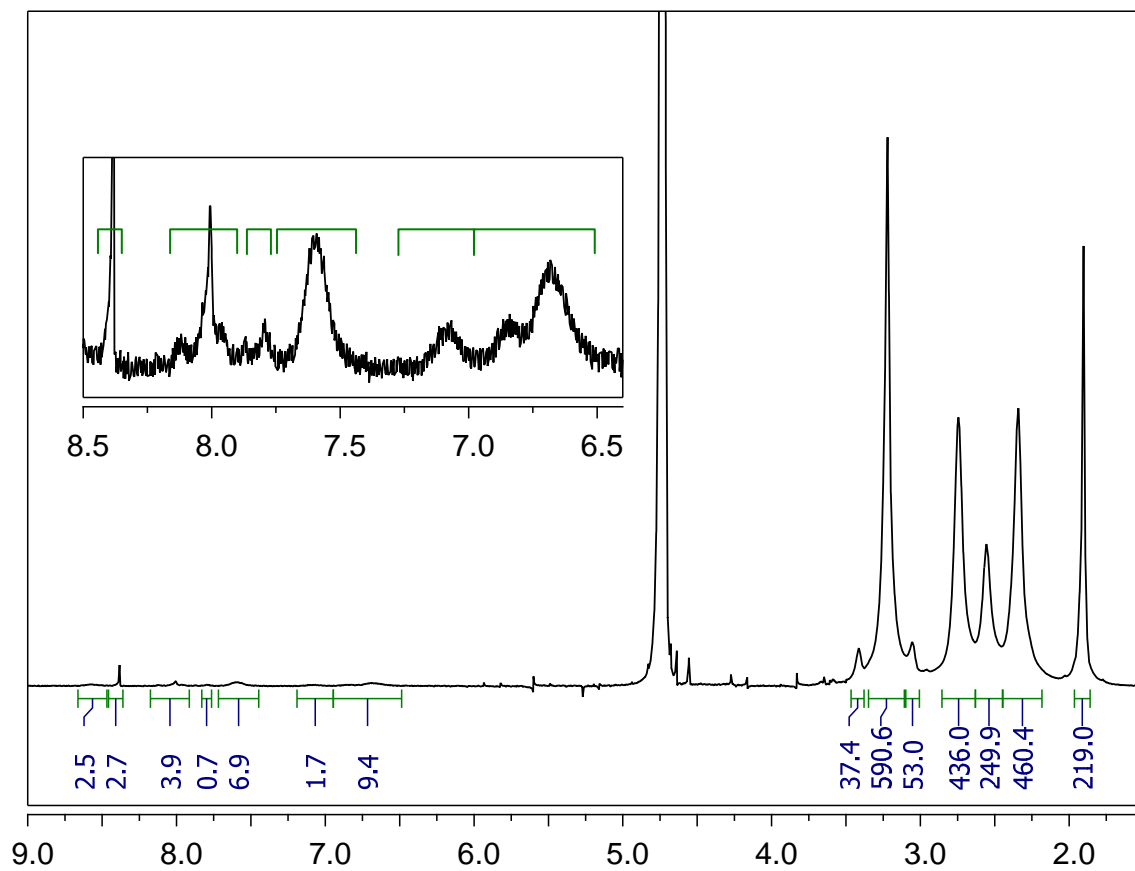
13. G5-Ac₁₀₇-Alkyne₁.₆-FA₃.₅

185
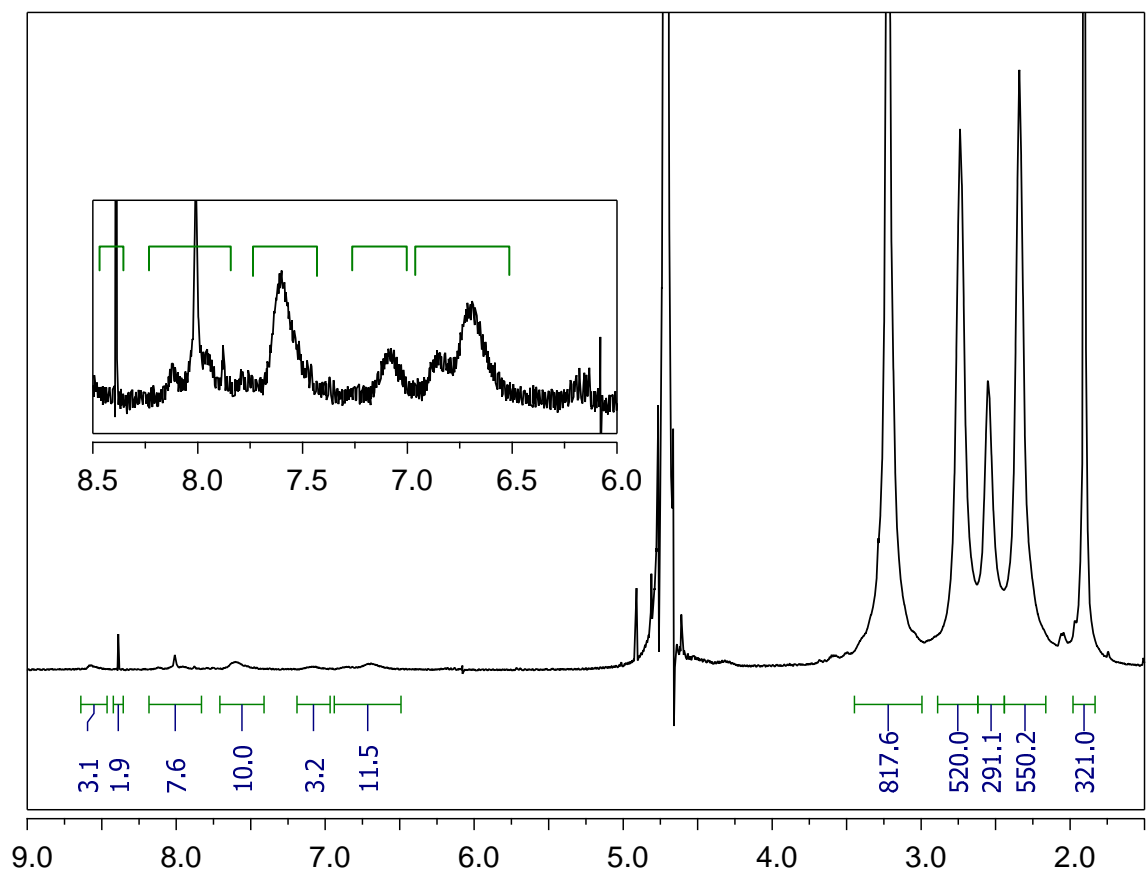
14. G5-Ac₁₀₆-Azide_{2.5}-FITC_{3.2}
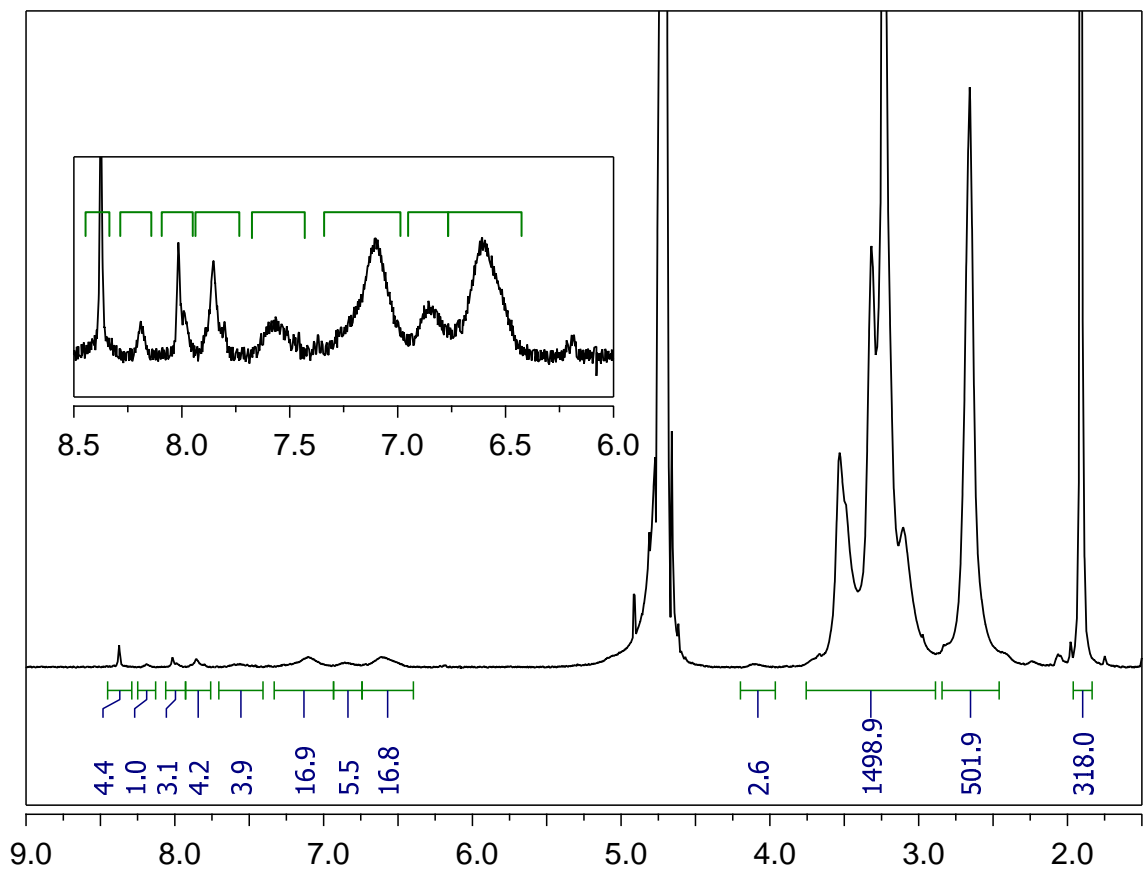
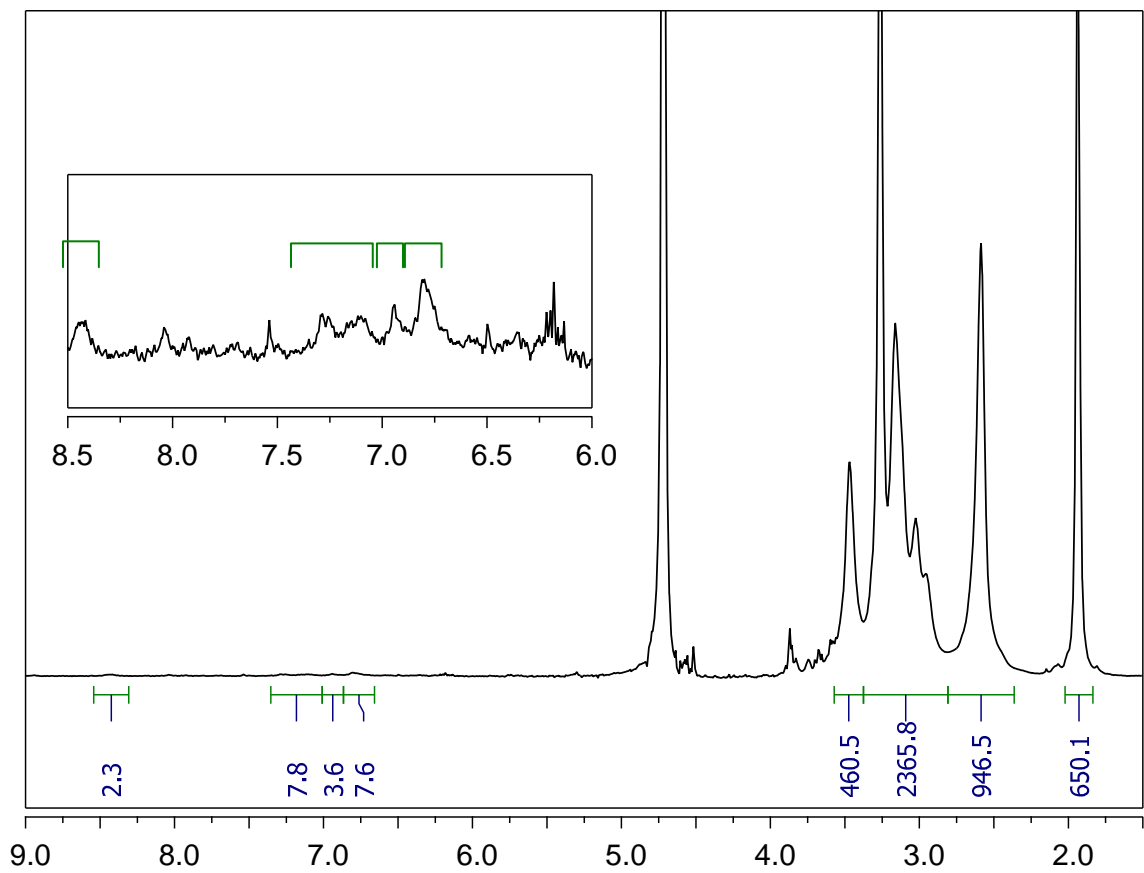**15. Folic Acid Targeted Dendrimer System FA$_{3.5}$-G5-Ac$_{107}$-L-G5Ac$_{106}$-FITC$_{3.2}$**
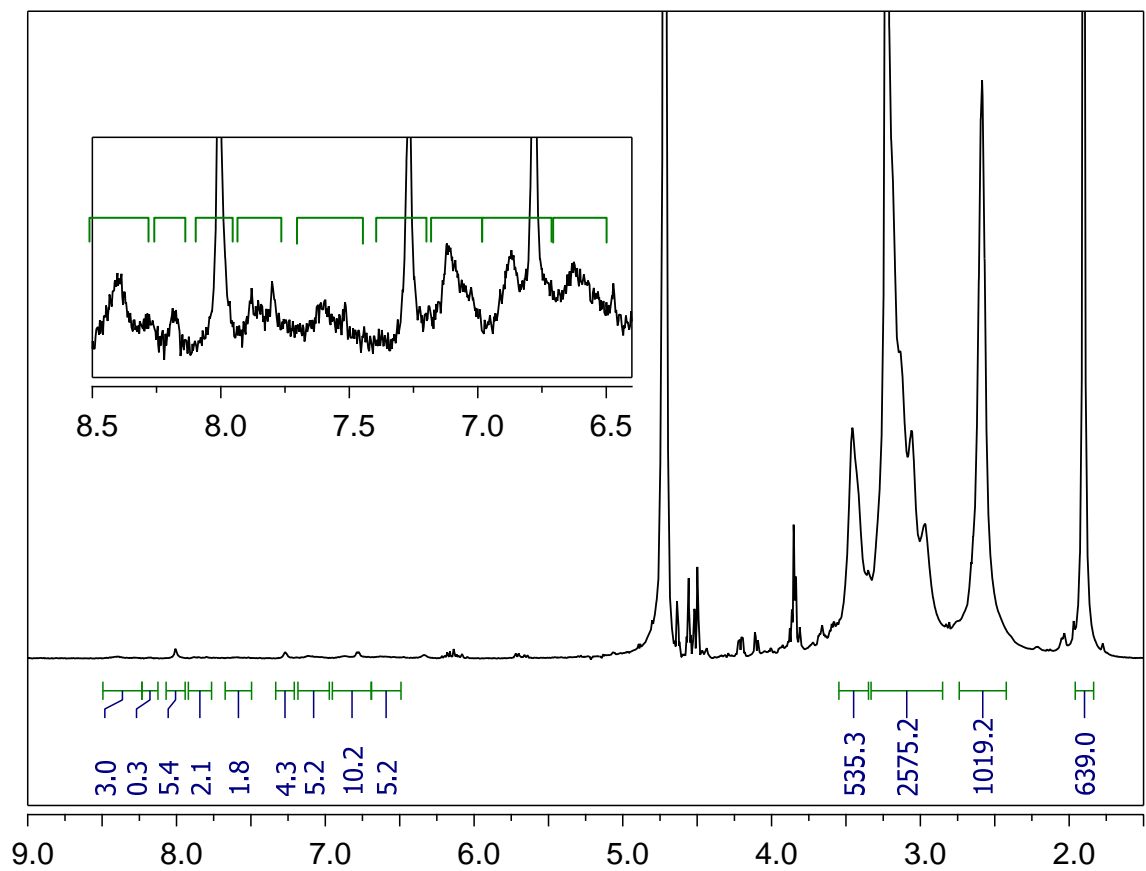
16. Synthesis of G5-Ac$_{67\%}$-Alkyne$_{1.3}$
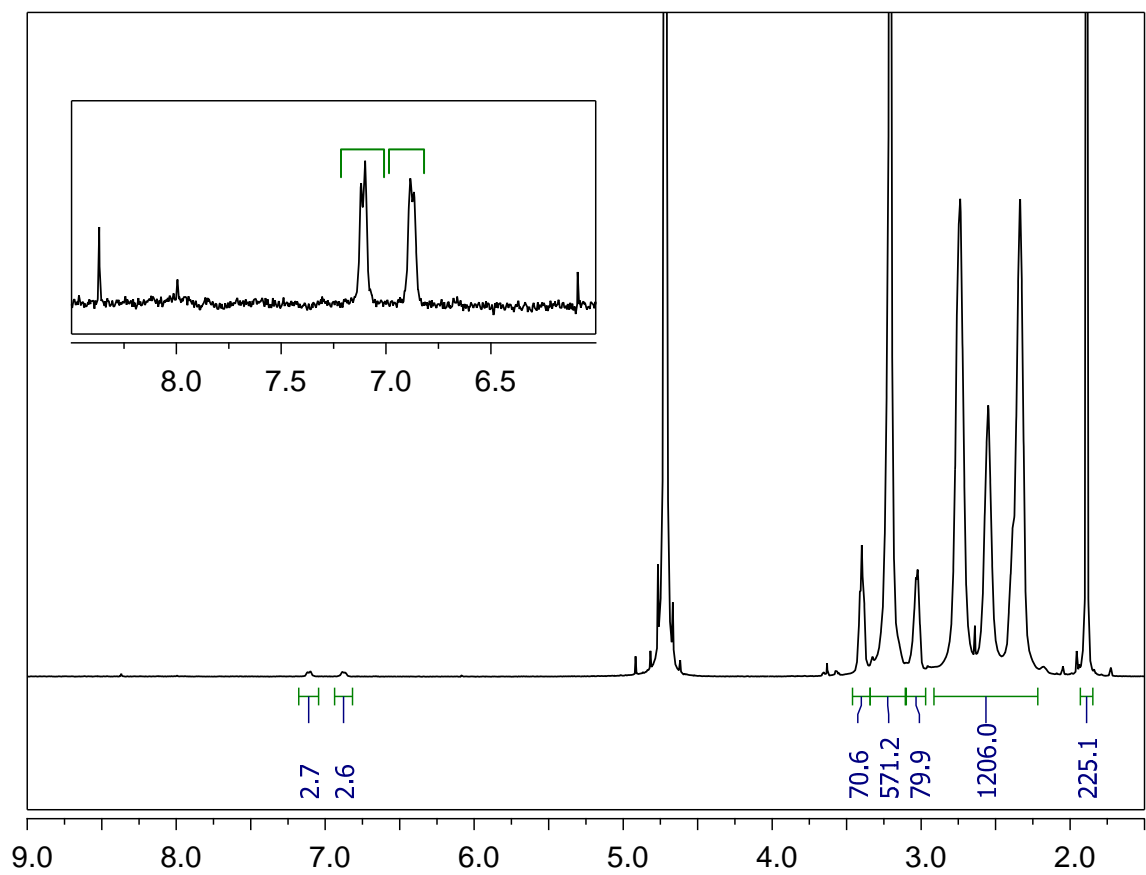
17. Synthesis of G5-Ac$_{110.7}$-Alkyne$_{1.3}$
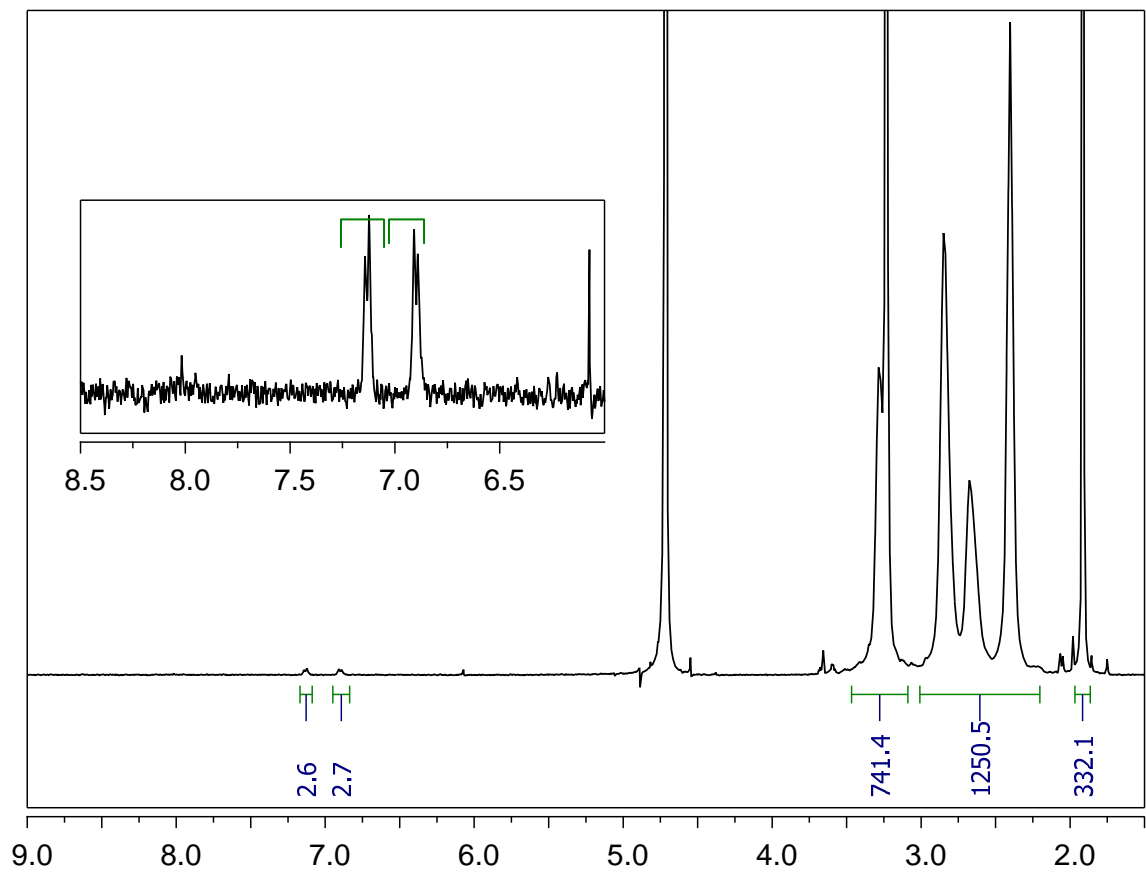
18. Synthesis of Un-targeted Dendrimer System G5-Ac$_{110.7}$-L-G5-Ac$_{106}$-FITC$_{3.2}$
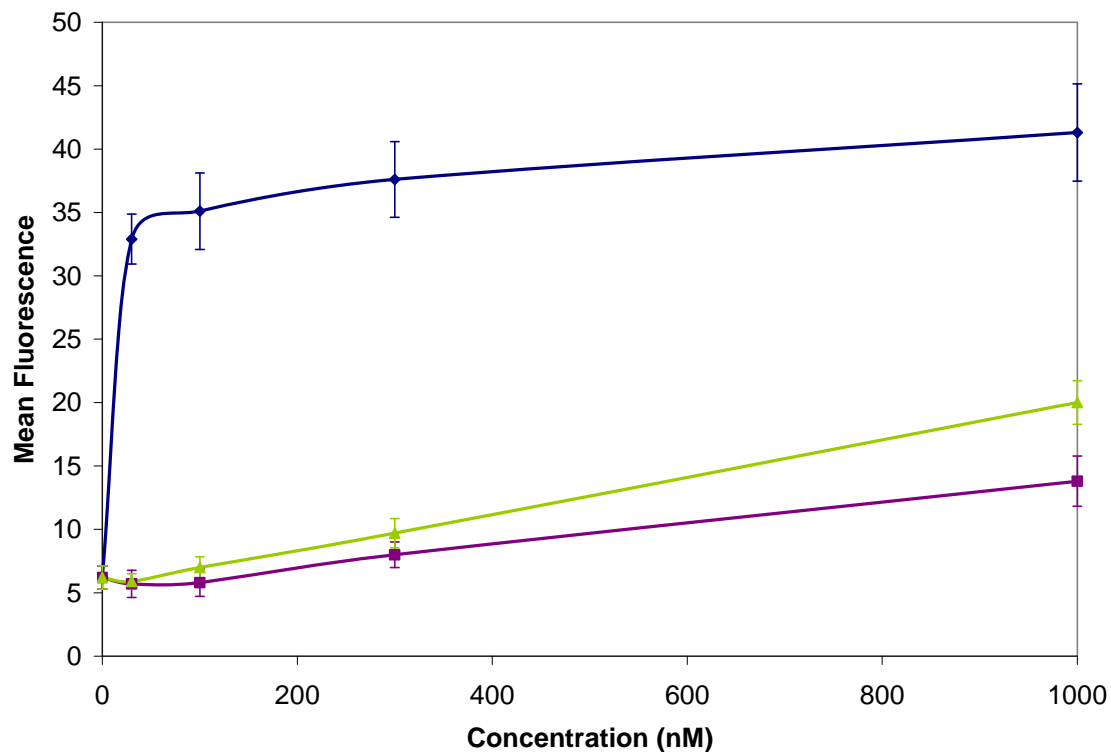
Figure 1: Binding and uptake of the fluorescent modular targeted dendrimer platform and controls in KB cells as measured by Flow Cytometry. Uptake of $FA_{3.5}$-G5-Ac_{107}-L-$G5Ac_{106}$-$FITC_{3.2}$ (**15**) is displayed in blue. Mean fluorescence values for the un-targeted platform G5-$Ac_{110.7}$-L-G5-Ac_{106}-$FITC_{3.2}$ (**18**) is shown in green. Last, mean fluorescence values for the imaging module G5-Ac_{106}-$Azide_{2.5}$-$FITC_{3.2}$ (**14**) can be found in purple. Error bars indicate standard deviation as computed from half-peak coefficient of variation (HPCV) values.